RESEARCH DIVISION

COLLEGE OF ENGINEERING

NEW YORK UNIVERSITY

DEPARTMENT OF METEOROLOGY

A UNIFIED MATHEMATICAL THEORY FOR THE ANALYSIS, PROPAGATION, AND REFRACTION OF STORM GENERATED OCEAN SURFACE WAVES

PART I

WHOI
DOCUMENT
COLLECTION

Prepared for

BEACH EROSION BOARD DEPARTMENT OF THE ARMY

Contract No. W 49-055-eng-1

OFFICE OF NAVAL RESEARCH DEPARTMENT OF THE NAVY

Contract No. N onr-285(03)

7

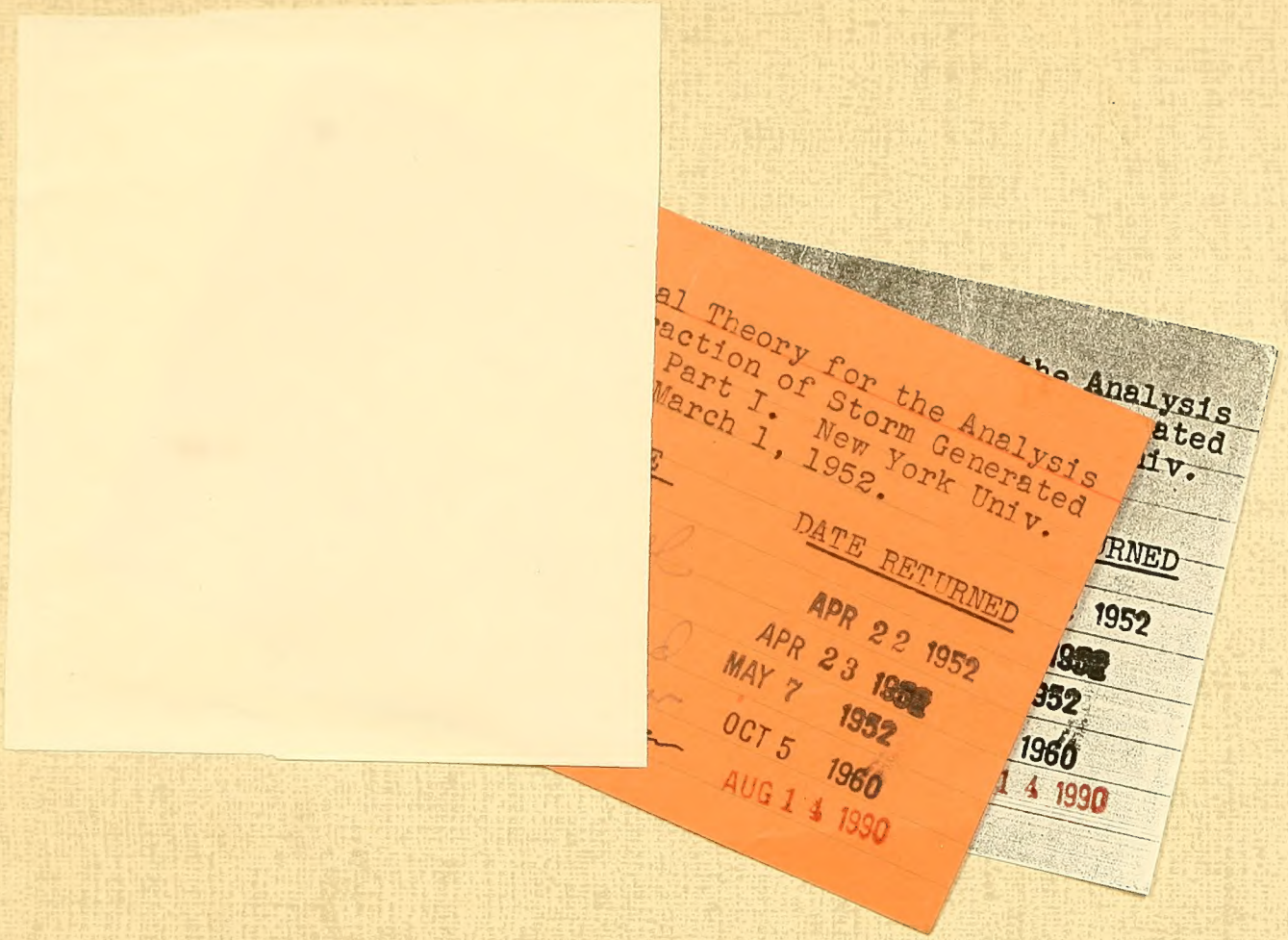
al Theory for the Analysis
action of Storm Generated
Part I. New York Univ.
March 1, 1952.
DATE RETURNED
APR 22 1952
APR 23 1952
MAY 7 1952
OCT 5 1960
AUG 14 1990
the Analysis
ated
niv.
RNED
1952
352
1960
4 1990

A UNIFIED MATHEMATICAL THEORY FOR THE ANALYSIS, PROPAGATION, AND REFRACTION OF STORM GENERATED OCEAN SURFACE WAVES

Part I

By

Willard J. Pierson, Jr.

Preliminary Distribution

Prepared under contracts sponsored by the Office of Naval Research and the Beach Erosion Board, Washington, D. C.

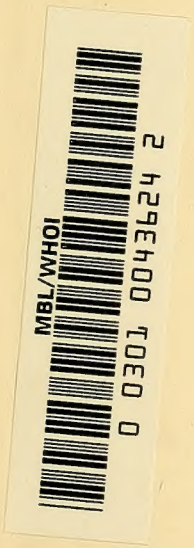

New York University
College of Engineering
Department of Meteorology

March 1, 1952

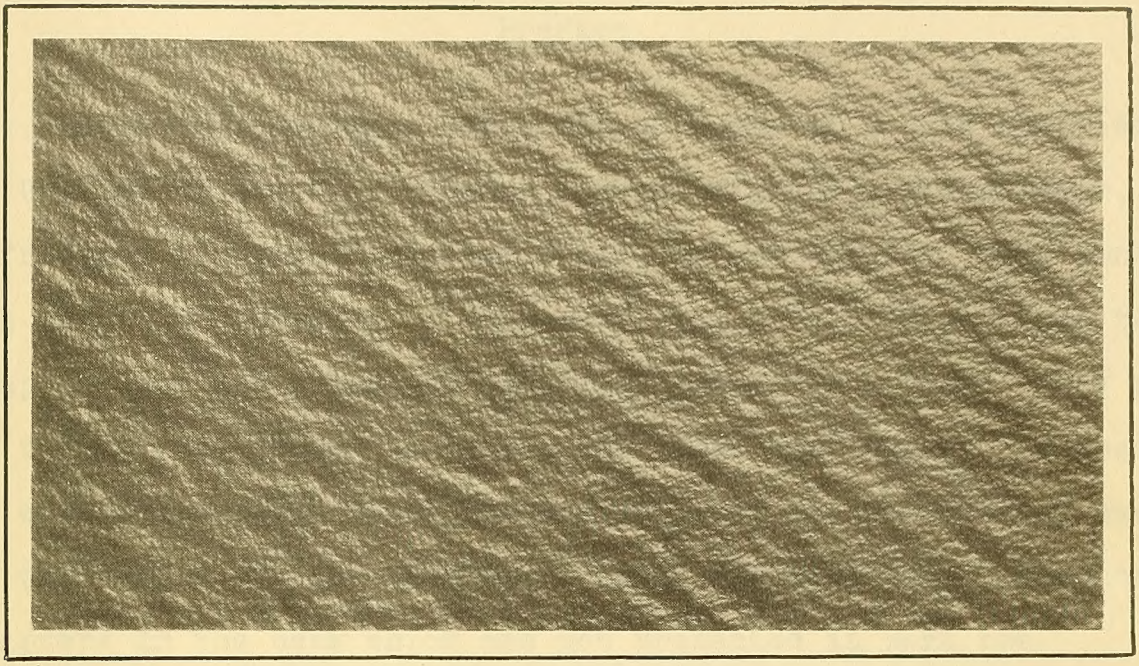

$$\eta(x,y,t) = \int_0^{\infty}\int_{-\frac{\pi}{2}}^{\frac{\pi}{2}} \cos\left[\frac{\mu^2}{g}(x\cos\theta + y\sin\theta) - \mu t + \psi(\mu,\theta)\right]\sqrt{d^2 E_2(\mu,\theta)}$$

FRONTISPIECE

Preface

The following pages represent part one of a book entitled "A Unified Mathematical Theory for the Analysis, Propagation, and Refraction of Storm Generated Ocean Surface Waves." They contain the first ten chapters of this projected book. These first ten chapters are not a logical stopping place in the book. Only part of the unified theory is presented. That part covers the theory of wave propagation (wave forecasting) and the theoretical part of the theory of wave analysis. There are also many references to chapters in the book which are not presented in part one.

Part one is presented in this disjointed form with all the apparent loose ends because more of the book could not be completed before the publication deadline and because an error was made by the author in estimating the date of completion of the book. There are many important decisions which have to be made soon in connection with the problem of adequate methods of wave analysis and wave recording and it is hoped that the contents of part one will help in these decisions.

The remainder of the book will be presented in bi-monthly installments until the book is completed. It is planned to present the mathematical theory of additional properties of waves in deep water, the theory of waves in the transition zone, and the theory of wave refraction in the next chapters. The mathematical theory is complicated, but the practical application is straightforward and easily applied. After these chapters, the book will consist

of examples and applications of the theory, of examples from the work of others which substantiate the theory, and of suggested procedures for further verification.

The work presented herein has been sponsored by the Beach Erosion Board and the Office of Naval Research. The Office of Naval Research is supporting the research which applies to the problem of wave forecasting. The Beach Erosion Board is supporting the research which applies to the problem of wave analysis and wave refraction. If the reader wishes, he can select the various parts of each chapter which apply to each of the sponsors. However difficulties will occur in deciding what parts apply to which sponsor because adequate methods of analysis are a prerequisite for adequate methods of wave forecasting and a firm understanding of basic hydrodynamics is a prerequisite for any part of the theory.

One of the most important features of government sponsored research in science is the wide latitude of action permitted the researchers by the sponsoring agencies. This is especially true of the Office of Naval Research and the Beach Erosion Board. The original contracts were thought of as separate entities, and it was planned to present separate reports to each. However, as things worked out, it became possible to unify the entire theory and present the whole subject as an entity. It is hoped that both sponsors will be pleased with the final outcome.

March 1, 1952

Willard J. Pierson, Jr.
Department of Meteorology
New York University

INDEX

	Page
Chapter 1. Introduction	1
Chapter 2. Resumé of Classical Wave Theory	4
Chapter 3. Types of Periodic Functions and Non-Periodic Functions and their Representation by Discrete and Continuous Spectra	23
Chapter 4. The Propagation of a Finite Wave Group in Infinitely Deep Water	35
Chapter 5. The Propagation of a Finite Wave Train in Infinitely Deep Water	77
Chapter 6. Some Model Wave Systems in Which the Crests are Infinitely Long	102
Chapter 7. The Most Realistic Wave Systems with Infinitely Long Crests	122
Chapter 8. Short Crested Wave Systems	173
Chapter 9. The Mathematical Representation of a Short Crested Sea Surface by a Lebesgue Stieltjes Power Integral and the Problem of Forecasts for a Storm of Finite Width and Finite Duration over a Fetch of Length, F	206
Chapter 10. Methods for the Determination of Power Spectra	255
Appendix	311
Acknowledgements	321
Index to the Figures	324
Index to the Plates	326
Index to the Tables	331
Partial List of References	332

A UNIFIED MATHEMATICAL THEORY FOR THE ANALYSIS, PROPAGATION, AND REFRACTION OF STORM GENERATED OCEAN SURFACE WAVES

SIR HORACE LAMB M.A., LL.D., SC.D., F.R.S.

"SINCE THE CONDITIONS ARE UNIFORM WITH RESPECT TO X, THE SIMPLEST SUPPOSITION WE CAN MAKE IS THAT φ IS A SIMPLE HARMONIC FUNCTION OF X; THE MOST GENERAL CASE CONSISTENT WITH THE ABOVE ASSUMPTIONS CAN BE DERIVED BY SUPERPOSITION IN VIRTUE OF FOURIER'S THEOREM."

Chapter 1. INTRODUCTION

The origin of the remark is lost in antiquity, but many persons claim that ocean waves are just bumps on the water. Certainly, wave records show that the waves pattern is sometimes chaotic, sometimes irregular, and other times smooth. Wave records are not sinusoidal, nor are they obviously periodic. In this paper the supposition that waves are just bumps on the water will be admitted, and then it will be possible to show how waves can be represented by the sum of a number of sinusoidal terms in a way which will preserve many of their observed properties and which will be amenable to theoretical work.

The overall theory of wave forecasting is a mixture of various concepts which do not fit together well at the edges. Waves are treated partly as non-conservative waves and partly as classical waves. The significant waves are forecasted over a fetch and they are supposed to represent the average height and period of the one third highest waves. Admittedly, they are not classical

waves, and yet they are forecasted to travel with classical group velocities, and refracted as if they were purely sinusoidal waves of one single period.

The Sverdrup-Munk theory [1947, 1949a], as extended in part by Arthur [1948, 1949], depends on the validity of the assumption that two parameters, viz., the significant wave height and period, can adequately describe the sea surface at any time and any place. It will be shown that these parameters are not sufficient to characterize the sea surface and that the inadequacy of these parameters in part can explain the failure of the forecasting method to forecast the significant period as shown by Donn [1949], Isaacs and Saville [1949], and Pierson [1951b].

Wave records at present are frequently obtained by recording the pressure as a function of time at the bottom as the wave passes overhead. The pressure records are then analyzed for the significant period and significant pressure amplitude, and the significant height and period at the free surface are computed from these values. It will be shown that this procedure is incorrect.

The use of the significant period in problems in wave refraction is also a most doubtful procedure. A method will be developed in this paper which will be far more applicable to actual sea conditions than the present techniques.

The overall plan of this paper is to start with the simple and proceed to the complex in the derivation of various models of waves on the sea surface. Models of the sea surface will finally be obtained which will prove to be adequate for a correct description of the sea surface.

After these models have been obtained, they will be discussed in connection with the problem of wave forecasting, wave recording, and wave refraction. It will be shown that they form a basis for a correct forecasting theory of ocean waves. It will also be shown that the current debate in the literature about whether friction against the atmosphere or eddy viscosity in the moving water causes the decrease of wave height with travel into the decay area is an argument about nothing, because this decrease of height of waves with travel can mostly be explained by classical concepts without the use of any type of friction in the theory.

Many of the points which will be discussed in this paper are purely theoretical. Some of the instrumentation and methods of analysis which will have to be devised in order to place the techniques which will be described into practical use have yet to be developed. The data which are obtained at present are inadequate. Procedures for obtaining data which will adequately characterize waves produced by a storm at sea will be described.

The final result of this paper will be to obtain a unified mathematical theory for the representation of ocean surface waves as they are. The behavior of irregular waves will be described completely from the time they leave their source until they enter the breaker zone. Applications to problems in beach erosion and ship design and other far-reaching implications will be described.

Chapter 2. RESUMÉ OF CLASSICAL WAVE THEORY

Introduction

Classical wave theory has discussed rotational waves such as Gerstner's waves and irrotational waves such as shallow water waves, waves of finite height, deep water waves of infinitesimal height, and solitary waves. This paper will be concerned with the theory of deep water waves of infinitesimal height at first, and later the refraction and diffraction of these waves will be discussed.

Before the theory of waves of infinitesimal height is applied to the sea surface, a reason should be given for not using the theory of waves of finite height. The reason is simply that the waves of infinitesimal height combine linearly whereas waves of finite height do not combine linearly. The irregularity of the sea surface is its dominant feature. As such, it can be treated mathematically. The non-linearity of the sea surface cannot be treated mathematically without suppressing the irregularity of the sea surface. These points will be clarified in the resumé of the theory of waves which follows.

Non-linear equations

If irrotational motion is assumed, the problems connected with gravity wave motion on a free surface approximated by a plane despite the curvature of the earth can all be considered to be solutions of equations (2.1), (2.2), (2.3), (2.4), and (2.5) which are shown in Plate I and which for example are given by Lamb [1932].

Irrotational Non-linear Equations for Motion Bounded by a Free Surface and a Bottom of Variable Depth.

Potential equation $$\Phi_{xx} + \Phi_{yy} + \Phi_{zz} = 0 \qquad (2.1)$$

Bernoulli's equation $$\frac{p}{\rho} = \Phi_t - \frac{1}{2}\left(\Phi_x^2 + \Phi_y^2 + \Phi_z^2\right) - gZ \qquad (2.2)$$

Boundary conditions:

at $Z = -h(x,y)$ $$\Phi_n = 0 \qquad (2.3)$$

at $Z = \eta$ $$\eta = \frac{1}{g}\Phi_t - \frac{1}{2g}\left(\Phi_x^2 + \Phi_y^2 + \Phi_z^2\right) \qquad (2.4)$$

at $Z = \eta$ $$\eta_t = -\Phi_z \qquad (2.5)$$

Irrotational Linear Equations for Motion Bounded by a Free Surface and a Bottom of Variable Depth.

Potential equation $$\Phi_{xx} + \Phi_{yy} + \Phi_{zz} = 0 \qquad (2.6)$$

Bernoulli's equation $$\frac{p}{\rho} = \Phi_t - gZ \qquad (2.7)$$

Boundary conditions:

at $Z = -h(x,y)$ $$\Phi_n = 0 \qquad (2.8)$$

at $Z = 0$ $$\eta = \frac{1}{g}\Phi_t \qquad (2.9)$$

at $Z = 0$ $$\eta_t = -\Phi_z \qquad (2.10)$$

PLATE I

Equation (2.1) is the potential equation which originally comes from the equation of continuity. Equation (2.2) is Bernoulli's equation where an arbitrary function of time has been neglected. Equation (2.2) need not be considered explicitly in solving wave problems; it simply gives the pressure after φ has been obtained. Equation (2.3) is a boundary condition equation and states that there is no fluid motion normal to the bottom. Equation (2.4) is the free surface boundary condition for pressure continuity where η is the free surface. Finally, equation (2.5) is the kinematic boundary condition at the free surface. It states the condition that a particle at the free surface must remain at the free surface. In this paper, partial derivatives will be denoted by subscripts; for example, Φ_t means $\partial\Phi/\partial t$.

These equations have never been solved completely. Partial solutions have been obtained only after simplifying the equations. Even the known solutions for waves of finite height are approximations. The difficulty arises in equation (2.4). The term $(\varphi_x^2 + \varphi_y^2 + \varphi_z^2)/2g$ is the cause of the difficulty. It is a non-linear term. Suppose, for example, that φ_1 satisfies equations (2.1), (2.2), (2.3), (2.4), and (2.5), and that φ_2 also satisfies the same equations. Then φ_1 plus φ_2 will not satisfy the equations, and P_1 plus P_2 and η_1 plus η_2 have no meaning.

Thus the original equations for wave motion are non-linear. At this point, then, in the study of wave motions there are two possible ways to proceed. One way to proceed is to concentrate on the non-linear properties of the equations. The second way to proceed is to reduce the equations to a linear form with the small-

height assumption so that the property that the sum of two solutions is also a solution will be obtained.

If the non-linearity of the problem is of the greatest interest, the work of Stokes [1847] as summarized by Lamb [1932] illustrates the type of results which are obtained. In Chapter IX, Section 250 of Lamb, for example, the problem of waves of finite amplitude in water of infinite depth is treated "as a case of steady motion" under the assumption that the wave is periodic in time. The notation is somewhat different from that which is used here, but equation 4 in Lamb shows that the non-linearity of the free surface and of Bernoulli's equation is considered in the derivation to find the speed of the wave. The solution is approximate because it is in series form. The wave profile is approximated for the first three terms by a trochoid, and the whole wave profile moves forward with the speed

$$C = \left[\frac{g}{k}\,(1 + k^2a^2)\right]^{1/2} \quad , \quad k = \frac{2\pi}{L} \quad .$$

Davies' Results

A recent monograph by Lowell [1950] on gravity waves of finite amplitude describes some results which have been obtained by T.V. Davies [1951] of King's College, University of London. Lowell's summary of his monograph is quoted in full below. Davies' work has unified the previous theories of waves of finite height and has yielded some improved theoretical relationships about the ratio of wave height to wave length.

GRAVITY WAVES OF FINITE AMPLITUDE

"T. V. Davies of King's College, University of London, has discovered a new method for treating the classical problem of steady gravity waves in an irrotational, incompressible fluid. He has been able to solve the problems of (a) periodic waves in a channel of infinite depth, (b) the solitary wave, (c) periodic waves in a channel of finite depth, and (d) periodic waves at the interface of two streams of finite depth.

"The method used by Davies is a development of that of Levi-Civita in his paper of 1925. The first approximate solution contains a variable parameter μ which satisfies $0 \leq \mu \leq \mu_o$, (μ_o being known in each case); the lower range of μ corresponds to the classical waves of small amplitude, the upper limit corresponds to the case in which breaking occurs at the crest. The Stokes result, that the angle of breaking at the crest is 120°, is verified in each case and the problems of wave velocity, energy, form of the free surface, and the drift at the base of the fluid, have in the main been solved. The first approximation is in error by 13% at the extreme case of breaking at the crest, but the error decreases when the crest is horizontal and when the ratio of wave height to wave length is smaller. The higher approximations have been derived in cases (a) and (b)."*

---

* The μ in this quotation has a meaning here which is different from its meaning in the rest of the text.

In the theory of waves of finite height, it is not possible to take two solutions, add them, and find a solution for the combined effect of the two profiles. Thus the known solutions for waves of finite height are all purely periodic, and they do not apply to the sea surface if the sea is irregular.

Linearized Equations

Since the irregularity of the sea surface will be of the greatest interest in this paper, the equations must be linearized if known mathematical techniques are to be applied to the analysis. The assumption can be made that φ is so small that the square of φ and its partial derivatives can be neglected compared to the magnitude of φ and its partial derivatives. Under this assumption equations (2.1), (2.2), (2.3), (2.4) and (2.5) can be replaced by equations (2.6), (2.7), (2.8), (2.9) and (2.10) which are also given in Plate I.

Equations (2.6) through (2.10) are very much simpler than the first set of equations. The non-linear terms have been omitted from equations (2.2) and (2.4), and to the same degree of validity, it is possible to evaluate the free surface boundary conditions at $z = 0$ instead of at $z = \eta$. These equations are linear. If φ_1 is a solution of equations (2.6), (2.7), (2.8), (2.9), and (2.10), and if φ_2 is a solution of the same equations, then $\varphi_1 + \varphi_2$ is also a solution. In addition, $P_1 + P_2$ and $\eta_1 + \eta_2$ are defined. Strictly speaking the equations hold exactly only for waves of infinitesimal amplitude. In what follows, they will be applied to waves of finite height with the reservation that

the higher the ratio of the wave amplitude to the wave length the more inaccurate the results. This linearized theory is used in nearly all practical wave studies and especially in the theory of wave refraction and diffraction.

General solutions

The above set of equations is, nevertheless, still complicated, and the manifold of possible solutions is extremely large. The number of known solutions is quite small.

There are two general types of solutions to those linearized equations. One is the periodic solution in time, and the other is the non-periodic solution. A periodic solution in time is a solution such that at any point in the fluid or at the free surface, the same conditions are found one period later as were found at the time of the initial observation. The conditions must be the same for all time. Thus, the conditions for a periodic solution can be stated as in equation (2.11) in Plate II. From equation (2.11), it follows that the free surface is also periodic.

The concept of periodicity will be investigated in detail in the next chapter. It should be noted at this point, that the sum of two periodic solutions need not be periodic unless some additional conditions are satisfied.

In addition, a whole class of non-periodic solutions can be obtained from integration by Fourier's Integral Theorem over a continuous spectrum of periods. The quotation at the start of this paper emphasizes the fact that the way to obtain non-periodic solutions is to build them up mathematically from

periodic solutions by the use of Fourier's Integral Theorem. One purpose of this paper is to show what information is needed to carry out this process for the sea surface. It will be found that classical wave theory is not quite general enough to represent the sea surface. The more recent extensions of Fourier Theory to stationary time series have to be employed in order to represent waves from a storm at sea adequately.

Periodic solutions

To return to the linear equations, then, it becomes necessary to study the nature of purely periodic solutions. In order to do this, it is possible to split off the periodicity in time by use of the equations (2.12) and (2.13) in Plate II. In equations (2.12) and (2.13), Re is read "the real part of." η and φ are complex quantities, and some examples will be given later.

If equations (2.12) and (2.13) are substituted into the linearized equations, a set of reduced equations is obtained in which φ and η' are not functions of time. However, (2.12) and (2.13) yield the progressive wave solutions. Equation (2.7) will not be used for a while and it will not be given in modified form.

The reduced linear equations given in Plate II have been solved exactly for a constant depth and for a linearly sloping beach. They have not been solved for $z = - h(x,y)$ where $h(x,y)$ is an arbitrary function of x and y.

There are two solutions for constant depth. One solution yields an infinite train of traveling infinitely long straight parallel wave crests with a free surface which varies sinusoidally

Form of the Irrotational Linear Equations when the Requirement that the Solution be Periodic in Time is Imposed.

Definition of periodicity $\bar{\Phi}(x,y,z,t) = \bar{\Phi}(x,y,z,t+T)$ (2.11)

then $\bar{\Phi}(x,y,z,t) = \mathcal{R}e\, \Phi(x,y,z) e^{-i\frac{2\pi t}{T}}$ (2.12)

$\eta(x,y,t) = \mathcal{R}e\, \eta'(x,y) e^{-i\frac{2\pi t}{T}}$ (2.13)

and, potential equation $\phi_{xx} + \phi_{yy} + \phi_{zz} = 0$ (2.14)

boundary conditions:

at $Z = -h(x,y)$ $\qquad \phi_n = 0$ (2.15)

at $Z = 0$ $\qquad \eta' = -\frac{i2\pi}{gT}\phi$ (2.16)

at $Z = 0$ $\qquad -\frac{i2\pi}{T}\eta' = -\phi_z$ (2.17)

Known solutions if $Z = -h$ (h constant)

Straight wave crests

$$\phi = \frac{AgTi\, e^{i\left[\frac{2\pi}{L}(x\cos\Theta + y\sin\Theta) + \delta\right]} \cosh\frac{2\pi}{L}(Z+h)}{\cosh\frac{2\pi}{L}h} \tag{2.18}$$

$$\eta = A\cos\left[\frac{2\pi}{L}(x\cos\Theta + y\sin\Theta) + \delta - \frac{2\pi t}{T}\right] \tag{2.19}$$

$$C^2 = \frac{L^2}{T2} = \frac{gL}{2\pi}\tanh\frac{2\pi h}{L} \tag{2.20}$$

Circular wave crests

$$\phi = \text{const}\, H_0^1\left(\frac{2\pi}{L}r\right)\cosh\frac{2\pi}{L}(Z+h) \tag{2.21}$$

$$\phi \cong \frac{\text{const}\, e^{i\frac{2\pi}{L}\sqrt{(x-x_0)^2+(y-y_0)^2} - i\frac{\pi}{4}} \cosh\frac{2\pi}{L}(Z+h)}{\sqrt{(x-x_0)^2+(y-y_0)^2}} \tag{2.22}$$

$$\eta \cong \frac{\text{const}\, \cos\left(\frac{2\pi}{L}\sqrt{(x-x_0)^2+(y-y_0)^2} - \frac{\pi}{4} - \frac{2\pi t}{T}\right)}{\sqrt{(x-x_0)^2+(y-y_0)^2}} \tag{2.23}$$

PLATE III

in one direction. The other solution, given by a Hankel function, yields circular wave crests which radiate from a point source.

The first solution is found in the Cartesian coordinate system which has been used so far. φ is given by equation (2.18). δ is an arbitrary phase lag, and A is the amplitude of the wave crest.

From equations (2.18), (2.13), and (2.16), it follows that η is given by equation (2.19). This representation for the free surface has been chosen in order to point out all the arbitrary parameters in the solution. The most important one to note is the θ which permits the choice of any wave direction, if θ varies through 2π radians. The equation for the speed of waves in water of constant depth follows from equations (2.18), (2.16), and (2.17). The fact that the depth is constant permits the easy treatment of the problem. The speed of the crests is given by equation (2.20). Equation (2.19) is the only wave with straight crests, which travels with the classical wave velocity of waves with small amplitude. As written, it states that there are an infinite number of crests present, that the wave record will be observed for an infinite time at any point, that the period and wave length are everywhere the same and everywhere constant, and that the heights of all crests are the same. If any single one of these requirements is not satisfied in nature, then the equation is not valid, and a more refined analysis is needed.

The second solution is found in cylindrical coordinates, and the solution is given in terms of the distance r from a fixed point, $r_o = 0$. φ is given by equation (2.21) where $H_o^1 (2\pi r/L)$ is the first Hankel function of order zero (see Sommerfeld [1949]). If r is large and x_o, y_o are the coordinates where r = 0, then φ is approximated by equation (2.22).

The free surface, η, is then given by equation (2.23) under the same assumption that r is large. The same condition for the speed of the wave crests holds that was given in equation (2.20). The point of origin of the circular wave crest is arbitrary.

Equations (2.21), (2.22), and (2.23) will not be used in this paper. Mathematical techniques similar to the ones which will be employed in this paper (but more difficult) are applicable to problems involving these equations. They are given here in the interest of completeness, and in order to make one very important point.

For narrow fetches with very turbulent and extremely variable winds, and for wave generating areas such as those found in hurricanes, a detailed study of the sea surface would have to be made with these equations as a starting point. Problems in wave decay in particular must be studied because the form of equation (2.23) provides a means for the decrease of wave height with distance traveled. In view of these considerations, the results of this paper will be based upon the assumption that the elemental unit of analysis is a wave of the form of equation (2.19). The consequences of this assumption will be

discussed in detail in a later chapter.

The remaining known solutions to these reduced equations have been obtained by Stoker, [1947], and his co-workers for the problem of a linearly sloping beach with waves parallel to the beach and recently by Peters for waves at an angle to the beach (unpublished).* For additional information, see the paper referred to above.

No exact solutions for the reduced equations have been obtained under the condition that the depth is an arbitrary function of x and y. Graphical methods of solution based upon the principles of geometrical optics have been given by Sverdrup and Munk [1944], and by Johnson, O'Brien and Isaacs [1948]. Pierson [1951a] has discussed these results and formulated the problem which would have to be solved in order to proceed from equations (2.14) through (2.17) to a result which would prove that the principles of geometrical and physical optics are applicable to problems of ocean wave refraction and diffraction. Eckart [1951] has obtained an approximate solution to the completely general problem, accurate everywhere to within a few percent.

The solutions which have been discussed so far apply to depths which range from infinite to one or two tenths of the deep water wave length. The solutions do reduce to the shallow water theory, if h is picked smaller and smaller, but a wave of the finite height progressing from deep to shallow water in Stoker's work [1947] becomes infinitely high as it approaches

*See References.

the shore and thus the linearized theory breaks down.

Another class of solutions can be obtained under the assumption that the water is shallow. The shallow water theory of the solitary wave, for example, as obtained by Airy is treated in Lamb [1932]. Recent refinements in the theory have been obtained by Keller [1949]. Lowell [1949a] has studied the propagation of waves in shallow water. Munk [1949] has studied the breaking of solitary waves in shallow water. Stoker [1949] has applied the non-linear shallow water theory to the formation of breakers and bores and to the breaking of waves in shallow water.

The results which will be obtained in this paper will hold only up to the shallow water zone. It will be possible to generalize the theory of ocean wave refraction to the disturbances studied herein. The breaker zone, however, will not be treated, although an extension of the results obtained by Biesel [1951] may make this possible. Biesel's graphs of waves just before breaking appear to be the most realistic mathematical breakers ever presented.

Non-periodic solutions

One final important class of solutions which has been obtained in classical wave theory remains to be discussed. They are the solutions which have been obtained by the use of Fourier's Integral Theorem for waves in infinitely deep water. The general procedure is to integrate the potential function and the representation of the free surface given in equations (2.18) and (2.19) over a continuous spectrum of angular wave frequencies

($\mu = 2\pi/T$) and thus obtain some special case non-periodic solutions.

For infinitely deep water (for practical purposes about five hundred feet for waves with periods of ten seconds or less), the potential function, the free surface, the pressure (z decreases from zero), the wave speed and the wave length are given by equations (2.24), (2.25), (2.26), (2.27) and (2.28) where $\mu = 2\pi/T$. The equations follow from equations (2.7), (2.9), (2.12), (2.13), (2.18) and (2.19).

In these equations (Plate III), Φ is a function of the three space coordinates and time. Φ also depends upon the parameters, μ , θ, A, and δ. If $\Phi_1 = \Phi_1(x,y,z,t,\mu_1,\theta_1,A_1,\delta_1)$* is one potential function, and if $\Phi_2 = \Phi_2(x,y,z,t,\mu_2,\theta_2,A_2,\delta_2)$ is a second potential function, then $\Phi = \Phi_1 + \Phi_2$ is a third potential function.

Moreover, if A and δ are functions of μ and θ, then a double integral of Φ over μ and θ is also a potential function. $A(\mu,\theta)$ and $\delta(\mu,\theta)$ must behave properly in a mathematical sense for large μ . In particular equation (2.29) is a potential function which satisfies equation (2.6) and (for $z = -\infty$) equation (2.8). Also η can be found from equation (2.9) and the pressure can be found from equation (2.7). The condition, (2.10), is satisfied.

If one picks some functional form for $A(\mu,\theta)$ and $\delta(\mu,\theta)$ and if then the indicated integration can be performed on equation (2.29), the resulting expression for the potential function

*i.e., Φ is a function of the time and space variables and one set of fixed values for the parameters.

Periodic Wave Solutions For Infinitely Deep Water Expressed in Terms of Angular Wave Frequencies.

$$\mu = \frac{2\pi}{T}$$

Potential function

$$\Phi = \frac{-Ag}{\mu} e^{\mu^2 z/g} \sin\left(\frac{\mu^2}{g}(x\cos\theta + y\sin\theta) - \mu t + \delta\right) \qquad (2.24)$$

Free surface

$$\eta = A\cos\left(\frac{\mu^2}{g}(x\cos\theta + y\sin\theta) - \mu t + \delta\right) \qquad (2.25)$$

Pressure

$$p = \rho g A e^{\mu^2 z/g} \cos\left(\frac{\mu^2}{g}(x\cos\theta + y\sin\theta) - \mu t + \delta\right) - g\rho Z \qquad (2.26)$$

Wave speed $C = \frac{g}{\mu}$ (2.27)

Wave length $L = \frac{2\pi g}{\mu^2}$ (2.28)

A non periodic potential function results from integration over μ and θ.

$$\Phi = \int_{-\infty}^{+\infty}\int_{-\pi}^{+\pi} \frac{-gA(\mu,\theta)}{\mu} e^{\mu^2 z/g} \sin\left(\frac{\mu^2}{g}(x\cos\theta + y\sin\theta) - \mu t + \delta(\mu,\theta)\right) d\mu\, d\theta \qquad (2.29)$$

PLATE III

will yield all the usual information about the effects of the disturbance on the free surface.*

Lamb [1932] summarizes some of the results which have been obtained by the use of the Fourier Integral Theorem. Among the results, the Cauchy Poisson Wave problems are of the greatest interest as far as this paper is concerned. One problem gives the wave system propagated from an initially concentrated elevation of the free surface, and the other problem gives the wave system propagated from an initially concentrated impulse applied to the free surface.

The first problem gives the wave system which would result, if at the given time t = 0, an infinitely high, infinitesimally wide, infinitely long column of water were to start falling into the ocean at the point x = 0. The free surface, η, is given by equation (2.30) if $gt^2/4x$ is large.

$$\eta = \frac{g^{\frac{1}{2}} t}{2^{3/2} \pi^{1/2} x^{3/2}} \left[\cos\left(\frac{gt^2}{4x}\right) + \sin\left(\frac{gt^2}{4x}\right) \right] \qquad (2.30)$$

At any x as t approaches infinity, η oscillates more and more rapidly and approaches infinite values of height. Since the original formulas upon which this solution is based were founded upon the assumption that the height of the initial disturbance is small, the physical reality of the problem is seriously open to question.

The second problem gives the wave system which results from the action of an infinitely intense impulse upon the line

*Note also that the u, v, and w components of the fluid velocity can be found from Φ .

$x = 0$ at the time $t = 0$. The free surface for large $gt^2/4x$ is found by partial differentiation of equation (2.30) with respect to t and multiplication by $1/g\rho$. Again the physical reality of the problem is seriously open to question.

The two problems described above have been used (frequently in a most uncritical way) by many authors in attempts to devise methods for forecasting ocean waves. Until some ship reports an infinitely high, infinitely long, infinitesimally wide column of water over the ocean or an infinitely intense local impulse concentrated on a line, it will be necessary to interpret these results "cum grano salis."

There is one remaining classical application of the Fourier Integral Theorem which is of great interest in this study. It is the Gaussian wave packet. Coulson [1943] gives a readily available summary of the chief results obtained (see reference, pp. 135-138). The representation for the free surface obtained from the Gaussian wave packet depended upon the integration of equation (2.31) where to transform to the notation of equation (2.29), K would be given by $K = \mu^2/g$ and n would be given by $n = \sqrt{Kg} = \mu$.*

$$\eta(x,t) = \mathcal{R}_e \int_{-\infty}^{\infty} A e^{-\sigma(K-K_o)^2} e^{i2\pi(Kx-nt)} dK \qquad (2.31)$$

For $t = 0$, the integral can easily be evaluated and the free surface is found to be given by equation (2.32).

*Coulson [1943] uses ϕ for the free surface and not the potential function.

$$\eta(x,0) = \mathcal{R}_e A\sqrt{\frac{\pi}{\sigma}}\, e^{-\frac{\pi^2 x^2}{\sigma}} e^{2\pi i K_o x} \qquad (2.32)$$

Equation (2.32) represents a wave as a function of x on the free surface with a wave length, $L_o = 2\pi/K_o$, which is modulated by a probability curve envelope. In order to evaluate (2.31) as a function of time also, n was expanded as a function of K in a Taylor series about the point $n_o = \sqrt{K \cdot g}$. Only the first two terms of the expansion were used in the integration.

The solution thus obtained was an approximation because of the series approximation of n. It showed that the probability curve envelope advanced with the group velocity appropriate to waves with a wave length, $L_o = 2\pi/K_o$, that the envelope flattened out with time and decreased in maximum amplitude, and that there was a gradual phase shift of the individual waves under the envelope.

The Gaussian wave packet is a far more realistic problem than the Cauchy-Poisson problem because the condition that the height of the waves be small is satisfied everywhere if it is satisfied at the time t = 0. As it stands, however, it is probably not applicable for moderately large values of σ and for large values of time or displacement in the x direction because the effect of dispersion is partially neglected in the series approximation of n.

It should be noted that none of the classical solutions have considered the possible variation in the direction of propagation of the wave crests as indicated in equation (2.29).

This will be done in great detail in this paper when models which describe waves from a storm at sea are obtained.

Chapter 3. TYPES OF PERIODIC FUNCTIONS AND NON-PERIODIC FUNCTIONS AND THEIR REPRESENTATION BY DISCRETE AND CONTINUOUS SPECTRA

Introduction

The surface of the oceans, if represented accurately everywhere, would have to be given by a function of latitude, longitude, and time. The function would include the effects of tides, piled up water due to wind stress, other things, capillary waves, and gravity waves. This representation for the sea surface would be an extremely complicated function. In fact, it is so complex that it is necessary to restrict the scope of the problem and to study the various effects separately.

This study will be restricted to the mathematical analysis of ocean gravity waves with periods ranging from one or two minutes through one half seconds. Even this restriction is not enough. It is also necessary to restrict attention to homogeneous areas of the ocean over which conditions can be expected to be relatively the same and to line segments on which the waves as they pass are the same in essential character for a relatively long time. A generating area or fetch such as the ones treated in the Sverdrup-Munk Theory [1944a, 1947] might be such an area of study if the waves have reached a steady state condition. It will be shown that the usual measurements of significant height and period are not sufficient to characterize such a steady state condition.

Frequently the character of recorded wave data changes

slowly over time intervals of the order of four hours. In the same sense that sin t can be approximated in the neighborhood of t = 0 by t, it will be possible to represent wave records obtained at a certain time by the functions which will be studied. The more rapidly the sea surface characteristics change, the less valid some of the techniques described here will be.

The nature of available data

Ocean waves are recorded by two methods at the present time. Either the actual height of the free surface is recorded at a fixed point as a function of time, or the pressure at some depth below the free surface and at a fixed point is recorded as a function of time. Neither method is sufficient to determine completely the actual space and time distribution of the free surface, the pressure, and the fluid motions. By a sufficient number of simplifying assumptions, it is possible to draw a few conclusions about the distribution in space and time of the above properties.

The actual height of the free surface is frequently measured on the open ocean by an upright graduated pole with a large disk on the bottom to damp out the motions of the pole. On the end of piers or at fixed installations such as oil drilling structures in the Gulf of Mexico as reported by Glenn [1950], it is possible to use the instrument developed by the Beach Erosion Board and described by Caldwell [1948]. In either case a record is obtained of the height of the free surface as a function of time at a fixed point. Or in terms of the equations employed in this paper, $\eta = \eta(x_o, y_o, z = 0, t)$ is known.

Most wave records at the present time are not actual measurements of the free surface. They are measurements of the pressure at some depth below the free surface. In all but one known case, the depth is the bottom at a short distance (relatively speaking) from the shore. In this one case, the pressure was recorded by a submarine below the sea surface as reported by Ewing and Press [1949]. In terms of the equations employed herein, $P = P(x_o,y_o,z_o,t)$ is known where usually z_o is equal to $- h(x_o,y_o)$, the depth of the water below the (x_o,y_o) point of installation of the instrument.

From either $\eta = \eta(x_o,y_o,0,t)$ or $P = P(x_o,y_o,z_o,t)$, the problem is to find out what $P = P(x - x_o, y - y_o, z, t)$, $\eta = \eta(x - x_o, y - y_o, t)$ and (say) $U = U(x - x_o, y - y_o, z, t)$ are like. The problem is not simple. In fact, with the given data, the problem cannot be solved.

As a start, though, it is necessary to study what is most accurately known, namely either $\eta = \eta(x_o,y_o,0,t)$ or $P = P(x_o,y_o,z_o,t)$. The free surface will be used in this part of the discussion although the remarks can be modified so that they apply to the pressure. The question is, "What ways are there to analyze the free surface as a function of time?"

Over time intervals of the order of days, $\eta = \eta(t)$, at any fixed point, is not even remotely periodic. The amplitude of η may vary from small departures from zero to storm wave heights. The problem, then, is how to analyze η under the assumption that some property of η is preserved for time intervals of the order of twenty minutes or so, with the reservation that

the situation is still undefined outside of some possibly larger time interval.

Consider a wave record, say twenty minutes long. Is it possible to pick some functional representation for η (t) which will coincide with the wave record for the twenty minutes over which our attention is concentrated? Many functional representations are so obviously inadequate that they will not even be considered, but for other functional representations it is not immediately obvious that they do or do not apply.

As a start consider a wave record which is not too irregular.* Such a wave record might appear as sketched in Plate IV. The essential feature of the record for this part of the discussion is that there are groups of high waves and that between the groups of high waves there are time intervals where the amplitude of the disturbance of the free surface is small compared to the amplitude near the center of the group. These groups of high waves will simply be referred to as "wave groups."

One discrete period

One way to analyze the actual wave record would be by the significant wave method of analysis as defined by Sverdrup and Munk [1947]. Suppose that the significant height and period are ten feet and eight seconds. Now Sverdrup and Munk carefully state that the significant wave does not behave like a classical wave, yet in many applications it is tacitly assumed that the free surface at a point in relatively deep water can be represented by equation (3.1) of Plate IV where in this case A = 5 and T = 8.

* Irregular wave records will be discussed very much later.

Types of Periodic Functions and Non Periodic Functions and Their Representation by Discrete and Continuous Spectra

Actual wave record $\eta = \eta_a(t)$

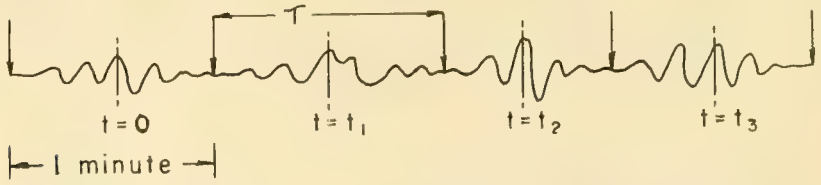

Analysis no. 1 Purely periodic with one discrete spectral component.

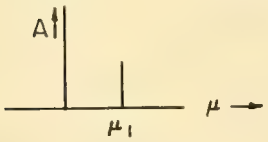

$$\eta_1(t) = A_1 \cos \frac{2\pi t}{T_1} = A_1 \cos \mu_1 t \qquad (3.1)$$

$$\eta_1(t) = \eta_1(t + T_1) \qquad (3.2)$$

Portion of graph of $\eta_1(t)$

Analysis no. 2 Purely periodic with many discrete spectral components.

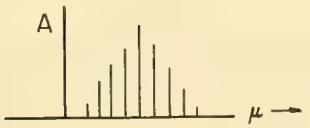

$$\eta_2(t) = \sum_{n=1}^{\infty} A_n \cos\left(\frac{2\pi n t}{T} + \delta_n\right) = \sum_{n=1}^{\infty} A_n \cos(\mu_n t + \delta_n) \qquad (3.3)$$

$$\eta_2(t) = \eta_2(t + T) \qquad (3.4)$$

$$T_n = \frac{T}{n} \quad \text{and} \quad \mu_n = \frac{2\pi n}{T} \qquad (3.5)$$

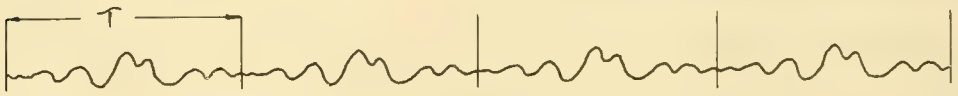

Portion of graph of $\eta_2(t)$

Analysis no. 3 Not periodic with a continuous spectral representation.

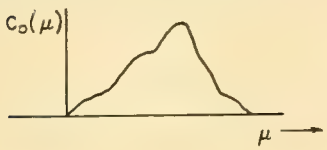

$$\eta_3(t) = f_0(t) + f_1(t - t_1) + f_2(t - t_2) + f_3(t - t_3) \qquad (3.6)$$

$$a_0(\mu) = \frac{1}{\pi}\int_{-\infty}^{+\infty} f_0(t)\cos\mu t\, dt \qquad b_0(\mu) = \frac{1}{\pi}\int_{-\infty}^{+\infty} f_0(t)\sin\mu t\, dt \qquad (3.7)$$

$$f_0(t) = \int_0^{\infty} a_0(\mu)\cos\mu t\, d\mu + \int_0^{\infty} b_0(\mu)\sin\mu t\, d\mu \qquad (3.8)$$

$$c_0(\mu) = +\sqrt{(a_0\mu)^2 + (b_0\mu)^2} \qquad (3.9)$$

Graph of $\eta_3(t)$

PLATE IV

This representation implies that the spectrum of the wave amplitude is concentrated at one value, T_1. It also implies that the wave record repeats itself every $T_1 = 8$ seconds and that the wave amplitude is constant and that therefore equation (3.2) holds.

Now try to match the graph of $\eta_1(t)$ with the actual wave record. A point for t to be equal to zero can be chosen at a sharply defined crest in the actual wave record. The two records will coincide in apparent phase near t = 0, but they will soon get out of phase. In addition, the heights of the two wave records will rarely coincide. Five sixths of the time the actual wave heights will be lower than the heights in the function which is supposed to represent the wave record.

One property which the function which is to represent the actual wave record should have is that that function should represent the potential energy of the sea surface averaged over time at the point of observation. Thus equation (3.10) should hold where $\bar{T}$ represents a time interval which is long compared to the length of a wave group but short compared to the rate at which the features of the wave record change (say, twenty minutes).

$$\frac{1}{\bar{T}}\int_{t^*}^{t^*+\bar{T}} (\eta_1(t))^2 dt \cong \frac{1}{\bar{T}}\int_{t^*}^{t^*+\bar{T}} (\eta_A(t))^2 dt \qquad (3.10)$$

Obviously this particular method of representing the sea surface is an overestimate of the potential energy of the sea surface. In addition, many different actual wave records could have the same significant height and period and completely different values for the potential energy.

It is possible to assign a value to A in equation (3.1) so that equation (3.10) will hold. The value of A would not be one half of the significant height. If this were done, equation (3.1) would still not be a good representation for the actual wave record for reasons which will become apparent later.

In summary, if the actual wave record is represented by a purely periodic function with one discrete spectral component, there are only two parameters which can be chosen. These two parameters do not adequately describe the actual wave record as a function of time.

Many discrete periods

A second way to analyze the actual wave record would be to pick out a well defined wave group (if there is one) in the record and assume that that wave group repeated itself every τ seconds exactly. Here τ is the time interval separating either the relative low wave height areas or the relative maxima from wave group to wave group. By a proper choice of the origin of the time axis, and by the assumption that the wave group is repeated periodically, it is then possible to analyze that one wave group by a Fourier series. The wave record will then be given by equation (3.3). It must repeat itself every τ seconds. The discrete spectral wave periods which determine those component waves which vary sinusoidally are determined by dividing the period of repitition by the integers.

Suppose such an analysis were carried out on the records shown by some computational method such as the one given by Conrad [1946]. The record would be multiplied by $\cos 2\pi t/\tau$. The area

under the curve would be computed with proper regard for positive and negative areas. A similar computation with sin $2\pi t/\tau$ would be carried out. Then by proper correction factors and by elementary computations, the amplitude and phase of the first harmonic could be found.

If this were done for an actual wave record, or for the one sketched, the amplitude of the first harmonic would undoubtedly come out to be negligible. In fact if τ were, say, one hundred seconds, in most records, the amplitude of the harmonic components would not become appreciable until n were equal to five or six. It would become a maximum with n about twelve (if the significant period was near eight seconds) and die out again as n became higher than 25 or 30.

Such a computation would be extremely tedious. But it would emphasize the fact that the areas of low wave height are essentially caused by the phase cancellation of a great many sinusoidal waves of low amplitude and the fact that the areas of high wave height are essentially caused by the phase reinforcement of the same sinusoidal waves of low amplitude.

The representation thus obtained would be a true representation of the one wave group studied. However, if the representation for the actual wave record were compared to the actual wave record, it would only match up for the one wave group chosen. It would not match the following or preceding wave groups because they are not exact duplicates of the chosen wave group. The other wave groups would vary in amplitude and phase, they would not occur at regularly spaced time intervals, and they might possibly have a different apparent period and/or frequency spectrum. Also

there might be long stretches of the original record which do not show any groups.

If equation (3.10) is applied to $\eta_2(t)$ instead of $\eta_1(t)$, there is a much better chance that the potential energy of the representative wave record will be approximately equal to the potential energy of the actual wave record. However, the wave group chosen and the time interval, τ, might not be representative of the entire wave record.

There are several other, not so important, ways in which the actual wave record could be analyzed which would yield a discrete spectrum. For example, it could be assumed that a ten or twenty minute length of record repeats itself periodically every ten or twenty minutes. Such an analysis would be carried out along the lines of the one described above. The harmonics would not become appreciable until n was of the order of forty-five or fifty. The analysis would be even more tedious than the one described above, and the results would not be too amenable to theoretical work. The portion of the wave record studied would be repeated exactly, but the record and its representation would not agree outside of the time interval studied.

It could also conceivably happen that a wave record was composed of discrete spectral components which were irrational. For example, $\eta(t) = \cos 2\pi t/\sqrt{2} + \sin 2\pi t/\sqrt{3}$ is not periodic. There is no time interval, τ, such that $\eta(t) = \eta(t + \tau)$. Such a representation for the free surface would be called an almost periodic function. For additional theoretical considerations, reference is made to the book by Bohr [1947] on the subject.

For additional comment on this point, see Chapter Seven.

Continuous spectrum

A third possible way to analyze the actual wave record would be to pick out the well defined wave groups and analyze them by means of the Fourier Integral Theorem. For instance, the wave group centered at t = 0 could be defined to be identically zero beyond the arrows which bracket it. The function $f_o(t)$ could be given by the wave group between the arrows and by the zero outside of the arrows. Then equation (3.7) could be applied to the function and finally, $f_o(t)$ could be represented by equation (3.8). For conditions on $f_o(t)$ and for definitions of the symbols used, see Sommerfeld [1949].

Similar analyses of $f_1(t - t_1)$, $f_2(t - t_2)$, and $f_3(t - t_3)$ in (3.6) could be carried out. Each analysis would yield a continuous spectrum of wave frequencies given by the appropriate form of equation (3.7) and the relative importance of various parts of the spectrum would be given by equations of the form of (3.9). There is no known precise procedure with which one could start with the wave record and find the appropriate $a_i(\mu)$ and $b_i(\mu)$, but such a procedure is theoretically possible. Finally, $\eta_3(t)$ can represent the wave record exactly over any length of time chosen for analysis.

If equation (3.10) were applied to the actual wave record, the two sides of the equation would be exactly equal. Thus this method of analysis represents exactly the potential energy averaged over the wave record as a function of time at a fixed point.

Such an analysis would make it possible to represent a wave

record as a function of time as observed at a fixed point. However, it tells us very little about what to expect for times outside of the interval in which the analysis was performed. There is also the difficulty that the wave groups as defined above do not seem to be really persistent phenomenon, that is, there is no mean time, τ , which separates the wave groups.

Time series analysis

A fourth method of analysis, which has not been illustrated in Plate IV, can be carried out with the aid of the more recent concepts of time series analysis. These concepts will be discussed in Chapter 7 where it will be shown that they form the most realistic method of wave analysis. In this method of analysis, equation (3.10), for example, has a most convenient interpretation.

The problem of variable direction

When η (t) has been represented as a function of time by one of the methods described above, the problem of representing the short crested appearance of the sea surface is still unsolved, and the representation of η (t) is not enough to yield the complete solution. More information is needed to solve the short crested wave problem. The exact information needed will be described from Chapter 8 onward in this paper.

Critique and plan of the next three chapters

The first three methods of analysis are all inadequate. Various simple models which have the properties of the second and third models and which have infinitely long crests will be considered mathematically in Chapters 4, 5, and 6. When these models

are compared to the realistic models which will be obtained from time series analysis, the reasons for their inadequacy will become evident. It will also be evident that the analysis based on method number one is completely inadequate.

Chapter 4. THE PROPAGATION OF A FINITE WAVE GROUP IN INFINITELY DEEP WATER

Introduction

Some interesting results can be obtained by the application of Fourier Integral Theory to the problem of a finite wave group. In this chapter, a special wave group will be studied in order to show some of the properties of dispersion in infinitely deep water. The particular form of the wave group studied in this chapter will be employed in studies of various not-too-realistic models of the sea surface. This particular form of the wave group is too specific for reality, but if it is imagined that the steps taken with reference to the specific modulation envelope employed are taken with reference to arbitrary forms for the envelope, then it is possible to see how some of the properties of ocean waves can be studied. There are a great many possible forms for the finite wave groups discussed in the previous chapter. A very special one will be picked for this chapter.

Formulation

Suppose then that the origin of the space coordinate system is located at the point $x = 0$, $y = 0$, $z = 0$ on the surface of an ocean of very great depth. At this point the height of the free surface as a function of time is measured and it is found that the equation for the observed free surface is given by equation (4.1) of Plate V.

Equation (4.1) has three parameters. The parameter, A, determines the amplitude of the disturbance which is greatest

The Propogation of a Finite Wave Group in Infinitely Deep Water.

$$\eta(o,o,t) = A\, e^{-\sigma^2 t^2} \sin\frac{2\pi t}{T} \tag{4.1}$$

$$b(\mu) = \frac{A}{\pi}\int_{-\infty}^{+\infty} e^{-\sigma^2 t^2} \sin\frac{2\pi t}{T} \sin\mu t\, dt$$

$$= \frac{A}{2\pi}\int_{-\infty}^{+\infty} e^{-\sigma^2 t^2}\left(-\cos\left(\frac{2\pi}{T}+\mu\right)t + \cos\left(\frac{2\pi}{T}-\mu\right)t\right) dt$$

$$= \frac{\sqrt{\pi}A}{2\pi\sigma}\left(-e^{\frac{-(\mu+2\pi/T)^2}{4\sigma^2}} + e^{\frac{-(\mu-2\pi/T)^2}{4\sigma^2}}\right) \tag{4.2}$$

$$\eta(o,o,t) = \frac{\sqrt{\pi}A}{2\pi\sigma}\int_o^\infty -e^{\frac{-(\mu+2\pi/T)^2}{4\sigma^2}} \sin\mu t\, d\mu$$

$$+ \frac{\sqrt{\pi}A}{2\pi\sigma}\int_o^\infty e^{\frac{-(\mu-2\pi/T)^2}{4\sigma^2}} \sin\mu t\, d\mu \tag{4.3}$$

$$\eta(x,t) = \frac{\sqrt{\pi}A}{2\pi\sigma}\int_o^\infty -e^{\frac{-(\mu+2\pi/T)^2}{4\sigma^2}} \sin\left(\frac{\mu^2 x}{g}+\mu t\right) d\mu$$

$$+ \frac{\sqrt{\pi}A}{2\pi\sigma}\int_o^\infty -e^{\frac{-(\mu-2\pi/T)^2}{4\sigma^2}} \sin\left(\frac{\mu^2 x}{g}-\mu t\right) d\mu \tag{4.4}$$

$$\int_o^\infty f(\mu)\, d\mu = -\int_o^{-\infty} f(-\mu)\, d\mu = \int_{-\infty}^{o} f(-\mu)\, d\mu \tag{4.5}$$

$$\eta(x,t) = \frac{\sqrt{\pi}A}{2\pi\sigma}\int_{-\infty}^{+\infty} -e^{\frac{-(\mu-2\pi/T)^2}{4\sigma^2}} \sin\left(\frac{\mu^2 x}{g}-\mu t\right) d\mu \tag{4.6}$$

$$p(x,z,t) = \frac{\rho g A\sqrt{\pi}}{2\pi\sigma}\int_{-\infty}^{+\infty} -e^{\frac{-(\mu-2\pi/T)^2}{4\sigma^2}+\frac{\mu^2 z}{g}} \sin\left(\frac{\mu^2 x}{g}-\mu t\right) d\mu - g\rho z \tag{4.7}$$

PLATE V

near t = 0. The parameter, σ , determines the rate at which the probability curve envelope dies out from t = 0 as t becomes large either positively or negatively. The parameter, T, determines the period of the sinusoidal term which is modulated by the probability curve. For example if σ = 1/30 sec^{-1}, A = 3 meters, and t = 10 seconds, in three cycles of the sinusoidal term the amplitude of the disturbance would die down from a peak near 3 meters to a value of about 1.1 meters. In six cycles the amplitude would be .4 meters; in nine cycles it would be .15 meters; and in twelve cycles it would be .055 meters. Thus for these values of the parameters, the disturbance would essentially pass completely in two hundred and forty seconds (four minutes). For this reason, the wave group will be referred to as a finite wave group because it lasts for only a finite length of time at the origin.

Two hours later at the point x = 0, y = 0, z = 0, the sea surface is essentially undisturbed. It would be nice to know where the disturbance is at two hours after the time t = 0, and what disturbance of the free surface it is causing wherever it is. It would also be nice to know what pressure disturbance at depths below the free surface is being caused by the passage of the wave group overhead.

Method of solution

The first step in solving the problem is to find the continuous Fourier spectrum of the function given by equation (4.1). The expression, η (0,0,t), is an odd function, that is, η (0,0,t) equals $-\eta$ (0,0,-t), and so only b(μ) must be found as given by

equation (3.7). The expression, $b(\mu)$, is given in equation (4.2) for the particular problem under study. The integral is evaluated in Bierens de Haan [1867].

It follows that equation (4.3) is just another way to write equation (4.1), and if it were integrated (4.1) would be obtained. As written, equation (4.3) is more informative than equation (4.1) because it is an integral which contains a term which varies sinusoidally as a function of time, and, from Chapter 2, a great deal is known about how such waves travel.

Neither equation (4.1) nor equation (4.3) gives sufficient information to determine the solution of the problem completely. There are many disturbances of the free surface which could have produced the observed variation in time at the point of observation. The various spectral components which combine at the point $x = 0$ and $y = 0$ to produce the disturbance might have come from many different directions. It will be assumed that most of the disturbance came from the negative x direction and is traveling in the positive x direction. Thus variation in y does not occur and η will be a function of x and t alone. This assumption is definitely an approximation to what occurs in nature because it implies that the crests of the disturbance are infinitely long in the y direction.

The first term in equation (4.3) contributed only a very small amount to the total integral because, with μ positive, the magnitude of the exponential term is small to start with and becomes smaller as μ increases. Let these spectral components travel in the negative x direction.

The second term in equation (4.3) contributes a major part

to the integral because, for $\mu = 2\pi/T$, the exponential term is unity. Let these spectral components travel in the positive x direction. Under these conditions, the variation of η with x can be expressed, and equation (4.4) follows from equation (4.3).

Equation (4.4) reduces to equation (4.3) if x is set equal to zero. In addition, a correct spectral wave length has been assigned to each spectral frequency, μ . Equation (2.25) applies where δ is equal to $-\pi/2$ and θ is zero.

In the first term of equation (4.4), the limits of integration can be changed from zero through infinity to minus infinity through zero by the relations given in equation (4.5), and finally η (x,t) can be expressed by equation (4.6). Again equation (4.6) reduces to equation (4.3) if x is set equal to zero.

If equation (4.6) were integrated at this stage of the derivation, an expression for the free surface as a function of x and t would be obtained. It is better to delay the integration and consider the possibility of obtaining some information about the pressure at the depth z below the free surface.

The pressure can be found immediately from consideration of equations (2.9), (2.6), (2.7), (2.25), (2.24), and (2.26). From equation (2.9), the value of Φ is known for z = 0. From equation (2.6), Φ and Φ_t as a function of z follow, and substitution of Φ_t as a function of x, z, and t into equation (2.7) gives the pressure. Equations (2.9), (2.6), and (2.7) are perfectly general.* In particular, if equation (2.25) is the free surface, then equation (2.24) must be the potential function, and equation (2.26) must represent the pressure. Integration over the parameter, μ , does not affect these relationships and the pressure as a function

* Within the linear approximation.

of time, distance, and depth is given by equation (4.7).

The pressure given by equation (4.7) is evidently a rather complicated function. It is complicated because infinitely deep water is a dispersive medium. The various spectral components of the pressure are attenuated at different rates with depth and the various spectral wave components travel at different speeds along the surface. It is therefore to be expected that the shape of the wave profile as a function of time at different values of x will not be the same as the shape of the wave profile at x equal to zero and that the apparent period of the pressure variation at a depth z below the surface will not be the same as the apparent period of the disturbance at the surface.

Solution

The next step is to integrate equation (4.7). The value of the integral is given in Table 269 on page 375 of the table of definite integrals compiled by Bierens de Haan [1867]. After some algebraic manipulations the result can be put into the form of equation (4.8) of Plate VI.

The free surface can be found from equation (4.8), with the use of equation (2.9), by substituting $p = 0$ on the left, $z = 0$ into the first term on the right, and $z = \eta$ into the second term on the right. Equation (4.9) then gives the free surface.

The pressure as a function of time and depth at the point $x = 0$, is also of interest because the expression is simpler. By substituting $x = 0$ into equation (4.8) and clearing fractions, the pressure can be found below the original point of observation. The pressure is given by equation (4.10).

The derivation given in Plate V and the results obtained

Finite Wave Group (Solution)

$$p(x,z,t) = \frac{-Ag\rho e^{-\left\{\frac{\frac{16\pi^2\sigma^2}{g^2T^2}\left[Z^2 - \frac{gZ}{4\sigma^2} - \frac{\sigma^2 gT^2 Zt}{4} + \left(x - \frac{gTt}{4\pi}\right)^2\right]}{\left(1 - \frac{8\sigma^2 Z}{g} + \frac{16\sigma^4(Z^2+x^2)}{g^2}\right)}\right\}}}{\left(1 - \frac{8\sigma^2 Z}{g} + \frac{16\sigma^4(Z^2+x^2)}{g^2}\right)^{1/4}} \cdot \sin\left[\frac{\frac{4\pi^2 x}{gT^2} - \frac{2\pi t}{T} - \frac{4\sigma^4 t^2 x}{g} + \frac{8Z\pi\sigma^2 t}{gT}}{1 - \frac{8\sigma^2 Z}{g} + \frac{16\sigma^4(Z^2+x^2)}{g^2}} + \frac{1}{2}\tan^{-1}\frac{4\sigma^2 x}{g\left(1 - \frac{4\sigma^2 Z}{g}\right)}\right]$$

$$- g\rho Z \qquad (4.8)$$

$$\eta(x,t) = \frac{-Ae^{-\left\{\frac{\frac{16\pi^2\sigma^2}{g^2T^2}\left(x - \frac{gTt}{4\pi}\right)^2}{\left(1 + \frac{16\sigma^4 x^2}{g^2}\right)}\right\}}}{\left(1 + \frac{16\sigma^4 x^2}{g^2}\right)^{1/4}} \cdot \sin\left[\frac{\frac{4\pi^2 x}{gT^2} - \frac{2\pi t}{T} - \frac{4\sigma^4 t^2 x}{g}}{1 + \frac{16\sigma^4 x^2}{g^2}} + \frac{1}{2}\tan^{-1}\frac{4\sigma^2 x}{g}\right] \qquad (4.9)$$

$$p(o,z,t) = \frac{-Ag\rho e^{-\left\{\frac{\frac{4\pi^2 Z}{gT^2} - \sigma^2 t^2}{1 - \frac{4\sigma^2 Z}{g}}\right\}^2}}{\left(1 - \frac{4\sigma^2 Z}{g}\right)^{1/2}} \cdot \sin\left[\frac{-2\pi t}{T\left(1 - \frac{4\sigma^2 Z}{g}\right)}\right] - g\rho Z \qquad (4.10)$$

PLATE VI

in Plate VI could just as easily have been carried out if the sin $2\pi t/T$ in equation (4.1) had been replaced by the cos $2\pi t/T$. All that is needed is a few changes in sign in appropriate parts of the derivation. An arbitrary phase lag, δ, can be inserted into the sinusoidal term of equations (4.8), (4.9) and (4.10) and the equations will still be valid.

Evaluation

Now that the solutions have been obtained, some graphs and tables will be presented in order to show how the functions vary, why they vary the way they do, and what physically significant conclusions can be drawn from the data assembled. When the parameters of the solution are varied, the behavior of the solution varies markedly.

The behavior of the solution depends most strongly on the parameter, σ , which, in equation (4.1) determines the rate at which the envelope of the sinusoidal term goes to zero. For large values of σ the duration in time of the original disturbance is short. For small values of σ the duration of the original disturbance is long.

Spectrum

Thus σ is an interesting parameter to trace through the remaining equations. Consider, for example, the effect of σ in equation (4.6) in which it determines the nature of the continuous spectrum. The amplitude of the continuous spectrum is given by $c(\mu)$ as shown in figure 1 where the minus sign is omitted by virtue of equation (3.9).

The graph of the spectrum is a probability curve with a

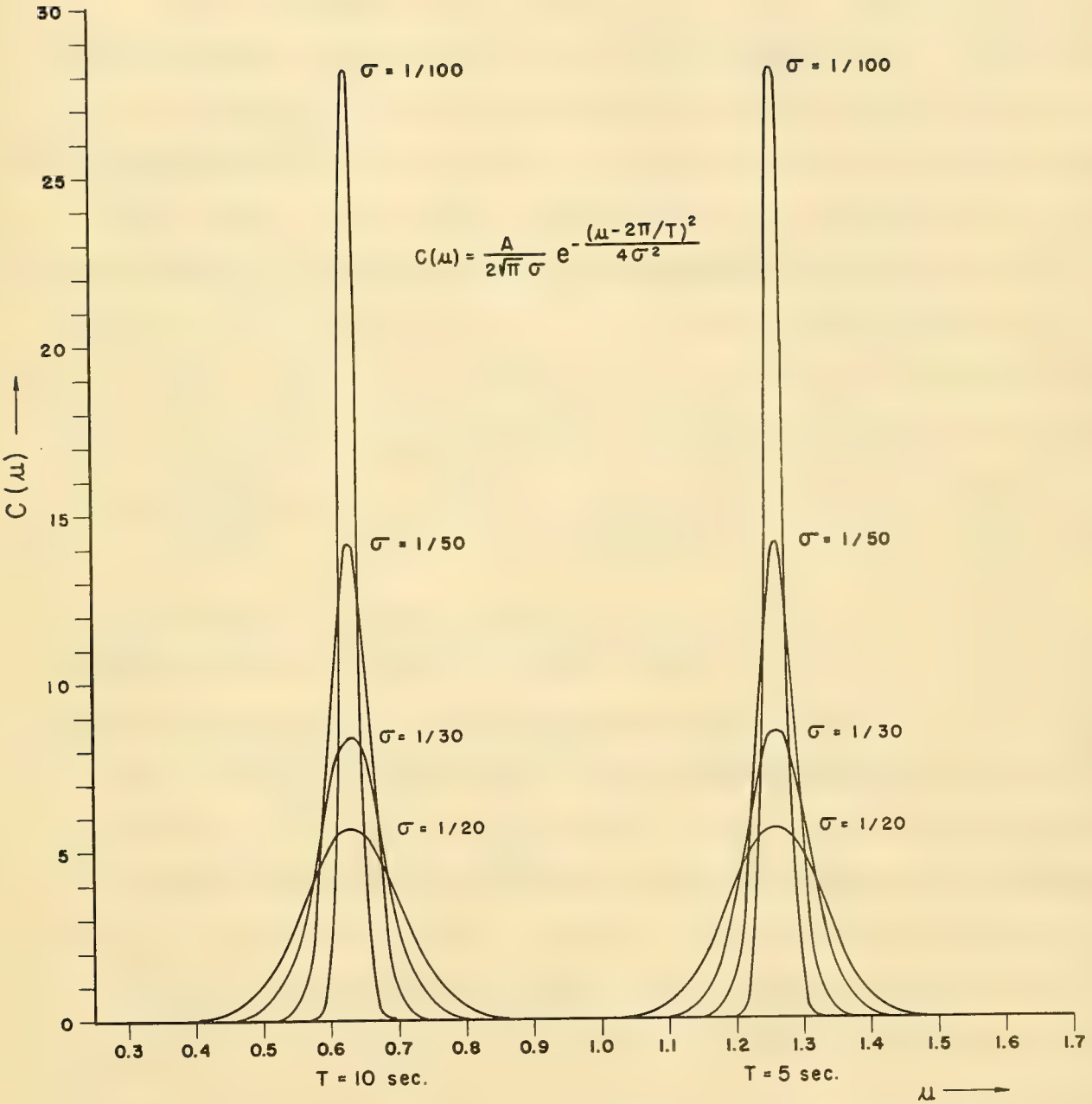

Fig 1. GRAPHS OF THE CONTINUOUS SPECTRA OF FINITE WAVE GROUPS FOR VARIOUS VALUES OF σ AND T.

maximum amplitude given by $A/2\sqrt{\pi}\sigma$ when $\mu = 2\pi/T$. The larger the value of σ the more slowly the probability curve dies down to zero as μ varies and the lower the peak amplitude. As σ approaches zero, $c(\mu)$ approaches an infinitely high spike at the point $\mu = 2\pi/T$. Note that as σ approaches zero, equation (4.1) approaches η (t) = A sin $2\pi t/T$, that equation (4.8) approaches the correct expression for the pressure which would be caused by a purely sinusoidal wave, and that equation (4.9) approaches η (x,t) = A sin$(2\pi x/L - 2\pi t/T)$ where L is the appropriate wave length for a wave with a period, T, in deep water.

The continuous spectrum of the disturbances is graphed in figure 1 for A equal to unity, σ = 1/20, 1/30, 1/50, and 1/100 sec^{-1} and T = 5 and 10 sec. The shorter the duration of the wave group, the wider the spread of the wave spectrum, and it should be expected that the more rapidly the shape of the disturbance will change as it travels onward.

In the formulation of the problem, part of the spectrum of the wave group at x = 0 was made to travel in the negative x direction. As a result an integral form of the solution was obtained which could be evaluated in closed form. If this had not been done at that time, the solution could only have been obtained in series form and it would have been more difficult to interpret and evaluate. Figure 1 shows that the contribution to the total spectrum of these components is indeed so small that it does not show on the graphs for the values of the parameters employed. It can be concluded that the effect of this tail of the probability curve which exists for negative values of μ will not affect the properties of the solution very much.

Properties of the Solution

definition $$D = 1 + \frac{16\sigma^4 x^2}{g^2} \tag{4.11}$$

$$E(\eta) = \frac{A}{D^{\frac{1}{4}}} e^{-\frac{16\pi^2\sigma^2}{Dg^2t^2}\left(X - \frac{gTt}{4\pi}\right)^2} \tag{4.12}$$

$$t = \frac{4\pi x_1}{gT} + t' = t_g + t' \tag{4.13}$$

$$E(\eta) = \frac{A}{D^{\frac{1}{4}}} e^{-\frac{\sigma^2(t')^2}{D}} \tag{4.14}$$

$$S(\eta) = -\sin\left[\frac{4\pi^2 x}{DgT^2} - \frac{2\pi t}{DT} - \frac{4\sigma^4 t^2 x}{Dg} + \frac{1}{2}\tan^{-1}\frac{4\sigma^2 x}{g}\right] \tag{4.15}$$

$$-\frac{2\pi t}{DT} - \frac{4\sigma^4 t^2 x_1}{Dg} = \text{const} \tag{4.16}$$

$$-\frac{2\pi(t+T_1^*)}{DT} - \frac{4\sigma(t+T_1^*)^2 x_1}{gD} = \text{const} - 2\pi \tag{4.17}$$

$$\frac{4\sigma^4 x_1 (T_1^*)^2}{g} + \left(\frac{2\pi}{T} + \frac{8\sigma^4 t x_1}{g}\right)T^* - 2\pi D = 0 \tag{4.18}$$

$$\frac{1}{(T^*)^2} - \frac{1}{T}\left(1 + \frac{4\sigma^4 t' x_1 T}{g\pi D}\right)\frac{1}{T_1^x} - \frac{4\sigma^4 x_1}{2\pi g D} = 0 \tag{4.19}$$

$$T_1^* = 2T\left(\frac{1}{\sqrt{\left(1+\frac{4\sigma^4 t' x_1 T}{g\pi D}\right)^2 + \frac{8\sigma^4 x_1 T^2}{g\pi D}} + \left(1 + \frac{4\sigma^4 t' x_1 T}{g\pi D}\right)}\right) \tag{4.20}$$

$$-\frac{2\pi(t-T_2^*)}{DT} - \frac{4\sigma^4(t-T_2^*)^2 x_1}{gD} = \text{const} + 2\pi \tag{4.21}$$

$$T_2^* = 2T\left(\frac{1}{\sqrt{\left(1+\frac{4\sigma^4 t' x_1 T}{g\pi D}\right)^2 - \frac{8\sigma^4 x_1 T^2}{g\pi D}} + \left(1 + \frac{4\sigma^4 t' x_1 T}{g\pi D}\right)}\right) \tag{4.22}$$

$$T^* = \frac{T}{1 + \frac{4\sigma^4 t' x_1 T}{g\pi D}} \tag{4.23}$$

Plate VII

The assumption made in the formulation essentially poses the form of $\eta_x(0,t)$ which can be arbitrarily given in such a problem. The possibility of very low waves traveling in the opposite direction out of the group is indeed a very small price to pay for a closed complete easily evaluated solution.

Envelope

The free surface given by equation (4.9) is a product of a slowly varying term which determines the envelope of the disturbance times a term which is the sine of a complicated function of x and t and which varies rapidly as a function of x and t in order to give the individual waves in the wave group. Consider, first, the envelope of the free surface given by $E(\eta)$ in equation (4.12) where D is defined in equation (4.11). The minus sign can be considered to be part of the phase of the sinusoidal term. At x = 0, the envelope becomes $Ae^{-\sigma^2 t^2}$.

Substitute some constant value for x into the equation for the envelope, say $x = x_1$ and keep that value. As the time varies, what happens to the amplitude of the disturbance? The disturbance is greatest when $t = 4\pi x_1/gT$ which shows that the envelope moves in the positive x direction with the group velocity of waves of the period T. The maximum value of the envelope is given by $A/(D)^{1/4}$ and so the greatest value of the amplitude of the disturbance decreases as the wave group travels in the positive x direction.

Let $t = 4\pi x_1/gT + t' = t_g + t'$ (Equation (4.13)), so that attention can be concentrated on the times near the time when the wave group passes the point x_1. The exponent of e in the

equation for the envelope takes the form $-(\sigma^2/D)(t')^2$ (equation (4.14)). This shows that it takes longer for the envelope to decrease to 1/e of its maximum value at $x = x_1$ than it does at $x = 0$.

The behavior of the envelope as a function of time at a fixed point is shown by Tables 1 through 4 for the same values of σ and T which were employed in graphing figure 1 and for $\sigma = 1/20$, T = 20 sec. Table 1 shows the appropriate values for σ equal to 1/100 sec^{-1} and T equal to either 5 seconds or 10 seconds. At x equal to zero and t equal to zero the amplitude of the envelope is one. Thirty-two and four tenths seconds before or after t equal to zero the amplitude of the envelope at x equal to zero is nine tenths. On hundred fifty-two seconds before or after t equal to zero the amplitude of the envelope is one tenth. The highest part of the wave group passes the point x equal to zero in three hundred and four seconds (5.07 min). Of course, the wave group never completely passes a given point. For example, it takes five hundred twenty-two seconds (or 8.7 minutes) for the .01 values of the envelope to pass.

When the maximum amplitude of the wave group reaches the point x equal to 17.7 km, the maximum possible value of the envelope is 0.90. The maximum amplitude of the wave group passes that point x = 1.77 km at the time indicated by t_g, which in this case is given by 4,560 seconds (or 1.27 hours) if the period of the waves under the envelope is 5 seconds and by 2280 seconds (or .635 hours) if the period of the waves under the envelope is 10 seconds. This shows that the envelope of the 10 second waves travels twice as fast as the envelope of the five second waves.

Table 1

Values of the envelope of the free surface at fixed points as a function of time for σ = 1/100 sec^{-1} and T = 5 and T = 10 sec.

	T = 5	T = 10	Envelope Value										
x_1 km	t_g	hrs.	1.0	0.9	0.8	0.7	0.6	0.5	0.4	0.3	0.2	0.1	.01
0	0	0	0	32.4	47.2	60.0	71.6	83.2	95.8	110	129	152	215
17.7	1.27	.633		0	42.4	62.0	78.6	94.6	111.2	129	152	183	262
29.6	1.87	.933			0	62.4	83.8	107	130	155	184	225	327
43.6	3.11	1.56				0	80	120	154	188	228	284	420
78.0	4.83	2.42					0	119	177	231	291	372	562
99.8	6.75	3.51						0	190	286	383	508	791
124.0	11.0	5.49							0	335	520	715	1200
272	19.4	9.72								0	707	1165	2049
612	43.6	21.8									0	2152	4031
2452	174.4	87.2										0	15150

$t = t_g + t'$ t' tabulated above.

x_1 is the point of observation in kilometers

t_g is the time at which the maximum value of the envelope passes the point x_1. Column one gives the value of t_g for T = 5 seconds. Column two gives the value of t_g for T = 10 seconds. t_g given in hours.

t' is the time before and after t_g in seconds at which the envelope has the indicated value.

Table 2

Values of the envelope of the free surface at fixed points as a function of time for $\sigma = 1/50$ sec^{-1} and T = 5 and T = 10 sec.

	T = 5	T = 10	Envelope value										
x_1 km	t_g	hrs.	1.0	0.9	0.8	0.7	0.6	0.5	0.4	0.3	0.2	0.1	.01
0	0	0	0	16.2	23.6	29.9	35.8	41.6	47.9	54.9	64.9	75.9	108
4.43	.317	.154		0	21.2	31.0	39.3	47.3	55.6	64.7	75.7	91.5	131
7.35	.522	.266			0	31.2	41.9	53.6	65.0	77.4	92.0	112	164
10.90	.778	.389				0	40.0	59.1	76.5	94.0	114	142	210
17.0	1.21	.61					0	59.2	88.4	116	145	186	281
23.7	1.69	.85						0	95	143	191	254	395
38.6	2.75	1.38							0	167	260	358	600
68.0	4.86	2.43								0	354	583	1025
153	10.9	5.5									0	1076	2016
613	43.6	21.8										0	7575

$t = t_g + t'$ t' tabulated above

x_1 is the point of observation in kilometers.

t_g is the time at which the maximum value of the envelope passes the point x_1. Column one gives the value of t_g for T = 5 sec. Column two gives the value of t_g for T = 10 sec. t_g given in hours.

t' is the time before and after t_g in seconds at which the envelope has the indicated value.

Table 3

Values of the envelope of the free surface at fixed points as a function of time for $\sigma = 1/30$ sec^{-1} and T = 5 and T = 10 sec.

	T = 5	T = 10	Envelope Value										
x_1 km	t_g	hrs.	1.0	0.9	0.8	0.7	0.6	0.5	0.4	0.3	0.2	0.1	.01
0	0	0	0	9.7	14.2	17.9	21.5	25.0	28.7	33.0	38.0	45.6	64.5
1.6	.114	.057		0	12.8	18.5	23.7	28.7	33.3	38.9	45.2	54.8	78.6
2.65	.189	.094			0	19.0	25.2	32.2	39.0	46.5	55.2	68.5	98.1
3.12	.281	.140				0	24.0	35.6	45.8	56.3	68.5	85.4	126
6.13	.436	.218					0	36.0	53.0	69.4	87.3	112	169
8.54	.608	.304						0	57.9	85.9	115	152	237
13.9	.988	.494							0	107	156	221	360
24.5	1.74	.870								0	221	349	615
55.1	3.92	1.96									0	645	1210
221	15.7	7.85										0	4550

$t = t_g + t'$ t' tabulated above.

x_1 is the point of observation in kilometers.

t_g is the time at which the maximum value of the envelope passes the point x_1. Column one gives the value of t_g for T = 5 sec. Column two gives the value of t_g for T = 10 sec. t_g given in hours.

t' is the time before and after t_g in seconds at which the envelope has the indicated value.

Table 4

Values of the envelope of the free surface at fixed points as a function of time for $\sigma = 1/20$ sec^{-1} and T = 5, T = 10, and T = 20 sec.

	T = 5	T = 10	T = 20											
x_1 km	t_g	hrs.		1.0	0.9	0.8	0.7	0.6	0.5	0.4	0.3	0.2	0.1	.01
0	0	0	0	0	6.5	9.4	11.9	14.3	16.6	19.1	21.9	25.4	30.3	42.9
.71	.051	.025	.012		0	8.5	12.4	15.7	18.9	22.2	25.9	30.4	36.6	52.4
1.18	.075	.037	.019			0	12.6	16.8	21.4	26.0	30.9	36.8	45.1	65.9
1.74	.124	.062	.031				0	16.0	23.6	30.5	37.6	45.7	56.9	84.1
3.12	.193	.097	.049					0	23.7	35.3	46.2	58.2	74.4	112.4
4.79	.27	.135	.068						0	37.8	57.2	76.6	101.5	158
4.96	.44	.22	.11							0	67.1	104	147	240
10.9	.775	.388	.194								0	141	221	410
24.5	1.74	.87	.435									0	417	806
98.1	6.98	3.49	1.75										0	3030

$t = t_g + t'$ t' tabulated above.

x_1 is the point of observation in kilometers.

t_g is the time at which the maximum value of the envelope passes the point x_1. Column one gives the value of t_g for T = 5 sec, column two the value of t_g for T = 10 sec, and column three for T = 20 sec. t_g given in hours.

t' is the time before and after t_g in seconds at which the envelope has the indicated value.

Put another way, for the same value of σ , the amplitude of the envelope decreases twice as fast for 10-second waves as it does for 5-second waves. Forty-two and four tenths seconds before and after the time, t_g, the amplitude of the envelope is 0.80. One hundred eighty-three seconds before and after t_g the ampitude is 0.10.

The above examples show that this method of computation breaks down the dependence on time of the amplitude of the envelope into two different parts. The time is given by $t = t_g + t'$. The part, t_g, evaluates the gross effect of the speed of travel and it is of the order of magnitude of hours in the computations. t_g depends only on the value of x_1 considered and the period of the waves under the envelope. The part t', evaluates the time it actually takes the wave group to pass a given point, and it is measured in seconds. t' depends only on the value of x_1 considered and the value of σ . Computation of the actual time t would require prohibitive accuracy in order to compute the time of passage of the wave group at large values of x_1 because t' is essentially the difference between two large numbers.

Now compare Table 4 with Table 1. In Table 4, σ equals 1/20 sec^{-1}. The maximum amplitude of the envelope dies down much more rapidly. In fact, x_1, need be only four hundredths of the distance given in Table 1 for the amplitude to decrease a corresponding amount. In Table 1, the envelope could travel 17.7 km before the amplitude would decrease to nine tenths of its original value. In Table 4, the envelope would travel only .71 km and then its amplitude would decrease to nine tenths of its

original value. Thus the larger the value of σ , the wider the spectrum of the disturbance, and the more rapidly the disturbance dies down in amplitude as it travels along.

The time required for the wave group to pass the point of interest is simply two tenths of the time required for the wave group to pass the corresponding point of interest in Table 1. Thus, the modification of the wave group with a large value of σ occurs much more rapidly than it does for a small value of σ .

In summary, the envelope travels in the positive x direction with a speed determined by the group velocity of waves with a period T. The larger the value of T, the more rapidly the group travels in the x direction. Its maximum amplitude decreases as it travels along, and it spreads out over the sea surface more and more the further it gets away from the origin. The larger the value of T and the larger the value of σ , the more rapidly the group disperses in time.

Apparent local period

The rapidly varying sinusoidal term which determines the nature of the waves as modulated by the envelope can now be considered. The sinusoidal term is given by $S(\eta)$ in equation (4.15). The term varies between plus one and minus one as x and t are varied and it is defined everywhere in the x,t plane. It is not periodic in t since there exists no constant τ such that $S(\eta)[t] = S(\eta)[t + \tau]$. In addition, the sinusoidal term is not periodic in x. In fact, the entire solution is not periodic.

Consider the term in the brackets in equation (4.15) for a fixed positive value of x_1. As a function of t, it is a parabola

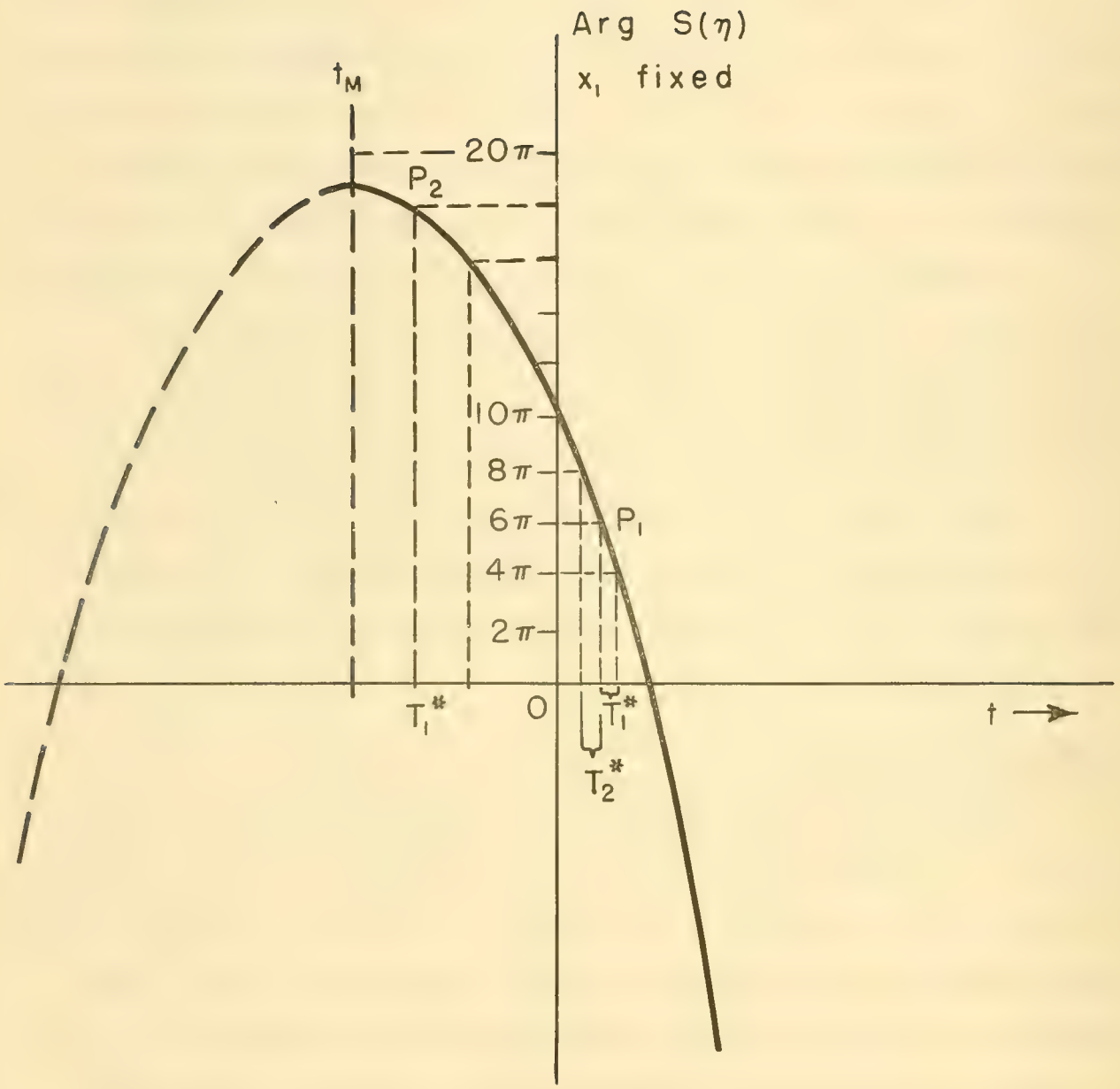

Fig 2

Form of the Graph of the Argument of $S(\eta)$.
T_1^* and T_2^* are defined at P_2.
The figure is not to scale.

which achieves some maximum value when t is negative at the point $t = t_M$ as graphed in figure 2. For $t > t_M$, an increase in t results in a decrease of the argument of the sine curve. The minus sign at the front of the expression can be put inside by adding π to the term in brackets.

Since the original problem was, in a sense, an initial value problem, the main point of interest will be in the behavior of $S(\eta)$ for $t > 0 > t_M$. For this reason, consider the point P_1. The terms which are constant for constant x_1 can be ignored and equation (4.16) can be written. Then if t is increased by the amount, T_1^*, the new constant value will be equal to the old constant value minus 2π, and $S(\eta)$ will have the same value as before. Equation (4.18) can then be obtained by subtracting equation (4.17) from equation (4.16). Equation (4.18) transforms easily into equation (4.19) with the use of equation (4.13). Finally equation (4.20) can be obtained if equation (4.19) is solved for $1/T_1^*$, and the reciprocal of the solution is taken.

By an exactly similar procedure, T_2^* can be found from equation (4.16) and equation (4.21). T_2^* is given by equation (4.22).

The only difference between equation (4.22) and (4.20) is that the second term under the radical is negative in equation (4.22). Thus for certain values of t' near $t' = -t_g + t_M$, the value of the term under the radical is negative and T_2^* is imaginary. Such a value of t' (or t) is shown at the point P_2 in figure 2. An increase in the value of t by T_1^* results in a decrease in the value of the argument by 2π, but there is no

possible way to decrease the value of t by T_2^* and cause an increase in the value of the argument by 2π. This is the reason why T_2^* is imaginary for certain values of t'.

The derivation given above applies only to values of $t > t_M$ (or $t' > - t_g + t_M$) and $x_1 > 0$. For the other three possible combinations of inequalities, similar derivations can be carried out. One of the two quantities T_1^* or T_2^*, will always exist for the entire range of applicability. The other will be imaginary only over a very short range.

Although $S(\eta)$ is not periodic, it now becomes convenient to define a term which is somewhat analogous to the period of a periodic function. This term will be denoted by T^* and it will be defined to be the average value of T_1^* and T_2^*. T^* will be called the apparent local period of $S(\eta)$.

It has been shown that the maximum value of the envelope occurs for $t' = 0$, and therefore T^* is most important near $t' = 0$. For the values of σ, x_1 and T employed in Tables 1 through 4, $8\sigma^4 x_1 T^2/g\pi D$ is always less than 10^{-2}, and it can be shown from the expansion of the radicals in the expressions for T_1^* and T_2^* that T^* depends essentially only on the square of this term as a slight correction factor. Therefore T^* can be given by equation (4.23) to four significant figures in the neighborhood of $t' = 0$.

The apparent local periods which correspond to the times and distances given in Tables 1 through 4 are given in Tables 5 through 13. The apparent local periods are given to three significant places. Table 5 can be interpreted as follows with

the use of Table 1. In Table 1, after the envelope has traveled 29.6 kilometers in 1.87 hours, the envelope is 0.5 units high, 107 seconds before its maximum value of 0.8 and 107 seconds after its maximum value. Then in Table 5 at the time $t = t_g - 107$ seconds, the apparent local period is 5.04 seconds and at the time $t = t_g + 107$ seconds, the apparent local period is 4.96 seconds. Thus the first waves to arrive at the point of observation have the longest apparent local period.

Tables 5 through 13 combined with equation (4.20) show that the larger the values of σ and T, the more rapidly the value of T* departs from T as the wave group travels away from $x = 0$. In Table 8, for example, after the group has traveled only 10.9 kilometers, the apparent local period for the waves which arrive first is 5.42 seconds and for those which arrive last, 4.64 seconds. In Table 5, after the group has traveled 612 kilometers, the apparent local period is 5.08 for the waves which arrive first and 4.92 seconds for those which arrive last. The dispersive effects of the various spectra graphed in figure 1 are evident.

The overall variation of equation (4.9) at a fixed point as a function of time can now be described. A wave height recorder at some distance x_1 from the origin would not detect any significant variations in height until a time corresponding to t_g had elapsed. At a time in seconds before and after t_g corresponding to t' waves of the amplitude given in the tables with an apparent local period given in the tables would be recorded. For times much greater than t_g, the sea surface would be essentially

Table 5

Apparent local period of the free surface at fixed points given by Table 1 for $\sigma = 1/100$ and T = 5 seconds.

T = 5		Envelope Value										
xkm	t_g hrs	1.0	0.9	0.8	0.7	0.6	0.5	0.4	0.3	0.2	0.1	.01
0	0	5.00	5.00	5.00	5.00	5.00	5.00	5.00	5.00	5.00	5.00	5.00
17.7	1.27		5.00	5.02 4.98	5.02 4.98	5.03 4.97	5.04 4.96	5.04 4.96	5.05 4.95	5.06 4.94	5.07 4.93	5.10 4.90
29.6	1.87			5.00	5.02 4.98	5.03 4.97	5.04 4.96	5.05 4.95	5.06 4.94	5.07 4.93	5.09 4.91	5.13 4.87
43.6	3.11				5.00	5.03 4.97	5.04 4.96	5.05 4.95	5.06 4.94	5.08 4.92	5.10 4.90	5.15 4.86
78.0	4.83					5.00	5.04 4.96	5.06 4.94	5.08 4.93	5.10 4.91	5.13 4.88	5.19 4.82
99.8	6.75						5.00	5.04 4.97	5.06 4.94	5.08 4.92	5.11 4.90	5.17 4.89
124.0	11.0							5.00	5.04 4.96	5.06 4.95	5.08 4.92	5.13 4.88
272	19.4								5.00	5.05 4.95	5.08 4.92	5.15 4.86
612	43.6									5.00	5.08 4.92	5.16 4.88
2452	174.4										5.00	5.12 4.88

For the appropriate values of t', and the definition of the symbols employed see Table 1. T* tabulated above. The largest value of T* applies when t' is negative.

Table 6

Apparent local period of the free surface at fixed points given by Table 2 for $\sigma = 1/50$ and T = 5 seconds.

T = 5		Envelope Value										
xkm	t_g hrs	1.0	0.9	0.8	0.7	0.6	0.5	0.4	0.3	0.2	0.1	.01
0	0	5.00	5.00	5.00	5.00	5.00	5.00	5.00	5.00	5.00	5.00	5.00
4.43	.217		5.00	5.03 4.97	5.05 4.95	5.06 4.94	5.07 4.93	5.08 4.92	5.10 4.90	5.12 4.89	5.12 4.87	5.21 4.81
7.35	.522			5.00	5.05 4.95	5.07 4.93	5.08 4.92	5.10 4.90	5.12 4.88	5.15 4.86	5.18 4.83	5.32 4.76
10.90	.778				5.00	5.06 4.95	5.08 4.92	5.11 4.90	5.13 4.88	5.16 4.85	5.20 4.82	5.30 4.73
17.0	1.21					5.00	5.07 4.93	5.10 4.90	5.14 4.87	5.17 4.84	5.22 4.79	5.34 4.70
23.7	1.69						5.00	5.08 4.93	5.11 4.89	5.15 4.86	5.21 4.81	5.33 4.71
38.6	2.75							5.00	5.09 4.91	5.14 4.87	5.20 4.82	5.33 4.71
68.0	4.86								5.00	5.10 4.90	5.17 4.84	5.31 4.73
153	10.9									5.00	5.13 4.88	5.25 4.77
613	43.6										5.00	5.25 4.77

For the appropriate values of t' and the definition of the symbols employed see Table 2. T* tabulated above.

Table 7

Apparent local period of the free surface at fixed points given by Table 3 for $\sigma = 1/30$ and T = 5 seconds.

T = 5		Envelope Value										
xkm	t_g hrs	1.0	0.9	0.8	0.7	0.6	0.5	0.4	0.3	0.2	0.1	.01
0	0	5.00	5.00	5.00	5.00	5.00	5.00	5.00	5.00	5.00	5.00	5.00
1.6	.114		5.00	5.05 4.95	5.08 4.92	5.10 4.90	5.12 4.84	5.14 4,86	5.17 4.84	5.20 4.82	5.26 4.78	5.35 4.69
2.65	.189			5.00	5.10 4.92	5.11 4.89	5.14 4.86	5.17 4.84	5.21 4.81	5.25 4.77	5.31 4.72	5.47 4.61
3.12	.281				5.00	5.09 4.91	5.14 4.87	5.18 4.83	5.22 4.80	5.27 4.76	5.34 4.70	5.53 4.57
6.13	.436					5.00	5.11 4.89	5.17 4.84	5.23 4.79	5.29 4.74	5.43 4.67	5.60 4.52
8.54	.608						5.00	5.13 4.88	5.19 4.82	5.26 4.76	5.35 4.69	5.57 4.54
13.9	.988							5.00	5.16 5.85	5.24 4.78	5.34 4.70	5.58 4.53
24.5	1.74								5.00	5.18 4.83	5.29 4.74	5.54 4.56
55.1	3.92									5.00	5.22 4.79	5.44 4.63
221	15.7										5.00	5.44 4.73

For the appropriate values of t', and the definition of the symbols employed see Table 3. T* tabulated above.

Table 8

Apparent local period of the free surface at fixed points given by Table 4 for $\sigma = 1/20$ and T = 5 seconds.

T = 5		Envelope Value										
xkm	t_g hrs	1.0	0.9	0.8	0.7	0.6	0.5	0.4	0.3	0.2	0.1	.01
0	0	5.00	5.00	5.00	5.00	5.00	5.00	5.00	5.00	5.00	5.00	5.00
.71	.051		5.00	5.08 4.92	5.12 4.87	5.11 4.86	5.18 4.83	5.22 4.89	5.26 4.77	5.30 4.73	5.37 4.68	5.55 4.55
1.18	.075			5.00	5.13 4.88	5.17 4.84	5.22 4.80	5.27 4.76	5.33 4.71	5.39 4.66	5.49 4.59	5.74 4.43
1.74	.124				5.00	5.14 4.87	5.21 4.80	5.28 4.75	5.34 4.70	5.42 4.64	5.54 4.56	5.84 4.38
3.12	.193					5.00	5.22 4.80	5.33 4.71	5.45 4.62	5.51 4.53	5.76 4.42	6.24 4.17
3.99	.27						5.00	5.20 4.81	5.31 4.73	5.42 4.64	5.58 4.53	5.96 4.31
4.96	.44							5.00	5.18 4.83	5.29 4.74	5.42 4.64	5.72 4.44
10.9	.775								5.00	5.26 4.76	5.44 4.63	5.85 4.37
24.5	1.74									5.00	5.34 4.70	5.63 4.46
98.1	6.98										5.00	5.63 4.46

For the appropriate value of t' and the definition of the symbols employed see Table 4. T* tabulated above.

Table 9

Apparent local period of the free surface at fixed points given by Table 1 for σ = 1/100 and T = 10 seconds.

T = 10		Envelope Value										
xkm	t_g hrs	1.0	0.9	0.8	0.7	0.6	0.5	0.4	0.3	0.2	0.1	.01
0	0	10	10	10	10	10	10	10	10	10	10	10
17.7	.633		10	10.06 9.94	10.10 9.90	10.12 9.88	10.14 9.86	10.17 9.84	10.20 9.81	10.24 9.78	10.28 9.73	10.41 9.62
29.6	.933			10	10.09 9.91	10.13 9.87	10.17 9.84	10.21 9.80	10.25 9.76	10.30 9.72	10.37 9.66	10.53 9.51
43.6	1.56				10	10.11 9.89	10.17 9.84	10.23 9.79	10.26 9.75	10.33 9.70	10.40 9.63	10.57 9.46
78.0	2.42					10	10.16 9.85	10.24 9.73	10.33 9.67	10.40 9.63	10.51 9.54	10.75 9.31
97.8	3.51						10	10.16 9.87	10.29 9.77	10.32 9.70	10.43 9.60	10.69 9.39
124	5.49							10	10.14 9.86	10.22 9.79	10.32 9.70	10.53 9.32
272	9.72								10	10.20 9.80	10.33 9.68	10.61 9.45
6.12	21.8									10	10.33 9.69	10.64 9.43
2452	87.2										10	10.51 9.54

For the appropriate values of t' and the definition of the symbols employed see Table 1. T* tabulated above.

Table 10

Apparent local period of the free surface at fixed points given by Table 2 for $\sigma = 1/50$ seconds.

T = 10		Envelope Value										
x km	t_g hrs	1.0	0.9	0.8	0.7	0.6	0.5	0.4	0.3	0.2	0.1	.01
0	0	10	10	10	10	10	10	10	10	10	10	10
4.43	.154		10	10.13 9.87	10.19 9.81	10.25 9.77	10.30 9.72	10.34 9.68	10.41 9.63	10.44 9.56	10.59 9.48	10.86 9.27
7.35	.216			10	10.20 9.81	10.27 9.75	10.35 9.68	10.47 9.57	10.51 9.54	10.61 9.46	10.75 9.35	11.14 9.07
10.9	.389				10	10.22 9.78	10.33 9.65	10.43 9.60	10.54 9.52	10.66 9.42	10.83 9.29	11.28 8.98
17.0	.61					10	10.28 9.79	10.42 9.61	10.56 9.50	10.71 9.38	10.92 9.22	11.46 8.87
23.7	.85						10	10.30 9.71	10.47 9.57	10.64 9.43	10.87 9.26	11.39 8.91
38.6	1.38							10	10.36 9.66	10.57 9.49	10.83 9.29	11.43 8.89
38.6	1.38								10	10.42 9.62	10.71 9.38	11.31 8.96
68.0	2.48									10	10.54 9.51	11.07 9.12
613	21.8										10	11.07 9.12

For the appropriate values of t' and the definition of the symbols employed above see Table 2. T* tabulated above.

Table 11

Apparent local period of the free surface at fixed points given by Table 3 for $\sigma = 1/30$ and T = 10 seconds.

	t = 10	Envelope Value										
x km	t_g hrs	1.0	0.9	0.8	0.7	0.6	0.5	0.4	0.3	0.2	0.1	.01
0	0	10	10	10	10	10	10	10	10	10	10	10
1.6	.057		10	10.22 9.79	10.32 9.70	10.42 9.62	10.51 9.54	10.59 9.47	10.70 9.39	10.83 9.29	11.00 9.15	11.52 8.83
2.65	.094			10	10.34 9.68	10.46 9.59	10.59 9.47	10.73 9.37	10.88 9.25	11.06 9.13	11.33 8.95	12.05 8.55
3.12	.140				10	10.38 9.65	10.57 9.49	10.74 9.36	10.43 9.22	11.15 9.07	11.48 8.86	12.35 8.40
6.13	.218					10	10.58 9.57	10.72 9.37	10.46 9.19	11.24 9.00	11.65 8.76	12.72 8.24
8.54	.304						10	10.53 9.52	10.80 9.31	11.10 9.10	11.51 8.84	12.56 8.31
13.9	.494							10	10.66 9.42	10.66 9.17	11.46 8.87	12.63 8.79
24.5	.87								10	10.75 9.35	11.23 9.01	12.40 8.38
55.1	1.96									10	10.98 9.18	11.91 8.62
221	7.85										10	11.92 8.61

For the appropriate values of t' and the definition of the symbols employed above see Table 3. T* tabulated above.

Table 12

Apparent local period of the free surface at fixed points given by Table 4 for $\sigma = 1/20$ and T = 10 seconds.

T = 10		Envelope Value										
x km	t_g hrs	1.0	0.9	0.8	0.7	0.6	0.5	0.4	0.3	0.2	0.1	.01
0	0	10	10	10	10	10	10	10	10	10	10	10
.71	.025		10	10.33 9.69	10.49 9.56	10.63 9.44	10.76 9.34	10.91 9.23	11.07 9.12	11.29 8.98	11.60 8.79	12.45 8.35
1.18	.037			10	10.52 9.53	10.70 9.48	10.92 9.22	11.14 9.07	11.39 8.91	11.70 8.73	12.16 8.49	13.98 7.95
1.74	.062				10	10.58 9.48	10.89 9.25	11.17 9.05	11.47 8.87	11.85 8.66	12.40 8.38	14.03 7.78
3.12	.097					10	10.92 9.23	11.43 8.89	11.96 8.59	12.59 8.29	13.59 7.91	16.61 7.15
3.99	.135						10	10.73 9.37	11.32 8.96	11.85 8.65	12.63 8.28	14.75 7.56
4.96	.22							10	10.75 9.35	11.23 9.02	11.83 8.66	13.38 7.99
10.9	.388								10	11.11 9.09	11.87 8.64	14.08 7.75
24.5	.87									10	11.47 8.86	12.63 8.07
98.1	3.49										10	12.19 8.05

For the appropriate values of t' and the definition of the symbols employed above see Table 4. T* tabulated above.

Table 13

Apparent local period of the free surface at fixed points given by Table 4 for $\sigma = 1/20$ and T = 20 seconds.

T = 20		Envelope Value										
x km	t_g hrs	1.0	0.9	0.8	0.7	0.6	0.5	0.4	0.3	0.2	0.1	.01
0	0	20	20	20	20	20	20	20	20	20	20	20
.71	.012		20	21.36 18.80	22.06 18.29	22.68 17.89	23.31 17.51	24.00 17.14	24.81 16.75	25.92 16.28	27.59 15.68	33.00 14.35
1.18	.019			20	22.20 18.20	23.03 17.67	24.06 17.22	25.15 16.60	26.46 16.08	28.17 15.50	31.00 14.76	41.32 13.19
1.74	.031				20	22.44 18.04	23.90 17.19	25.30 16.53	26.87 15.93	28.98 15.27	32.59 14.43	46.73 12.72
3.12	.049					20	24.03 17.13	26.20 15.99	24.73 15.07	34.01 14.16	42.37 13.09	98.04 11.14
3.99	.068						20	23.13 17.62	26.08 16.22	29.09 15.24	34.25 14.12	56.18 12.17
4.96	.11							20	23.26 17.54	25.56 16.44	28.97 15.27	40.32 13.30
10.9	.194								20	24.99 11.69	29.22 15.20	47.62 12.66
24.5	.435									20	26.90 15.92	38.46 13.51
98.1	1.75										20	38.76 13.48

For the appropriate values of t' and the definition of the symbols employed above see Table 4. T* tabulated above.

undisturbed again. Figures 3 and 4 are a group of graphs which show the wave records which would be observed at various fixed x_1, as a function of time. The graphs have been obtained by considering Tables 4, 12, and 13 and hence values of σ equal to 1/20 sec^{-1} and of T equal to 10 and 20 seconds. The phase of the wave crests has been chosen to go through zero at $t_g = 0$. A slight variation in x' and t_g within the accuracy of the last significant figure given for them would make this possible. The wave crests have been sketched in from the data given in these tables. It is simply too long and difficult a procedure to evaluate equation (4.9) by letting t vary through 2 second increments throughout a range of several thousand seconds in order to graph the free surface. Figures 3 and 4 are sufficiently accurate, however, to show the major features in the transformation of the wave group.

From equation (4.12), it would also be possible to discuss the shape of the envelope as a function of x for a fixed time. The envelope is not a normal probability curve as a function of x for a fixed t since D varies with x. This aspect of the problem of evaluating the solution has not been investigated in as much detail as the problem of the variation in time at a fixed x. For T = 10 sec and σ = 1/100 sec^{-1}, the graphs shown in figure 5 have been obtained. The slight skewness shown by equation (4.12) (which is not so great as one might expect because the D's in the two places where they occur counteract each other) is not evident in the graphs. It might show up for other values of the parameters.

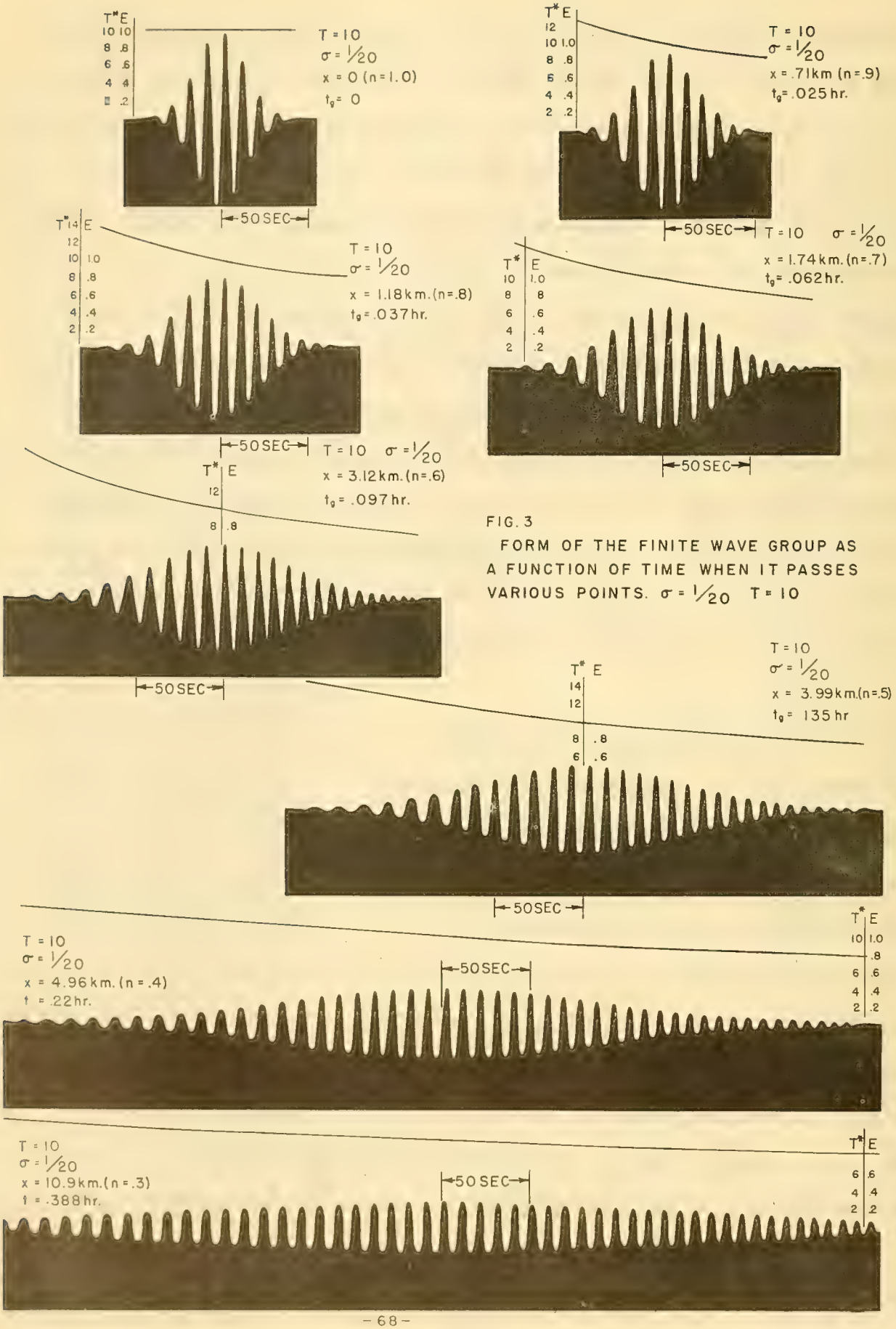

FIG. 3

FORM OF THE FINITE WAVE GROUP AS A FUNCTION OF TIME WHEN IT PASSES VARIOUS POINTS. $\sigma = 1/20$ $T = 10$

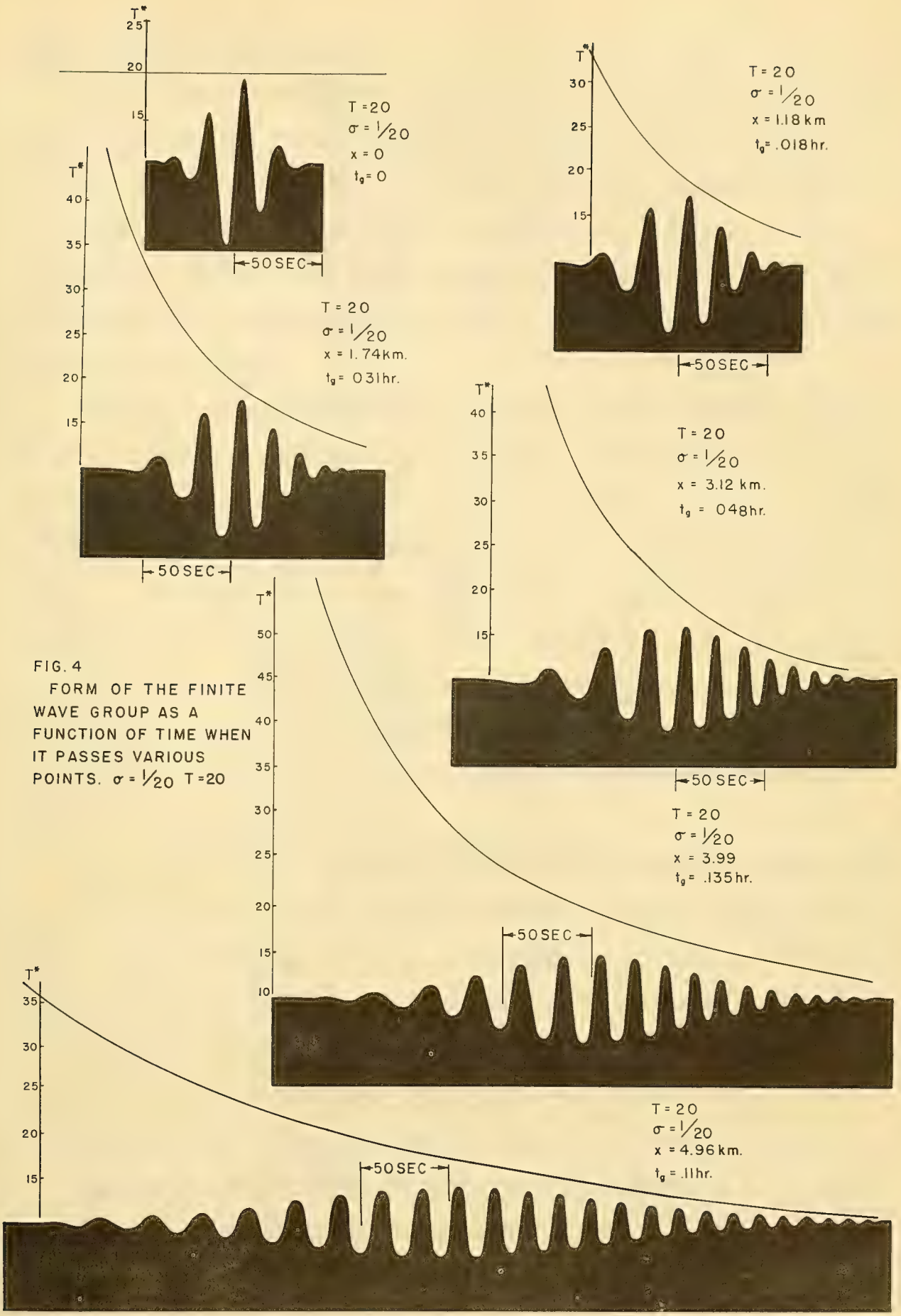

FIG. 4
FORM OF THE FINITE WAVE GROUP AS A FUNCTION OF TIME WHEN IT PASSES VARIOUS POINTS. $\sigma = 1/20$ T = 20

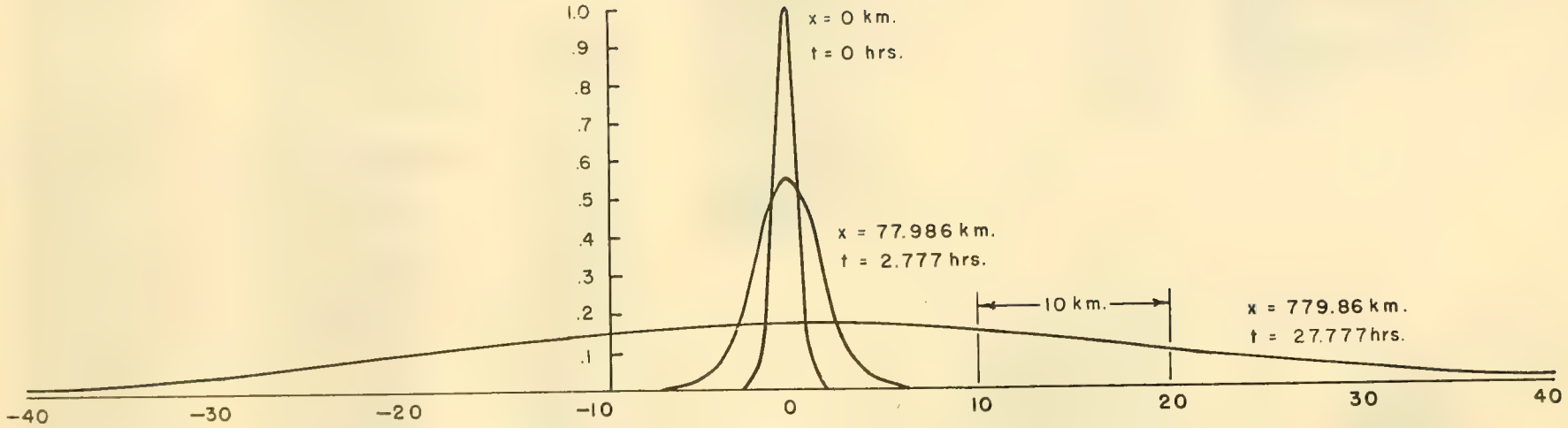

FIG.5 ENVELOPE OF THE FINITE WAVE GROUP AS A FUNCTION OF X FOR FIXED TIMES. $\sigma = 1/100\ \text{sec.}^{-1}$ T = 10 sec.

Apparent local wave length

An apparent local wave length can be obtained by an analysis similar to the one carried out for the apparent local period. In the derivation of the apparent local period, no approximations were made until equation (4.23) was obtained. The derivation showed that higher order effects could be neglected, and so it is possible to simplify the derivation of the apparent local wave length on this basis.

Equation (4.24) defines the argument of the sinusoidal part of the solution as a function of x and t. If equation (4.24) is partially differentiated with respect to time, and then if finite increments are taken as in equation (4.25), T* can be found immediately in the form of equation (4.26). Equation (4.13) would then give equation (4.23) from equation (4.26).

Now the derivation of the apparent local wave length can be carried out easily. Equation (4.27) leads to the apparent local wave length as given in equation (4.28). Note that L* is not equal to $g(T^*)^2/2\pi$.

Equation (4.29) shows that t can be considered a fixed value and redefined in terms of a fixed x by means of the group velocity relationship. Also x can be treated as the sum of two terms. The x_1 is the large term which determines the location of the maximum amplitude of the wave group, and the x' determines the distance from this maximum. With these equations, an alternate relationship for L* can be given by equation (4.31).

Equation (4.31) shows that L* is almost equal to the wave length of a sinusoidal wave of period T in infinitely deep water

$$\text{Arg } S(\eta) = \frac{\frac{4\pi^2 x}{gt^2} - \frac{2\pi t}{T} - \frac{4\sigma^4 t^2 x}{g}}{1 + \frac{16\sigma^4 x^2}{g^2}} + \frac{1}{2}\tan^{-1}\frac{4\sigma^2 x}{g} = f(x,t) \quad (4.24)$$

$$\frac{\partial f(x,t)}{\partial t} = \frac{\Delta f}{\Delta t} = \frac{-2\pi}{T^*} \quad (4.25)$$

$$T^* = \frac{TD}{\left(1 + \frac{4\sigma^4 T t x}{g\pi}\right)} \quad (4.26)$$

$$\frac{\partial f(x,t)}{\partial x} = \frac{\Delta f}{\Delta x} = \frac{+2\pi}{L^*} \quad (4.27)$$

$$L^* = \frac{\frac{gT^2D^2}{2\pi}}{\left(1 + \frac{4\sigma^4 T t x}{g\pi}\right)^2 - \sigma^4\left(\frac{4x}{g} - \frac{tT}{\pi}\right)^2 + \frac{T^2\sigma^2 D}{2\pi^2}} \quad (4.28)$$

$$t_1 = \frac{4\pi x_1}{gT} = t_g \quad (4.29)$$

$$x = x_1 + x' \quad (4.30)$$

$$L^* = \frac{\frac{gT^2}{2\pi}\left(1 + \frac{32\sigma^4 x_1 x'}{g^2 D} + \frac{16\sigma^4 (x')^2}{g^2 D}\right)^2}{\left(1 + \frac{16\sigma^4 x_1 x'}{g^2 D}\right)^2 - \frac{\sigma^4}{D^2}\left(\frac{4x'}{g}\right)^2 + \frac{T^2\sigma^2}{2\pi^2 D}} \quad (4.31)$$

$$df = \frac{\partial f}{\partial t}dt + \frac{\partial f}{\partial x}dx = \frac{-2\pi}{T^*}dt + \frac{2\pi}{L^*}dx = 0 \quad (4.32)$$

$$\frac{dx}{dt} = C^* = \frac{L^*}{T^*} \quad (4.33)$$

Another form of the Cauchy Poisson wave problem

$$A = A'\sigma \quad (4.34)$$

$$\eta(x,t) = \frac{A'\sqrt{g}}{2\sqrt{x}}\left(\cos\frac{gt^2}{4x} + \sin\frac{gt^2}{4x}\right) \quad (4.35)$$

Plate VIII

when x' is zero. The term $T^2\sigma^2/2\pi^2 D$ is small compared to one for the values of T and σ employed in the evaluation. For a fixed x_1, as x' increases positively, the apparent local wave length increases. As x' decreases the apparent local wave length decreases. Thus for a fixed t as a function of x, the longer waves are in the front of the group.

One final point needs to be made. It was shown that a positive increase in t by the amount T* caused a decrease in f(x,t) by the amount 2π. In equation (4.27), it was assumed that a positive increase in x by the amount L* caused a positive increase in f(x,t) by the amount 2π. Equation (4.31) then gave a positive value for L* over the range of x and t where the maximum value of the envelope occurs. The derivation therefore shows that those wave crests which are under the maximum value of the envelope as it travels along are moving forward in the positive x direction.

Apparent local speed

The total change in f(x,t) at a wave crest should be zero if the observer moves with the speed of the crest. Equation (4.32) imposes this condition and yields the result that the wave crests advance with an apparent local speed given by C* in equation (4.33). In equation (4.33) it should be understood that L* and T* are given by equation (4.26) and (4.29). For values of x and t which give a maximum value for the envelope, it then follows that the wave crests are moving forward with a speed twice that of the envelope.

Summary of wave group behavior

In summary, the wave group studied travels forward with the group velocity appropriate to the value of T employed. It dies down in amplitude as it travels along and spreads out over the ocean surface. The individual waves under the envelope form in the rear of the envelope as waves with a short apparent local period, travel through the envelope with a gradually increasing apparent local period to a maximum amplitude where they have an apparent local period nearly equal to T, and finally race ahead with a longer and longer apparent local period to disappear at the front of the group. At any instant of time, the longest apparent waves are at the front of the group, if x and t are greater than zero.

The study in this section of the behavior of the solution for values of the parameters employed in the tables is now completed. A study of the pressure caused by the surface disturbance will be made in a later chapter.

New form of Cauchy-Poisson problem

One very special modification of the solution can be found which yields another fascinating form of the Cauchy-Poisson wave problem. If in equation (4.1), $\sin 2\pi t/T$ is replaced by $\cos 2\pi t/T$, then in equation (4.9), the negative sine term can be replaced by a positive cosine term. Then in these new equations replace A by a modified form given in equation (4.34), where A* is constant.

As σ approaches infinity, the modified form of equation (4.1) approaches an infinitely high spike which lasts only for an instant in time. The spectrum given by $a(\mu)$ is equal to

a constant value everywhere and thus degenerates into a white noise spectrum. Then for x not equal to zero, the free surface assumes the form of equation (4.35).

In this modified form of the Cauchy-Poisson wave problem, the amplitude of the waves at a fixed point, x, does not increase with time and is finite at all x not equal to zero. The disturbance, as in one of the previous cases, is caused by an infinitely high, infinitely long,* infinitesimally wide column of water at the origin, but in this case it lasts only for an instant of time. Thus there is not enough energy to produce an infinitely high disturbance at points other than x = 0.

Physical reality of problem

The physical reality of the whole problem discussed in this section should be considered. If such a wave group were generated on the surface of the ocean, would it travel as predicted? It might not because no ocean is infinitely deep, because the low periods associated with high values of μ are really capillary waves, and because such effects as internal viscosity, and the friction of the atmosphere against the moving waves have been neglected.

The wave length of a sinusoidal wave in water of finite depth is less than the values employed here.** Since the spectrum of the waves is defined near $\mu = 0$ where the period of the waves is infinite, the group will not travel exactly as predicted in water of finite depth.

In figure 1, for the values of the parameters employed, it can be seen that that portion of the spectrum which is affected

* In the y direction.
**For the same period.

by a depth equal to that of the average depth of the ocean is very small. Note that this is not the case in the Cauchy-Poisson problem where the spectrum is a white noise spectrum.

The wave length of a sinusoidal wave when surface tension is considered, is greater than the values employed here if the period is very small. For the range of the parameters considered this effect is very small. Again this is not the case in the Cauchy-Poisson problem.

The effect of internal viscosity has been shown to be negligible by Sverdrup and Munk [1947] for the dominant spectral components employed although Johnson [1949] has shown that it is important for very short period waves. Internal viscosity would not be important until the group had traveled a distance equivalent to several times around the earth.*

The action of the air against the traveling wave group or of some type of internal eddy viscosity in the motion is possibly an important effect which could modify its actual travel. For the present, there will be no speculation about the modification of the solution obtained in this section by these mechanisms.

---

*See Lamb [1932], sec. 348 equation (9). For the ten second spectral component, traveling with the group velocity of a ten second wave, the distance the group would travel before dying down to the 1/e of its former height due to molecular viscosity would be of the order of 10^6 kilometers.

Chapter 5. THE PROPAGATION OF A FINITE WAVE TRAIN IN INFINITELY DEEP WATER

Introduction

There is considerable interest in the problem of what happens to a train of waves of constant height, finite duration, and constant apparent local period as it travels along. Sverdrup and Munk [1947] have given a physical argument based upon the fact that the energy of the wave train advances with the group velocity which shows that the major rise of the amplitude advances with the group velocity of the apparent local period and that only very low waves travel out in front of the main group.

Such a finite wave train has a continuous Fourier spectrum. In order to determine the effects of dispersion, it is necessary to investigate the problem mathematically with the techniques of the previous problem.

Despite Munk's [1947] assertion to the contrary, dealing with the recorded period, "without recourse to the nature of the underlying continuous Fourier spectrum" always tacitly assumes something about the underlying spectrum which may not be theoretically justified. There is considerable confusion in the technical literature about the difference between the apparent local period of the previous section and the period of a periodic function. In addition the use of the formula $c = gT/2\pi$ in the above reference is not valid because the formula applies only to a purely periodic wave train of one constant period.

Formulation

Suppose that a wave record defined by equation (5.1) is observed at the point x = 0 and y = 0, as a function of time. The sea surface would be perfectly flat for all times before t = -nT. After that time waves all of the same height with an apparent local period equal numerically to T would be observed until t = nT. There would be 2n complete wave crests. After t = nT the sea surface would become and remain flat again. Thus the wave train lasts only for a finite length of time, and it is therefore referred to as a finite wave train. It would be nice to know what the sea surface looks like at other places and other times. It would also be nice to know how the pressure varies as a function of depth as the wave train passes overhead.

Method of solution

The continuous spectrum, $b(\mu)$, can be found as usual by integrating equation (5.2). The last result in equation (5.2) has the same property that was found in the previous chapter in that for $\mu > 0$ the second term dominates the first term.

By arguments exactly parallel to the ones in the previous chapter, the equation for the free surface can be written in the form of equation (5.3). For x = 0, equation (5.3) reduces to equation (5.1).

It was possible to obtain a representation for the pressure caused by the disturbance in an integral form similar to equation (4.7) of the previous section. However the indicated integration could not be carried out, so, although it would be nice to know something about the pressure caused by the disturbance, that aspect

The Propagation of a Finite Wave Train in Infinitely Deep Water

$$\eta(o,o,t) = \begin{cases} A \sin \frac{2\pi t}{T}, & \text{if } -nT < t < nT \\ & (n \text{ an integer}) \\ 0 & , \text{ otherwise} \end{cases} \tag{5.1}$$

$$b(\mu) = \frac{A}{\pi}\int_{-\infty}^{+\infty} \eta(o,o,t) \sin \mu t \, dt = \frac{A}{\pi}\int_{-Tn}^{Tn} \sin \frac{2\pi t}{T} \sin \mu t \, dt$$

$$= \frac{A}{2\pi}\int_{-Tn}^{Tn} \left[-\cos\left(\frac{2\pi}{T} + \mu\right)t + \cos\left(\frac{2\pi}{T} - \mu\right)t\right] dt$$

$$= \frac{A}{\pi}\left[- \frac{\sin\left(\frac{2\pi}{T} + \mu\right)Tn}{\left(\frac{2\pi}{T} + \mu\right)} + \frac{\sin\left(\frac{2\pi}{T} - \mu\right)Tn}{\left(\frac{2\pi}{T} - \mu\right)} \right]$$

$$= \frac{A}{\pi}\left[- \frac{\sin \mu T n}{\left(\frac{2\pi}{T} + \mu\right)} - \frac{\sin \mu T n}{\left(\frac{2\pi}{T} - \mu\right)} \right] \tag{5.2}$$

$$\eta(x,t) = \frac{A}{\pi}\int_{-\infty}^{+\infty} \frac{\sin \mu Tn}{\left(\frac{2\pi}{T} - \mu\right)} \sin\left(\frac{\mu^2 x}{g} - \mu t\right) d\mu \tag{5.3}$$

$$\frac{2\pi}{T} - \mu = -\alpha \tag{5.4}$$

$$\eta(x,t) = \frac{A}{\pi}\int_{-\infty}^{+\infty} \sin\left[\left(\frac{4\pi^2 x}{gT^2} - \frac{2\pi t}{T}\right) + \left(\frac{\alpha^2 x}{g} + \alpha\left(\frac{4\pi x}{gT} - t\right)\right)\right] \frac{\sin \alpha n T}{-\alpha} \, d\alpha$$

$$= \frac{A}{\pi} \sin\left(\frac{4\pi^2 x}{gT^2} - \frac{2\pi t}{T}\right)\int_{-\infty}^{+\infty} \cos\left[\frac{\alpha^2 x}{g} + \alpha\left(\frac{4\pi x}{gT} - t\right)\right] \frac{\sin \alpha n T}{-\alpha} \, d\alpha$$

$$+ \frac{A}{\pi} \cos\left(\frac{4\pi^2 x}{gT^2} - \frac{2\pi t}{T}\right)\int_{-\infty}^{+\infty} \sin\left[\frac{\alpha^2 x}{g} + \alpha\left(\frac{4\pi x}{gT} - t\right)\right] \frac{\sin \alpha n T}{-\alpha} d\alpha \tag{5.5}$$

PLATE IX

of the problem will have to be unknown for the present.

The next step is to integrate equation (5.3). A few manipulations in the form of trigonometric identities and a transformation of variable make it possible to put the equation into a form where the integral can be evaluated. The transformation of variable given by equation (5.4) and the formula for the sine of the sum of two angles yields equation (5.5). The trigonometric identity for the product of two sinusoidal terms can then be used to obtain equation (5.6). The assumption that n is an integer is used.

Consider the first term in equation (5.6) (Plate X). The term under the integral can be expanded by the trigonometric identity for the sine of the sum of two angles and thus this integral can be written as the sum of two integrals. One of these integrals is given by equation (5.7). The integrand is an odd function, and the integral of an odd function from minus infinity to plus infinity is zero. The other term is even and its integral from minus infinity to plus infinity is equal to twice its integral from zero to infinity. The contribution of the first term is therefore only the first term in equation (5.8). If this operation is carried out on each term in equation (5.6) the corresponding terms result in equation (5.8).

The terms in equation (5.8) can be written as a double Fourier Integral by means of an interesting mathematical detour, and the double Fourier Integral can be evaluated by an interchange of the order of integration. The mathematics will be carried out for the first term in equation (5.8).

The Propagation of a Finite Wave Train in Infinitely Deep Water (Continued)

$$\eta(x,t) = \frac{-A}{2\pi}\sin\left(\frac{4\pi^2 x}{gT^2} - \frac{2\pi t}{T}\right)\int_{-\infty}^{+\infty}\sin\left(\frac{\alpha^2 x}{g} + \alpha\left(\frac{4\pi x}{gT} - t + nT\right)\right)\frac{d\alpha}{\alpha}$$

$$+ \frac{A}{2\pi}\sin\left(\frac{4\pi^2 x}{gT^2} - \frac{2\pi t}{T}\right)\int_{-\infty}^{+\infty}\sin\left(\frac{\alpha^2 x}{g} + \alpha\left(\frac{4\pi x}{gT} - t - nT\right)\right)\frac{d\alpha}{\alpha}$$

$$+ \frac{A}{2\pi}\cos\left(\frac{4\pi^2 x}{gT^2} - \frac{2\pi t}{T}\right)\int_{-\infty}^{+\infty}\cos\left(\frac{\alpha^2 x}{g} + \alpha\left(\frac{4\pi x}{gT} - t + nT\right)\right)\frac{d\alpha}{\alpha}$$

$$- \frac{A}{2\pi}\cos\left(\frac{4\pi^2 x}{gT^2} - \frac{2\pi t}{T}\right)\int_{-\infty}^{+\infty}\cos\left(\frac{\alpha^2 x}{g} + \alpha\left(\frac{4\pi x}{gT} - t - nT\right)\right)\frac{d\alpha}{\alpha} \qquad (5.6)$$

$$\int_{-\infty}^{+\infty}\sin\frac{\alpha^2 x}{g}\cos\left(\alpha\left(\frac{4\pi x}{gT} - t + nT\right)\right)\frac{d\alpha}{\alpha} = 0 \qquad (5.7)$$

$$\eta(x,t) = \frac{-A}{\pi}\sin\left(\frac{4\pi^2 x}{gT^2} - \frac{2\pi t}{T}\right)\int_{0}^{\infty}\cos\frac{\alpha^2 x}{g}\sin\left(\alpha\left(\frac{4\pi x}{gT} - t + nT\right)\right)\frac{d\alpha}{\alpha}$$

$$+ \frac{A}{\pi}\sin\left(\frac{4\pi^2 x}{gT^2} - \frac{2\pi t}{T}\right)\int_{0}^{\infty}\cos\frac{\alpha^2 x}{g}\sin\left(\alpha\left(\frac{4\pi x}{gT} - t - nT\right)\right)\frac{d\alpha}{\alpha}$$

$$- \frac{A}{\pi}\cos\left(\frac{4\pi^2 x}{gT} - \frac{2\pi t}{T}\right)\int_{0}^{\infty}\sin\frac{\alpha^2 x}{g}\sin\left(\alpha\left(\frac{4\pi x}{gT} - t + nT\right)\right)\frac{d\alpha}{\alpha}$$

$$+ \frac{A}{\pi}\cos\left(\frac{4\pi^2 x}{gT} - \frac{2\pi t}{T}\right)\int_{0}^{\infty}\sin\frac{\alpha^2 x}{g}\sin\left(\alpha\left(\frac{4\pi x}{gT} - t - nT\right)\right)\frac{d\alpha}{\alpha} \qquad (5.8)$$

$$2\int_{0}^{\infty}\cos\frac{x}{g}\alpha^2\cos\beta\alpha\,d\alpha = \left(\cos\frac{\beta^2 g}{4x} + \sin\frac{\beta^2 g}{4x}\right)\sqrt{\frac{\pi g}{2x}} \qquad (5.9)$$

$$\cos\frac{x}{g}\alpha^2 = \int_0^{\infty}\frac{1}{\pi}\sqrt{\frac{\pi g}{2x}}\left[\cos\frac{\beta^2 g}{4x} + \sin\frac{\beta^2 g}{4x}\right]\cos\beta\alpha\,d\beta \qquad (5.10)$$

$$\sin\frac{x}{g}\alpha^2 = \int_0^{\infty}\frac{1}{\pi}\sqrt{\frac{\pi g}{2x}}\left[\cos\frac{\beta^2 g}{4x} - \sin\frac{\beta^2 g}{4x}\right]\cos\beta\alpha\,d\beta \qquad (5.11)$$

Plate X

The first step is to find the Fourier Spectrum of cos $\alpha^2 x/g$ as a function of α. Equation (5.9) gives this spectrum as a function of the new variable, β. It then follows that cos $\alpha^2 x/g$ is given by equation (5.10). Equation (5.11) would be the corresponding equation for the sin $x\alpha^2/g$. Note that this step involves the assumption that x is greater than zero. Slight modifications of the analysis from this point on would also yield valid results for x less than zero.

In the second expression in equation (5.12), (Plate XI), equation (5.10) has been substituted for cos $\alpha^2 x/g$ in the integral which occurs in the first term of equation (5.8). In the third expression, the order of integration has been interchanged as indicated by the rearrangement of the brackets. The change in the order of integration can be justified theoretically. The term in brackets in the third expression leads to the conclusion that integration of the term, cos $\beta^2 g/4x$ + sin $\beta^2 g/4x$, from zero to the indicated variable upper limit is equal to the original integral as in the fourth expression. Finally a change in variable gives the last expression in equation (5.12).

The term in brackets in the third expression in equation (5.12) is considered in equation (5.12) and designated with the letter I. It can be shown easily that this integral as a function of β, after integration over α, is either constant or zero, and its values are given below the integral (see Pierce, [1929]).

Now that the integral over α has been evaluated, consider the integration over β when $4\pi x/gT - t + nT > 0$. For $\beta < 4\pi x/gT - t + nT$, the integrand as a function of β is equal to cos $\beta^2 g/4x$ + sin $\beta^2 g/4x$

The Propagation of a Finite Wave Train in Infinitely Deep Water (Continued)

$$\int_0^\infty \cos\frac{\alpha^2 x}{g}\sin\left(\alpha\left(\frac{4\pi x}{gT}-t+nT\right)\right)\frac{d\alpha}{\alpha}$$

$$=\frac{1}{\pi}\sqrt{\frac{\pi g}{2x}}\int_0^\infty\left[\int_0^\infty\left(\cos\frac{\beta^2 g}{4x}+\sin\frac{\beta^2 g}{4x}\right)\cos\beta\alpha\,d\beta\right]\sin\left(\alpha\left(\frac{4\pi x}{gT}-t+nT\right)\right)\frac{d\alpha}{\alpha}$$

$$=\frac{1}{\pi}\sqrt{\frac{\pi g}{2x}}\int_0^\infty\left(\cos\frac{\beta^2 g}{4x}+\sin\frac{\beta^2 g}{4x}\right)\left[\int\frac{\cos\beta\alpha\sin\left(\alpha\left(\frac{4\pi x}{gT}-t+nT\right)\right)d\alpha}{\alpha}\right]d\beta$$

$$=\frac{\pi}{2\pi}\sqrt{\frac{\pi g}{2x}}\int_0^{\left(\frac{4\pi x}{gT}-t+nT\right)}\left(\cos\frac{\beta^2 g}{4x}+\sin\frac{\beta^2 g}{4x}\right)d\beta$$

$$=\frac{\pi}{2}\int_0^{\sqrt{\frac{g}{2\pi x}}\left(\frac{4\pi x}{gT}-t+nT\right)}\left(\cos\frac{\pi}{2}\sigma^2+\sin\frac{\pi}{2}\sigma^2\right)d\sigma \qquad (5.12)$$

$$I=\int_0^\infty\frac{\cos\beta\alpha\sin\left(\alpha\left(\frac{4\pi x}{gT}-t+nT\right)\right)}{\alpha}d\alpha \qquad (5.13)$$

$I=0$ if $\beta>\frac{4\pi x}{gT}-t+nT>0$ or $\beta<\frac{4\pi x}{gT}-t+nT<0$

$I=\frac{\pi}{4}$ if $\beta=\frac{4\pi x}{gT}-t+nT>0$

$I=-\frac{\pi}{4}$ if $\beta=\frac{4\pi x}{gT}-t+nT<0$

$I=\frac{\pi}{2}$ if $0<\beta<\frac{4\pi x}{gT}-t-nT$

$I=-\frac{\pi}{2}$ if $\frac{4\pi x}{gT}-t+T<\beta<0$

$$\frac{\pi}{2}\sigma^2=\frac{g}{4x}\beta^2 \qquad \beta=+\sqrt{\frac{2\pi x}{g}}\,\sigma \qquad (5.14)$$

Plate XI

times a positive constant. For $\beta > 4\pi x/gT - t + nT$, the integrand is equal to cos $\beta^2 g/4x$ + sin $\beta^2 g/4x$ times zero, which is zero. But since the integrand is zero beyond this value of β, the integral can be evaluated by integrating cos $\beta^2 g/4x$ + sin $\beta^2 g/4x$ from zero to $4\pi x/gT - t + nT$ as in the fourth expression in equation (5.12). Then the transformation given by equation (5.14) yields the final expression in equation (5.12). The theory of integration also shows that if $4\pi x/gT - t + nT$ had been negative, the integrals would still be correct as written.

The integral given in the last expression for equation (5.12) is the sum of two known integrals. They are the Fresnel Integrals which are tabulated, for example, by Jahnke-Emde [1945]. For any particular value of x, t, n, and T, the upper limit of integration is some number, and the table gives the value of the integral.

Solution

Each term in equation (5.8) can be treated in the same manner as the first term was treated. The final form of the solution is then given by equation (5.15) where G(x,t,T,n) and H(x,t,T,n) are defined by equations (5.16) and (5.17). These three equations then are the solution, because they can be evaluated for all values of t, n, and T, and for all x greater than zero.

In order to show that it is the solution of the problem, equation (5.15) must reduce to equation (5.1) as x approaches zero through positive values of x. If the upper limits of integration are plus or minus infinity the values of the integrals are given by equations (5.18) and (5.19).

Consider the expression for G in equation (5.16). Pick any

Finite Wave Train (Solution)

$$\eta(x,t) = G(x,t,T,n)\sin\left(\frac{4\pi^2 x}{gT^2} - \frac{2\pi t}{T}\right)$$

$$+ H(x,t,T,n)\cos\left(\frac{4\pi^2 x}{gT^2} - \frac{2\pi t}{T}\right) \tag{5.15}$$

$$G = \frac{A}{2}\left[-\int_0^{\sqrt{\frac{g}{4\pi x}}\left(\frac{4\pi x}{gT} - t + nT\right)}\left(\cos\frac{\pi}{2}\sigma^2 + \sin\frac{\pi}{2}\sigma^2\right)d\sigma + \int_0^{\sqrt{\frac{g}{4\pi x}}\left(\frac{4\pi x}{gT} - t - nT\right)}\left(\cos\frac{\pi}{2}\sigma^2 + \sin\frac{\pi}{2}\sigma^2\right)d\sigma\right] \tag{5.16}$$

$$H = \frac{A}{2}\left[\int_0^{\sqrt{\frac{g}{4\pi x}}\left(\frac{4\pi x}{gT} - t - nT\right)}\left(\cos\frac{\pi}{2}\sigma^2 - \sin\frac{\pi}{2}\sigma^2\right)d\sigma - \int_0^{\sqrt{\frac{g}{4\pi x}}\left(\frac{4\pi x}{gT} - t + nT\right)}\left(\cos\frac{\pi}{2}\sigma^2 - \sin\frac{\pi}{2}\sigma^2\right)d\sigma\right] \tag{5.17}$$

$$\int_0^{\infty}\cos\frac{\pi}{2}\sigma^2 d\sigma = \int_0^{\infty}\sin\frac{\pi}{2}\sigma^2 d\sigma = \frac{1}{2} \tag{5.18}$$

$$\int_0^{-\infty}\cos\frac{\pi}{2}\sigma^2 d\sigma = \int_0^{-\infty}\sin\frac{\pi}{2}\sigma^2 d\sigma = -\frac{1}{2} \tag{5.19}$$

$$\lim_{x\to 0^+} G = -A \quad \text{if } -nT < t < nT \tag{5.20}$$

$$\lim_{x\to 0^+} G = 0 \quad \text{if } t < -nT \text{ or } t > nT \tag{5.21}$$

$$\lim_{x\to 0^+} H = 0 \quad \text{if } t \neq -nT \text{ and } t \neq nT \tag{5.22}$$

Plate XII

value of t such that $-nT < t < nT$. Then as x approaches zero through positive values the upper limits of integration of the first term in G approaches plus infinity. The upper limit of the second term approaches minus infinity. The total contribution of the bracket is then minus 2, and equation (5.20) holds.

Similarly if $t < -nT$ or $t > nT$, equation (5.21) holds. The sine term approaches - sin $2\pi t/T$. The expression for H can be analyzed similarly and H is zero if t is not equal to either nT or -nT. Therefore equation (5.15) reduces to equation (5.1) when x approaches zero except possibly at two points, namely $t = nT$ and $t = - nT$.

At these two points, the actual behavior of the solution is clarified if, now, after passing to the limiting value of x equal to zero, t is allowed to approach $t = nT$ and $t = - nT$ from both positive and negative values. The free surface approaches the value zero as t approaches nT or -nT from either direction, and therefore (5.15) can be defined to be equal to zero at $t = -nT$ and $t = +nT$. Therefore (5.15) equals (5.1) everywhere as x approaches zero through positive values of x.

There is a reason for the particular care which must be employed in the study of the solution near these two special points. It is that the slope of the original expression, equation (5.1), is discontinuous at these points. The effect of this discontinuity in slope causes the solution to have a very peculiar appearance as a function of time for values of x near $x = 0$.

Evaluation

Now that a solution to the problem has been obtained, the properties of the solution will be discussed and graphed as in the

previous chapter. The nature of the continuous spectrum, the behavior of the wave train as it travels along, and its variation with n will be described.

Spectrum

The part of the continuous spectrum which was used in the integral form of the solution is given as $b^*(\alpha)$ in equation (5.23). The second form, in terms of α, can be obtained with the use of equation (5.4), if n is an integer. As μ approaches $2\pi/T$ or as α approaches zero, the spectrum has an indeterminate form, but the application of standard methods shows that the value of $b^*(\alpha)$ approaches ATn/π at this point. Thus for larger values of n, the contribution to the spectrum near values which are equal to values associated with the apparent local period becomes large compared to other values of the spectrum. As n approaches infinity, however, the spectrum does not reduce to one infinitely high spike as in the problem in Chapter 4. The actual behavior of the spectrum is shown in the graphs of $b^*(\alpha)$ which are shown in figure 6. If n equals a small value as in the top graph of figure 6, the spectrum is a smooth curve with important contributions for all spectral values. Such a disturbance of the sea surface would travel only a short distance and rapidly die out. In the bottom graph of figure 6, there are three different scales on the ordinate, $(b(\alpha'))$, and abscissa (α'), axes. The inner scales apply for n = 10. If n is increased by a factor of ten, the ordinate scale is increased by a factor of 10 and the abscissa scale is decreased by a factor of 10 as in the middle set of scales. Thus, the important part of the spectrum is increasingly concentrated near $\mu = 2\pi/T$,

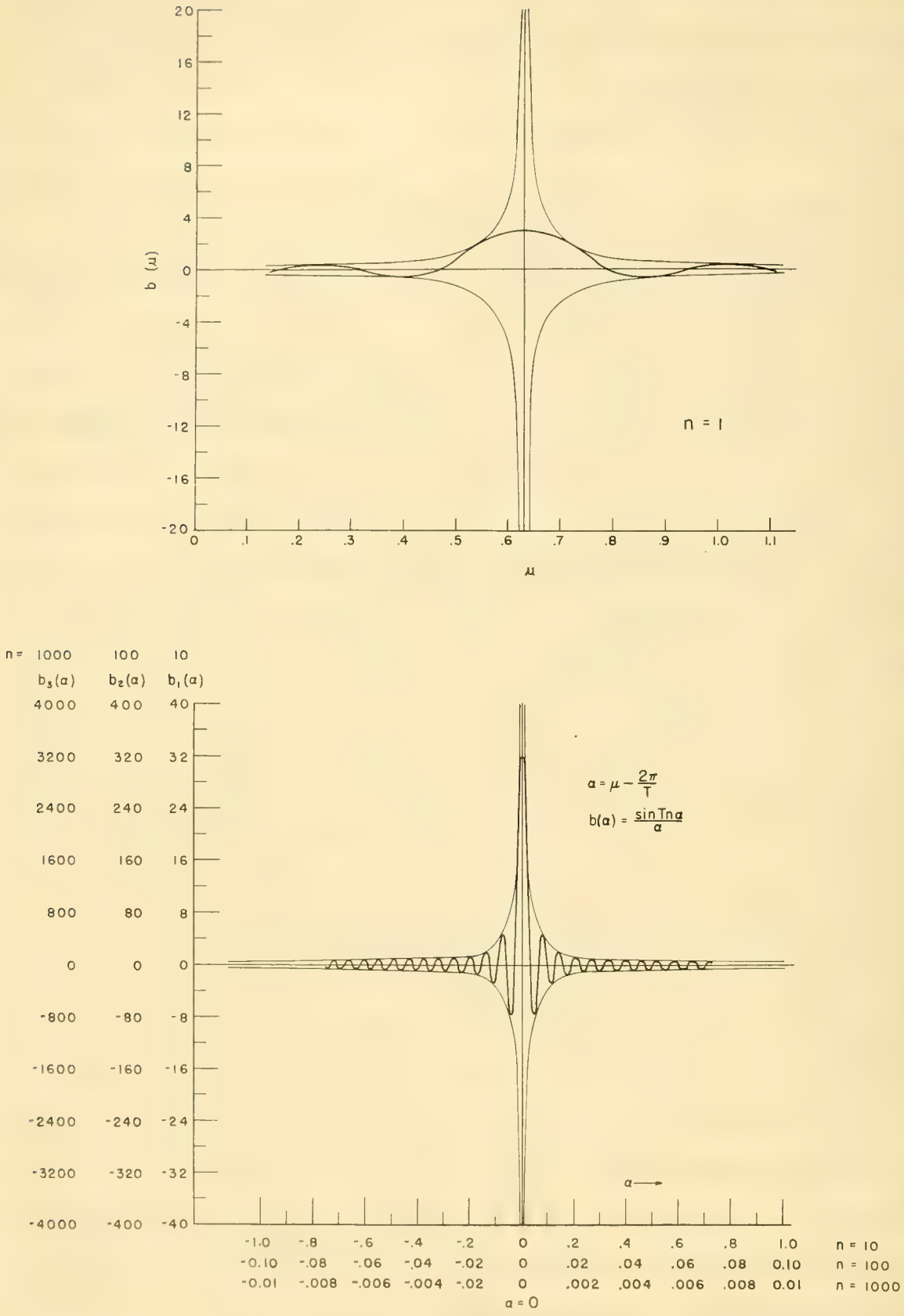

Fig 6 Graphs of b(α) for various values of n. Co-ordinate scales differ for different n for bottom graph as shown

($\alpha' = 0$), and the side spectral components oscillate more and more rapidly and tend to cancel. For large values of n, the same remarks about the spectral components which travel in the negative x direction are applicable which were made in the comments about the spectrum of this finite wave group.

As n approaches infinity, for any finite values of t and x, equation (5.15) reduces to $\eta\ (x,t) = A \sin(4\pi^2 x/gT^2 - 2\pi t/T)$ which is a simple sine wave traveling toward the right. Only when the wave train is infinitely long and lasts for an infinite length of time is it possible to apply the usual formula for wave speed and wave length without qualification. Also equation (4.9) reduces to the above form as σ approaches zero.

An interesting question is, "Why are the two continuous spectra so different in their limiting forms?" The explanation lies in the way that the free surface at x equal to zero approaches its limiting form. The free surface studied in Chapter 4 deforms continuously into its limiting form, namely $\eta\ (0,t) = A \sin 2\pi t/T$, as σ approaches zero. The free surface studied in this chapter does not deform continuously into its limiting form. The sharp discontinuity from full amplitude to zero amplitude is always present, and an increase in the value of n just displaces the discontinuity in time. This difference in behavior thus explains the differences in the type of continuous spectra obtained.

The solution to the problem studied in this chapter is valid for all integer values of n. For n equal to one, there would be two complete wave crests under the envelope. The evaluation of the solution for other values of x and t would then be somewhat difficult

because all terms in equations (5.15), (5.16) and (5.17) would have to be evaluated carefully over small increments in the variable quantities. The disturbance would die down in amplitude and spread out over the surface quite rapidly. In addition, the variation in amplitude and sign of the terms G and H would be as rapid as the variation of the sine and cosine terms so that the simplifying concept of a slowly varying envelope and a relatively rapidly varying sinusoidal term under the envelope would not be applicable.

Simplification of results

For large values of n the analysis of the solution and the physical interpretation of the results are simpler. One could consider the problem to represent a train of waves of constant apparent local period which takes, say, ten hours to pass a given point, $x = 0$. Then if T equals ten seconds, n equals 1800, and nT equals 18,000.

Now consider the integrals in equation (5.18) and (5.19). If the upper limit were replaced by plus or minus ten in these integrals, the values of the integrals would still be very close to plus or minus one half. Thus, interest should be concentrated on times and places where the upper limits of integration in equations (5.16) and (5.17) lie between minus ten and plus ten. One way to do this is to study the variation of the solution at a fixed value of x as a function of time. Pick a fixed value of x and call it x_1 as in Chapter 4. Then the forward edge of the wave train arrives at x_1 at a time, t, determined by the group velocity of waves with a period equal to the apparent local period of the wave train. When

$t = 4\pi x_1/gT - nT$, the upper limit of integration in the second term of (5.16) and the first term of (5.17) is zero. The upper limits of integration of the other two terms is given by $(g/4\pi x_1)^{1/2}$ 2nT and its value is greater than 10 for all values of x_1 less than ten thousand kilometers. Note also that a wave train with 3600 waves of 10 second period in it would be about 600 km long.

For a fixed point, x_1, then, if x_1 is less than approximately ten thousand kilometers, the transformation of variable given by equation (5.24) can be applied where the time of passage of the forward part of the wave train occurs near t' equal to zero. Equation (5.15) then simplifies to equation (5.25). The first integral in equation (5.16) is practically a constant; the second integral in equation (5.17) is practically zero; and some algebraic manipulations then yield equation (5.25) where G* and H* are defined in (5.26) and (5.27). The value of x_1 is fixed; equation (5.25) does not imply that the waves are traveling in the negative x direction.

G* and H* are functions of the variable upper limit of integration. For x_1 small, the upper limit of integration is greater than ten or less than minus ten after t' has varied through a small range of values. For x_1 large, t' must vary through a much larger range of values. G* and H* are graphed in figure 7 for A = 1 as a function of $(g/4\pi x_1)^{1/2}t'$.

The appearance of the solution as a function of t' for a fixed x_1 depends upon the choice of x_1. For small values of x_1, the effect of G* and H* is to put ripples on the first two or three waves in the wave train and to leave the remaining waves

$$b^*(u) = -\frac{A \sin u T n}{\pi\left(\frac{2\pi}{T} - u\right)} = \frac{A \sin \alpha T n}{\pi \alpha} \tag{5.23}$$

$$t = \frac{4\pi x_1}{gT} - nT + t' = t_g + t' \tag{5.24}$$

$$\eta(x_1, t') \cong G^*(x_1, t', n, T) \sin\left(\frac{4\pi^2 x_1}{gT^2} + \frac{2\pi t'}{T}\right)$$

$$+ H^*(x_1, t', n, T) \cos\left(\frac{4\pi^2 x_1}{gT^2} + \frac{2\pi t'}{T}\right) \tag{5.25}$$

$$G^* = \frac{A}{2}\left[1 + \int_0^{\sqrt{\frac{g}{4\pi x_1}}\, t'} \left(\cos\frac{\pi}{2}\sigma^2 + \sin\frac{\pi}{2}\sigma^2\right) d\sigma\right] \tag{5.26}$$

$$H^* = \frac{A}{2}\left[-\int_0^{\sqrt{\frac{g}{4\pi x_1}}\, t'} \left(\cos\frac{\pi}{2}\sigma^2 - \sin\frac{\pi}{2}\sigma^2\right) d\sigma\right] \tag{5.27}$$

if x_1 is large enough.

$$\eta(x_1, t) \cong \sqrt{(G^*)^2 + (H^*)^2}\, \sin\left(\frac{2\pi t'}{T} + \frac{4\pi^2 x_1}{gT} + \tan^{-1}\frac{H^*}{G^*}\right) \tag{5.28}$$

$$E_p = \frac{g\rho}{2}\left(\eta(x, t'')\right)^2 \tag{5.29}$$

$$\overline{E}_p \cong \frac{1}{T}\int_{t'}^{t'+T} \frac{g\rho}{2}\left(\eta(x_1, t'')\right)^2 dt'' \cong \frac{g\rho}{4}\left((G^*)^2 + (H^*)^2\right) \tag{5.30}$$

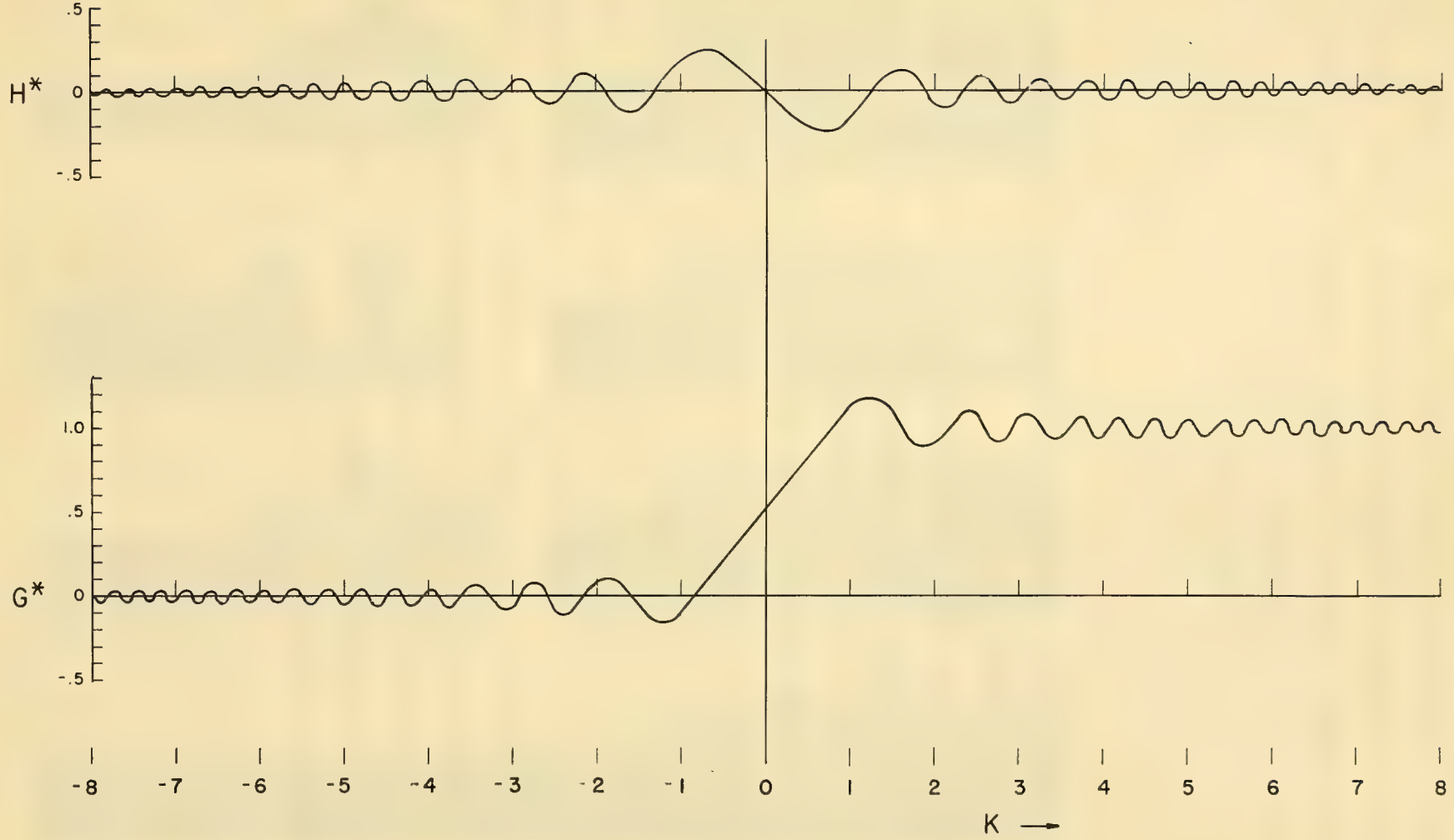

Fig 7 G* and H* graphed as a function of $(g/4\pi x_1)^{\frac{1}{2}} t'$

unaltered. For slightly larger values of x_1, the effect of G* and H* is to produce strangely distorted wave crests shortly after t' = 0 and crests with many different apparent local periods shortly before t' = 0. For moderate values of x_1, the effect of G* and H* is to cause the individual wave crests to be modulated in amplitude and phase and to have an apparent local period equal to T for all values of t'. Finally for values of x_1 near ten thousand kilometers, G* and H* are no longer appropriate and the original form of the solution must be studied.

Figure 8 shows the forward edge of the finite wave train as a function of t' for various values of x_1 in order to illustrate the above remarks. T is ten seconds, n is 1800, and x_1 has been chosen to be 1/2 centimeter, one twelfth of a wave length, five wave lengths and one hundred wave lengths. The time scales for the graphs on the left are different in order to show the fine details, and the times scales for the graphs on the right are the same in order to show the overall behavior. For x_1 equal to 1/2 centimeter, the effect of G* and H* is to put a few high frequency ripples on the very first wave crest as in the graph at the upper left. The graph on the upper right shows that the major portion of the train is essentially unaffected. For x = L/12 and x = 5L a few crests at the forward edge are affected but the major portion of the train is still unaffected. For X = 100L, about ten crests are found of substantial amplitude in advance of t' = 0, and about twenty crests are modulated in amplitude behind t' = 0. The transition from constant amplitude to small amplitude is quite gradual.

For values of x_1 which are large enough, G* and H* are slowly

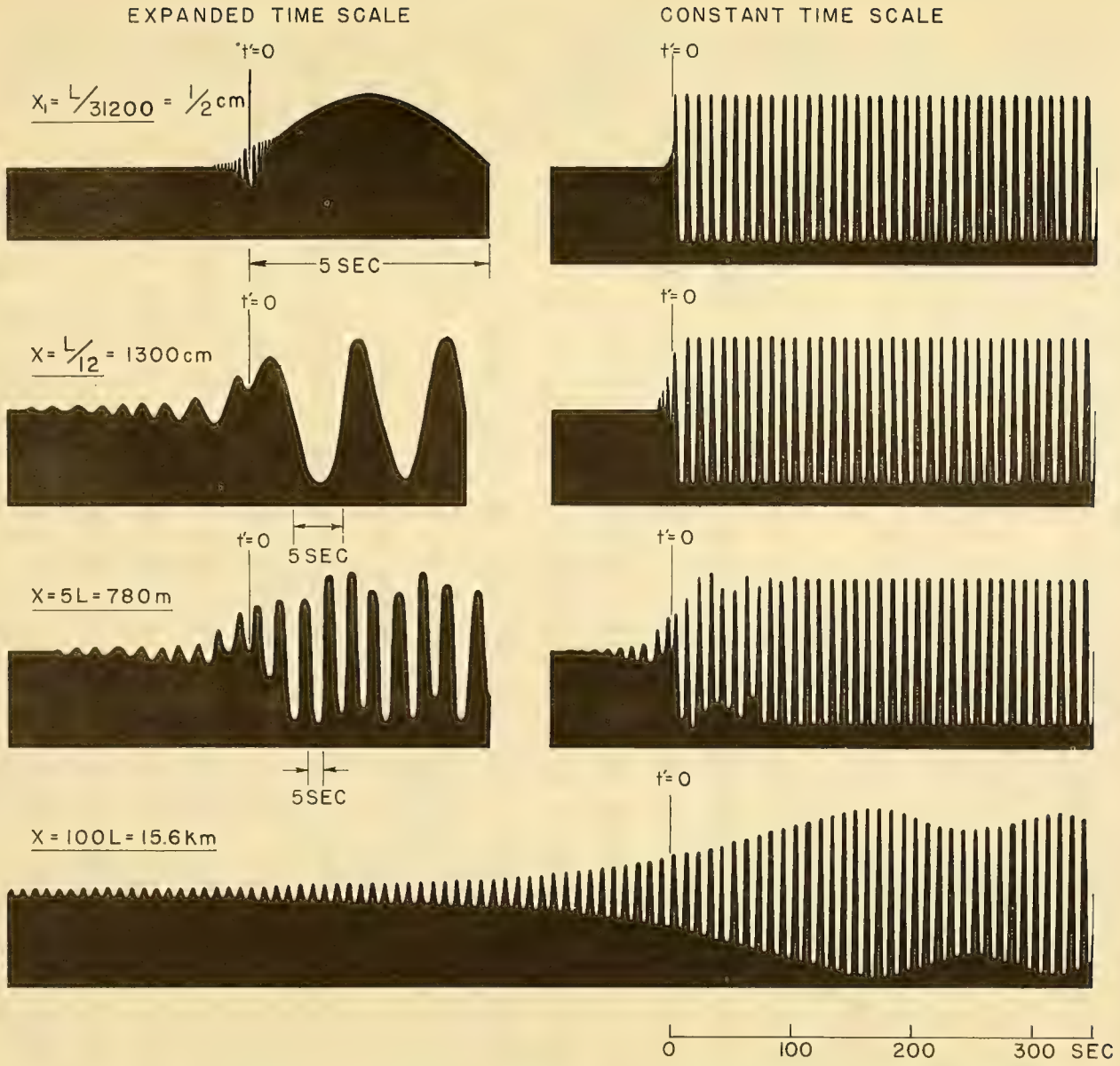

FIG 8. GRAPHS OF THE FINITE WAVE TRAIN AS A FUNCTION OF t' FOR VARIOUS VALUES OF X_1
T = 10 SEC n = 1800

varying functions of time such that they change slowly over several hundred seconds. Under these conditions, η (x_1,t') can be approximated by equation (2.8). The wave train now has an envelope given by $(G^*)^2 + (H^*)^2)^{1/2}$. Also since the most rapidly varying term is the sinusoidal term, the apparent local period is everywhere equal to T. However H^* and G^* still vary slowly with time so that the wave crests under the envelope will not all be in phase. The gradual phase shift with time is given by $\tan^{-1} H^*/G^*$.

It is also possible to compute the potential energy at each point by the use of equation (5.29). The potential energy can be averaged over one cycle; and by suitable approximations the averaged potential energy can be given as a slowly varying function of time by (5.30).

Figure 9 is a nomogram which permits the determination of the amplitude of the envelope of the wave train as a function of t' for fixed x_1 (and consequently t_g). The straight lines of various slopes in the bottom part of the figure are graphs of $t' = (4\pi x_1/g)^{1/2}K$ for various x_1 where K is the numerical value of the upper limit of integration in equations (5.26) and (5.27). When t' equals 2,000 seconds as in the example, and x_1 equals 439 kilometers, K equals 2.7. The envelope is graphed as a function of K in the upper graph. Thus, 2,000 seconds after t_g equals 10.63 hours which corresponds to x_1 equal to 439 km, the envelope is .92 times the amplitude of the waves in the original train. Note that the forward edge of the wave train passes the point x = 0 five hours before t = 0, and the forward edge actually takes 15.63 hours to travel the 439 kilometers. For this particular value of x_1 the waves build up from an amplitude

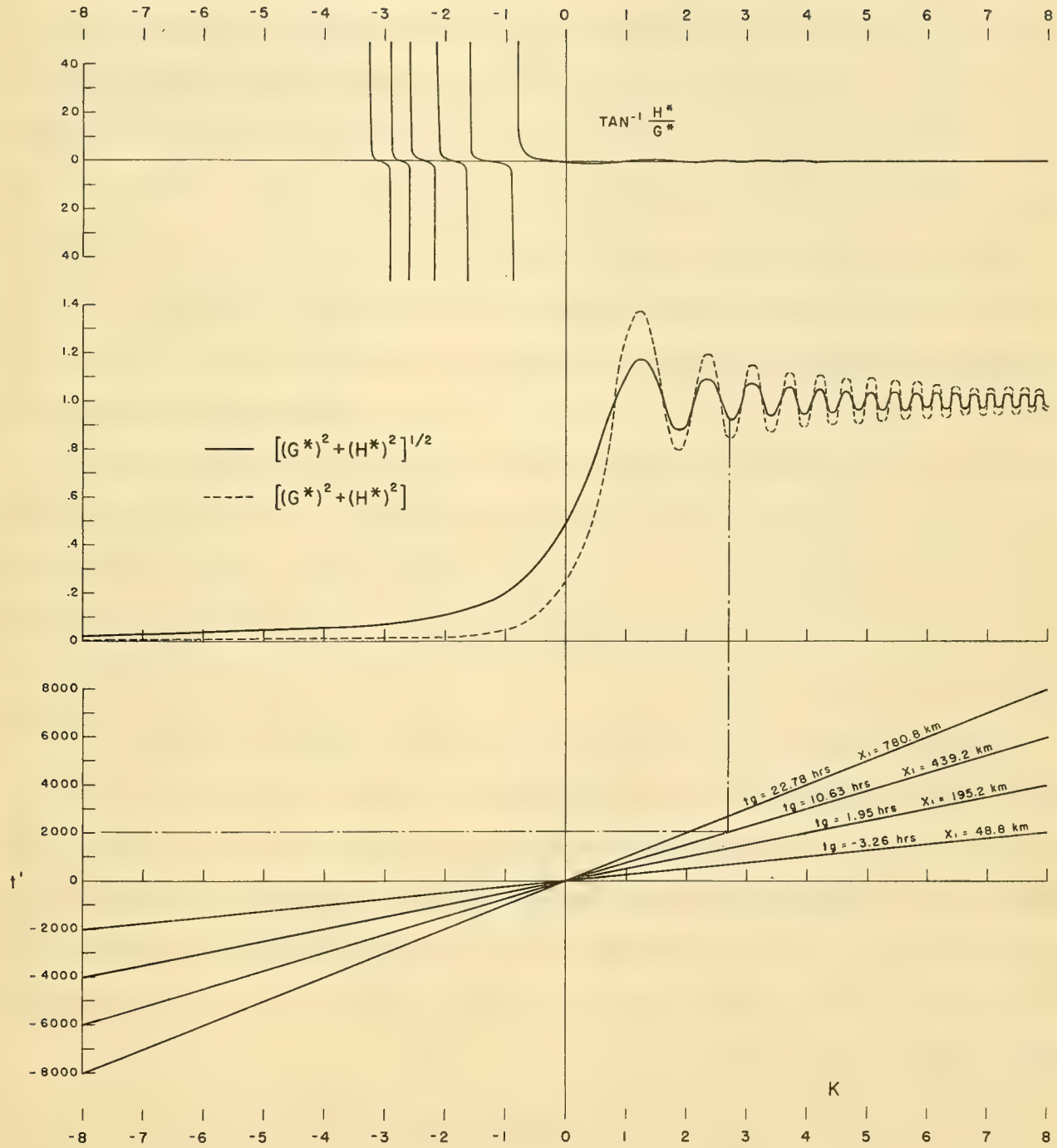

Fig. 9. Variation of the envelope, the average potential energy, and the phase of the crests for relatively large values of x_t as a function of t'.

of less than one tenth to maximum amplitude in 2300 seconds (38 minutes). This means that after the passage of 230 waves, the train is essentially constant in amplitude.

An analysis of equations (5.15), (5.16) and (5.17) would show that the trailing end of the wave train would pass near the time $t' = 2nT$ after the forward end. The procedure employed in the study of the forward end of the wave train could be employed to study the trailing end of the wave train, and similar equations and results could be obtained.

Between the time t' equals zero and $t' = 2nT$, for the example considered above there would always be essentially 3600 wave crests in the wave train. A few extra would be found before $t' = 0$ and after $t' = 2nT$. From $K = 0$ to $K = 4$ in figure 10, for the example considered above when x_1 equals 439 km there would be only 300 waves which are not quite of constant amplitude. At the trailing end, there would be another 300 waves. Thus only a total of 600 waves out of the 3600 waves, or 16.7%, would be modulated at the ends of the train.

Other quantities of interest are also graphed in figure 9. The relative amplitudes of the potential energy at various times is shown by the dashed graph. The gradual phase shift as a position of t' is also shown above the graphs of the envelope and the potential energy. In the forward part of the wave train before $t' = 0$, the phase shifts might cause waves which are not approximately sinusoidal in form.

For the relatively large values of x_1 employed in figure 9, the wave record as a function of t' which would be observed at x_1

can be graphed by first constructing the envelope and then by drawing in the wave crests with appropriate regard to phase.

There will be some point x_1, at which the approximations employed in equations (5.25), (5.26) and (5.27) begin to fail because the modulation on the rear edge of the wave train will lap over and combine with the modulation of the forward edge of the wave train. Figure 9 shows that the modulation is only important for 6000 seconds if x_1 = 439 km. Modulation which is effective for more than 18,000 seconds would affect the rear half of the train. Therefore an estimate of nine times 439 km or approximately 4,000 km is better than the previous crude estimate of 10,000 km for the point at which the use of equation (5.15) directly would be required in evaluating the solution.

Some objection might be raised on the physical reality of the problem because of the behavior of the solution near x_1 equal to zero. The unrealistic behavior is due to the discontinuous character of the functions employed. Wave trains in nature would not be so sharply delineated. To eliminate this objection, just consider the wave train as a function of time as it passes the point x_1 = 5 km. Let this value of x_1 be the new point of origin of the wave train. Then the new wave train at its starting point would have smoothed ends, and beyond the new reference point for all times the solution would be a well behaved function.

Summary

The behavior of the finite wave train can now be summarized. If the wave train takes a given number of hours to pass a given point, it will take essentially the same number of hours to pass

each subsequent point reached by the train in its forward travel. There will be a few extra low waves in advance of the train and a few more lagging behind the train, but there will be only a small percentage of extra crests produced which are of any appreciable amplitude. The forward end of the train will advance with the group velocity of the apparent local period of the waves in the train, and the trailing end will follow with that same group velocity. After a given distance of travel, the ends of the train will be modulated by a Fresnel interference pattern.

Eventually when x becomes very, very large, the wave train will have a much lower amplitude. As x approaches infinity, for n finite, the amplitude of the wave train approaches zero everywhere. All disturbances of initially finite duration and amplitude must eventually approach zero amplitudes because of dispersion.

The individual waves will be essentially constant in amplitude and period over the central part of the train. The crests will travel forward with a speed appropriate to the apparent local period of the waves in the train. Thus the individual crests are traveling with twice the speed of the train. Therefore they must form in the rear of the train, grow in amplitude, travel through the train, and die out again at the front of the train. At the ends of the train, a particular crest will not have a speed exactly equal to the speed in the center of the train, because of the effect of the phase shifts shown in equation (5.28). Wave crests are created and destroyed.

Agreement with classical theory

Finally, it should be pointed out that many of the abstract

points made by Lamb [1932] concerning the propagation of gravity waves in infinitely deep water, are illustrated in these two concrete exact solutions which have been presented. Two quotations from Lamb follow which illustrate this point.

> "It has often been noticed that when an isolated group of waves, of sensibly the same length, is advancing over relatively deep water, the velocity of the group as a whole is less than that of the individual waves composing it. If attention be fixed on a particular wave, it is seen to advance through the group, gradually dying out as it approaches the front, whilst its former place in the group is occupied in succession by other waves which have come forward from the rear."

> "Hence in the case of an isolated group the supply of energy is sufficient only if the group advance with half the velocity of the individual waves."

Note also that the solutions obtained in this paper give some information which is not described by Lamb [1932]. For example the solution for the finite wave group gives information about how the amplitude dies down and how the apparent wave periods change with time. The solution for the finite wave train gives information about how the ends of the train are modulated.

Comments

The finite wave train is an interesting study. It still has infinitely long crests, and it is still unrealistic in that respect. However, properly interpreted and modified it will be a building block in the formulation of the more realistic models.

Chapter 6. SOME MODEL WAVE SYSTEMS IN WHICH THE CRESTS ARE INFINITELY LONG

Introduction

The usual wave record today in deep water is observed as a function of time at a fixed point. A question arises as to whether this one record is enough to characterize the sea surface and as to whether it can be used as a forecasting tool. The actual short crested appearance of the sea surface and the finite width of the storm cannot be determined from this one observation. Some elementary results (without the use of time series theory) can be obtained which demonstrate some of the effects of dispersion, but they will be shown to be inadequate even for the case of infinitely long crests.

Equations (6.1) through (6.6) describe free surfaces as a function of time which might be observed at the edge of a storm at sea at the point $x = 0$ and $y = 0$. They increase in complexity, and they are described less and less precisely as functions. In equation (6.6), for example, $a_n(\mu)$ and $b_n(\mu)$ are unknown functions which would have to be described before anything could be said about the behavior of the sea surface either at the origin as a function of time or at other points.

Figure 10 shows portions of the graphs of $\eta_{II}(o,o,t)$, $\eta_{III}(o,o,t)$, and $\eta_{IV}(o,o,t)$. The first graph is regular and repeats itself exactly. The second graph was constructed by picking different values of A_n, δ_n, and θ_n at random for a few values and graphing the resulting function.

Model Wave Systems with Infinitely Long Crests

$$\eta(0,0,t) = A \sin \frac{2\pi t}{T} \tag{6.1}$$

$$\eta(0,0,t) = \begin{cases} A \sin \dfrac{2\pi t}{T} & -n\,T < t < n\,T \\ 0 & \text{otherwise} \end{cases} \tag{6.2}$$

$$\eta_{I}(0,0,t) = \sum_{n=-\infty}^{n=+\infty} A\, e^{-\sigma^2 (t-n\tau)^2} \sin \frac{2\pi(t-n\tau)}{T} \tag{6.3}$$

$$\eta_{II}(0,0,t) = \sum_{n=-p}^{n=+p} A\, e^{-\sigma^2 (t-n\tau)^2} \sin \frac{2\pi(t-n\tau)}{T} \tag{6.4}$$

$$\eta_{III}(0,0,t) = \sum_{n=-p}^{n=+p} A_n e^{-\sigma^2 (t-n\tau+\delta_n)^2} \sin\left(\frac{2\pi(t-n\tau+\delta_n)}{T} - \theta_n\right) \tag{6.5}$$

$$\eta_{IV}(0,0,t) = \sum_{n=-p}^{n=+p} \int_0^{\infty} \left[a_n(u)\cos u(t-n\tau+\delta_n) + b_n(u)\sin u(t-n\tau+\delta_n)\right] du \tag{6.6}$$

Examples.

$$\eta'_{IV}(0,0,t) = \frac{(t+300)^2}{100} e^{\frac{-(t+300)^2}{100}} \sin\left(\frac{2\pi}{T}(t+300) + \frac{\pi}{6}\right) + \frac{3}{2} e^{\frac{(t+200)^2}{20^2}} \sin\left(\frac{2\pi(t+200)}{10}\right)$$
$$+ \frac{20}{2\pi(t-100)} \sin \frac{2\pi(t+100)}{20} \cdot \cos\left(\frac{2\pi(t+100)}{10}\right) + \frac{(20)^2}{(2\pi)^2 t^2} \left(\sin \frac{2\pi t}{10}\right)^2 \sin\left(\frac{2\pi t}{10} + \frac{\pi}{4}\right)$$
$$+ \frac{3}{4} e^{\frac{-(t-100)^2}{10^2}} \sin\left(\frac{2\pi(t-100)}{10}\right) + \left(1 - \left(\frac{t-200}{20}\right)^2\right) e^{\frac{-(t-200)^2}{10^2}} \sin\left(\frac{2\pi(t-200)}{10} - \frac{\pi}{4}\right)$$
$$+ \frac{3}{4} \frac{25}{2\pi(t-300)} \sin \frac{2\pi(t-300)}{25} \sin\left(\frac{2\pi(t-300)}{10}\right). \tag{6.6a}$$

$$\eta''_{IV}(0,0,t) = \left[\frac{(t+300)^2}{100} e^{\frac{-(t+300)}{100}} + \frac{3}{2} e^{\frac{(t+200)^2}{400}} + \frac{20}{2\pi(t+100)} \sin \frac{2\pi(t+100)}{20}\right.$$
$$+ \frac{(20)^2}{(2\pi)^2 t^2} \left(\sin \frac{2\pi t}{20}\right)^2 + \frac{3}{4} e^{\frac{-(t-100)^2}{10^2}} + \left(1 - \frac{(t-200)^2}{20^2}\right) e^{\frac{(t-200)^2}{100}}$$
$$\left. + \frac{3}{4} \frac{25}{2\pi(t-300)} \sin \frac{2\pi(t-300)}{25}\right] \cdot \sin \frac{2\pi t}{10} \tag{6.6b}$$

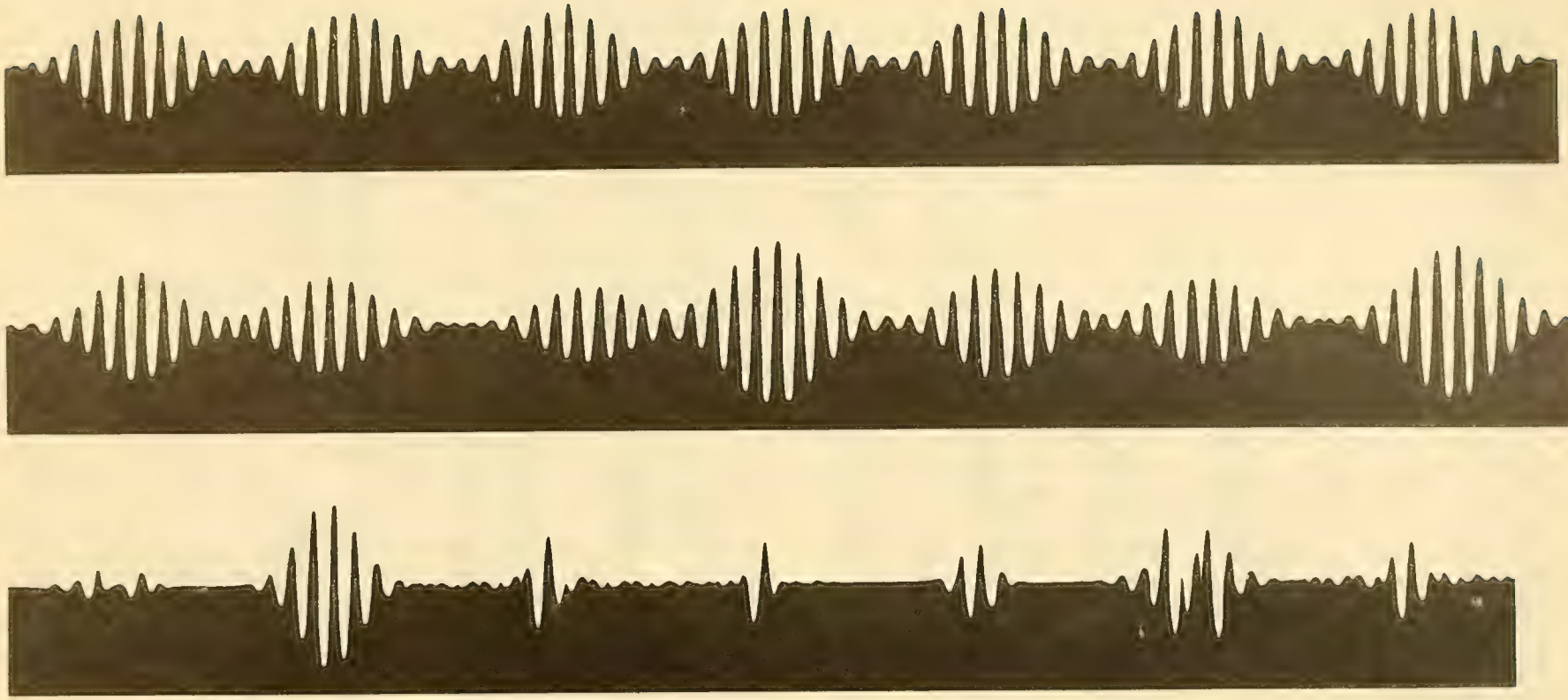

Fig.10. Graphs of Segments of Equations (6.4) (6.5) and (6.6 B)

Equation (6.6a) is a specific example of what equation (6.6) might look like after different functions had been picked for $a_n(\mu)$ and $b_n(\mu)$ and after integration over μ. It could be graphed as a function of t but the phase shifts indicated from group to group would require more precision than is warranted for the purposes of illustration. An easier function for purposes of illustration can be found by setting $a_n(\mu)$ equal to zero and the δ_n equal to zero. The "waves" under the envelope then factor out and the term in the bracket represents the overall envelope in equation (6.6b). Equation (6.6b) is the last graph in figure 10. The number of different functions which could be constructed according to equation (6.6) is limited only by the imagination. It will be left as a problem for the reader to solve to find out what the functions $a_n(\mu)$ and $b_n(\mu)$ are which yield equations (6.6a) and (6.6b). They are all smooth piecewise continuous and piecewise differentiable functions.

In this chapter, it will be assumed that the wave crests are infinitely long in the y direction. The results will then be independent of y, and a y could be substituted for the second zero in all of the equations of Plate XIV. It will therefore be omitted and the free surface will be treated as a function of x and t.

Equation (6.1) is trivial. If the wave is traveling in the positive x direction, the only possible motion is given by equation (2.19) where $\theta = 0$, $\delta = 3\pi/2$, and for infinitely deep water, $L = gT^2/2\pi$. The comments made on equation (2.19) still apply. If the observation were to represent a storm at sea, the storm would have started before the start of time, and it would never

end. Conditions would be the same at all points.

Equation (6.2) has been solved in Chapter 5. It is far too regular to represent a storm at sea. However it does start and stop at the origin, and the wave train actually travels and disperses so that it is observed at different times at different values of x. If 2nT is of the order of several hours, at each point, x, there is a time interval of several hours where the disturbance can be thought of as having the properties of equation (6.1). Outside of this time interval the waves have either not arrived at a point x, or they have passed the point x, and the sea surface is essentially undisturbed.

An infinite periodic train of wave groups

Equation (6.3) has not been treated before. It has the faults of equation (6.1), but it also has some other interesting features which make it worth studying. The function represented by equation (6.3) is periodic with a period, τ . Therefore it can be expanded into a Fourier Series of simple sine waves with discrete spectral components. Thus equation (6.7) shows that it is possible to represent the infinitely long periodic train by a sum such as the one given by the last expression in equation (6.8).

Each side of equation (6.8) is multiplied by $\sin 2\pi pt/\tau$ in equation (6.9). The function is odd and there will be no cosine terms. Integration of both sides of the equation from $-\tau/2$ to $\tau/2$, as shown by equations (6.10) and (6.11) yields the values of a_m. Equation (6.12) is then another representation for $\eta_I(o,t)$.

Equation (6.12) is much more informative than equation (6.3) because it is a sum of simple sine terms, and the classical theory

An Infinite Periodic Train of Wave Groups.

For Equation (6.3) $$\eta_I(0,t) = \eta_1(0,t+\tau) \tag{6.7}$$

$$\eta_I(0,t) = \sum_{n=-\infty}^{n=+\infty} A\, e^{-\sigma^2(t-n\tau)^2} \cdot \sin\left(\frac{2\pi}{T}(t-n\tau)\right) = \sum_{m=1}^{\infty} a_m \sin\frac{2\pi m t}{\tau} \tag{6.8}$$

$$\sum_{n=-\infty}^{n=+\infty} A e^{-\sigma^2(t-n\tau)^2} \sin\frac{2\pi}{T}(t-n\tau)\sin\frac{2\pi p t}{\tau} = \sum_{m=1}^{\infty} a_m \sin\frac{2\pi m t}{\tau}\sin\frac{2\pi p t}{\tau} \tag{6.9}$$

$$\int_{-\frac{\tau}{2}}^{\frac{\tau}{2}} a_m \sin\frac{2\pi m t}{\tau}\sin\frac{2\pi p t}{\tau}\,dt = \begin{cases} 0 & m \neq p \\ a_m\ \frac{\tau}{2} & m = p \end{cases} \tag{6.10}$$

$$\int_{-\frac{\tau}{2}}^{\frac{\tau}{2}} \sum_{n=-\infty}^{n=+\infty} A e^{-\sigma^2(t-n\tau)^2} \sin\frac{2\pi}{T}(t-n\tau)\sin\frac{2\pi m t}{\tau}\,dt = \int_{+\infty}^{-\infty} A e^{-\sigma^2 t^2} \sin\frac{2\pi t}{T}\sin\frac{2\pi m t}{\tau}\,dt$$

$$= \frac{\sqrt{\pi}A}{2\sigma}\left(-e^{-\left(\frac{2\pi m}{\tau}+\frac{2\pi}{T}\right)^2/4\sigma^2} + e^{-\left(\frac{2\pi m}{\tau}-\frac{2\pi}{T}\right)^2/4\sigma^2}\right) \tag{6.11}$$

$$\eta_I(0,t) = \sum_{m=1}^{\infty} \frac{\sqrt{\pi}A}{\sigma\tau}\left(-e^{-\left(\frac{2\pi m}{\tau}+\frac{2\pi}{T}\right)^2/4\sigma^2} + e^{-\left(\frac{2\pi m}{\tau}-\frac{2\pi}{T}\right)^2/4\sigma^2}\right)\sin\frac{2\pi m t}{\tau} \tag{6.12}$$

$$\eta_I(x,t) = \sum_{m=1}^{\infty} \frac{\sqrt{\pi}A}{\sigma\tau}\left[-e^{-\left(\frac{2\pi m}{\tau}+\frac{2\pi}{T}\right)^2/4\sigma^2}\sin\left(\frac{4\pi^2 m^2 x}{g T^2} + \frac{2\pi m t}{\tau}\right)\right.$$

$$\left. - e^{-\left(\frac{2\pi m}{\tau}-\frac{2\pi}{T}\right)^2/4\sigma^2}\sin\left(\frac{4\pi^2 m^2 x}{g\tau^2} - \frac{2\pi m t}{\tau}\right)\right] \tag{6.13}$$

gives information on the correct spectral wave length to assign to each discrete spectral period. In equation (6.13), these wave lengths are assigned to the periods, and complete knowledge of the behavior of equation (6.3) at other x has now been obtained. Some of the waves are assigned to travel in the negative x direction in order to obtain complete agreement with the results of Chapter 4.

For a fixed t, the sea surface as described by equation (6.13) is periodic as a function of x. The wave lengths involved are given by $L = g\tau^2/2\pi m^2$, and they decrease in length by one over the square of the integers.

Alternate solution

An alternate solution to equation (6.3) is also possible with the use of the results of Chapter 4. If, in equation (4.9), $t - n\tau$ is substituted for t, and then if the equation is summed from n equals minus infinity to plus infinity, an alternate solution is the result. The alternate solution is horribly difficult to evaluate and interpret. It represents a sort of blind alley with little practical application. The difficult terms and derivations of Chapter 4 would have to be analyzed and summed over many values of n before a result would be obtained. For comparison, in equation (6.13) for typical values of σ and T, only about ten terms are important in the sum, and the evaluation and interpretation is quite simple.

A finite train of regular wave groups

In equation (6.12), for typical values of σ , τ , and T, the first term in parenthesis is negligible and it is therefore neglected

in equation (6.14). Also for typical values of σ , τ , and T, the finite wave groups in equation (6.4), are essentially zero outside of the interval $n\tau - \tau/2 < t < n\tau + \tau/2$. It then follows that an adequate representation for equation (6.4) is given by equation (6.14) by simply chopping off the infinitely long (in time) function given by equation (6.12).

Equation (6.14) is a sum of terms each of which is similar to the finite wave train studied in Chapter 5. The apparent period of the wave is given by τ/m, and if $p\tau + \tau/2$ is equal to an integer, say, q times τ/m, the results of Chapter 5 will apply. (Note, q τ/m corresponds to nT of Chapter 5.) Equation (6.15) then yields equation (6.16) which shows that q is an integer if m is even.

For even values of m, then, equation (6.14) can be expressed as the first condition of equation (6.17), and for odd m, the second expression can be applied. The results of Chapter 5 apply directly to each of the terms in the sum for even m. For odd values of m, a problem similar to the one solved in Chapter 5 would have to be solved. Formulated in terms of the notation of Chapter 5, the problem would be to find $\eta(x,t)$ given that $\eta(o,t) = A \sin 2\pi t/T$ for $-nt - T/2 < t < nT + T/2$ and $\eta(o,t) = 0$ otherwise. The solution can be found easily by the methods employed before, and the results are not essentially different from the results of Chapter 5.

The finite regular train of wave groups is therefore composed of a sum of finite wave trains of amplitude, a_m, and period, τ/m. Each train requires $(2p + 1)\tau$ seconds to pass the point x equal to zero.

The forward edge and the trailing edge of each train advance

A Finite Train of Regular Wave Groups.

$$\eta_{II}(0,t) = -\sum_{m=1}^{\infty} \frac{\sqrt{\pi}A}{\sigma\tau} e^{-\left(\frac{2\pi m}{\tau} - \frac{2\pi}{T}\right)^2 / 4\sigma^2} \sin\frac{2\pi m t}{\tau} = \sum_{m=1}^{\infty} a_m \sin\frac{2\pi m t}{\tau}$$

$$\text{if } -\left(p+\tfrac{1}{2}\right)\tau \le t \le \left(p+\tfrac{1}{2}\right)\tau$$

$$\eta_{II}(0,t) = 0 \qquad \text{otherwise} \tag{6.14}$$

$$\left(p+\tfrac{1}{2}\right)\tau = q\frac{\tau}{m} \tag{6.15}$$

$$q = mp + \frac{m}{2} \tag{6.16}$$

$$\eta_{II}(0,t) = \begin{cases} \sum_{m=2,4,\cdots}^{\infty} a_m \sin\frac{2\pi m t}{\tau} \\ \sum_{m=1,3,5\cdots}^{\infty} a_m \sin\frac{2\pi m t}{\tau} \\ 0 \end{cases} \quad \begin{array}{l} \text{if } -\left(mp+\frac{m}{2}\right)\frac{\tau}{m} \le t \le \left(mp+\frac{m}{2}\right)\frac{\tau}{m} \\ \\ \text{otherwise} \end{array} \tag{6.17}$$

Plate XVI

with the group velocity appropriate to waves with a period τ/m, and the edges are modulated by the Fresnel pattern discussed in detail in Chapter 5. The first train has a period of τ seconds and an amplitude of $(\sqrt{\pi}A/\sigma\tau)\exp(-(2\pi/\tau - 2\pi/T)^2/4\sigma^2$. The second train has a period of $\tau/2$ seconds and an amplitude of $(\sqrt{\pi}A/\sigma\tau)\exp(-(2\pi 2/\tau - 2\pi/T)^2/4\sigma^2)$. The periods of the waves which would propagate into the area of decay, for τ = 100 seconds, would be 100 seconds, 50 seconds, 33.3 seconds, 25 seconds, 20 seconds, 16.7 seconds, 14.3 seconds, 12.5 seconds, 11.1 seconds, 10 seconds, and so forth through 4 seconds for m = 25, 2 seconds for m = 50, and 1 second for m = 100. If T were 10 seconds the train with a 10 second period would have a maximum amplitude and for typical values of σ the trains with one and one hundred second periods would be very low.

For the values of σ = 1/20 $\sec^{-1}$, T = 10 sec, and A = 5 meters, and for τ = 100 seconds, the amplitude of the 100 second component would be less than 10^{-12} meters, and the amplitude of the 10 second component would be 3.55 meters.

If p were equal to 180, the wave system represented by equation (6.4) would require ten hours and two minutes (36,100 seconds) to pass the point x = 0. From the derivation, this wave system can be broken down into a number of wave trains of different spectral periods and each wave train would advance with its own group velocity into the area of decay. Each wave train would take essentially 10 hours to pass a point in the area of decay, but they would pass at different times.

For the chosen values of parameters for equation (6.4), only

periods ranging from 17 seconds to 7 seconds are important. All others are associated with wave trains less than one-half centimeter in height. The spectral periods, the wave train amplitude, and the 1000 km travel times are shown in Table 14. The sum of the heights (crest to trough) in Table 14 is 10 meters within the accuracy of the computations so that the amplitude at phase reinforcement equals the maximum crest to trough height of the wave groups in equation (6.4).

Table 14. Component periods, amplitudes, and 1000 km travel times for the important wave trains in equation (6.4).

m	Period (seconds)	Amplitude (meters) (crest to trough)	Travel time of forward edge to a point 1000 km away
1	100	$< 10^{-12}$	-----
6	16.7	.006	21.4 hrs.
7	14.3	.094	25.0 hrs
8	12.5	.755	28.5 hrs
9	11.1	2.39	32.0 hrs
10	10.0	3.53	35.6 hrs
11	9.09	2.39	39.2 hrs
12	8.33	.755	42.7 hrs
13	7.69	.094	46.3 hrs
14	7.14	.006	49.8 hrs

Figure 11 shows the effect of dispersion on the original wave system. The waves which would be observed at a point 1000 km away are shown on a time-period coordinate system. A sinusoidal wave train with a crest to trough height of .6 cm would arrive 21.4 hours after the wave system started at x equal to zero, as shown on the first bar in the upper left of the figure. It would pass

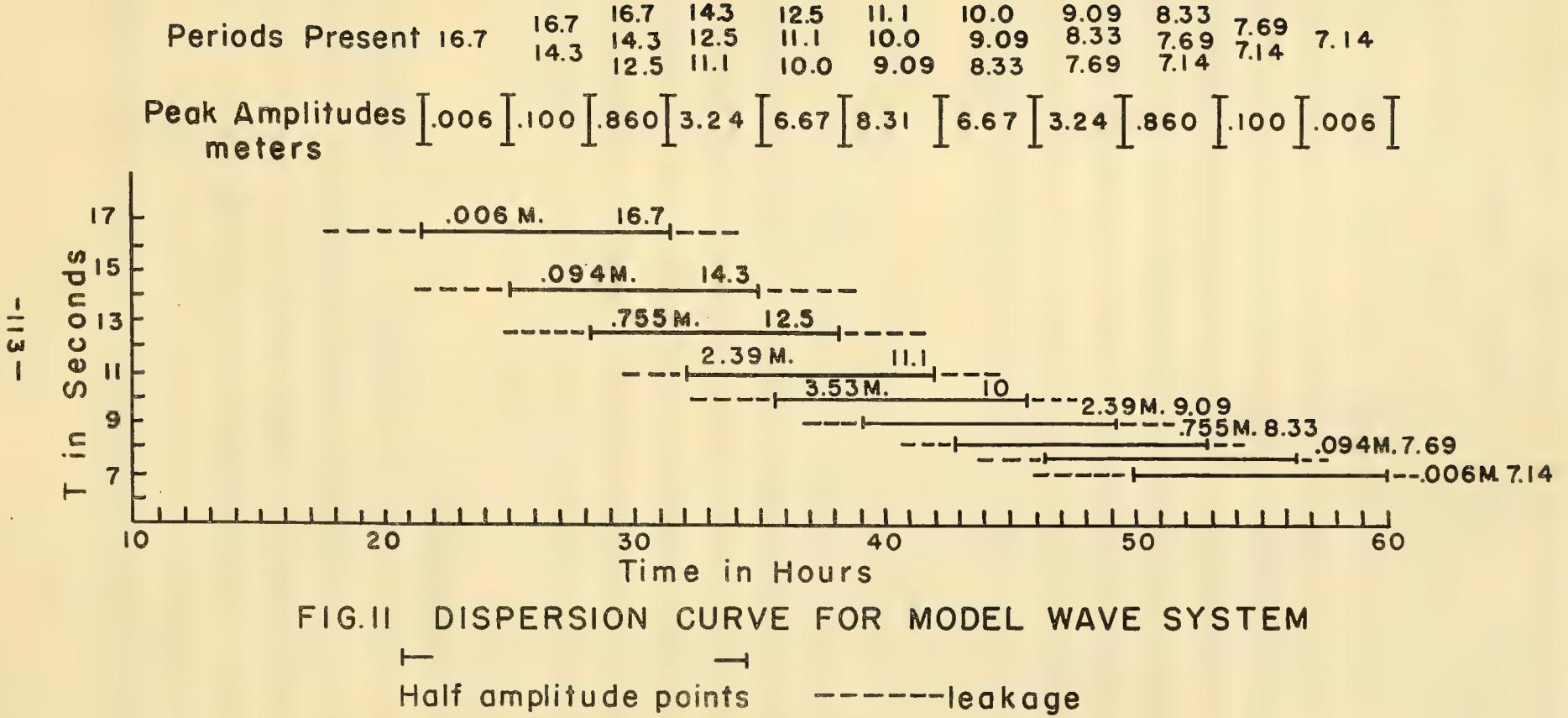

FIG. II DISPERSION CURVE FOR MODEL WAVE SYSTEM

Half amplitude points ------leakage

completely in ten hours, and 31.4 hours after the start of the wave system at x equal to zero the component would no longer be present. Similar remarks can be made about each bar in the diagram. When the various bars of the diagram overlap the sea surface is the sum of the various sinusoidal terms indicated. Sine waves of different periods will sometimes add to a maximum and sometimes cancel to a minimum. In fact, there will be a point of phase reinforcement every 100 seconds in this model. The maximum wave heights present are therefore just the sums of the amplitudes of the components. The peak amplitudes are shown above the dispersion diagram as a function of time along with the periods which go to make up the peak heights.

The forerunners of swell discussed in the literature are clearly shown in this model. This swell will be more regular than the original model waves. What is of more interest is the trailing end of short period waves which is not discussed or emphasized as much in the literature. The waves which arrive after 42 hours will have periods less than the apparent period in the original storm, and the question as to why they are not observed more often arises.

Alternate formulations

The results shown by equations (6.14) through (6.17) can be obtained in an alternate form by finding the spectrum of equation (6.4), and by making an approximation to the integration to be carried out. The alternate derivation is given by Pierson [1951] in another paper.

An exact solution can also be found by the substitution of

$t - n\tau$ for t in equation (4.9) followed by a summation from $n = -p$ to $n = +p$. The same difficulties apply to this formulation of the solution that applied to the alternate solution for the infinitely long (in time) periodic train of finite wave groups.

Energy considerations

The results so far obtained have been derived from the classical theory. There is no physical mechanism in the mathematics which would result in the degradation of energy from kinetic and potential energy to heat energy from the effects of friction. There is one effect present, namely dispersion, which spreads out the energy in time and space that was originally concentrated at the origin.

The potential energy at an instant of time for a unit area of the sea surface is given by equation (6.18). In classical theory in which waves are considered to be purely sinusoidal, it is permissible to average over one wave length or over one period and to discuss the average as an average over one cycle of the potential energy. For irregular wave records, such as equation (6.5), this process is inadequate.

Any record of the sea surface obtained as a function of time can be treated by equation (6.19). If $\overline{T}$ is increased, for different t^*, then the average potential energy may settle down to a constant value in which $\overline{P.E.}$ would be independent of time.

All of the wave records discussed herein are built up of simple sine waves, and for sine waves the potential energy averaged over time at a fixed point equals the kinetic energy averaged over time at a fixed point. This principle is also true if the disturbance

is composed of infinitesimal waves added together by means of Fourier Integrals. If the potential energy can be accounted for, the kinetic energy can be accounted for; and the total energy is therefore accounted for. For additional information, see Lamb [1932].

The problem, then, is to construct a balance sheet for all the energy in the system at $x = 0$ and show that that energy is finally observed at $x = x_1$ without loss. The potential energy will be traced, and since an equal amount of kinetic energy must be present, the total energy will be accounted for.

Equation (6.19) can be applied to an ordinary sinusoidal wave for an introductory elementary example. This is done in equation (6.20) where η equals $-A \sin(4\pi^2 x/gT^2 - 2\pi t/T)$. The last expression in equation (6.20) is a function of $\bar{T}$, t^*, and x. For any x and t^* as $\bar{T}$ becomes large, $\overline{P.E.}$ is given by equation (6.21). The two sine terms can be at most two in absolute value for a fixed x, t^*, and $\bar{T}$, and if $\bar{T}$ is of the order of ten times the period, $\overline{P.E.}$ differs from its limiting value by less than two per cent. The result shows that the same average potential energy is present at any point in space at any time.

Energy balance for the infinite period train of wave groups

The infinite periodic train of wave groups (equation (6.3)) can be written as an infinite sum of sinusoidal waves as in equation (6.8) and (6.13). If the waves which travel in the negative x direction are omitted because they are negligible, the a_m would be defined by the top part of equation (6.14). (See the discussion at the beginning of the section on the finite

Energy Considerations.

Potential Energy per unit area.

$$P.E. = \rho g \frac{\eta^2}{2} \tag{6.18}$$

Potential Energy per unit area averaged over time

$$\overline{P.E.} = \frac{1}{\bar{T}} \int_{t^*}^{t^*+\bar{T}} \rho g \frac{\eta^2}{2} dt \tag{6.19}$$

$$\overline{P.E.} = \frac{1}{\bar{T}} \int_{t^*}^{t^*+\bar{T}} \frac{\rho g}{2} A^2 \left(\sin\left(\frac{4\pi^2 x}{gT^2} - \frac{2\pi t}{T}\right)\right)^2 dt = \frac{\rho g A^2}{4\bar{T}} \int_{t^*}^{t^*+\bar{T}} \left(1 - \cos\left(\frac{8\pi^2 x}{gT^2} - \frac{4\pi t}{T}\right)\right) dt$$

$$= \frac{\rho g A^2}{4} \left[1 + \frac{T}{4\pi\bar{T}} \left(\sin\left(\frac{8\pi^2 x}{gT^2} - \frac{4\pi(t^*+\bar{T})}{T}\right) - \sin\left(\frac{8\pi^2 x}{gT^2} - \frac{4\pi t^*}{T}\right)\right)\right] \tag{6.20}$$

for $\bar{T} = kT$ or as $\bar{T} \longrightarrow \infty$

$$\overline{P.E.} = \frac{\rho g A^2}{4} \tag{6.21}$$

$$\overline{P.E.} = \frac{1}{\bar{T}} \int_{t^*}^{t^*+\bar{T}} \rho \frac{g}{2} \left(-\sum_{m=1}^{\infty} a_m \sin\left(\frac{4\pi^2 m^2 x}{g\tau^2} - \frac{2\pi m t}{\tau}\right)\right)^2 dt = \frac{1}{\bar{T}} \int_{t^*}^{t^*+\bar{T}} \rho \frac{g}{2} \sum_{m=1}^{\infty} a_m^2 \left(\sin\left(\frac{4\pi^2 m x}{g\tau^2} - \frac{2\pi m t}{\tau}\right)\right)^2 dt$$

$$+ \frac{1}{\bar{T}} \int_{t^*}^{t^*+\bar{T}} \rho \frac{g}{2} \sum_{m=1}^{\infty} \sum_{\substack{q=1 \\ m \neq q}}^{\infty} a_m a_q \sin\left(\frac{4\pi^2 m^2 x}{g\tau^2} - \frac{2\pi m t}{\tau}\right) \sin\left(\frac{4\pi^2 q^2 x}{g\tau^2} - \frac{2\pi q t}{\tau}\right) dt \tag{6.22}$$

$$\lim_{\bar{T} \to \infty} \overline{P.E.} = \sum_{m=1}^{\infty} \frac{\rho g}{4} a_m^2 = \frac{\rho g}{4} \frac{\pi A^2}{4\sigma^2 T^2} \sum_{m=1}^{\infty} e^{-\left(\frac{2\pi m}{\tau} - \frac{2\pi}{T}\right)^2 / 2\sigma^2} \tag{6.23}$$

for fixed $x = x_1$ and $t = t^*$

$$\overline{P.E.} \cong \begin{cases} \rho \frac{gA^2}{4} & \text{if } -nT + E(x_1, n, T) < \frac{4\pi x_1}{gT} - t^* - \bar{T} < nT - E(x_1, n, T) \\ & \text{and} \\ 0 & \text{if } -nT + E(x_1, n, T) < \frac{4\pi x_1}{gT} - t^* < nT - E \\ & \text{if } \frac{4\pi x_1}{gT} - t^* < -nT - E(x_1, n, T) \\ & \text{or if } 4\pi x_1 - t^* + \tau < nT + E(x_1, n, T) \end{cases} \tag{6.24}$$

$$\overline{P.E.} \cong \frac{\rho g}{4} \sum_{m=k}^{m=k+n} a_m^2$$

if m satisfies the inequalities

$$-p(\tau + \tau/2) + E(x_1, \tau/m, p) < \frac{4\pi m x_1}{g\tau} - t_1^* < p(\tau + \tau/2) - E(x_1, \tau/m, p)$$

$$\text{and } -p(\tau + \tau/2) + E(x_1, \tau/m, p) < \frac{4\pi m x_1}{g\tau} - t^* - \bar{T} < p(\tau + \tau/2) - E(x_1, \tau/m, p) \tag{6.25}$$

regular train of wave groups.) $\overline{P.E.}$ can then be given by equation (6.22).

The process of squaring a sum of terms is carried out in the second expression in equation (6.22). The sum of the squared terms occurs in the first integral, and a sum of cross product terms involving two different wave lengths and two different periods (τ/m and τ/q) occurs in the second integral. In the second integral, the product of two sines with two different arguments is given by half the cosine of the difference of the arguments minus half the cosine of the sum of the arguments. Thus each term in the second integral is sinusoidal, with τ as the greatest possible period, and the average of a sinusoidal term is zero.

The first integral in the second expression for equation (6.22) is a sum of integrals like those treated in equation (6.20). Each term can be treated like equation (6.20) was treated. Since each term of the first integral yields an average if $\overline{T}$ is large, the limit for large $\overline{T}$ is given by equation (6.23). More refined investigation would show that if $\overline{T}$ were of the order of ten or twenty times τ , the averaged value of the potential energy would be within a few per cent of the limiting value.

The results show that the potential energy of the sea surface averaged over a fairly long time for the infinite periodic train of wave groups is the same everywhere at any time. The disturbance studied never started and it will never stop. It covers the whole xy plane.

Energy balance for the finite wave train

In Chapter 5, it was shown that the forward edge and the rear edge of the finite wave train travel forward with the group velocity of the waves under the envelope and that the edges are modulated by appropriate combinations of the Fresnel Integrals. The disturbance is present at a given x_1 for only 2nT seconds approximately. Therefore if equation (6.19) is applied to the solution, for any t^*, and if $\bar{T}$ is allowed to approach infinity $\overline{P.E.}$ will become zero. The potential energy averaged over a long long time after any initial time at any fixed point is zero.

But at a given $x_1 > 0$, the disturbance is present for 2nT seconds, and the 2nT seconds could stand for ten or twenty hours. If, in equation (6.19), t^* were a time after the train had arrived and if $t^* + \bar{T}$ were a time before the train had passed, then $\overline{P.E.}$ would very nearly equal $\rho g A^2/4$. Note that for the elementary cases discussed above, the average over ten cycles is only two per cent in error.

The modulation of the edges has to be considered, and the value of $\overline{P.E.}$ is not given by $\rho g A^2/4$ if equation (6.19) is evaluated in the modulation zone.

Equation (6.24) formulates the above discussion in terms of inequalities. Apart from the modulation effects of the edges expressed schematically by $E(x_1, n, T)$ (a positive number), the value of $\overline{P.E.}$ will be approximately $\rho g A^2/4$ if the first inequalities indicated are satisfied and it will be approximately zero if the second two inequalities are satisfied. If none of the

four inequalities are satisfied, $\overline{P.E.}$ is of some value between $\rho g A^2/4$ and zero.

The average potential energy at the modulated edge of the train was discussed in Chapter 5. Figure 9 shows that at least to the eye the area under the dashed curve is equal to the area under a jump function given by $f(t) = 0$ for $t < t_g$ and by $f(t) = 1$ for $t > t_g$.

To a good degree of approximation, then, the potential energy averaged over a time short compared to the total duration of the train but long compared to a cycle is constant when the train is present at the point of observation. Since the train, if it has not traveled too far, takes $2nT$ seconds to pass, the total amount of energy present is the same as at the origin at each point of observation.

For great distances of travel, dispersion modifies the results, and $\overline{P.E.}$ decreases. No energy is lost; it is just spread out over a greater time interval.

Energy balance for the finite regular train of wave groups

The finite regular train of wave groups was broken up into finite wave trains of different periods. At a given point of observation, x_1, some trains will be present, some will have passed, and some will not have arrived as shown by figure 11. If the train for m equal to K is present, and if the train for m equal to K + M is present, then the trains for m for values in between will be present. Equation (6.25) expresses this formally. Over a long enough time, all of the energy in the original record is accounted for at each point of observation.

The inadequacy of all of the models in this chapter

Even if the waves on the sea surface had infinitely long crests, the models studied in this chapter would be inadequate for very subtle reasons which will be discussed in the next chapter. For these reasons, equations (6.5) and equations (6.6) were only indicated in Plate XIV. Various approximate results based upon the assumption that the individual groups in the sum of wave groups do not overlap to the extent that the potential energy associated with one group is affected by the presence of the neighboring groups can be obtained. The difficulty in the analysis of equations (6.5) and (6.6) lies in the fact that it appears that the wave record cannot be expressed as the sum of a number of sine waves in a form which applies to the whole sea surface. Even the most general model described by $\eta_{IV}(o,o,t)$ could not be made to fit an actual observation of waves on the sea surface. The methods of Fourier Integral theory have been pushed as far as practicable, and it becomes necessary to introduce new concepts in order to obtain more realistic models.

Chapter 7. THE MOST REALISTIC WAVE SYSTEMS WITH INFINITELY LONG CRESTS

Introduction

In Chapter 6, model wave systems were derived which became increasingly more complex throughout the chapter. The most general wave system mentioned only briefly in the last chapter depended on the assumption that the waves came in groups separated by an average time interval, τ , throughout the storm and that the waves were low near the times $t = n\tau + \tau/2$.

If sample wave records are examined, it will be found that portions of the record do exhibit groups which appear to be of a length τ . But also it will be found that there are long stretches of the record which do not show groups, and which appear to be just irregular bumps of assorted heights and various time separations of the crests. Such records are not adequately described by any of the models which were discussed in the previous chapter.

The author has spent many hours in conversations with those whose activities are connected with waves. Along the New Jersey coast, for example, a fisherman once solemnly informed him that "every seventh wave was the highest." Another fisherman was equally positive that every fifth wave was the highest. In fact, opinion was well scattered over all values from three to seven. A fisherman (or for that matter, any one) with a profound faith in any one of these particular integers will some day be bowled over by a wave higher than either its

predecessors or successors with a label "favorite integer plus two." The sea surface is irregular; it does appear that the waves sometimes come in groups, but the groups do not persist, they do not have a mean time of separation, and they do not contain the same number of waves.

Figure 12 shows some wave records. They are on a greatly condensed time scale such that the crests are all crowded together. Note the basic features of these wave records. Isolated high waves frequently occur as at the points marked A. Sometimes groups appear as in the intervals marked B. At times the trend in the amplitudes is quite high as in the intervals marked C. And at other times the trend in the amplitudes is quite low as in the intervals marked D. The basic feature of the records is their irregularity, which is a type of irregularity which would almost appear to defy an adequate mathematical representation. Obviously any of the mathematical models employed in the past chapters do not represent such a wave record. Consequently, better models must be found.

The next step then in increasing complexity is to find some way to represent the sea surface which is general enough to include this very irregular pattern. It will be found that Fourier Integral Theory is not enough and that an extension to a type of Lebesgue Stieltjes Integral is needed.* The extension to this type of integral and the inclusion of some very interesting statistical methods simplify the problem once the basic concepts are understood and permits a tremendous stride

*The Lebesgue-Stieltjes Integral is defined in James and James [1949] for example.

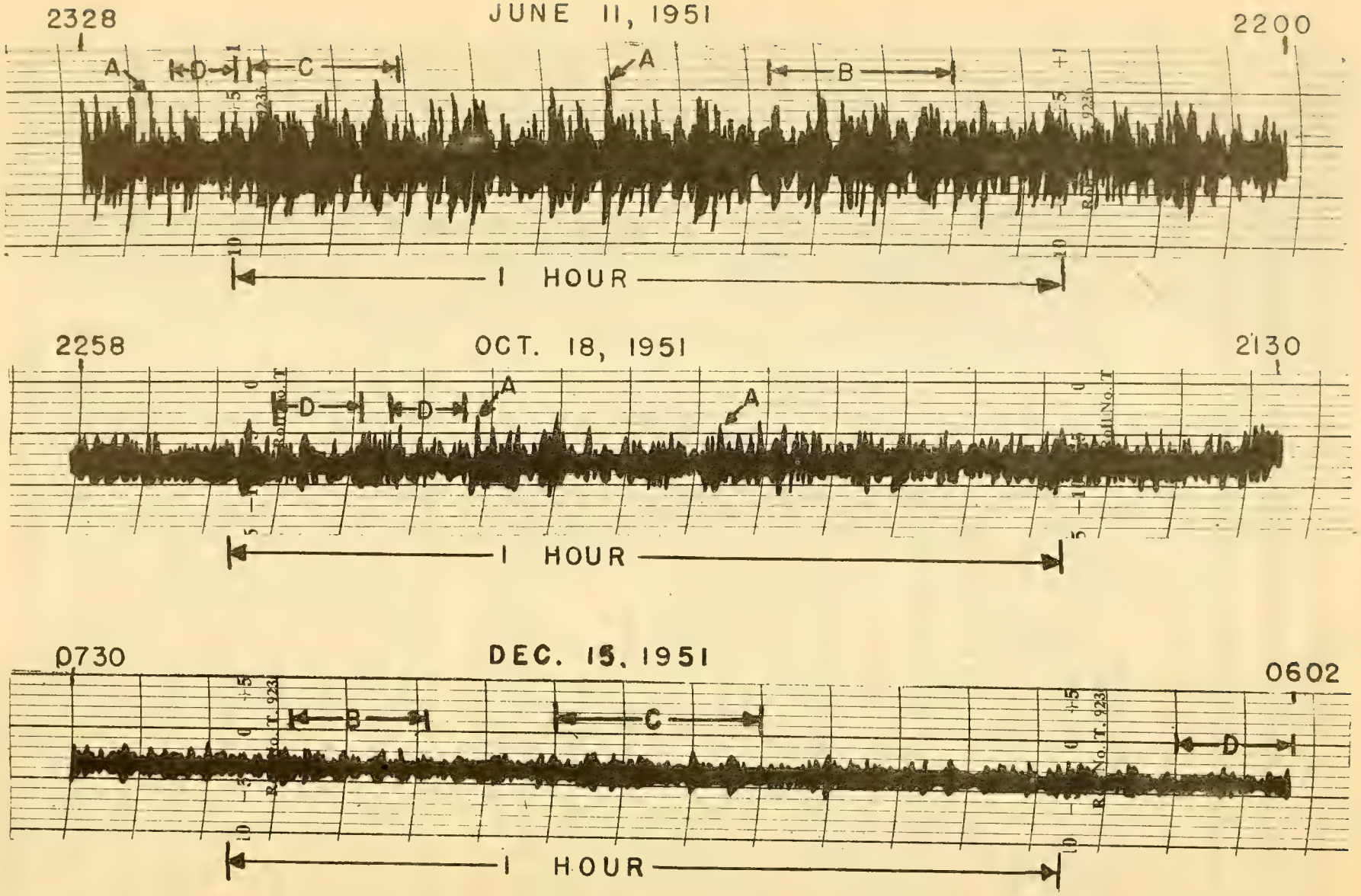

FIG. 12 SOME VERY CONDENSED SAMPLE WAVE RECORDS.

forward in the problem of understanding and forecasting ocean waves.

The generalization which will be developed in this chapter will make it apparent that the finite irregular train of wave groups mentioned in the last chapter as given in equation (6.5) involves too many special assumptions to permit its development to a completely realistic case.

The Lebesgue Stieltjes Power Integral

In order to extend the techniques of wave analysis, it is necessary to discuss a new type of integral which is well established in theoretical mathematics, but which is unfamiliar to many people. The ordinary Riemann Integral is the one which is well known. The concepts of the Lebesgue Integral and the Stieltjes Integral are employed in theoretical statistics, and Cramer [1946] is a reference for such a study. No attempt will be made for complete mathematical detail and for complete generality, but the derivation will be general enough to include those properties which are needed for wave record analysis. The reader who is interested in greater detail is referred to Tukey and Hamming [1949], Tukey [1949], Levy [1948], Cramer [1946], and Wiener [1949]. The methods by which these concepts can be applied to wave analysis most directly are given by Tukey and Hamming [1949], and many of the arguments herein will be based upon quotations from and explanations by Tukey and Hamming [1949] and Tukey [1949].

Consider the Lebesgue Stieltjes Power Integral given by equation (7.1). $\eta(t)$ is the free surface as a function of

$$\eta(t) = \int_0^{\infty} \cos(\mu t + \psi(\mu)) \sqrt{dE(\mu)} \tag{7.1}$$

where $E(\mu) = 0$ for $\mu \leq 0$ (7.2)

and $E(\mu_1) \leq E(\mu_2)$ if $0 \leq \mu_1 < \mu_2$ (7.3)

and $E(\mu) < M$ for all μ (7.4)

which implies that

$$\lim_{\mu \to \infty} E(\mu) = E_{MAX} \tag{7.5}$$

consider a one dimensional net given by

$$0 < \mu_1 < \mu_2 < \mu_3 < \cdots < \mu_k < \mu_{k+1} < \mu_{k+2} < \cdots < \infty \tag{7.6}$$

then

$$\eta(t) = \lim_{\substack{\max(u_{k+1} - u_k) \to 0 \\ \mu_{2R} \to \infty}} \sum_{n=0}^{r} \sqrt{E(\mu_{2n+2}) - E(\mu_{2n})} \cdot \cos(\mu_{2n+1} t + \Psi(\mu_{2n+1})) \tag{7.7}$$

where $0 \leq \Psi(\mu_{2n+1}) \leq 2\pi$ (7.8)

Partial Sum

$$\eta(t) = \sum_{n=0}^{r} \sqrt{E(\mu_{2n+2}) - E(\mu_{2n})} \cdot \cos(\mu_{2n+1} t + \Psi(\mu_{2n+1})) \tag{7.9}$$

$\min(\mu_{k+1} - \mu_k) = \Delta_1 \mu$

$\max(\mu_{k+1} - \mu_k) = \Delta_2 \mu$

$$\overline{P.E.} = \lim_{\bar{T} \to \infty} \frac{\rho g}{2\bar{T}} \int_{t^*}^{t^* + \bar{T}} (\eta(t))^2 dt = \lim_{\substack{r \to \infty \\ \Delta_2 \mu \to 0}} \sum_{n=0}^{r} \left[E(\mu_{2n+2}) - E(\mu_{2n}) \right] \cdot \left[\frac{\rho g}{4} \right]$$

$$= \lim_{\substack{\mu_2 \bar{T} \to \infty \\ \Delta_2 \mu \to 0}} \frac{\rho g}{4} \sum_{n=0}^{r} \left[-E(\mu_{2n}) + E(\mu_{2n+2}) \right]$$

$$= \lim_{\substack{\mu_2 \bar{T} \to \infty \\ \Delta_2 \mu \to 0}} \frac{\rho g}{4} \left[(-0 + E(\mu_2)) + (-E(\mu_2) + E(\mu_4)) + \cdots (-E(\mu_{2r}) + E(\mu_{2r+2})) \right]$$

$$= \lim_{\substack{\mu_2 \bar{T} \to \infty \\ \Delta_2 \mu \to 0}} \frac{\rho g}{4} E(\mu_{2r+2}) = \frac{\rho g}{4} E_{max} \tag{7.10}$$

Plate XVIII

time at the point of observation. The function, $\psi(\mu)$, is a point set function which will be defined later. The notation $\sqrt{dE(\mu)}$ at first does not make sense, until the process by which the integration is to be carried out is defined.

The properties of $E(\mu)$ are given by equations (7.2) through (7.5). It is zero for μ less than or equal to zero. It is monotonically non-decreasing for μ greater than zero; that is, if μ_2 is greater than μ_1, then $E(\mu_2)$ is greater than or equal to $E(\mu_1)$ as stated by equation (7.3). Finally, for all μ, $E(\mu)$ is less than some positive constant, M, as required by equation (7.4). If $E(\mu)$ is monotonically non-decreasing and if it is bounded from above, then it follows that $E(\mu)$ has a definite maximum value E_{max} (equation (7.5)) which is either actually reached at a finite value of μ or which is approached asymptotically as μ approaches infinity. In statistics, a function with similar properties is referred to as the cumulative frequency function, or ogive, as defined, for example by James and James [1949].

$E(\mu)$ will be referred to as the cumulative power density. It measures that part of the averaged squared value of $\eta(t)$ which is contributed by those spectral frequencies less than or equal to μ. The word "power" in the definition is unfortunate for wave theory because the averaged squared value of $\eta(t)$ is most nearly connected with the potential energy of the record averaged over time. In electronic theory where these concepts were originally developed, equation (7.1) usually described a voltage produced by an alternating current, and the voltage

squared working into a known load was a measure of the power involved. By extension anything involving the square of the sample studied has been described in terms of power which explains the origin of the term cumulative power density. Later on when actual wave power is studied, it will always be referred to as wave power in order to eliminate confusion.

To proceed with the definition of the integral given by equation (7.1),* in equation (7.6) the μ axis has been marked by a series of points, $0, \mu_1, \mu_2, \mu_3 \cdots\cdots \mu_{2R}$. Such a division of the range of integration into a number of small intervals is called a net. The μ_j are not necessarily equally spaced, and they are not necessarily rational points. Now form the sum of terms represented by equation (7.7) before the limiting process is applied. The first term is given, for example, by the square root of the difference (which is greater than or equal to zero) between $E(\mu_2)$ and $E(\mu_o)$ times the cosine of $\mu_1 t$ plus $\psi(\mu_1)$ where, as yet, $\psi(\mu_1)$ is not defined.

The function, $\psi(\mu_1)$, can be defined in many ways. One definition would be to give a set of points between 0 and 2π from which a value could be picked by some rule once ψ_{2n+1} was given, and the fact that the integral involved such a set of points would then make it a Lebesgue integral. Suppose then that such a rule is given for picking the value of $\psi(\mu_{2n+1})$.

Then the integral of equation (7.1) is the limit of the sum given by equation (7.7) as the mesh of the net approaches

*For additional information, see Levy [1948].

zero. That is, the integral is the limit of the process defined by equation (7.7) and the law for picking $\psi(\mu_{2n+1})$, as the greatest distance between two successive μ's in the net, say μ_{k+1} and μ_k, is shrunk to zero. Note that the partial sums in equation (7.7) are almost periodic functions as defined by Bohr [1947] if the μ's are irrational.

This integral has one very valuable property. The square of the function given by the integral averaged over time, is equal to $(1/2)E_{max}$. This can most easily be shown by considering the partial sum given by equation (7.9) in which the smallest distance between two successive μ's is $\Delta_1\mu$, a small but finite value and in which the largest distance between two successive μ's is $\Delta_2\mu$.* The potential energy of $\eta(t)$ averaged over time is given by the integral expression in equation (7.10) (see equation (3.10)). Since the μ_{2n+1} are different, the cross product terms in the square average to zero when (7.9) is substituted for $\eta(t)$, and the second expression in (7.10) results (see, for example, equation (6.22)). Upon rearrangement and evaluation of the sum, the plus $E(\mu_2)$ in the first parenthesis is cancelled by the minus $E(\mu_2)$ in the second parenthesis, and the r'th partial sum is $E(\mu_{2r+2})$. As r approaches infinity, $\overline{P.E.}$ equals $(\rho g/4)E_{max}$. Equation (7.10) holds for arbitrarily small values of $\Delta_2\mu$ and hence it holds in the limit.

---

*$\Delta_1\mu$ is the smallest segment in the net; $\Delta_2\mu$ is the largest. The lengths of all others lie in between.

Some examples

The Lebesgue Stieltjes Power Integral just defined includes as special cases all of the representations of the sea surface in the previous chapters which were infinitely long in duration. From the definition of the integral, it is evident that the function $\eta(t)$ never attains a constant value of zero.

Example one is another way to express equation (2.19) when x and y are zero and δ equals $3\pi/2$. $E(\mu)$ is given by equation (7.11) which shows that it is piecewise constant with a value of zero below $2\pi/T$ and of A^2 above $2\pi/T$. The function, $\psi(\mu)$, could be given, for this example, by equation (7.12), but actually $\psi(\mu)$ could be anything outside of a small interval about $2\pi/T$.

If the limiting process defined by equation (7.7) is carried out, the value of $[E(\mu_{2n+2}) - E(\mu_{2n})]^{1/2}$ is zero for all n except for that particular n, say n = p, for which $\mu_{2p} < 2\pi/T < \mu_{2p+2}$. The square root for this particular interval is equal to A. Also since $\mu_{2p} < \mu_{2p+1} < \mu_{2p+2}$, the expression $|\mu_{2p+1} - 2\pi/T|$ can be made as small as one pleases. As the mesh approaches zero, μ_{2p+1} falls on the interval $\mu = 2\pi/T \pm \epsilon$ and determines the phase. In the limit then, equation (7.13) is the result. The potential energy is given by equation (7.14), and since E_{max} equals A^2 the results confirm equation (7.10).

The various functions employed in example one are shown in the graphs applicable to the example in figure 13. In this example, since $E(\mu)$ is a step function, another function defined as $JE(\mu)$, the jump in $E(\mu)$, can be defined and graphed.

Some Examples

Example 1

$$E(u) = \begin{cases} 0 & 0 \le 2\pi/T \\ A^2 & 2\pi/T \le \mu < \infty \end{cases} \tag{7.11}$$

$$\Psi(u) = \begin{cases} 3\pi/2 & \text{for } \mu = 2\pi/T \pm \epsilon \\ 0 & \text{otherwise} \end{cases} \tag{7.12}$$

$$\text{then } \eta(t) = A \sin 2\pi/T \tag{7.13}$$

$$\overline{P.E.} = \frac{\rho g}{4} A^2 \tag{7.14}$$

Example 2

$$E(\mu) = \begin{cases} 0 & 0 \le \mu < 2\pi/T_1 \\ A_1^2 & 2\pi/T_1 \le \mu < 2\pi/T_2 \\ A_1^2 + A_2^2 & 2\pi/T_2 \le \mu < 2\pi/T_3 \\ A_1^2 + A_2^2 + A_3^2 & 2\pi/T_3 \le \mu < \infty \end{cases} \tag{7.15}$$

$$\Psi(\mu) = \begin{cases} \pi & \mu = 2\pi/T_1 \pm \epsilon \\ 3\pi/2 & \mu = 2\pi/T_2 \pm \epsilon \\ 0 & \mu = 2\pi/T_3 \pm \epsilon \end{cases}$$

$$\Psi(\mu) = \text{anything otherwise} \tag{7.16}$$

$$\text{then } \eta(t) = -A_1 \cos\frac{2\pi t}{T_1} + A_2 \sin\frac{2\pi t}{T_2} + A_3 \cos\frac{2\pi t}{T_3} \tag{7.17}$$

$$\overline{PE} = \frac{\rho g}{4}(A_1^2 + A_2^2 + A_3^2) \tag{7.18}$$

Example 3

$$E(\mu) = \begin{cases} 0 & \mu < 2\pi/\tau \\ a_1^2 & 2\pi/\tau \le \mu < 4\pi/\tau \\ \sum_{m=1}^{K} a_m^2 & K(2\pi/\tau) \le \mu < K+1(2\pi/\tau) \\ \sum_{m=1}^{\infty} a_m^2 & \mu = \infty \end{cases} \tag{7.19}$$

$$\Psi(\mu) = 3\pi/2 \qquad 0 < \mu < \infty \tag{7.20}$$

$$\text{then } \eta(t) = \sum_{m=1}^{\infty} a_m \sin\frac{2\pi m t}{\tau} \tag{7.21}$$

$$\overline{P.E.} = \frac{\rho g}{4} \sum_{m=1}^{\infty} a_m^2 \tag{7.22}$$

Example 4

$$E(\mu) = \begin{cases} a\mu & 0 < \mu < 2\pi/T_1 \\ a\,2\pi/T_1 & 2\pi/T_1 \le \mu < \infty \end{cases} \tag{7.23}$$

$$\Psi(\mu) = 0 \tag{7.24}$$

$$\text{then } \lim_{m\to\infty} \eta(0) = \lim_{m\to\infty} m\sqrt{a\mu} = \lim_{m\to\infty} \sqrt{\frac{ma\,2\pi}{T_1}} = \infty \tag{7.25}$$

$$\text{but} \qquad \overline{P.E.} = \lim_{T\to\infty} \frac{\rho g}{T4} \int_{-T/2}^{T/2} (\eta(t))^2 dt = \frac{\rho g a 2\pi}{4 T_1} \tag{7.26}$$

Plate XIX

$JE(\mu)$ equals A^2 at $2\pi/T$.

Example two is a slight extension of the concepts in example one. $E(\mu)$ has three steps. $\psi(\mu)$ can be arbitrary except in the intervals surrounding the points $2\pi/T$, $2\pi/T_2$, and $2\pi/T_3$ where it is given by equation (7.15). The value of the integral is given by equation (7.17) and $\overline{P.E.}$ is given by equation (7.18). The graphs of the appropriate functions are given in figure 13.

Example three is the formulation of the Power Integral for the infinite train of regular wave groups defined by equation (6.8). $E(\mu)$, as defined by equation (7.19), is a step function with an infinite number of steps which become small like $\exp[-\mu^2]$ as μ approaches infinity. E_{max} therefore exists. $\psi(\mu)$ can be defined by equation (7.20) as one of many possible ways. The integral and the average potential energy are then given by equations (7.21) and (7.22). The various functions involved are graphed in figure 13.

Example four shows how it is possible to pick $E(\mu)$ and $\psi(\mu)$ in a way which will yield physically unrealistic results for $\eta(t)$. If $E(\mu)$ is continuous and, for example, a linearly increasing function of μ over part of the μ axis as given by equation (7.23), and if $\psi(\mu)$ is zero, the limit, as the mesh approaches zero in equation (7.7), becomes infinite at $t = 0$. Let the net points be equally spaced at intervals of $\Delta\mu$ such that $m\Delta\mu = 2\pi/T_1$. Then at $t = 0$, the cosine term is unity and the value of $\eta(o)$ is given by equation (7.25). As m approaches infinity, and $\Delta\mu$ approaches zero, $\eta(o)$ becomes

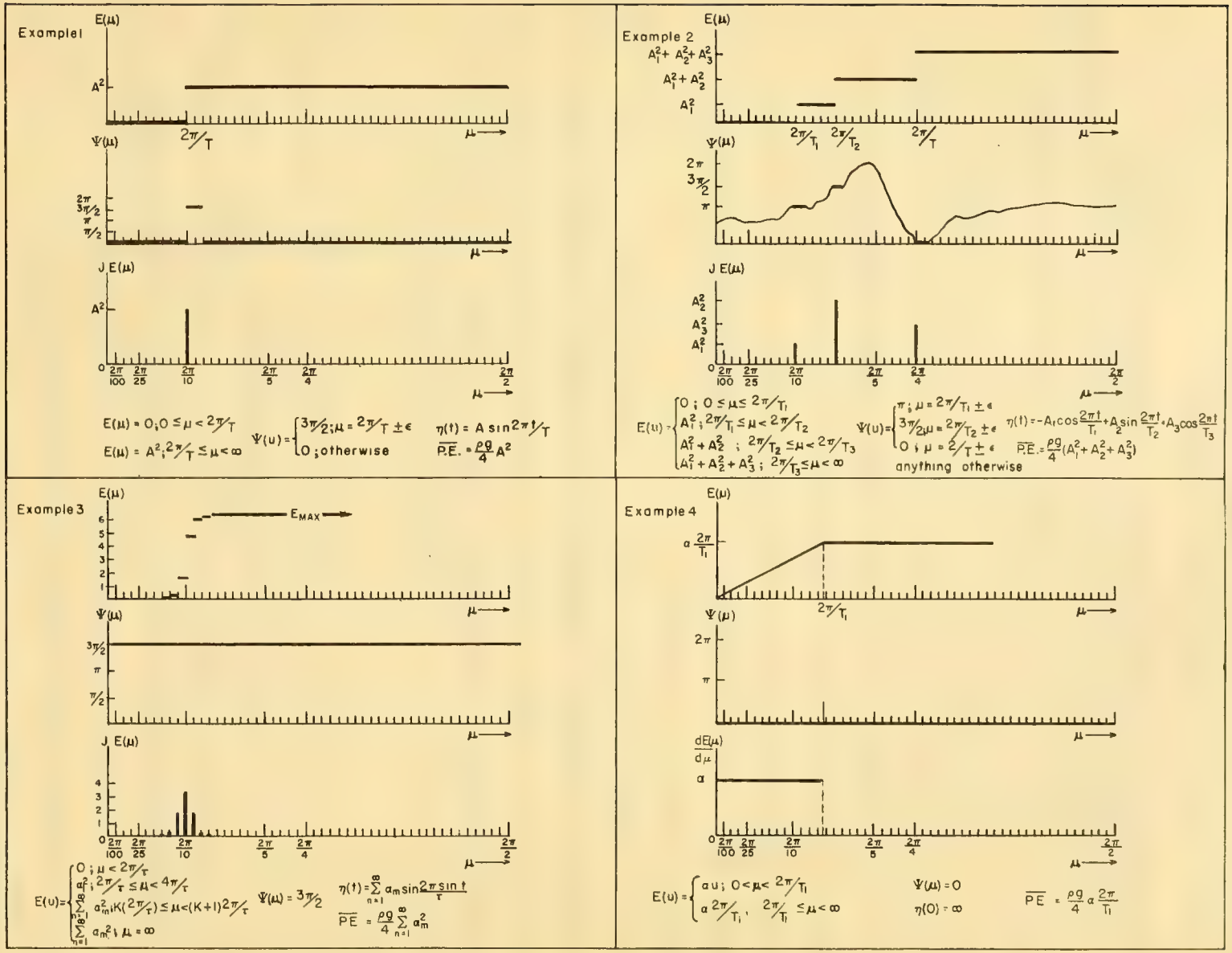

Fig.13 Graphs of the Functions Involved in the various Examples of the Lebesgue Stieltjes Power Integral.

infinite. However, $\overline{P.E.}$ as defined by equation (7.26), is still finite. The appropriate graphs for example four are given in figure 13. In this case, there is no jump in $E(\mu)$, and $dE(\mu)/d\mu$ equals α if μ is less than $2\pi/T_1$.

The Gaussian case, or the principle of independent phases

The examples of the integration of equation (7.1) which have been given so far have not introduced anything basically new in the nature of the sea surface. The integral is so general, however, that it includes many cases which can only be represented by such an integral. One special case is the Gaussian case which is of extremely great importance in the theory of noise and which will prove to be of equal importance in wave theory.

The integral considered is still equation (7.1), and the conditions given by equations (7.2), (7.3), (7.4), and (7.5) are still imposed. In addition, the condition that $E(\mu)$ be a continuous function is added, and the point set which defines $\psi(\mu)$ is very specially defined. Continuity in $E(\mu)$ yields all necessary qualities. It permits a very peculiar mathematical form for the derivative of $E(\mu)$ which will be discussed later in Chapter 10.

Continuity of $E(\mu)$ is imposed by equation (7.27), which states that the difference between $E(\mu_{2n+2})$ and $E(\mu_{2n})$ can be made smaller than some delta if $\mu_{2n+2} - \mu_{2n}$ is made smaller than some epsilon (which may depend on delta). * In examples one, two, and three, this condition is not fulfilled at the jumps. In example four, $E(\mu)$ is continuous.

* See Courant [1937].

The Gaussian Case

Equations(7.2), (7.3), (7.4) and (7.5) hold

in addition $0 < E(\mu_{2n+2}) - E(\mu_{2n}) < \epsilon$

if $\mu_{2n+2} - \mu_{2n} < \delta(\epsilon)$ (7.27)

and $0 \leq \psi(\mu_{2n+1}) \leq 2\pi$

such that $p(\psi(\mu_{2n+1}) < a\,2\pi) = a$ (7.28)

when $0 \leq a \leq 1$

Then Equation (7.7) has a limit and

$$\lim_{\bar{T}\to\infty} \frac{1}{\bar{T}} \int_{t}^{t^*+\bar{T}} (\eta(t))^2\, dt = \frac{E_{max}}{2} \tag{7.29}$$

and if $(A(\mu))^2$ is piecewise continuous

$$dE(\mu) = (A(\mu))^2\, d\mu \tag{7.30}$$

$$\text{and } \eta(t) = \int_0^\infty \cos(\mu t + \psi(\mu)) \sqrt{(A(\mu))^2\, d\mu} \tag{7.31}$$

partial sum

$$\eta(t) = \lim_{R\to\infty} \sum_{n=0}^{r} \sqrt{(A(\mu_{2n+1}))^2 (\mu_{2n+2}\mu_{2n})} \cdot \cos(\mu_{2n+1} t + \psi(\mu_{2n+1}))$$

$$\min(\mu_{K+1} - \mu_K) = \Delta_1\mu$$

$$\max(\mu_{p+1} - \mu_p) = \Delta_2\mu$$

$$= \mathcal{R}_e \lim_{r\to\infty} \sum_{n=0}^{r} \sqrt{(A(\mu_{2n+1}))^2 (\mu_{2n+2} - \mu_{2n})} \cdot e^{i(\mu_{2n+1} t + \psi(\mu_{2n+1}))} \tag{7.32}$$

$$\min(u_{K+1} - u_K) = \Delta_1 u$$

$$\max(u_{p+1} - u_p) = \Delta_2 u$$

Gaussian Distribution of Amplitudes

$$p(\eta(t_1) < K) = \frac{1}{\sqrt{\pi E_{max}}} \int_{-\infty}^{K} e^{-\xi^2/E_{max}}\, d\xi \tag{7.33}$$

$$p(K < \eta(t_1) < K + dK) = \frac{1}{\sqrt{\pi E_{max}}} e^{-K^2/E_{max}}\, dK \tag{7.34}$$

Plate XX

The conditions on $\psi(\mu)$ are that $\psi(\mu)$ be between 0 and 2π and that its value be random and equally probable for any particular μ. Equation (7.28) states this condition in statistical terms. The equation is read, "The probability that $\psi(\mu_{2n+1})$ is less than $\alpha 2\pi$ equals α," where α lies between zero and one. Such a condition is equivalent to the statement that the phases are independent (Tukey and Hamming [1949]).

The integral can then be thought of as the limit of a sequence of sums such as equation (7.7) in which the $\psi(\mu_{2n+1})$ are chosen from a table of random numbers. Of course each time the process is carried out, the sum will be different because the phases are different. In addition, it is not possible to write down an expression for the result of the passage to the limit.

The function, $\psi(\mu)$, as defined by equation (7.28) is a point set function. It cannot be graphed. It is continuous no where. For a particular net over the axis, and after the choices from a table of random numbers have been made, it is a definite function.

Now consider all possible point set function, $\psi(\mu)$, which could be chosen by the probability law which has been given. And consider all the corresponding $\eta(t)$ which could be determined from $\psi(\mu)$ once $E(\mu)$ is fixed. In the limit, a whole statistical class of functions $\eta(t)$ would be the result. What properties would they have in common? And if a part of one of these functions from this statistical class is given, how can $E(\mu)$ be found?

These questions can be answered in a statistical sense, but first some general properties will be obtained. The hope, of course, is that an actual wave record can be thought of best as one of the possible functions from the statistical class described above.

If equations (7.27) and (7.28) hold, then the limit of equation (7.7) exists, and the integral given by (7.29) has the value $(1/2)E_{max}$. In addition, if the derivative of $E(\mu)$ is continuous or piecewise continuous, it must be everywhere positive. Under these conditions, the derivative can be written as the square of some function $A(\mu)$ as in equation (7.30).

With this new representation for $dE(\mu)$, equation (7.1) can be rewritten as equation (7.31) which is no longer a Stieltjes Integral since there are no jumps in $E(\mu)$. It might be termed a Lebesgue Power Integral since the point set function $\psi(\mu)$ is still involved.

The function, $(A(\mu))^2$, is the power spectrum of $\eta(t)$. It has the dimensions $[L^2T]$, and since $d\mu$ has the dimensions of $[T^{-1}]$, the dimension of $\sqrt{(A(\mu))^2 d\mu}$ is [L]. The power spectrum is easily measured in a statistical sense, and the methods for such measurements have been presented by Tukey and Hamming [1949]. It will be assumed that $(A(\mu))^2$ can be determined with a known degree of statistical reliability. The procedures for so doing will be described in a later chapter when short crested waves will be considered.

The random walk

If the same net that was given in equation (7.6) is applied

to equation (7.31), the partial sum originally represented by equation (7.9) becomes equation (7.32). In equation (7.32), the second expression is simply a more informative way to write the first expression.

In the second expression, for each value of n, the term under the summation sign is a vector in the complex plane with an amplitude determined by the value of the radical, and a direction determined by the direction of the unit vector, $\exp[i(\mu_{2n+1}t + \psi(\mu_{2n+1}))]$. For any fixed t, say t_1, the direction of each vector is determined, and since $\psi(\mu_{2n+1})$ has the properties of equation (7.32), the individual vectors in the sum point in all possible directions.

To add vectors, the tail of the second is placed at the head of the first and the sum is the vector joining the head of the second with the tail of the first. The sum of the r vectors is this process repeated r times.

The sum of these vectors for $\Delta_1\mu$ and $\Delta_2\mu$ small but finite is considered in the classical statistical problem of the random walk. The random walk problem is described in detail by Margineau and Murphy [1943] and Kennard [1938], and Brownian motion is described by Levy [1948], but the statement of the problem will be given again here for the sake of completeness.

The classical problem concerns itself with a drunkard who starts out for home from a pub after a night of revelry. He strikes out in some direction and walks a distance y_1 in that direction, but becomes confused and turns in a completely

different direction at random and walks a distance y_2. He then walks a distance y_3 in another direction picked at random, and so on. The problem is to determine the probability that he will be within a distance R from the pub if the total distance he has walked is given by $Y = y_1 + y_2 + \ldots\ldots + y_n$, and if his choice of directions has been completely random.

The solution to the random walk problem as Y becomes larger and the y_i shrink smaller and smaller is the normal probability, or Gaussian, distribution. From the description of the problem, it would appear that the drunkard would not end up too far away from the pub. A whole statistical class of wayfarers would show most of them concentrated near the origin and a few scattered at greater distances away. The extension of the random walk problem into three dimensions is the problem of Brownian motion and similar results are obtained.

The connection of the random walk problem with equation (7.32) is that in the vector notation shown the partial sums are all basically random walks. The projection of the sum of the vectors on the real axis is also a Gaussian distribution in the limit as r approaches infinity and $\Delta_2 \mu$ approaches zero. Equation (7.33) is a consequence of this result. It states that the probability, at a time, t_1, chosen at random, that the amplitude of the sea surface will be less than the value K is given by the normal probability distribution. K is the departure from the mean, assumed to be zero, of the record. Equation (7.34) is another way to express this condition. It gives the probability that a point chosen at random in the record will lie between

the value of K and K + dK.

The representation of wave records by the Gaussian case of the Lebesgue Power Integral

If a portion of an actual wave record is to be represented by equations (7.1) through (7.10) and (7.27) through (7.32), then it must, at least, approximate the properties of the integral, and satisfy equations (7.33) and (7.34). One property of the integral is that $\eta(t)$ never repeats itself. Another is that if a time interval τ is chosen, which is large enough to eliminate autocorrelation effects, then the values of the heights of the sea surface measured at t_1, $t_1 + \tau$, $t_1 + 2\tau$ ..... and so on, will be distributed according to equation (7.34). Herein lies the fault of the models in Chapter 6. For different t_1 in this model, (since it was assumed that the groups were spaced τ units apart plus or minus a small deviation) the values of $\eta(t)$ will not all have the same probability distribution and therefore the model is not Gaussian.

It is very easy to test a wave record to see if the distribution of points chosen from $\eta(t)$ at time intervals sufficiently great is Gaussian. The test has been made on some actual amplitude wave records and on some pressure records. Some results of the tests are given in figure 14.

The first histogram in figure 14 is from a wave height record obtained with the Beach Erosion Board instrument described by Caldwell [1948], which was located on the pier at Long Branch, New Jersey. It shows that the distribution is not quite Gaussian because the median value of the histogram is below zero and the

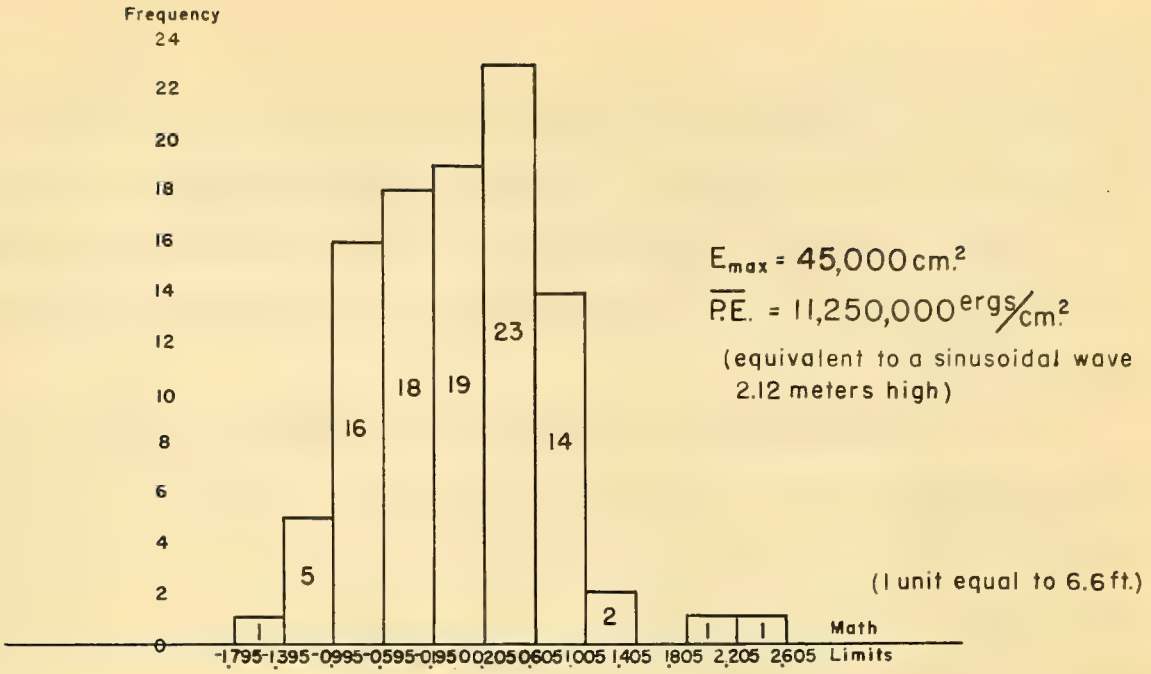

Histogram of samples from a wave record for 5-14-48 0000 to 0007 E.S.T., Long Branch, New Jersey. χ^2 = 23.1 with 8 degrees of freedom — Eliminate last group. χ^2=7.8 with 7 degrees of freedom. 35 out of 100 times sample could come from normal distribution.

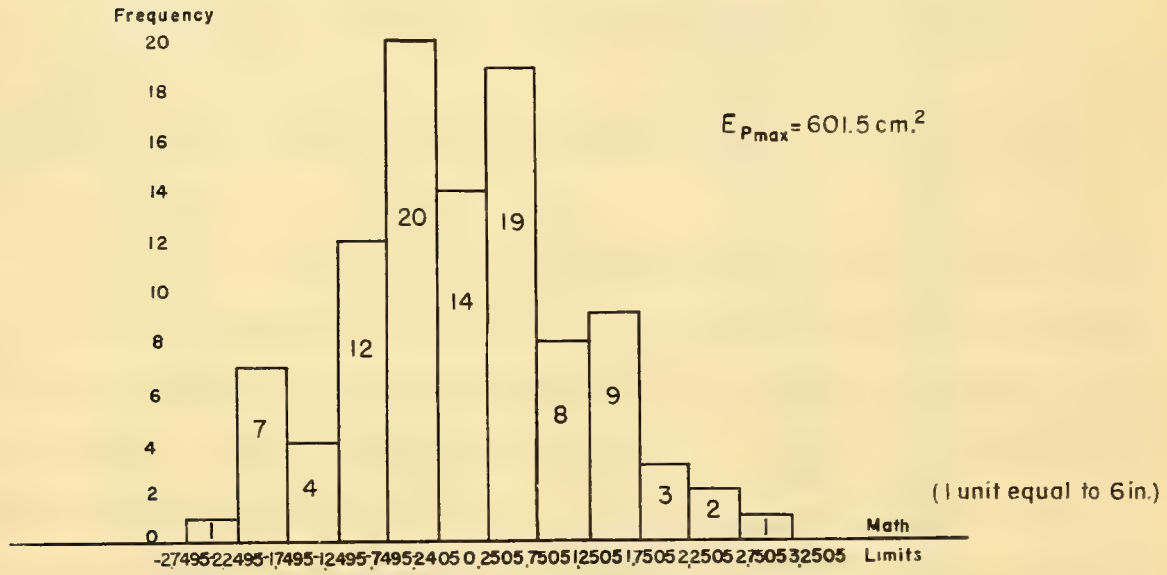

Histogram of samples from pressure record for 10-18-51, 2258 to 2323 E.S.T., Long Branch, New Jersey. χ^2=9.128 with 9 degrees of freedom. 43 out of 100 times sample could come from normal distribution.

Fig. 14. Histograms of wave height and pressure amplitude distributions from sample records.

frequency of large negative departures from the mean is not as great as the frequency of large positive departures from the mean. However, the departure from the Gaussian distribution is not so great that the resemblance to the Gaussian distribution is lost.

It is interesting to consider the probability that such a histogram composed of one hundred values chosen at random from a seven minute wave record could have come from a Gaussian distribution. The Chi-Square Test can be employed to determine this probability by standard statistical methods. The needed values computed by the methods described, for example, in Hoel [1947] are given in Table 15.

Table 15. Chi Square Test of the upper histogram in figure 14.

X_i	$\varphi(X_i)$	F_i	$f_i - F_i$	$(f_i - F_i)^2$	$(f_i - F_i)^2/F_i$
2.30	.029	1.67	- .669	0.448	0.268
1.72	.091	5.24	-..237	0.056	0.011
1.14	.207	11.9	4.09	16.70	1.40
0.568	.339	19.5	-1.51	2.28	0.117
0.00	.399	23.0	-3.96	15.70	0.684
0.583	.337	19.4	3.61	13.00	0.670
1.16	.204	11.7	2.26	5.11	0.435
1.73	.088	5.06	-3.06	9.39	1.854
2.30	.028	1.61	-1.61	2.60	1.611
2.89	.006	0.345	.655	0.26	0.754
3.46	.001	0.058	.942	0.89	15.29
				$(Chi)^2$ =	23.1
				Less last term	7.8

The value of Chi Square is 23.1 with eight degrees of freedom. It is highly improbable that such a distribution could come from a normal distribution. But note that it is the very last value in the sum which makes the sum so high. If this last term is omitted Chi Square is 7.8, and the sample could have come from a normal distribution 34 out of 100 times if chosen at random.

The departure from the Gaussian case can be explained on the basis of the actual non-linearity of the sea surface. Because of the non-linearity, crests are higher and troughs are lower than in a surface described by the Gaussian case. The peak values of the crests are what have produced the high value of Chi Square. It was pointed out in the second chapter that little could be done about the essential non-linearity of the sea surface, and these histograms show remarkable agreement with the hypothetical Gaussian case within the limits of the linearization assumption.

The potential energy of an actual wave record averaged over time can be computed by squaring the wave record and averaging over time. Such a computation would require rather lengthy computations. The histograms show that E_{max} can be estimated easily be taking the second moment about the mean (square of the variance) of a sample of one hundred or so points from the record. The computations involved would be considerably less than by the other method, and the reliability of the estimate would depend on the size of the sample, on the magnitude of E_{max}, and on the function $E(\mu)$. The value of E_{max} and of $\overline{P.E.}$

as computed from the histogram is given beside the histogram. E_{max} and $\overline{P.E.}$ are reliable and theoretically definite statistical quantities obtained from wave records. These points will be considered in more detail later.

The remaining histogram in figure 14 was obtained from a pressure record which was taken by a pressure recorder in 30.5 feet of water (mean low water) offshore from Long Branch, New Jersey. It was obtained in October 1951, while an east coast storm passed Long Branch just a short distance out over the ocean. This histogram is more nearly distributed according to the Gaussian law than the height record was. In fact, 43 out of 100 times at random, this histogram could have come from a normal distribution. The better agreement can be explained on the basis of the fact that the second order non-linear terms die out more rapidly with depth. Consequently in the pressure record the higher ridges and shallower troughs which were at the surface are less accentuated. From these histograms, $E_{p_{max}}$ has been computed which is analogous to the quantity E_{max} in the height record. However, $\overline{P.E.}$ cannot be computed from $E_{p_{max}}$. $\overline{P.E.}$ can be computed if either $E_p(\mu)$ or $(A_p(\mu))^2$ is known, and if a certain linear operator is applied to $E_p(\mu)$ in order to get the value of E_{max} which applies to the free surface (see the discussion of pressure records in a later chapter).

A number of other samples of points equally spaced in time were picked from this same pressure wave record. Of these, several values of Chi Square were so high that they were not in the tables. Other values were quite reasonable, and the

probabilities that the samples could have been picked from a normal distribution were 30 in 100, and 50 in 100. There were two cases in which Chi Square was very large.

The skewness of the histogram of the surface records is one way in which $\eta(t)$ does not follow a Gaussian distribution. A second way in which the distribution will not be Gaussian comes from the fact that equation (7.34) yields a finite probability for very high crests and very low troughs. For low waves, this finite but very small probability is not important. The Gaussian distribution is only a statistical ideal; for example, it predicts men twenty feet high from a population with a five foot mean and a variance of one foot. In short, all statistical theory must be used with judgment. Actual wave heights cannot exceed a certain value since the crests will break. It is to be expected that for high seas the histograms will be both skewed and chopped off at the extremes. The effect of breaking in a complex irregular sea surface is again a non-linear problem and cannot be treated by the methods under study.

Figure 14 shows consequently that actual wave records very closely approximate the requirement that $\eta(t)$ have a Gaussian distribution of the amplitudes. Berkoff and Kotig [1951] have commented on the fact that certain symmetry requirements for $\eta(t)$ are not met in actual wave records. This failure is a consequence of the actual non-linearity of the problem, but again the departure from the Gaussian case is small.

This fact is indeed fortunate. The theory of the statistical analysis of functions of the form of equation (7.1) in

the Gaussian case has been presented by Tukey and Hamming [1949]. For the non-Gaussian case very little is known. Paraphrasing Tukey, it can be said that "This restriction to Gaussian (wave records) will presumably not be a serious hindrance to our analysis of actual (wave records) which will be non-Gaussian to a greater or less extent, if we use the quantitative expressions for the fluctuations as warning signs, and realize that fluctuations larger than those predicted by Gaussian theory are likely. The recommended procedures (in the paper) are known to be good for Gaussian (wave records). For moderately non-Gaussian cases, the analogy with simple problems suggests that the procedures will be quite good." For wave records the modifying effects of non-linearity must be kept in mind, at least in a qualitative sense. Tukey (personal communication) says that the values of Chi Square given before are just what one might expect from random noise and that the better results for the pressure records show that the system is non-linear in the high frequency components.

If the qualifications and explanations in the above section are taken into consideration, it can be concluded that the best possible known way to represent a wave record and consequently the sea surface as a function of time at a fixed point is given by the Gaussian case of the Lebesgue Power Integral. Any portion of a record of the sea surface as observed as a function of time, if the sea surface is in a stationary state, can therefore be thought of as a segment of one of the statistical ensemble of functions which would result from the indicated limiting process

which defines the integral.

Stationary processes and stationary time series

The first three examples given in Plate XIX and the Gaussian case of the Lebesgue Power Integral are all specific examples of stationary processes. A stationary process is simply a function of time, say $\eta(t)$, such that the essential properties of the function are not altered by the substitution of $t + h$ for t in the functional representation. Substitution of $t + h$ for t in the first three examples simply changes the phase of the various sinusoidal waves in the function. The power spectrum is still the same, and the function is still composed of the same sine waves. Similarly, in the Gaussian case, substitution of $t + h$ for t simply changes the values of $\psi(\mu)$, and the function is still an element in the class of all possible functions which can be found by the procedure of integration defined above for a particular $E(\mu)$.

A stationary time series can be made from any of these functions by giving their values only at separate points; say, at $t_1, t_2, t_3 \ldots\ldots t_n$, preferably separated by the same length of time. The height of the water against a wave pole in successive frames of a motion picture film strip would be a practical example.

Special note

The Gaussian case of the Lebesgue Power Integral does not have to have any special form for $E(\mu)$. $E(\mu)$ can be any function as long as it is continuous. In previous chapters, the normal probability curve has been used as a special example

of an ordinary Fourier spectrum to study the propagation of a finite wave group and to study the propagation of various finite wave trains. The accidental fact that the spectrum was connected with a normal probability (or Gaussian) curve should not be confused with the very important fact that values of $\eta(t)$ at greatly separated values of t, chosen at random, are distributed according to the Gaussian probability law.

Wave record analysis

Any given wave record as a function of time can be considered to be a short piece of an infinitely long record which is one of the infinite number of records possible from the integration of the Gaussian case of the Lebesgue Power Integral. The problem is to find $(A(\mu))^2$, given the short piece of the record. This problem is the basic problem of wave analysis if it is generalized to permit representation of short crested waves. The function, $(A(\mu))^2$, and the extension to what corresponds to it for a short crested sea surface can only be estimated because of the finite length of the record. The longer the record, the more reliable the estimate of $(A(\mu))^2$. The problem of wave analysis will be considered for the short crested case in a later chapter.

Wave forecast models for wave systems with infinitely long crests in the Gaussian case

Consider again equation (7.1), for the Gaussian case. Instead of $\eta(t)$, equation (7.35) employs $\eta(o,t)$ to point out the fact that the function is presumably known only at the origin of the x coordinate system. Assume that $(A(\mu))^2$ is known. This wave record as a function of time at the origin never started

The Forcasting Problem for a Sea Surface Represented by the Gaussian Case of the Lebesgue Power Integral with Infinetely Long Crests in the Y Direction

$$\eta(0,t) = \int_0^\infty \cos(\mu t + \psi(\mu))\sqrt{d\,E(\mu)} \tag{7.35}$$

$$\eta(x,t) = \int_0^\infty \cos\left(\frac{\mu^2 x}{g} - \mu t - \psi(\mu)\right)\sqrt{dE(\mu)} \tag{7.36}$$

$$\eta(x,t) = \int_0^\infty \cos\left(\mu t + \left(\psi(\mu) - \frac{\mu^2 x}{g}\right)\right)\sqrt{dE(\mu)} \tag{7.37}$$

$$0 \le \psi(\mu_{2n+1}) - \frac{(\mu_{2n+1})^2 x_1}{g} + 2\pi N = \psi'(\mu_{2n+1}) \le 2\pi \tag{7.38}$$

$$\tilde{F}(t)\cdot\eta(0,t) = \tilde{F}(t)\cdot\int_0^\infty \cos(\mu t + \psi(\mu))\sqrt{dE(\mu)}$$

$$\cong \tilde{F}(t)\sum_{n=0}^{r}\sqrt{E(\mu_{2n+2}) - E(\mu_{2n})}\cdot\cos(\mu_{2n+1}t + \psi(\mu_{2n+1})) \tag{7.39}$$

$$\min(\mu_{K+1} - \mu_K) = \Delta_1\mu$$

$$\max(\mu_{p+1} - \mu_p) = \Delta_2\mu$$

Special Case $\tilde{F}(t) = \begin{cases} 1 & 0 < t < D_w \\ 0 & \text{otherwise} \end{cases}$ (7.40)

The Square Cornered Filter

$$t_f = \frac{2\mu x}{g} \tag{7.41}$$

$$t_r = \frac{2\mu x}{g} + D_w \tag{7.42}$$

if $t_r \ge t_{ob} \ge t_f$ band for a particular μ is present (7.43)

$$\frac{2\mu x}{g} + D_w \ge t_{ob} \ge \frac{2\mu x}{g} \tag{7.44}$$

$$\frac{g(t_{ob} - D_w)}{2x} \le \mu \le \frac{g\,t_{ob}}{2x} \tag{7.45}$$

$$\mu_u = \frac{g t_{ob}}{2x} \tag{7.46}$$

$$\mu_L = \frac{g(t_{ob} - D_w)}{2x} \tag{7.47}$$

$$\Delta\mu = \mu_u - \mu_L = \frac{g D_w}{2x} \tag{7.48}$$

$$\text{S.F.G.} = \begin{cases} 1 & \text{if } \dfrac{g(t_{ob} - D_w)}{2x} \le \mu \le \dfrac{g t_{ob}}{2x} \\ 0 & \mu \text{ otherwise} \end{cases} \tag{7.49}$$

$$\text{F.F.G.} = \frac{1}{2}\left[\left(\int_{\sqrt{\frac{x}{\pi g}}\left(\mu - \frac{g(t_{ob} - D_w)}{2x}\right)}^{\sqrt{\frac{x}{\pi g}}\left(\mu - \frac{g t_{ob}}{2x}\right)} \cos\frac{\pi}{2}\delta^2\,d\delta\right)^2 + \left(\int_{\sqrt{\frac{x}{\pi g}}\left(\mu - \frac{g(t_{ob} - D_w)}{2x}\right)}^{\sqrt{\frac{x}{\pi g}}\left(\mu - \frac{g t_{ob}}{2x}\right)} \sin\frac{\pi}{2}\delta^2\,d\delta\right)^2\right] \tag{7.50}$$

Plate XXI

and will never stop. Consequently this representation lacks reality in the same sense that equations (6.1) and (6.3) lacked reality in that the storm which produced the record would have to last forever at the origin. If $\eta(o,t)$ is given by equation (7.35) then by virtue of the linearity of the problem, $\eta(x,t)$ is given by equation (7.36).

Equation (7.37) is another way to express equation (7.36) and the variation with x has been absorbed in $\psi(\mu)$. For any partial sum such as equation (7.9), and for a fixed x, (say positive), it is always possible to add an integral number of 2π's to $\psi(\mu_{2n+1}) - (\mu_{2n+1})^2 x_1/g$ and obtain a new value, $\psi'(\mu_{2n+1})$, which satisfies equation (7.38). The $\psi'(\mu_{2n+1})$ will be distributed according to the same probability laws that govern the distribution of the original $\psi(\mu_{2n+1})$, and consequently $\psi'(\mu)$ is another point set function like $\psi(\mu)$. Consequently $\eta(x,t)$ at any x is Gaussian and has the same cumulative power distribution that the record at the origin had. $\eta(x,t)$ also has the same power spectrum. In a statistical sense, then, the sea surface has the same properties at all points.

Wave record of finite duration

In order to generalize the model to a record at the source of finite duration, consider the multiplication of $\eta(o,t)$ by $\tilde{F}(t)$. $\tilde{F}(t)$ is any function of time which varies very slowly compared to the individual waves in $\eta(t)$. $\tilde{F}(t)$ should also be essentially zero outside of a certain range of t. $\tilde{F}(t)$ operating on the integral as in equation (7.35) is equal to the effect in the limit of $\tilde{F}(t)$ operating on one of the partial sums which represent $\eta(t)$.

But it is relatively easy to determine the effect of $\tilde{F}(t)$ on a simple trigonometric term of angular frequency, μ_{2n+1}. The result of operating on any partial sum with $\tilde{F}(t)$ can consequently be found very easily. In the limit, then, the complete effect on the integral can be determined by considering μ to be a variable.

One of the many possible $\tilde{F}(t)$ is given by equation (7.40) where D_w is the duration of the waves. The wave record builds up to full amplitude instantaneously at t = 0 and dies out instantaneously at $t = D_w$. When this particular $\tilde{F}(t)$ is applied to one of the terms in the partial sum indicated in equation (7.39), it can be seen that the problem is essentially the same problem that was solved in Chapter 5 except for a shift in the time axis. If $\tilde{F}(t)$ is applied to $\eta(t)$, the result is no longer a stationary process, but a sample taken during a time interval in which $\tilde{F}(t)$ is essentially one would yield a power spectrum upon analysis indistinguishable from the one obtainable from the unmodified function, $\eta(t)$.

In Chapter 5 it was found that the forward edge and the rear edge of the wave train advanced with the group velocity, and that the edges were modulated by Fresnel Integrals. For the moment, although it is physically impossible, assume that the amplitude of the train is either zero or one at any x and that the Fresnel modulation effects are not present.

The square cornered or sharp cutoff filter

The time, t_f, required for the forward edge of the wave train to reach the point x for a fixed μ is given by equation (7.41). The rear edge, t_r, passes D_w seconds later. Consequently, for a

particular μ and for a fixed value of x, if the time of the observation, t_{ob}, lies between t_r and t_f then the component sinusoidal wave for that particular μ is present as shown by equation (7.42). Substitution of equations (7.41) and (7.42) into (7.43) yields equation (7.44). Rearrangement of equation (7.44) then yields equation (7.45).

For a fixed time and place of observation, and for a fixed duration of the waves, those spectral values of μ are present which lie between the values $g(t_{ob} - D_w)/2x$ and $gt_{ob}/2x$. The other values in this simplified case are not present. The upper value of μ which is present is given by equation (7.46), and the lower value, by equation (7.47). The band width present, $\Delta\mu$, depends directly on D_w and inversely on x as shown by equation (7.48).

Figure 15 shows how these considerations can be used to construct a forecasting diagram. The top part of the figure is a graph of the straight lines given by equation (7.46) and (7.47) as functions of t and μ for various fixed values of x and for D_w equal to 10 hours. Pick a time, $t = t_{ob}$, say, twenty hours and a fixed x, say, 200 kilometers. The line for t = 20 hours intersects the two parallel lines which apply to x = 200 km, and a segment of the μ axis is cut off between the two parallel lines. The projection of this segment onto the μ axis then gives the band of frequencies present at x = 200 km, 20 hours after the start of the storm.

Practically nothing is known about the power spectrum of waves at the edge of an area of generation in a storm at sea.

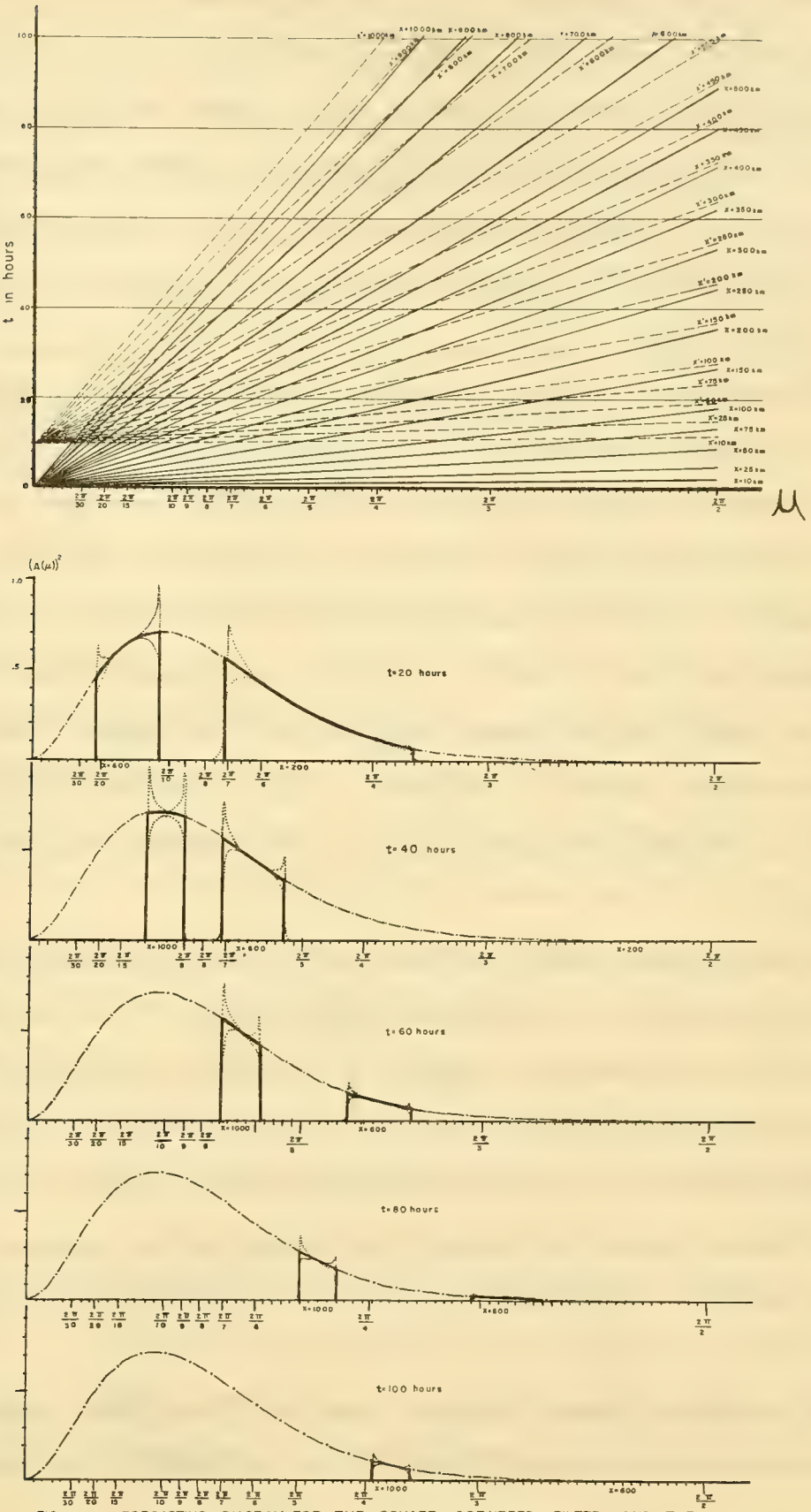

FIG. 15. FORCASTING DIAGRAM FOR THE SQUARE CORNERED FILTER AND THE FRESNEL FILTER FOR THE CASE OF A VERY SHORT FETCH

Consequently, for purposes of illustration, a form for the power spectrum has been assumed. The assumed form of the power spectrum has been plotted below the part of the figure just discussed. It represents what needs to be known about the power spectrum at the source before the power spectrum at any other point of observation can be forecasted. The power spectrum at the source is given by the dash dot curve.

The band width determined above has been used to multiply the power spectrum at the source by the square cornered filter in order to find the power spectrum at the point and time of observation. The square cornered filter is given by equation (7.49), and to apply it to the given power spectrum set the forecasted power spectrum equal to zero outside of the segment described above and set it equal to the power spectrum at the source inside of the segment described above. The heavy solid lines show the effect of applying the square cornered filter to the power spectrum at the source.

The forecasted power spectrum is an instantaneous power spectrum, and in terms of our original definition, it has no meaning. However, if a wave record taken at x = 200 km from twenty hours minus ten minutes to twenty hours plus ten minutes is analyzed for its power spectrum, it might be expected that something like the above pattern, except for slight smoothing at the edges, would be obtained because the filter function is a slowly moving function of time.

The remaining power spectra show the forecasted power spectra for various x's and various times. For a fixed x, as time increases,

the filter tunes through the power spectrum at the source. High period waves are received first followed by low period waves. The band width is constant for a constant D_w. For a larger fixed x, as time increases the filter tunes through the power spectrum at the source more slowly and its band width is narrower.

A square cornered sharp cutoff filter is physically impossible. It is, however, a relatively simple step to extend the forecast diagram to a Fresnel Filter. The procedure is to return to the methods of Chapter 5 and solve the problem given by

$$\eta(0,t) = \cos\left(\frac{2\pi t}{T_{2n+1}} + \psi(\mu_{2n+1})\right)$$

if $0 < t_{ob} < D_w$ and by $\eta(o,t) = 0$ otherwise. The transformation given by $t_{ob} = t' + D_w/2$ would break the function down into an odd and an even part about $t' = 0$. Formulas similar to those in Chapter 5 would result except that the original simplifications in the derivation permitted by the use of the whole number of waves and the oddness (in the sense of not even) of the function would not be available. Note that the third step in equation (5.2) shows that the Fourier spectrum will be continuous at $\mu = 2\pi/T_{2n+1}$. The result would be functions similar to equations (5.15), (5.16) and (5.17), and it would be possible to show that a modified form of $G^2 + H^2$ would give the square of the modulation envelope in the given wave train. The arbitrary phase would be in the trigonometric term.

Finally, the Fresnel Filter would be obtained as given by equation (7.50). In the filter, emphasis is placed on the variation with μ for a fixed x and t. If x is small, and if $\mu = gt_{ob}/2x$, then the range of integration is from a large positive number to

zero. The value of F.F.G. is then one fourth. Similarly, the value at $\mu = g(t_{ob} - D_w)2x$ is one fourth. For μ outside of this range, which is the same range as that of the square cornered filter, the Fresnel Filter falls to zero. Inside this range, it rises to one rapidly, overshoots and oscillates about one very rapidly, and finally settles down to one near the center of the band, if x is small. For very, very large x, the filter does not achieve the value one at the center of the band.

To employ the filter in the forecasting diagram, it is only necessary to evaluate equation (7.50) for t_{ob} equal to zero, and for various x as a function of μ . Then if the filter is located at the same place as the square cornered filter was located in the figure, which can be accomplished by setting the lower quarter power point at $\mu = g(t_{ob} - D_w)/2x$, the product of the Fresnel filter times the power spectrum at the source then gives the power spectrum at the point and time of the forecast.

The Fresnel filter has been applied to the power spectrum at the source according to the above rules. The line of dots above and below the results for the square cornered filter show the envelope of the very rapid oscillations at the edges of the band as produced by the Fresnel Filter. Since a wave record is of finite duration and since the filter tunes through the power spectrum at the source, these rapid fringe oscillations could be considered to cancel themselves out in a twenty minute record and the simplest filter to use would probably be a slightly smoothed square cornered filter.

A storm of finite duration with a fetch of finite length

The wave system given by $\tilde{F}(t)$ as given by equation (7.40) as it operates upon equation (7.35) is unrealistic in one sense which can be eliminated without requiring that the system be of finite width and contain short crested waves. The storm which would conceivably produce the waves would have to extend along the entire y axis of a coordinate system located at the forward edge of the storm. In addition, the winds which would conceivably produce the waves could not exist for any values of negative x. That is, the waves could not exist for negative x and they would have to build up very rapidly to a full stationary state (within the storm) within a very narrow zone at x = 0. Under these conditions when the storm lasts for D_S (Duration of Storm) seconds and then ends suddenly, the duration of the waves is D_W seconds, and $D_W = D_S$.

It is possible to formulate a somewhat more realistic case under the assumption that the same stationary conditions exist over a major portion of the fetch over which the waves passing x = 0 were generated that exist at x = 0 as the waves pass. This condition would occur in the fetch, or area of generation, if the wave spectrum had built up to the point where breaking at the crests due to non-linearity would dissipate the same amount of energy that is added to the wave system by the winds over the fetch. The exact mechanism is beyond the scope of this paper because of the non-linearity, but such a stationary state is within the realm of possibility.

Under these conditions, waves would leave the forward edge of the fetch while the winds are blowing over the fetch throughout the duration of the storm. But when the winds stop, there would also be a distance, F, behind the point, x = 0, such that for any point between x = 0 and x = - F there would be essentially the same time power spectrum for the waves as at the origin. The time power spectrum must be measured over a short enough time interval and at a time near $t = D_S$.

Consider the effect of operating on $\eta(o,t)$ as given by equation (7.35) with a new envelope function $F_F(t,\mu)$ at the source. The effect of $F_F(t,\mu)$ on $\eta(o,t)$ is by the definition of the integral the same as the limiting effect of $F_F(t,\mu)$ operating on a partial sum as the net of the partial sum goes to zero; and, as before, it is only necessary to consider the effect of $F_F(t,\mu)$ upon one sine wave in the partial sum.

At x = 0, no wave component of spectral frequency, μ_1, is observed for t less than zero. At t = 0, it appears instantaneously and at full amplitude to last at least until t equals the duration of the storm, D_S. The wave component does not cease when $t = D_S$ because it still exists over the fetch. The rear edge of the component must travel a distance F to reach the origin, and, if the spectral frequency is μ_1 and if the rear edge travels with the group velocity, then an additional time given by $2\mu_1 F/g$ is required. After $t = D_S + 2\mu_1 F/g$, this particular component will no longer be present.

$\tilde{F}_F(t)$ as given by equation (7.51 formulates these conditions for μ variable. The higher frequency (shorter period) components

The Forecasting Problem for a Sea Surface Represented by Infinitely Long Crests, a Gaussian Wave Record, and Winds that last D_s Seconds Over a Fetch of Length, F.

$$\underset{\text{at } x=0}{\widetilde{F}_F}(t,\mu)=\begin{cases}1 & 0<t<D_s+\dfrac{2\mu F}{g}\\ 0 & \text{otherwise}\end{cases} \tag{7.51}$$

$$t_f=\frac{2\mu x}{g} \tag{7.52}$$

$$t_r=\frac{2\mu x}{g}+D_s+\frac{2\mu F}{g} \tag{7.53}$$

$$t_f<t_{ob}<t_r \tag{7.54}$$

$$\mu_u=\frac{g\,t_{ob}}{2x} \tag{7.55}$$

$$\mu_L=\frac{g(t_{ob}-D_s)}{2(x+F)} \tag{7.56}$$

$$\frac{g(t_{ob}-D_s)}{2(x+F)}<\mu<\frac{g\,t_{ob}}{2x} \tag{7.57}$$

$$\mu_u-\mu_L=\Delta\mu=\frac{gD_s}{2(x+F)}+\frac{g\,t_{ob}F}{2x(x+F)} \tag{7.58}$$

$$\Delta\mu=\frac{gD_s}{2x}+\frac{gF(t_{ob}-D_s)}{2x(x+F)} \tag{7.59}$$

$$\text{S. F. G. F.}=\begin{cases}1;\ \text{if } \dfrac{g(t_{ob}-D_s)}{2(x+F)}\leqslant\mu\leqslant\dfrac{g\,t_{ob}}{2x}\\ 0;\ \text{otherwise}\end{cases} \tag{7.60}$$

$$\overline{\text{S. F. G. F.}}^{\,t_M}=\begin{cases}0 & ;\text{if } 0\leqslant\mu<\dfrac{g\left[(t_{ob}-\frac{t_M}{2})-D_s\right]}{2(x+F)}\\ \dfrac{1}{2}+\dfrac{2(x+F)\mu+g(D_s-t_{ob})}{g\,t_M} & ;\text{if } \dfrac{g\left[(t_{ob}-\frac{t_M}{2})-D_s\right]}{2(x+F)}\leqslant\mu<\dfrac{g\left[(t_{ob}+t_M)-D_s\right]}{2(x+F)}\\ 1 & ;\text{if } \dfrac{g\left[(t_{ob}-\frac{t_M}{2})+D_s\right]}{2(x+F)}\leqslant\mu<\dfrac{g\,(t_{ob}-\frac{t_M}{2})}{2x}\\ \dfrac{1}{2}+\dfrac{-2x\mu+g\,t_{ob}}{g\,t_M} & ;\text{if } \dfrac{g(t_{ob}-\frac{t_M}{2})}{2x}\leqslant\mu<\dfrac{g(t_{ob}+t_M)}{2x}\\ 0 & ;\text{if } \dfrac{g(t_{ob}+\frac{t_M}{2})}{2x}\leqslant\mu<\infty\end{cases} \tag{7.61}$$

PLATE XXII

take much longer to travel the length of the fetch and consequently they are observed for a greater length of time at the source. The wave system can be thought of as consisting of two parts. Within the time interval, $0 < t < D_S$, all spectral components are present at $x = 0$ with an intensity given by the original power spectrum. Then for t greater than D_S, there will be a value of μ such that, at the time of observation, $t = D_S + 2\mu F/g$, those values of μ which are less than the value of μ which satisfies this equation will no longer be present in the power spectrum at the source. The others will be present with the same intensity as before.

Now that the conditions have been given for $x = 0$, the conditions for positive x can be found for the case of the square cut-off filter. For any particular μ, under the assumption that the sine wave in the partial sum which applies to this particular μ has a forward edge with an amplitude which is either one or zero and which travels with the group velocity, the forward edge of that wave train requires $2\mu x/g$ seconds to reach the point x. The time of arrival of the forward edge of the train, t_f, is given by equation (7.52).

Similarly the rear edge of the train starts out $D_S + 2\mu F/g$ seconds after the forward edge. The time of passage of the rear edge of the train, t_r, is consequently given by equation (7.53).

If the time of observation, t_{ob}, lies between t_f and t_r as stated by equation (7.54) then that particular spectral component will be present. If t_{ob} is less than t_f the train will not have arrived, and if t_{ob} is greater than t_f the train will already

have passed.

Under these conditions the upper value of μ in the frequency band present at the point x at the time of observation, t_{ob}, as given by μ_u, can be found by setting $t_{ob} = t_f$ and $\mu = \mu_u$, and using equation (7.52). The result is equation (7.55). For those μ greater than μ_u, the wave trains will not yet have arrived.

The lower value of μ in the frequency band present at the point x at the time of observation, t_{ob}, as given by μ_L, can be found by setting $t_{ob} = t_r$ and $\mu = \mu_L$, and using equation (7.53). The result is equation (7.56). For those μ less than μ_L, the wave trains have already passed.

Those wave trains present at the point, x, at the time of observation, t_{ob}, are consequently associated with values of μ which satisfy the inequality given by equation (7.57). A slight extension of the forecasting graphs given by figure 15 will make it possible to devise a forecasting graph for this model with the use of equations (7.55), (7.56) and (7.57).

The band width, of the square cornered filter which applies to this case is given by equation (7.58). An alternate formulation is given by equation (7.59). The first term in equation (7.59) is the same as in the previous case and the second term is a correction for the finite length of the fetch. At a fixed x, the band width increases as t_{ob} increases. Stated another way, the band width is wider for higher values of μ at a fixed x as the filter tunes through the original spectrum at the source.

The square filter for a wave system at the source represented

by the Gaussian case for storms with a fetch of finite length is then given by the value of S.F.G.F. which is one if equation (7.57) holds and zero otherwise. The functional form of S.F.G.F. is given by equation (7.60).

Forecasting diagram for a storm of finite duration with fetch of finite length

A forecasting diagram for the application of equation (7.60) to the power spectrum given at the source in order to find the power spectrum at the point and time of observation is given by figure 16. The upper part is a copy of the corresponding part in figure 15 except that the lines which pass through the point $t = D_S$ are now labeled with the values of $x + F$. The diagram again applies for $D_S = 10$ hours. The lower lines are graphs of equation (7.55) for fixed x, with μ and t_{ob} variable. The upper lines are graphs of equation (7.56) for fixed $(x + F)$, with μ and t_{ob} variable.

As an example, suppose that a storm with winds that last for ten hours over a fetch one hundred miles long develops and then ceases. The fetch is defined over a strip on the x axis between $x = 0$ and $x = -F$ with $x = 0$ the forward edge of the storm; and positive values of x define the area of decay. Suppose also that the power spectrum at $x = 0$ during the time $0 < t < D_S$ is given by the same graph as in the previous figure.

Then to forecast the power spectrum at the point $x = 400$ km for the time $t_{ob} = 20$ hours, with the use of figure 16, locates the lines for $t_{ob} = 20$ hours, $x = 400$ km, and $x + F = 500$ km on the upper part of the figure. The intersection of $t_{ob} = 20$ hours

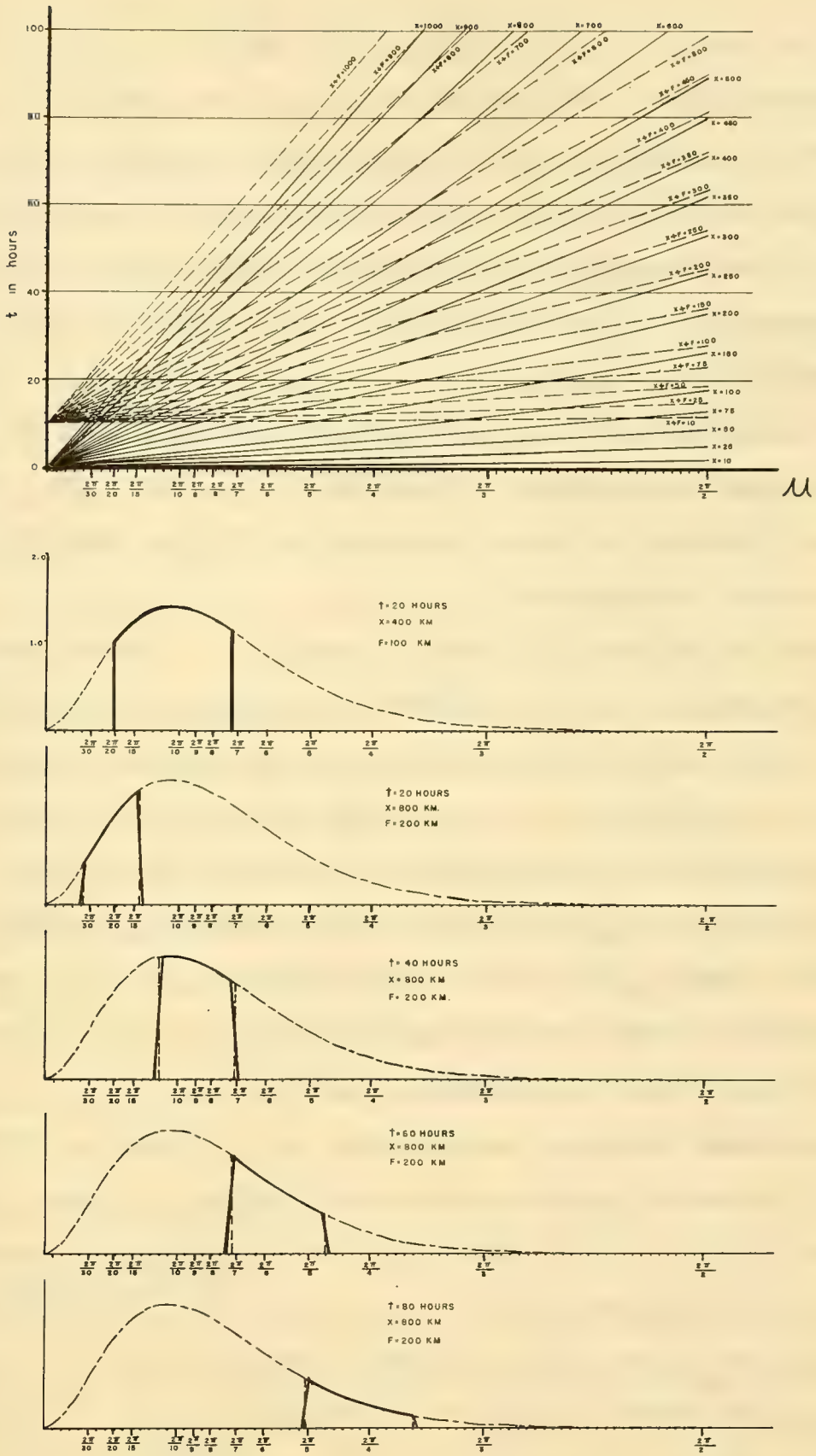

FIG. 16 FORECASTING DIAGRAM FOR THE SQUARE CORNERED FILTER AND THE SMOOTHED SQUARE CORNER FILTER FOR THE CASE OF A FETCH OF LENGTH, F.

and the curves for $x + F = 500$ km determine the value of μ_L , and the intersection of $t_{ob} = 20$ hours and the curve for $x = 400$ km determines the value of μ_u . The forecasted power spectrum then equals the power spectrum at the source between these values and zero otherwise. This case is illustrated in the first graph below the forecasting diagram.

For later values of t_{ob} and with F fixed, the band width of the power spectrum observed at the point x, becomes wider. In general, the longer the fetch the more rapidly the band width widens at the point of observation.

Figure 16 includes two special cases. If F equals zero, $x + F = x$, and the special case considered in figure 15 is the result. If D_S is zero, then the upper lines passing through the point $t = D_S$ coincide with the lines passing through $t = 0$. Then by considering the lines appropriate to, say, $x = 400$ km and $x + F = 500$ km and $t_{ob} = 20$ hours, the spectrum at the point $x = 400$ and time $t_{ob} = 20$ hours can be found in the same way as described above. This special case could occur when a strong wind blows for a very short time over a long fetch.

In general, the upper curves shift up and down for different values of D_S, and F varies from storm to storm. In some storms, the effect of D_S dominates the effect of F. For other storms, the effect of F dominates the effect of D_S. For the usual weather situation, the values of F and D_S must both be considered in order to forecast the power spectrum of the waves.

Correction of filter for the finite time of observation

At the point, x, and at the time, t_{ob}, an observation for some finite time must be made in order to obtain a wave record from which an observed power spectrum can be obtained in order to compare it with the forecasted power spectrum for verification purposes. If the observed record is too short, the measured power spectrum will be inaccurate. If the observed record is fairly long, the square filter will tune through part of the μ axis during the time required for the observation. The measured power spectrum will be more accurate, but the forecasted spectrum must be corrected for the effect of the finite time of observation.

If the wave record is observed at the point x, from the time $t = t_{ob} - t_M/2$ to the time $t = t_{ob} + t_M/2$, the smoothed filter can be computed by averaging the square filter given by equation (7.60) over the time, t_M. The smoothed filter is then given by equation (7.61) and it has the shape of a trapezoid.

In figure 16, for the other forecasted spectra indicated in the other curves of the figure, the effect of the trapezoidal figure given by equation (7.61) is shown by the heavy curves. The square filter is shown by the dashed curves. The appropriate Fresnel Filters have been eliminated because the fringe effects appear to be unrealistic. A t_M of one hour has been chosen. Note the varying width of the spectrum as t_{ob} increases.

Other smoother filters

The three filters which have just been described are not too realistic for the practical purpose of developing an easily applied wave forecasting theory. Probably an $\tilde{F}_F(t)$ which rose smoothly

to a constant value in the storm for the duration of the waves and then died out smoothly to zero again would be the most practical one to start with.

$$\tilde{F}_F(t,\mu) = (1/\pi)[\tan^{-1}(t/B_1) - \tan^{-1}(t - D_S + \frac{\mu F}{g})/B_2]$$

might be quite a practical one. The parameters, B_1 and B_2, could be related to the build up time of the waves. As the two values of B approach zero, $\tilde{F}_F(t)$ becomes in the limit equation (7.51). Such a representation would probably eliminate the Fresnel fringes.

Physical interpretation of the forecast diagrams

The waves at the source can be characterized as "sea." The waves at large x can be shown to have the properties of "swell." One of the ways in which the apparent period of ocean swell can increase with travel time is explained by this model. The analysis, however, is still incomplete because it does not contain any of the properties of short crested waves.

At the source, the power spectrum might look like the one assumed in figure 15. There is some indirect evidence which supports this general shape. The partial sum given by equation (7.32) shows that the sea surface can be represented by the sum of many vectors in the complex plane. These vectors have many different angular speeds. Suppose that at some instant of time, some number of the vectors add together to give a definite peak amplitude to the projection of the sum onto the real axis. And also suppose, as indeed must be the case, that the other vectors all add together to very nearly zero. These vectors which add to give the displacement are all rotating at widely different values of μ. Hence after they have gone around the circle several times they will

begin to cancel each other out, and the sea surface will go through several wavelike oscillations of decreasing amplitude. If t is varied negatively the vectors will cancel out with decreasing time. The process described above shows how a wave group is generated. At other times, different vectors could be involved, and the wavelike oscillations could have an entirely different apparent period. If the vectors which add by chance to give the peak wave have widely different angular frequencies, they cancel out very rapidly with time and the group is short. If by chance, these vectors have more nearly the same angular frequencies, then the group lasts longer. In the limit, these considerations show that the sea surface at the source is irregular and choppy, that groups of widely different durations can occur at random, and that the sea surface has the properties generally ascribed to the term "sea." The "significant" period, if it means anything at all in a source region, is probably the median value of the square root of the power spectrum.

At a large value of x, the power spectrum contains a much narrower band of frequencies. Consequently if the vectors in the partial sum which approximates the record, by chance add to a large displacement, these vectors will make a great many more rotations than in the case described above before they get out of phase. The wave groups (when they occur) are therefore longer and more regular. The wave record is still Gaussian, but the autocorrelation effect is greater, and points in the record would have to be taken at greater time intervals in order to show the Gaussian character. The Gaussian model of the Lebesgue Power

Integral therefore demonstrates the transformation of sea into swell without any effect of friction.

The period increase of ocean swell

One point which Sverdrup and Munk [1947] make in their studies of ocean waves is that the "significant period" of swell from a distant storm is higher than the "significant period" of the waves in the storm and that when the swell is highest the "significant period" is higher than the "significant period" in the storm. Sverdrup [1947] explains this observed fact by supposed selective attenuation of low periods. Figures 15 and 16 show another possible explanation. In these figures, the peak of the power spectrum is at a higher period than the median value of the square root of the power spectrum. From the figure the "significant period" in the storm would be probably around seven seconds. Now, the area under the power spectrum equals the square of the wave record; and at large x, when the band width is narrow, the highest waves occur with a "significant period" of ten seconds. Hence, this shows a period increase of ocean swell without selective attenuation. But the "significant period" of the swell does not increase indefinitely. It increases to ten seconds as the width of the filter narrows, and then stops increasing. It is known that the forecasted swell periods in the Sverdrup Munk theory fail for great decay distances,* and the above reasons could easily be an explanation.

---

*Personal communication, R. S. Arthur

Wave decay

In the Sverdrup Munk theory the decrease in wave height due to the travel of the waves into the area of decay is ascribed to selective attenuation of the waves against the atmosphere. The forecasting diagrams in figures 15 and 16, show that the square of the wave record averaged over time decreases with the band width of the filter. Therefore for a disturbance of finite duration over a fetch of finite length, the wave amplitudes die down essentially like $1/\sqrt{x}$ simply due to the properties of dispersion. This amount is not quite enough to fit the empirical forecasting graphs of Sverdrup and Munk as revised by Arthur [1948, 1949], but another factor approximately equal to $1/\sqrt{x}$ will result from consideration of short crested waves. It will eventually be shown in this paper that wave decay can be explained without friction effects. At this point, reference is made to figure 8 in the paper by Donn [1949]. Although the spectrum shown is not a power spectrum, (and the μ axis is plotted backwards), this figure already shows remarkable agreement with figure 16.

Comparison with the models of Chapter 6

The models studied in this chapter are far more realistic than the models studied in Chapter 6. In the first place, wave records appear to be actually Gaussian to a very good degree of approximation even if the records are swell records. Secondly, the models in this chapter provide for a smooth continuously varying record at large decay distances, whereas all of the models in Chapter 6 required discrete jumps in wave amplitude at distant

points of observation. Finally, the forecasting diagrams explain in part the observed change from sea into swell and the decrease in wave height with distance traveled.

Fourier Integral versus Lebesgue Power Integral

The introductory chapter of this paper began with a quotation from Lamb which stated that the most general case consistent with the assumption that the potential function was a simple harmonic function in x could be solved by the use of Fourier's Integral theorem. Interesting, but not completely general, results were obtained in Chapters 4, 5, and 6 with the use of Fourier's Integral theorem. Then suddenly strikingly realistic and completely general results were obtained by the use of a new integral referred to as the Lebesgue Power Integral. It would seem, at first approximation, that Lamb was wrong in the quotation.

This is not the case, however. Lamb was correct. If η (o,t) is given at x = 0 throughout the entire storm, no matter how complicated the function, and if η(o,t) is zero before and after the storm, then it is conceivably possible to find the Fourier spectrum for the entire wave system, and to solve a much more complicated problem somewhat along the lines of the problems solved in Chapters 4 and 5. Such a procedure would be impossible in a practical sense because of the length of the record and complexity of the function which would be required.

For an actual wave record it would also not be possible to attack the problem along the lines employed in Chapter 6 where the wave system was treated as if it were composed of wave groups repeating at fairly regular intervals, since a difficulty arises

upon attempting to find the average potential energy in the system when the wave groups overlap in time.

The Lebesgue Power Integral for the Gaussian case of a stationary time series eliminates these difficulties because it employs a function which is (apart from a constant) directly related to the average potential energy in the wave record. Methods of wave record analysis based upon this integral do not depend upon the entire wave record, upon the time the record was made, or upon the existence of groups of waves in the record. The analysis of the wave records is therefore much simpler, and the interpretation of results is much easier. The formulation of the wave record as a Lebesgue Power Integral is not a complete solution to the problems because such a record lasts forever, and theoretically at least, only has a meaning for an infinitely long record.

It should be noted that it is not necessary to include a section on energy considerations in this chapter. The potential energy averaged over time at the point and time of observation is given by the area under the forecasted power spectrum multiplied by $\rho g/4$, and the very nature of the filters employed shows that all of the energy is accounted for.

Fourier Integral theory was employed in order to find the filter functions for the forecasting diagrams since they are all based upon the results of Chapter 5. The Fourier Integral solution gave the effect of the finiteness of the record on the infinitely long record as represented by one of the terms of a partial sum which in the limit gave the Lebesgue Power Integral.

In conclusion for this chapter, the most realistic results

are obtained by a judicious combination of Fourier Integral theory, stationary time series theory, and statistical methods. The stationary time series concepts and the statistical methods apply to the wave system as a whole as if it were to last forever. Small pieces of the wave system when analyzed as wave records can be treated as if they were samples taken from a stationary process, and the statistical methods appropriate to such a treatment are valid. The concepts of Fourier Integral theory apply to the propagation of the system and to the fact that it lasts only for a given number of hours and is generated over a fetch of finite length.

Chapter 8. SHORT CRESTED WAVE SYSTEMS

Introduction

The possibilities of models with infinitely long crests have been analyzed in the past chapters of this paper. Unfortunately for theoretical purposes, storms are finite in width and waves at the edge of a storm at sea are short crested. These two facts have not been adequately treated in past forecasting theories and it is necessary to treat them adequately now. Waves are observed at angles up to forty-five degrees to the direction of the wind in a fetch of finite width. The waves therefore spread out over areas considerably wider than the width of the storm. The potential energy per unit area of the waves in the decay area must therefore be lower, and the waves must therefore be lower due to this effect.

In this chapter, then, the basic material for the analysis of short crested waves will be derived. In Chapter 9, the Lebesgue Power Integral for a short crested sea surface will be derived, and the behavior of the waves outside of a storm of finite width will be studied. In Chapter 9, the results will be so general that they will form an adequate theoretical base for a wave forecasting system.

Elementary short crested wave systems

Short crested waves are discussed somewhat briefly in Lamb [1932] and in most other references on wave theory. The usual analysis is of such an elementary nature that it is necessary to start from these elementary concepts and show how they can

be extended to the more complicated patterns.

The simplest short crested wave system could be represented by equation (8.1) where $0 < \alpha < 1$. The sea surface at $t = 0$ is an alternating sequence of elliptically shaped hills and valleys. As t varies they appear to move in the positive x direction. At any fixed y, the sea surface is sinusoidal in the x direction with an apparent length in the x direction given by $L_{(x)}$ in equation (8.2). The velocity in the x direction of the crests is given by $C_{(x)}$ in equation (8.3). Note that $L_{(x)}$ is not equal to $C_{(x)}T$.

Equations (8.1), (8.2) and (8.3) describe a possible configuration of the sea surface, but the particular method of presentation employed is limited to that one particular form and minor modifications and extensions thereof. By a trigonometric identity equation (8.1) can be written in the form of equation (8.4). The short crested waves then turn out to be simply the interference pattern between two long crested waves which are traveling in different directions. The first wave is traveling in the direction of the line $\sqrt{1 - \alpha^2}\, x + \alpha y = 0$. It has infinitely long crests oriented perpendicularly to this line. The individual crests have the classical wave length and travel with the classical speed. The second wave is traveling in the direction of the line $\sqrt{1 - \alpha^2}\, x - \alpha y = 0$. In this direction, it has all the properties of classical waves.

Equation (8.1) is thus another way to analyze equation (8.4). It can be employed only if the two waves have the same amplitude although interesting results can be found if the two waves in

Short Crested Waves

$$\eta(x,y,t) = A\cos\left(\frac{4\pi^2}{gT^2}\alpha y\right) \cdot \cos\left(\frac{4\pi^2}{gT^2}\sqrt{1-\alpha^2}\,x - \frac{2\pi t}{T}\right) \tag{8.1}$$

$$L_{(x)} = gT^2/2\pi\sqrt{1-\alpha^2} \tag{8.2}$$

$$C_{(x)} = gT\sqrt{1-\alpha^2}/2\pi \tag{8.3}$$

$$\eta(x,y,t) = \frac{A}{2}\cos\left(\frac{4\pi^2}{gT^2}\left(\sqrt{1-\alpha^2}\,x+\alpha y\right) - \frac{2\pi t}{T}\right)$$

$$+ \frac{A}{2}\cos\left(\frac{4\pi^2}{gT^2}\left(\sqrt{1-\alpha^2}\,x-\alpha y\right) - \frac{2\pi t}{T}\right) \tag{8.4}$$

$$\eta(x,y,t) = \sum_{i=1}^{N}\sum_{j=1}^{M} A_{ij}\cos\left(\frac{4\pi^2}{g\,T_j^2}\left(\sqrt{1-\alpha_i^2}\,x+\alpha_i y\right) - \frac{2\pi t}{T_j} + \delta_{ij}\right) \tag{8.5}$$

Plate XXIII

equation (8.4) have both different directions and periods. Difficulties arise when there are more than two terms in the sum and when the amplitudes are not the same. Under these conditions a sum of terms of different periods, directions, and amplitudes is the result such as in equation (8.5). The only method of analyzing the expression is to evaluate the expression term by term and sum them all in order to determine the actual appearance of the sea surface. There is no short cut to permit a form like equation (8.1).

Equation (8.5) yields a multitude of representations for the sea surface, depending on the number of terms chosen to be in the sum. Figure 17 is an example of what the sea surface might look like with five terms in the sum of equation (8.5). The equation given on the figure was evaluated for t = 0 as a function of x and y. The contour system begins to look like some of the aerial photographs of the sea surface which are found in the literature. In equation (8.5), if $-1 < a_i < 1$, and if the square root can have both positive and negative signs, then the expression is as general as possible.

A useful lemma

In order to derive many of the results which will follow, it is necessary to prove a very useful lemma (or auxiliary theorem*) which has many applications in Fourier Integral Theory. This lemma will not be proved for the most general conditions on the functions possible. The conditions which will be assumed are general enough to include all of the cases in which it will

*From lecture notes taken in a course in mathematics given by Professor Magnus of N.Y.U. Math Institute. Referred to also as Dirichlet's Limit formula. See Courant [1937] p. 321 for alternate proof.

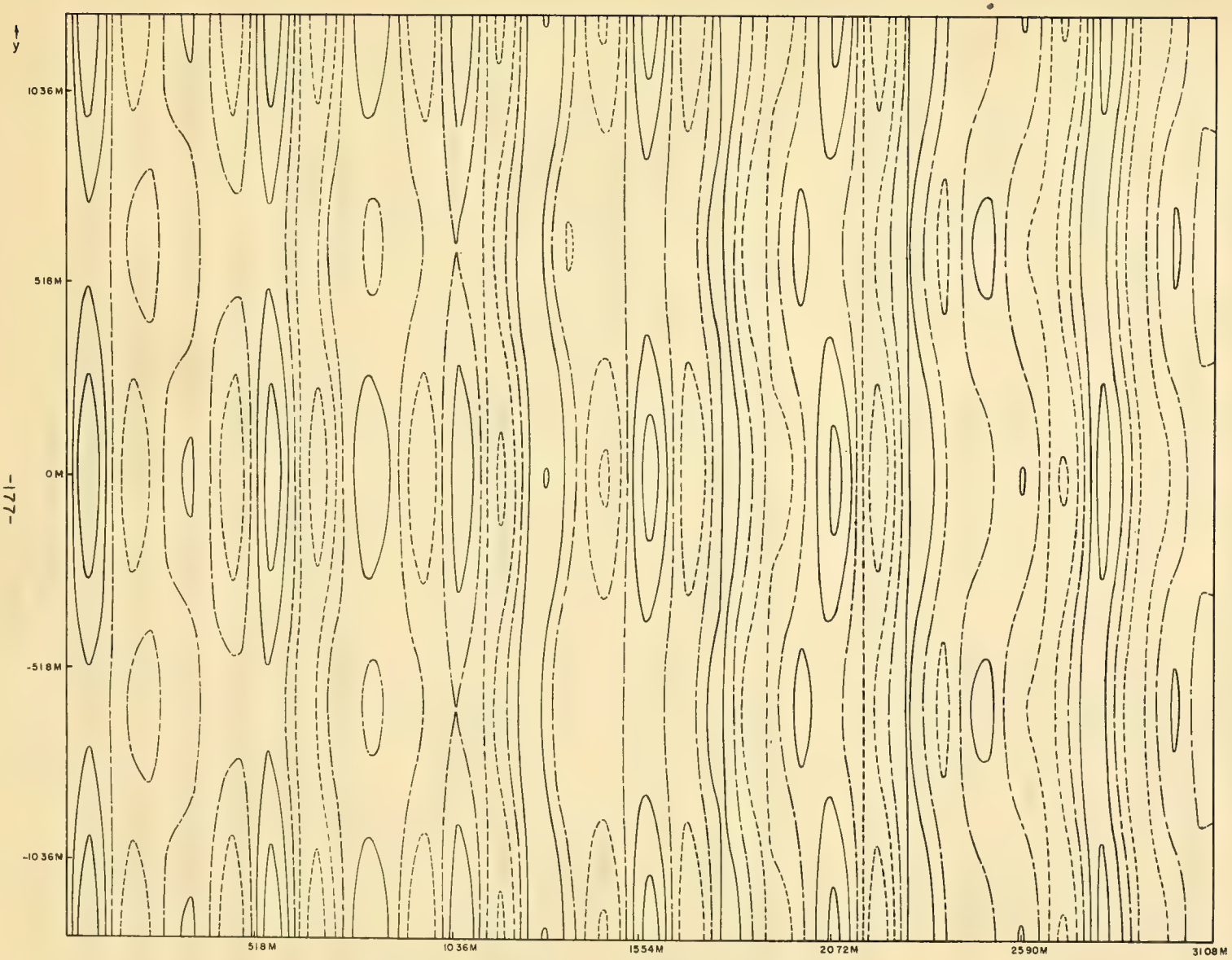

A PORTION OF A SHORT CRESTED SEA SURFACE

$\eta = +1 \text{ or } +2$ ——————

$\eta = 0$ —— — ——

$\eta = -1 \text{ or } -2$ - - - - - - -

$$\eta(x,y,0) = \sin\frac{4\pi^2 5^2}{g(2500)}x + \frac{1}{2}\sin\frac{4\pi^2 6^2}{g(2500)}x + \frac{1}{2}\sin\frac{4\pi^2 4^2}{g(2500)}x + \frac{1}{2}\sin\frac{4\pi^2 5^2}{g(2500)}\left(\sqrt{1-\left(\frac{1}{5}\right)^2}x + \frac{1}{5}y\right) + \frac{1}{2}\sin\frac{4\pi^2 5^2}{g(2500)}\left(\sqrt{1-\left(\frac{1}{5}\right)^2}x - \frac{1}{5}y\right)$$

Fig. 17

be applied in this paper.

The conditions which will be imposed are the following. First, the functions, f(x) and its first derivative, f'(x), are continuous as stated in (8.6). Secondly, the absolute value of f(x) is less than some positive constant M as stated by equation (8.7). And thirdly, the absolute value of the derivative of f(x) is less than M.

If these conditions are satisfied, then it can be proved that equation (8.9) holds. The proof follows. The integral from -A to A can be broken up into three parts as in equation (8.10) where ϵ is some small but fixed number. The integral from -A to $-\epsilon$ and the integral from ϵ to A can be shown to vanish. The integral from $-\epsilon$ to ϵ contributes the whole value to the entire integral.

Consider, first, the integral from ϵ to A. It can be integrated by parts, and if absolute values are taken, the first inequality in equation (8.11) is the result. Estimates based upon M, the value of ϵ, and the length of the path of integration, then yield the second inequality. The second inequality as N approaches infinity tends toward zero. Therefore the integrals from ϵ to A and from -A to $-\epsilon$ tend to zero as N approaches infinity.

Consider next, the integral from $-\epsilon$ to ϵ. In equation (8.12), the transformation of variables given by equation (8.13) yields the first expression. As n approaches infinity f(x'/N) approaches f(o) over a large range of x', and f(o) can be factored out of the integral as a constant. The integral from - N to N of (sin x')/x' approaches the integral from minus infinity

A Useful Lemma

Given $f(x)$ and $f'(x)$ continuous (8.6)

$$|f(x)| < M \tag{8.7}$$

$$|f'(x)| < M \tag{8.8}$$

$$\text{then } \lim_{N\to\infty}\int_{-A}^{A} \frac{\sin Nx}{x} f(x)\,dx = \pi f(0) \tag{8.9}$$

Proof :

$$\lim_{N\to\infty}\int_{-A}^{A} \frac{\sin Nx}{x} f(x)\,dx = \lim_{N\to\infty}\int_{-A}^{-\epsilon} \frac{\sin Nx}{x} f(x)dx + \lim_{N\to\infty}\int_{-\epsilon}^{\epsilon} \frac{\sin Nx}{x} f(x)\,dx$$

$$+ \lim_{N\to\infty}\int_{\epsilon}^{A} \frac{\sin Nx}{x} f(x)dx \tag{8.10}$$

$$\lim_{N\to\infty}\left|\int_{\epsilon}^{A} \frac{\sin Nx}{x} f(x)dx\right| \le \lim_{N\to\infty}\left| -\frac{f(x)}{x}\frac{\cos Nx}{N}\right|_{\epsilon}^{A} + \lim_{N\to\infty}\left|\int_{\epsilon}^{A}\frac{\cos Nx}{N}\left(\frac{f'(x)}{x} - \frac{f(x)}{x^2}\right)dx\right|$$

$$\le \lim_{N\to\infty}\left(\frac{2M}{\epsilon N} + \frac{2MA}{\epsilon^2 N}\right) \le 0 \tag{8.11}$$

$$\lim_{N\to\infty}\int_{-\epsilon}^{\epsilon} \frac{\sin Nx}{x} f(x)dx = \lim_{N\to\infty}\int_{-\epsilon N}^{\epsilon N} \frac{\sin x'}{x'} f\left(\frac{x'}{N}\right)dx' = \lim_{N\to\infty} f(0)\int_{-\epsilon N}^{\epsilon N}\frac{\sin x'}{x'}dx' = \pi f(0) \tag{8.12}$$

Where $x' = Nx$ (8.13)

Plate XXIV

to infinity of $(\sin x')/x'$ which has the value π. The final expression in equation (8.12) is thus the desired limiting value.

If A is permitted to approach infinity in equations (8.9), the same result will hold. The results hold for any preassigned A no matter how large, and therefore they hold for A infinite in the limit.

The initial value problem in the y,t plane for a disturbance of finite duration and width

In a storm at sea, the waves are quite irregular. There are high waves, and low waves. The high waves sometimes appear to come in groups followed by times when the waves are relatively low. In addition, even when the waves are high the crests are not very long, possibly only ten times the distance between successive crests. Consider then a wave record in deep water obtained by a whole line of wave recorders along a segment of the line $x = 0$ parallel to the dominant orientation of the crests. If all of the wave records were properly synchronized, it would be possible to obtain a plot of wave height as a function of time and the position of each of the recorders on the line $x = 0$. The free surface would then be expressible as a function of y and t inside of a closed curve given by some function of y and t. Inside of this closed curve let the sea surface be given by the observations. Outside of the closed curve, let the sea surface be identially zero in amplitude, and if desired smooth the sharp edges off the boundary. The result is a finite short crested wave system observed as a function of y and t at an arbitrary origin in deep water. It could represent a whole storm at sea

The Initial Value Problem in the y,t Plane for a Disturbance of Finite Duration and Width

$$\eta(x,y,t) = \int_{-\frac{\pi}{2}}^{\frac{\pi}{2}}\int_{0}^{\infty}\left[a(\mu,\theta)\cos\left(\frac{\mu^2}{g}(x\cos\theta + y\sin\theta) - \mu t\right) + b(\mu,\theta)\sin\left(\frac{\mu^2}{g}(x\cos\theta + \sin\theta) - \mu t\right)\right] d\mu\, d\theta \tag{8.14}$$

$$\eta(o,y,t) = \int_{-\frac{\pi}{2}}^{\frac{\pi}{2}}\int_{0}^{\infty}\left[a(\mu,\theta)\cos\left(\frac{\mu^2}{g}y\sin\theta - \mu t\right) + b(\mu,\theta)\sin\left(\frac{\mu^2}{g}y\sin\theta - \mu t\right)\right] d\mu\, d\theta \tag{8.15}$$

$$\eta(o,y,t) = \int_{-\frac{\pi}{2}}^{\frac{\pi}{2}}\int_{0}^{\infty}\left[a(\mu,\theta)\cos\left(\frac{\mu^2}{g}y\sin\theta\right)\cos\mu t + a(\mu,\theta)\sin\left(\frac{\mu^2}{g}y\sin\theta\right)\sin\mu t + b(\mu,\theta)\sin\left(\frac{\mu^2}{g}y\sin\theta\right)\cos\mu t\right.$$

$$\left. - b(\mu,\theta)\cos\left(\frac{\mu^2}{g}y\sin\theta\right)\sin\mu t\right] d\mu\, d\theta \tag{8.16}$$

$$\lim_{\substack{N\to\infty\\ M\to\infty}} \int_{-M}^{M}\int_{-N}^{N} \eta(o,y,t)\cos\left(\frac{(\mu^*)^2}{g}\sin\theta^* y\right)\cos\mu^* t\, dy\, dt$$

$$= \lim_{\substack{N\to\infty\\ M\to\infty}} \int_{-M}^{M}\int_{-N}^{N}\int_{-\frac{\pi}{2}}^{\frac{\pi}{2}}\int_{0}^{\infty}\left[a(\mu,\theta)\cos\left(\frac{\mu^2}{g}\sin\theta y\right)\cos\mu t\cos\left(\frac{(\mu^*)^2}{g}\sin\theta^* y\right)\cos\mu^* t\right] d\mu\, d\theta\, dy\, dt$$

+ terms which equal zero

$$= \lim_{\substack{N\to\infty\\ M\to\infty}} \int_{-\frac{\pi}{2}}^{\frac{\pi}{2}}\int_{0}^{\infty} a(\mu,\theta)\int_{-M}^{M}\int_{-N}^{N}\left[\frac{1}{2}\cos\left(\frac{\mu^2}{g}\sin\theta - \frac{\mu^{*2}}{g}\sin\theta^*\right)y\right] + \frac{1}{2}\cos\left[\left(\frac{\mu^2}{g}\sin\theta + \frac{\mu^{*2}}{g}\sin\theta^*\right)y\right]\Big]$$
$$\cdot\left[\frac{1}{2}\cos(\mu-\mu^*)t + \frac{1}{2}\cos(\mu+\mu^*)t\right] dy\, dt\, d\mu\, d\theta \tag{8.17}$$

Plate XXV

as it passes the line x = 0. Before a certain time its amplitude would be zero and after, say, ten hours had elapsed it would again be zero. In addition, outside of a certain range of y at x = 0 it would never be observed.

The immediate problem is to find out how this disturbance behaves at other values of x. In anticipation of what is to follow, though, think of a storm at sea as a sum of many elemental sine waves traveling in various directions but bounded by the closed curve described above. The disturbance is, by the principle of superposition, and due to the linearity of the system, equal to the sum of the individual disturbances, no matter how they differ in direction, amplitude, phase, and period.

The function, $\eta(o,y,t)$, has now been obtained. What is the function $\eta(x,y,t)$? Strictly speaking, $\eta(o,y,t)$ does not determine $\eta(x,y,t)$ because there is an ambiguity in the possible directions of the individual spectral components. For a completely general problem, $\eta_x(o,y,t)$ would also have to be measured. However waves in a storm at sea travel in the direction of the wind and if the reasonable assumption that each spectral component has a component of direction of travel in the positive x direction is made, then a solution can be obtained.

Equation (8.14) postulates that the free surface is composed of spectral sine waves of special frequency μ which travel in the spectral direction $x \cos \theta + y \sin \theta$ (see equation (2.29)). Note that the limits of integration are over only half a circle in the μ , θ polar coordinate system, and that μ is always positive since the integration is from zero to infinity. With this

assumption about the limits of integration, it is not necessary to know $\eta_x(y,t)$ because all spectral components have a direction component in the positive x direction.

If equation (8.14) represents the free surface everywhere, then equation (8.15) represents the sea surface at x = 0 and it can be expanded into the form of equation (8.16). Now the left hand side of equation (8.16) is a known function, and if the values of $a(\mu,\theta)$ and $b(\mu,\theta)$ were known then the step back to equation (8.14) would be simple and the problem would be solved.

Take the known function $\eta(y,t)$, multiply it by $\cos((\mu^{*2}/g)\sin\theta^{*}\cdot y)\cdot\cos\mu^{*}t$, and integrate it over y and t from minus N to plus N and from minus M to plus M. Consider the limit as M and N approach infinity. The first expression in equation (8.17) formulates this operation, and in the second expression (8.16) has been substituted for $\eta(o,y,t)$. The second, third, and fourth term in the bracket from equation (8.16) are not needed because the integration is even, and since, for example, $\cos\mu^{*}t\sin\mu t$ is odd the integration is zero. The third expression in equation (8.17) can be obtained from a trigonometric identity.

The integration under analysis is continued in equation (8.18). Two transformations of variable are employed in order to get from the second expression to the third expression. The second expression can be expanded into one integral which involves $(\sin(\mu-\mu^{*})M)/(\mu-\mu^{*})$ and another which involves $(\sin(\mu+\mu^{*})M)/(\mu+\mu^{*})$. In the first integral the transformation of variable given in equation (8.19) is used and in the

The Initial Value Problem in the y,t Plane for a Disturbance of Finite Duration and Width

$$\lim_{\substack{N\to\infty\\M\to\infty}} \int_{-M}^{M}\int_{-N}^{N} \eta(o,y,t)\cos\left(\frac{\mu^{*2}}{g}\sin\theta^{*}y\right)\cos\mu^{*}t\ dy\ dt$$

$$= \lim_{\substack{N\to\infty\\M\to\infty}} \int_{-\frac{\pi}{2}}^{\frac{\pi}{2}}\int_{-\mu}^{\infty} a(\mu,\theta)\left[\frac{\sin\left(\frac{\mu^{2}}{g}\sin\theta-\frac{\mu^{*2}}{g}\sin\theta^{*}\right)N}{\frac{\mu}{g}\sin\theta-\frac{\mu^{*2}}{g}\sin\theta^{*}}+\frac{\sin\left(\frac{\mu^{2}}{g}\sin\theta+\frac{\mu^{*2}}{g}\sin\theta\right)N}{\frac{\mu^{2}}{g}\sin\theta+\frac{\mu^{*2}}{g}\sin\theta^{*}}\right]\cdot\left[\frac{\sin(\mu-\mu^{*})M}{\mu-\mu^{*}}+\frac{\sin(\mu+\mu^{*})M}{\mu+\mu^{*}}\right]d\mu\ d\theta$$

$$= \lim_{\substack{N\to\infty\\M\to\infty}} \int_{-\frac{\pi}{2}}^{\frac{\pi}{2}}\int_{\mu^{*}}^{\infty} a(\mu+\alpha,\theta)\left[\frac{\sin\left(\frac{(\mu+\alpha)^{2}}{g}\sin\theta-\frac{\mu^{*2}}{g}-\sin\theta^{*}\right)N}{\left(\left(\frac{\mu^{*2}+\alpha}{g}\right)^{2}\sin\theta-\frac{\mu^{*2}}{g}\sin\theta^{*}\right)}+\frac{\sin\left(\frac{(\mu+\alpha)^{2}}{g}\sin\theta+\frac{\mu^{*2}\sin\theta^{*}}{g}\right)N}{\left(\frac{(\mu^{*}+\alpha)^{2}}{g}\sin\theta+\frac{\mu^{*2}}{g}\sin\theta^{*}\right)}\right]\frac{\sin\alpha M}{\alpha}\,d\alpha\ d\theta$$

$$+ \lim_{\substack{N\to\infty\\M\to\infty}} \int_{-\frac{\pi}{2}}^{\frac{\pi}{2}}\int_{\mu^{*}}^{\infty} a(-\mu^{*}+\alpha,\theta)\left[\frac{\sin\left(\frac{(-\mu+\alpha)^{2}\sin\theta}{g}-\frac{\mu^{*2}}{g}\sin\theta^{*}\right)N}{\frac{(-\mu^{*}+\alpha)^{2}}{g}\sin\theta-\frac{\mu^{*2}}{g}\sin\theta^{*}}+\frac{\sin\left(\frac{(-\mu^{*}+\alpha)^{2}}{g}\sin\theta+\frac{\mu^{*2}\sin\theta^{*}}{g}\right)N}{\frac{(-\mu^{*}+\alpha)^{2}}{g}\sin\theta+\frac{\mu^{*2}\sin\theta^{*}}{g}}\right]\frac{\sin\alpha M}{\alpha}\,d\alpha\ d\theta \quad (8.18)$$

first term let $\mu = \mu^{*}+\alpha$ (8.19)

second term let $\mu = -\mu^{*}+\alpha$ (8.20)

Plate XXVI

second, equation (8.20) is used.

As M approaches infinity, the results of the lemma given in equation (8.9) can be applied. In the first integral, the range of integration includes $\alpha = 0$, and in the second integral it does not. The limit in the first case is consequently a definite value. In the second case, it is zero. The second expression in equation (8.21) is the limiting value as M approaches infinity.

The limit as N approaches infinity can now be studied. There are two terms in the bracket in the second expression of equation (8.21) and the integration can be written as the sum of two terms. The transformation of variables given by the upper sign (where applicable) in equation (8.22), (8.23), and (8.24) can be used in the first term, and the corresponding relations with the lower sign can be used in the second term. The result is the third expression in equation (8.21).

The range of integration in both integrals includes the origin, and as N approaches infinity both integrals have a limit. The limiting value is given by the last expression in equation (8.21). It is an even function in θ^* as should be expected from the form of the original integral over η (o,y,t) times even cosine functions.

In equation (8.25), a similar integral is evaluated where the cosines have been replaced by sines. The result is an odd function in θ^*.

When the two equations (8.25) and (8.21), are taken together, it is possible to solve for $a(\mu^*,\theta^*)$, and the result is given by equation (8.26). Similar operations with $\cos[(\mu^*)^2/g \sin\theta]\sin \mu^* t$

$$\lim_{\substack{N\to\infty\\ M\to\infty}} \int_{-M}^{M}\int_{-N}^{N} \eta\,(o,y,t)\cos\left(\frac{\mu^{*2}}{g}\sin\theta^{*}y\right)\cos\mu^{*}t\;\,dy\,dt$$

$$=\lim_{N\to\infty}\int_{-\frac{\pi}{2}}^{\frac{\pi}{2}} \pi\, a\,(\mu^{*},\theta)\left[\frac{\sin\left(\frac{(\mu^{*})^2}{g}(\sin\theta-\sin\theta^{*})N\right)}{\frac{(\mu^{*})^2}{g}(\sin\theta-\sin\theta^{*})}+\frac{\sin\left(\frac{(\mu^{*})^2}{g}(\sin\theta+\sin\theta^{*})N\right)}{\frac{(\mu^{*})^2}{g}(\sin\theta-\sin\theta^{*})}\right]d\theta$$

$$=\lim_{N\to\infty}\int_{\frac{\mu^{*2}}{g}(-1-\sin\theta^{*})}^{\frac{\mu^{*2}}{g}(1-\sin\theta^{*})}\frac{\pi g\,a\left(\mu^{*},\sin^{-1}(\sin\theta^{*}+\frac{g\beta}{(\mu^{*})^2})\right)}{(\mu^{*})^2\sqrt{1-\left(\sin\theta^{*}+\frac{g\beta}{(\mu^{*})^2}\right)^2}}\cdot\frac{\sin\beta N}{\beta}\,d\beta+\lim_{N\to\infty}\int_{\frac{\mu^{*2}}{g}(-1+\sin\theta^{*})}^{\frac{\mu^{*2}}{g}(1+\sin\theta^{*})}\frac{\pi g\,a\left(\mu,\sin^{-1}(-\sin\theta^{*}+\frac{g\beta}{(\mu^{*})^2})\right)}{\frac{\mu^{*2}}{g}(\mu^{*})^2\sqrt{1-\left(-\sin\theta^{*}+\frac{g\beta}{(\mu^{*})^2}\right)^2}}\cdot\frac{\sin\beta N}{\beta}\,d\beta$$

$$=\frac{\pi^2 g\left[a\,(\mu^{*},\theta^{*})+a\,(\mu^{*},-\theta^{*})\right]}{(\mu^{*})^2\cos\theta^{*}} \qquad (8.21)$$

$$\frac{(\mu^{*})^2}{g}(\sin\theta\pm\sin\theta^{*})=\beta \qquad (8.22)$$

$$d\theta=\frac{g}{(\mu^{*})^2}\,\frac{d\beta}{\sqrt{1-\left(\pm\sin\theta^{*}+\frac{g\beta}{(\mu^{*})^2}\right)^2}} \qquad (8.23)$$

$$\theta=\sin^{-1}\left(\pm\sin\theta^{*}+\frac{g}{(\mu^{*})^2}\beta\right) \qquad (8.24)$$

and $\sin[((\mu^*)^2/g)\sin\theta]\cos\mu^* t$, make it possible to find $b(\mu^*,\theta^*)$.

The spectrum of the disturbance given by $a(\mu^*,\theta^*)$ and $b(\mu^*,\theta^*)$ has now been found from the function $\eta(o,y,t)$ which was known. These known values can now be substituted into the original formula given by equation (8.28) which is known once $\eta(o,y,t)$ is given. The integration in the square brackets must be carried out before the integration over μ^* and θ^*, and in order to emphasize this, the y and t which disappear due to the process of integration are not starred, and the ones which will remain in the final solution are starred.

The initial value problems in the x,y plane for a disturbance over a finite area

Given $\eta(x,y)$ at t equals zero, it is possible to find $\eta(x^*,y^*,t^*)$ by the methods used above. Formulated in terms of ν, where ν is the spectral wave number, equation (8.29) prescribes a motion such that each elemental wave in the motion has a component of travel in the positive x direction. A derivation which follows the procedures used above very closely then yields the final result as given by equation (8.30). The values of $a(\nu^*,\theta^*)$ and $b(\nu^*,\theta^*)$ are given in the brackets and can be found given $\eta(x,y)$.

The use of ν instead of μ is more convenient in the derivation but not essential. The variable could just as easily have been μ. The transformation of variables given by equations (8.31) and (8.32) then yields equation (8.33). The wave system consequently has the same form as the previous system.

The Initial Value Problem in the y,t Plane for a Disturbance of Finite Duration and Width

$$\lim \int_{-M}^{M}\int_{-N}^{N} \eta\,(o,y,t)\,\sin\left(\frac{\mu^{*2}}{g}\sin\theta^{*}y\right)\sin\mu^{*}t\,dy\,dt = \frac{2\pi^{2}g\left[a(\mu^{*},\theta^{*})-a(\mu^{*},-\theta^{*})\right]}{2\,(\mu^{*})^{2}\cos\theta^{*}} \qquad (8.25)$$

$$a(\mu^{*},\theta^{*}) = \frac{\mu^{*2}\cos\theta^{*}}{2\pi^{2}g}\left[\int_{-\infty}^{+\infty}\int_{-\infty}^{+\infty}\eta\,(o,y,t).\cos\left(\frac{\mu^{*2}}{g}\sin\theta^{*}y-\mu^{*}t\right)dy\,dt\right] \qquad (8.26)$$

$$b(\mu^{*},\theta^{*}) = \frac{\mu^{*2}\cos\theta^{*}}{2\pi^{2}g}\left[\int_{-\infty}^{+\infty}\int_{-\infty}^{+\infty}\eta\,(o,y,t).\sin\left(\frac{\mu^{*2}}{g}\sin\theta^{*}y-\mu^{*}t\right)dy\,dt\right] \qquad (8.27)$$

$$\eta\,(x^{*},y^{*},t^{*}) = \int_{-\frac{\pi}{2}}^{\frac{\pi}{2}}\int_{0}^{\infty}\left[\frac{\mu^{*2}\cos\theta^{*}}{2\pi^{2}g}\int_{-\infty}^{+\infty}\int_{-\infty}^{+\infty}\eta\,(o,y,t)\cos\left(\frac{\mu^{*2}}{g}\sin\theta^{*}y-\mu^{*}t\right)dy\,dt\right]\cos\left(\frac{\mu^{*2}}{g}(x^{*}\cos\theta^{*}-y^{*}\sin\theta^{*})-\mu^{*}t^{*}\right)d\mu^{*}\,d\theta^{*}$$

$$+\int_{-\frac{\pi}{2}}^{\frac{\pi}{2}}\int_{0}^{\infty}\left[\frac{\mu^{*2}\cos\theta^{*}}{2\pi^{2}g}\int_{-\infty}^{+\infty}\int_{-\infty}^{+\infty}\eta\,(o,y,t)\,\sin\left(\frac{\mu^{*2}}{g}\sin\theta^{*}y-\mu^{*}t\right)dy\,dt\right]\sin\left(\frac{\mu^{*2}}{g}(x^{*}\cos\theta^{*}+y^{*}\sin\theta^{*})-\mu^{*}t^{*}\right)d\mu^{*}\,d\theta^{*} \qquad (8.28)$$

Plate XXVIII

The Initial Value Problem in the x,y Plane for a Disturbance over a Finite Area

$$\eta(x,y,t) = \int_{-\frac{\pi}{2}}^{\frac{\pi}{2}} \int_0^\infty \left[a(\nu,\theta) \cdot \cos\left(\nu(x\cos\theta + y\sin\theta) - \sqrt{\nu g}\, t\right) + b(\nu,\theta) \sin\left(\nu(x\cos\theta + y\sin\theta) - \sqrt{\nu g}\, t\right) \right] d\nu\, d\theta \tag{8.29}$$

$$\eta(x^*,y^*,t^*) = \int_{-\frac{\pi}{2}}^{\frac{\pi}{2}} \int_0^\infty \frac{\nu^*}{2\pi} \left[\int_{-\infty}^\infty \int_{-\infty}^\infty \eta(x,y) \cdot \cos\left(\nu^*(x\cos\theta^* + y\sin\theta^*)\right) dy\, dx \right] \cdot \cos\left(\nu^*(x^*\cos\theta^* + y^*\sin\theta^*) - \sqrt{\nu^* g}\, t^*\right) d\nu^* d\theta^*$$

$$+ \int_{-\frac{\pi}{2}}^{\frac{\pi}{2}} \int_0^\infty \frac{\nu^*}{2\pi} \left[\int_{-\infty}^\infty \int_{-\infty}^\infty \eta(x,y) \cdot \sin\left(\nu^*(x\cos\theta^* + y\sin\theta^*)\right) dy\, dx \right] \cdot \sin\left(\nu^*(x^*\cos\theta^* + y^*\sin\theta^*) - \sqrt{\nu^* g}\, t^*\right) d\nu^* d\theta^* \tag{8.30}$$

let $\frac{\mu^{*2}}{g} = \nu^*$ (8.31) $\qquad 2\mu^* d\mu^* = g\, d\nu^*$ (8.32)

$$\eta(x^*,y^*,t^*) = \int_{-\frac{\pi}{2}}^{\frac{\pi}{2}} \int_0^\infty \left[\frac{\mu^{*3}}{\pi g^2} \int_{-\infty}^\infty \int_{-\infty}^\infty \eta(x,y) \cdot \cos\left(\frac{\mu^{*2}}{g}(x\cos\theta^* + y\sin\theta^*)\right) dy\, dx \right] \cos\left[\frac{\mu^{*2}}{g}(x^*\cos\theta^* + y^*\sin\theta^*) - \mu^* t^*\right] d\mu^* d\theta^*$$

$$+ \int_{-\frac{\pi}{2}}^{\frac{\pi}{2}} \int_0^\infty \left[\frac{\mu^{*3}}{\pi g^2} \int_{-\infty}^\infty \int_{-\infty}^\infty \eta(x,y) \cdot \sin\left(\frac{\mu^{*2}}{g}(x\cos\theta^* + y\sin\theta^*)\right) dy\, dx \right] \sin\left[\frac{\mu^{*2}}{g}(x^*\cos\theta^* + y^*\sin\theta^*) - \mu^* t^*\right] d\mu^* d\theta^* \tag{8.33}$$

Plate XXIX

The initial value problem in the y,t plane for a wave train of finite width and finite duration

The problem to be solved now is the logical extension of the problem in Chapter 5 to the case of a storm of finite width. Equation (8.28) is the starting point and when $\eta(o,y,t)$ is given, the problem consists of evaluating the indicated integrations.

The initial values are given by equation (8.34). Outside of a certain range of y at x = 0 given by plus and minus one half the width of the storm, W_s, no disturbance is observed at the source. Outside of a certain range of time at x = 0 given by plus and minus one half the duration of the waves, D_w, no disturbance is observed at the source. Inside of the indicated rectangle in the y,t plane, a disturbance given by $A \sin((\mu_1^2/g)y \sin\theta_1 - \mu_1 t)$ is observed. For y fixed, the disturbance inside the rectangle is a disturbance whose record, as a function of time, would look very much like the disturbance produced in Chapter 5. Since μ_1 is a fixed number, the apparent period of the disturbance would be given by $T_1 = 2\pi/\mu_1$ within the time interval given in equation (8.34). For a fixed θ_1, μ_1, and t, as y varies, the disturbance is a slowly varying sinusoidal function, if θ_1 is small. The smaller the value of θ_1, the more rapidly the crests of the disturbance move in the y direction. The crests in the y,t plane do not move in the y direction with the speed of gravity waves because they are really only a component of the wave as observed at x = 0. Given the graph of $\eta(o,y,t)$ the use of equation (8.34) determines μ_1 and θ_1 uniquely.

Several integrals must be evaluated in order to obtain the

The Initial Value Problem in the y,t Plane for a Wave Train of Finite Width and Finite Duration

INITIAL VALUES

$$\eta(o,y,t) = \begin{cases} A \sin\left(\frac{\mu_1^2}{g} y \sin\theta_1 - \mu_1 t\right) & \text{if } -D_w/2 < t < D_w/2 \text{ and } -W_s/2 < y < W_s/2 \\ 0 & \text{otherwise} \end{cases} \tag{8.34}$$

$$\int_{-\frac{D_w}{2}}^{\frac{D_w}{2}} \int_{-\frac{W_s}{2}}^{\frac{W_s}{2}} A \sin\left(\frac{\mu_1^2}{g} y \sin\theta_1 - \mu_1 t\right) \cos\left(\frac{\mu^{*2}}{g} \sin\theta^* y - \mu^* t\right) dy\, dt = 0 \tag{8.35}$$

$$\int_{-\frac{D_w}{2}}^{\frac{D_w}{2}} \int_{-\frac{W_s}{2}}^{\frac{W_s}{2}} A \sin\left(\frac{\mu_1^2}{g} y \sin\theta_1 - \mu_1 t\right) \sin\left(\frac{\mu^{*2}}{g} y \sin\theta^* - \mu^* t\right) dy\, dt$$

$$= \frac{A}{2} \int_{-\frac{D_w}{2}}^{\frac{D_w}{2}} \int_{-\frac{W_s}{2}}^{\frac{W_s}{2}} \left[\cos\left(\left(\frac{\mu_1^2}{g} \sin\theta_1 - \frac{\mu^{*2}}{g} \sin\theta^*\right) y\right) \cos(\mu - \mu^*) t - \cos\left(\left(\frac{\mu_1^2}{g} \sin\theta_1 + \frac{\mu^{*2}}{g} \sin\theta^*\right) y\right) \cos(\mu_1 + \mu^*) t \right] dy\, dt$$

$$= 2A \left[\frac{\sin\left(\frac{\mu_1^2}{g} \sin\theta_1 - \frac{\mu^*}{g} \sin\theta^*\right) \frac{W_s}{2}}{\left(\frac{\mu_1^2}{g} \sin\theta - \frac{\mu^{*2}}{g} \sin\theta^*\right)} \cdot \frac{\sin(\mu_1 - \mu^*) \frac{D_w}{2}}{(\mu_1 - \mu^*)} - \frac{\sin\left(\frac{\mu_1^2}{g} \sin\theta + \frac{\mu^*}{g} \sin\theta^*\right) \frac{W_s}{2}}{\left(\frac{\mu_1^2}{g} \sin\theta + \frac{\mu^{*2}}{g} \sin\theta^*\right)} \cdot \frac{\sin(\mu_1 + \mu^*) \frac{D_w}{2}}{(\mu_1 + \mu^*)} \right] \tag{8.36}$$

Plate XXX

spectrum of the disturbance. The first integral in equation (8.28) involves the evaluation of equation (8.35). All of the terms in the integrand are odd, the integration is even, and the result is that equation (8.35) is zero. The second integral in equation (8.28) involves the evaluation of equation (8.36). The integration is straight-forward and the result is given in equation (8.36).

The results of equation (8.36) can be substituted into equation (8.28). An integral would then result over the sum of two terms from zero to infinity. The integral is approximated in equation (8.37), for ease of evaluation, by an integration from minus infinity to plus infinity of the term which gives the important contribution for μ^* positive.

For all equations subsequent to equation (8.37), all of the starred quantities in equation (8.37) will be written without stars for simplicity of notation. By the transformations indicated in equations (8.38), (8.39), (8.40), and (8.41), equation (8.37) can be put in the form of equation (8.42).

The pair of equations given by equations (8.43) and (8.44) define a transformation of the space over which the integration is to be carried out. The inverse of the transformation is given by equations (8.45) and (8.46). The Jacobian of the transformation is given by equation (8.47). The application of this transformation to equation (8.42) yields equation (8.48) in which the original strip over which the integral was to have been evaluated in the μ, ρ plane now maps into the whole α, β plane.

Were it not for the very complicated coefficient of x in

The Initial Value Problem in the yt Plane for a Wave Train of Finite Width and Duration

$$\eta(x^*,y^*,t^*) \cong \int_{-\frac{\pi}{2}}^{\frac{\pi}{2}}\int_{-\infty}^{\infty} \frac{2A\mu^{*2}\cos\theta^*}{2\pi^2 g}\left[\frac{\sin\left(\frac{\mu_1^2\sin\theta'}{g}-\frac{\mu_1^{*2}\sin\theta^*}{g}\right)\frac{W_s}{2}}{\left(\frac{\mu_1^2\sin\theta'}{g}-\frac{\mu_1^{*2}\sin\theta^*}{g}\right)}\right]\left[\frac{\sin(\mu_1-\mu^*)\frac{D_w}{2}}{(\mu_1-\mu^*)}\right]\cdot\sin\left(\frac{\mu^*}{g}(x^*\cos\theta^*-y^*\sin\theta^*)-\mu^* t\right)d\mu^* d\theta^* \quad (8.37)$$

OMIT ALL *'S FOR SIMPLICITY

$$\sin\theta=\rho \quad (8.38) \qquad \cos\theta=\sqrt{1-\rho^2} \quad (8.39) \qquad d\theta = 1/\sqrt{1-\rho^2}\,d\rho \quad (8.40) \qquad \sin\theta'=\rho' \quad (8.41)$$

$$\eta(x,y,t) = A\int_{-1}^{1}\int_{-M}^{M}\frac{\mu^2}{\pi^2 g}\left[\frac{\sin\left(\frac{\mu_1^2\rho_1}{g}-\frac{\mu^2\rho}{g}\right)\frac{W_s}{2}}{\left(\frac{\mu_1^2\rho_1}{g}-\frac{\mu^2\rho}{g}\right)}\right]\left[\frac{\sin(\mu_1-\mu)\frac{D_w}{2}}{(\mu_1-\mu)}\right]\cdot\sin\left(\frac{\mu^2}{g}(x\sqrt{1-\rho^2}+y\rho)-\mu t\right)d\mu\,d\rho \quad (8.42)$$

$$\frac{\mu_1^2\rho_1}{g}-\frac{\mu_1^2\rho}{g}=-\beta \quad (8.43) \qquad \mu_1-\mu=-\alpha \quad (8.44) \qquad \mu=\alpha+\mu_1 \quad (8.45)$$

$$\rho=\frac{\mu_1^2\rho_1+\beta g}{(\mu_1+\alpha)^2} \quad (8.46) \qquad \text{JACOBIAN } \frac{\partial(\mu,\rho)}{\partial\alpha\,\partial\beta}=\frac{g}{(\mu_1+\beta)^2} \quad (8.47)$$

$$\eta(x,y,t) = A\int_{-\infty}^{\infty}\int_{-\infty}^{\infty}\frac{1}{\pi^2}\left[\frac{\sin\frac{\beta W_s}{2}}{\beta}\cdot\frac{\sin\frac{\alpha D_w}{2}}{\alpha}\right]\cdot\sin\left[\left(\frac{(\mu+\alpha)^2}{g}\sqrt{1-\left(\frac{\mu_1^2\rho_1+\beta g}{(\mu_1+\alpha)^2}\right)^2}\right)x+\left(\frac{\mu_1^2\rho_1}{g}\right)y+\beta y-\mu_1 t-\alpha t\right]d\alpha\,d\beta \quad (8.48)$$

Plate XXXI

the last sinusoidal term of the integrand, the integration of equation (8.48) would then yield the final result. Note that as D_w and W_s approach infinity, the application of the lemma given in equation (8.9) yields a simple sine wave of the form $A \sin((\mu_1^2/g)(x \cos\theta_1 + y \sin\theta_1) - \mu_1 t)$ without edges. The integration as it stands, for D_w and W_s finite, is too difficult to carry out and it must be approximated. The term involving x in the last sinusoidal term of the integrand is approximated in equation (8.49). The second expression in equation (8.49) is simply a way to rewrite the original expression. Since the major contribution of the integral occurs near α and β equal to zero from the behavior of the other terms in the integrand, higher order terms such as those involving α^3 and α^4 can be neglected. The third expression in equation (8.49) employs this approximation. Also since the major contribution is given near α and β equal to zero the square root can be approximated by the first term in its binomial expansion, and the fourth expression is obtained. The final expression in equation (8.49) is the result of clearing fractions.

Equation (8.50) is the approximate result which is obtained when the approximation given in equation (8.49) is substituted into equation (8.48). The first term in the argument of the last sinusoidal term of the integrand is simply a constant as far as the parameters of integration are concerned. The remaining terms are functions of α^2, α, β^2 and β alone without cross product terms of the form of, say, $\alpha \cdot \beta$.

For simplicity let $\sqrt{1 - \rho_1^2} = K$ as defined by equation (8.51).

The Initial Value Problem in the y t Plane for a Wave Train of Finite Width and Duration

$$\frac{x(\mu_1+\alpha)^2}{g}\sqrt{1-\left(\frac{\mu_1\rho_1+\beta g}{(\mu_1+\alpha)^2}\right)^2}=\frac{x\mu_1^2}{g}\sqrt{1-\rho_1^2+\frac{4\alpha}{\mu_1}+\frac{6\alpha^2}{\mu_1^2}+\frac{4\alpha^3}{\mu_1^3}+\frac{\alpha^4}{\mu_1^4}-\frac{2\rho_1\beta g}{\mu_1^2}-\frac{\beta^2 g^2}{\mu_1^4}}$$

$$\cong\frac{x\mu_1^2}{g}\sqrt{1-\rho_1^2}\sqrt{1+\frac{\frac{4\alpha}{\mu_1}+\frac{6\alpha^2}{\mu_1^2}-\frac{2\rho_1 g\beta}{\mu_1^2}-\frac{g\beta^2}{\mu_1^4}}{1-\rho_1^2}}=\frac{x\mu_1^2}{g}\sqrt{1-\rho_1^2}\left(1+\frac{\frac{2\alpha}{\mu_1}+\frac{3\alpha}{\mu_1^2}-\frac{\rho_1 g\beta}{\mu_1^2}-\frac{g\beta^2}{2\mu_1^2}}{1-\rho_1^2}\right)$$

$$=\frac{x\mu_1^2}{g}\sqrt{1-\rho_1^2}+\frac{2\alpha\mu_1 x}{g\sqrt{1-\rho_1^2}}+\frac{3\alpha x}{g\sqrt{1-\rho_1^2}}-\frac{\rho_1\beta x}{\sqrt{1-\rho_1^2}}-\frac{\beta^2 g x}{2\mu_1^2\sqrt{1-\rho_1^2}} \qquad (8.49)$$

$$\eta(x,y,t)=A\int_{-\infty}^{\infty}\int_{-\infty}^{\infty}\frac{1}{\pi^2}\left[\frac{\sin\beta\frac{ws}{2}}{\beta}\,\frac{\sin\alpha\frac{D_w}{2}}{\alpha}\right]\sin\left[\left(\frac{\mu_1^2}{g}(x\sqrt{1-\rho_1^2}+y\rho_1)-\mu_1 t\right)+\frac{3\alpha^2 x}{g\sqrt{1-\rho_1^2}}+\frac{2\alpha\mu_1 x}{g\sqrt{1-\rho_1^2}}-\alpha t-\frac{\beta^2 x g}{2\mu_1^2\sqrt{1-\rho_1^2}}-\frac{\rho_1 x\beta}{\sqrt{1-\rho_1^2}}+\beta y\right]d\alpha\,d\beta$$

(8.50)

Let $\sqrt{1-\rho_1^2}=K_1$ (8.51) $\qquad x K_1+y\rho_1=\overline{X}$ (8.52) $\qquad -\rho_1 x+K_1 y=\overline{Y}$ (8.53)

Note: $\overline{X}\perp\overline{Y}$

Plate XXXII

The terms, $xK_1 + y\rho_1$ and $-\rho_1 x + K_1 y$, occur as units in the integrand. The term, $xK_1 + y\rho_1$, is the direction in which the wave crests travel, and the term, $-\rho_1 x + K_1 y$ is the direction of orientation of the wave crests. They are the coordinates of a rectangular coordinate system which has been rotated through the angle θ_1, and they are designated by $\bar{X}$ and $\bar{Y}$ in equations (8.52) and (8.53). Note that $\bar{X}$ and $\bar{Y}$ are perpendicular.

The constant term with respect to the variables of integration can be factored out by a trigonometric identity, and the use of the notations given above them yields equation (8.54). The notation for the various constant terms can be shortened by the use of the symbols, C, D, E, and F, as defined by equations (8.55), (8.56), (8.57) and (8.58). Then the trigonometric terms under the double integral can be split into a product of two integrals by expanding them by a trigonometric identity and the result is equation (8.59).

Each of the integrals in equation (8.59) is an integral over only one variable and if one of them can be evaluated, all can be evaluated by similar techniques. The integral of one of integrals is given by equation (8.60). It is integrated by the very same techniques that were employed in the integration of a function of similar form in Chapter 5. The steps from equations (5.9) to equation (5.12) in Chapter 5 could be carried out (with a different variable for the notation) in order to obtain equation (8.60).

The integration of equation (8.59) would then result from the substitution of equations like (8.60) into equation (8.59). Delta is the dummy variable of integration for those expressions

The Initial Value Problem in the y,t Plane for a Wave Train of Finite Width and Finite Duration

$$\eta(x,y,t) = A\cos\left(\frac{\mu_1^2 X}{g} - \mu_1 t\right)\int_{-\infty}^{\infty}\int_{-\infty}^{\infty} \frac{1}{\pi^2}\,\frac{\sin\frac{\beta W_s}{2}}{\beta}\cdot\frac{\sin\frac{\alpha D_w}{2}}{\alpha}\cdot\sin\left(\frac{3x}{gK_1}\alpha^2 + \left(\frac{2\mu_1 x}{gK_1} - t\right)\alpha + \left(\frac{-X}{2\mu_1^2 K_1}\right)\beta^2 + \left(\frac{Y}{K_1}\right)\beta\right) d\alpha\, d\beta$$

$$+A\sin\left(\frac{\mu_1^2 X}{g} - \mu_1 t\right)\int_{-\infty}^{\infty}\int_{-\infty}^{\infty} \frac{1}{\pi^2}\,\frac{\sin\frac{\beta W_s}{2}}{\beta}\cdot\frac{\sin\alpha\frac{D_w}{2}}{\alpha}\cdot\cos\left(\frac{2x}{gK_1}\alpha^2 + \left(\frac{2\mu_1 x}{gK_1} - t\right)\alpha + \left(\frac{-X}{2\mu_1^2 K_1}\right)\beta^2 + \left(\frac{Y}{K_1}\right)\beta\right) d\alpha\, d\beta \quad (8.54)$$

$$C = \frac{3x}{gK_1} \quad (8.55) \qquad D = \frac{2\mu_1 x}{gK_1} - t \quad (8.56) \qquad E = \frac{-Xg}{2\mu_1^2 K_1} \quad (8.57) \qquad F = \frac{Y}{K_1} \quad (8.58)$$

$$\eta(x,y,t) = A\cos\left(\frac{\mu_1^2 X}{g} - \mu_1 t\right)\left[\int_{-\infty}^{\infty}\frac{1}{\pi}\,\frac{\sin\frac{\beta W_s}{2}}{\beta}\cdot\cos(E\beta^2 + F\beta)\,d\beta \int_{-\infty}^{\infty}\frac{1}{\pi}\,\frac{\sin\frac{\alpha D_w}{2}}{\alpha}\cdot\sin(C\alpha + D\alpha)\,d\alpha\right.$$

$$\left.+\int_{-\infty}^{\infty}\frac{1}{\pi}\,\frac{\sin\frac{\beta W_s}{2}}{\beta}\sin(E\beta^2 + F\beta)\,d\beta \int_{-\infty}^{\infty}\frac{1}{\pi}\,\frac{\sin\frac{\alpha D_w}{2}}{\alpha}\cos(C\alpha^2 + D\alpha)\,d\alpha\right] + A\sin\left(\frac{\mu_1^2 X}{g} - \mu_1 t\right)\left[\int_{-\infty}^{\infty}\frac{1}{\pi}\,\frac{\sin\frac{\beta W_s}{2}}{\beta}\cdot\cos(E\beta^2 + F\beta)\,d\beta\right.$$

$$\left.\cdot\int_{-\infty}^{\infty}\frac{1}{\pi}\,\frac{\sin\frac{\alpha D_w}{2}}{\alpha}\cdot\cos(C\alpha^2 + D\alpha)\,d\alpha - \int_{-\infty}^{\infty}\frac{1}{\pi}\,\frac{\sin\frac{\beta W_s}{2}}{\beta}\sin(E\beta^2 + F\beta)\,d\beta \int_{-\infty}^{\infty}\frac{1}{\pi}\,\frac{\sin\frac{\alpha D_w}{2}}{\alpha}\sin(C\alpha + D\alpha)\,d\alpha\right] \quad (8.59)$$

$$\int_{-\infty}^{\infty}\frac{1}{\pi}\,\frac{\sin\frac{\beta W_s}{2}}{\beta}\cdot\cos(E\beta^2 + F\beta)\,d\beta = \int_{0}^{\infty}\frac{1}{2\pi}\cos E\beta\left(\frac{\sin\left(\frac{W_s}{2} + F\right)\beta + \sin\left(\frac{W_s}{2} - F\right)\beta}{\beta}\right)d\beta = \frac{1}{2}\int_{\sqrt{\frac{1}{2\pi E}\left(F + \frac{W_s}{2}\right)}}^{\sqrt{\frac{1}{2\pi E}\left(F + \frac{W_s}{2}\right)}}\left(\cos\frac{\pi}{2}\delta^2 + \sin\frac{\pi}{2}\delta^2\right)d\delta = \int C\delta + \int S\delta \quad (8.60)$$

Plate XXXIII

which originally involved beta, and gamma is the dummy variable of integration for those expressions which involved alpha originally. Let the last expression in equation (8.60) be a short hand notation for the expression which precedes it.

Equation (8.61) is the result when this short hand notation is substituted into equation (8.59). Each of the indicated integrals is a Fresnel Integral and its value is consequently known. The terms preceding the two trigonometric terms in (8.61) determine the envelope of the traveling wave, and since an expression of the form G cosθ + H sinθ can be written in the form $(G^2 + H^2)^{1/2} \sin(\theta + \tan^{-1}G/H)$, the last expression in equation (8.61) shows the results of this transformation.

The expression, FF(x,y,t), is equal to the sum of the squares of the two coefficients in equation (8.61). It will turn out to be the two dimensional equivalent of the one dimensional Fresnel filter described in Chapter 7. When the process of squaring and clearing terms is carried out, the final result is the last expression in equation (8.62). FF(x,y,t) will be referred to as the Fresnel filter for a storm of finite width.

Interpretation of results

The expression for FF(x,y,t), given in equation (8.62), is a product of two terms which involve Fresnel Integrals. The function will first be treated for a fixed value of x as a function of y and t. Each of the terms in the large bracket is essentially two inside of a certain range of t and y for a fixed value of x. Outside of this range at least one of the terms is nearly zero and the product is therefore nearly zero. Consider the first

The Initial Value Problem in the y,t Plane for a Wave Train of Finite Width and Finite Duration

$$\eta(x,y,t) = \frac{A}{2}\left[\left(\int c\delta + \int s\delta\right)\left(\int c\gamma - \int s\gamma\right) + \left(\int c\delta - \int s\delta\right)\left(\int c\gamma + \int s\gamma\right)\right] \cos\left(\frac{\mu_1^2 X}{g} - \mu_1 t\right)$$

$$+ \frac{A}{2}\left[\left(\int c\delta + \int s\delta\right)\left(\int c\gamma + \int s\gamma\right) - \left(\int c\delta - \int s\delta\right)\left(\int c\gamma - \int s\gamma\right)\right] \sin\left(\frac{\mu_1^2 X}{g} - \mu_1 t\right)$$

$$= \left[A^2 . FF(x,y,t)\right]^{1/2} . \sin\left[\frac{\mu_1^2 X}{g} - \mu_1 t + \psi(x,y,t)\right] \qquad (8.61)$$

$$FF(x,y,t) = \frac{1}{4}\left[\left[\left(\int c\delta + \int s\delta\right)\left(\int c\gamma - \int s\gamma\right) + \left(\int c\delta - \int s\delta\right)\left(\int c\gamma + \int s\gamma\right)\right]^2 + \left[\left(\int c\delta + \int s\delta\right)\left(\int c\gamma - \int s\gamma\right)\right.\right.$$

$$\left.\left. - \left(\int c\delta - \int s\delta\right)\left(\int c\gamma - \int s\gamma\right)\right]^2\right] = \frac{1}{4}\left[\left(\int c\delta\right)^2 + \left(\int s\delta\right)^2\right]\left[\left(\int c\gamma\right)^2 + \left(\int s\gamma\right)^2\right]$$

$$= \frac{1}{4}\left[\left(\int_{\sqrt{\frac{2\mu_1^2 K_1}{2\pi x g}}\left(\frac{Y}{K_1} - \frac{W_s}{2}\right)}^{\sqrt{\frac{2\mu_1^2 K_1}{2\pi x g}}\left(\frac{Y}{K_1} + \frac{W_s}{2}\right)} \cos\frac{\pi}{2}\delta^2 d\delta\right)^2 + \left(\int_{\sqrt{\frac{2\mu_1^2 K_1}{2\pi x g}}\left(\frac{Y}{K_1} - \frac{W_s}{2}\right)}^{\sqrt{\frac{2\mu_1^2 K_1}{2\pi x g}}\left(\frac{Y}{K_1} + \frac{W_s}{2}\right)} \sin\frac{\pi}{2}\delta^2 d\delta\right)^2\right]\left[\left(\int_{\sqrt{\frac{g K_1}{6\pi x}}\left(\frac{2\mu_1 x}{g K_1} - t + \frac{D_w}{2}\right)}^{\sqrt{\frac{g K_1}{6\pi x}}\left(\frac{2\mu_1 x}{g K_1} - t - \frac{D_w}{2}\right)} \cos\frac{\pi}{2}\gamma^2 d\gamma\right)^2 + \left(\int_{\sqrt{\frac{g K_1}{6\pi x}}\left(\frac{2\mu_1 x}{g K_1} - t + \frac{D_w}{2}\right)}^{\sqrt{\frac{g K_1}{6\pi x}}\left(\frac{2\mu_1 x}{g K_1} - t - \frac{D_w}{2}\right)} \sin\frac{\pi}{2}\gamma^2 d\gamma\right)^2\right] \qquad (8.62)$$

Plate XXXIV

bracketed term. If $\bar{Y}$ is zero and W_s is fairly large, for an x which is not too large, the integrals will have to be evaluated from a large negative value to a large positive value and by the same arguments employed in Chapter 5, the value of the bracketed term will be essentially two. If, say, $\bar{Y} = K_1 W_s/2$ then the integrals will have to be evaluated from zero to a large positive value, and the value of the bracketed term will be one half. Thus when $\bar{Y} = K_1 W_s/2$ or $\bar{Y} = -K_1 W_s/2$, the potential energy, averaged over a relatively short interval of time, of the waves at that point under the envelope will be one fourth of its value near the center of the disturbance. Similarly in the second bracketed expression if $(2\mu_1 x/gK_1) - t - (D_w/2) = 0$, or if $(2\mu_1 x/gK_1) - t + (D_w/2) = 0$, the average potential energy will be one fourth the value at the center of the disturbance.

If the four equations treated above are put back into their original form as a function of x,y and t and θ_1 by the use of (8.51), (8.52), (8.53), and (8.41), then y and t can be found as a function of x and the other parameters of the solution. The result is equations (8.63), (8.64), (8.65) and (8.66). For a fixed value of x, θ_1, W_s, D_w, and μ_1, these equations are equations of four straight lines in the y,t plane. Segments of these straight lines are graphed for $x = x_1$ in the upper right of the y,t plane shown in figure 18. Their intersection determines a rectangle in the y,t plane. Inside the rectangle, the disturbance is at essentially full amplitude, and at the heavy boundaries as indicated on the figure, the average potential energy if one fourth of what it is in the center.

Interpretation of Results

Quarter Power Points of the Function FF(x, y, t)

For fixed x in the yt plane:

$$y = \frac{W_s}{2} + \tan\theta_1 x \tag{8.63}$$

$$y = -\frac{W_s}{2} + \tan\theta_1 x \tag{8.64}$$

$$t = \frac{D_w}{2} + \frac{2\mu_1 x}{g\cos\theta_1} \tag{8.65}$$

$$t = -\frac{D_w}{2} + \frac{2\mu_1 x}{g\cos\theta_1} \tag{8.66}$$

For fixed t in the xy plane:

$$Y = \cos\theta_1 \frac{W_s}{2} \tag{8.67}$$

$$Y = -\cos\theta_1 \frac{W_s}{2} \tag{8.68}$$

$$x = \frac{g\cos\theta_1\left(-\frac{D_w}{2} + t\right)}{2\mu_1} \tag{8.69}$$

$$x = \frac{g\cos\theta_1\left(\frac{D_w}{2} + t\right)}{2\mu_1} \tag{8.70}$$

PLATE XXXV

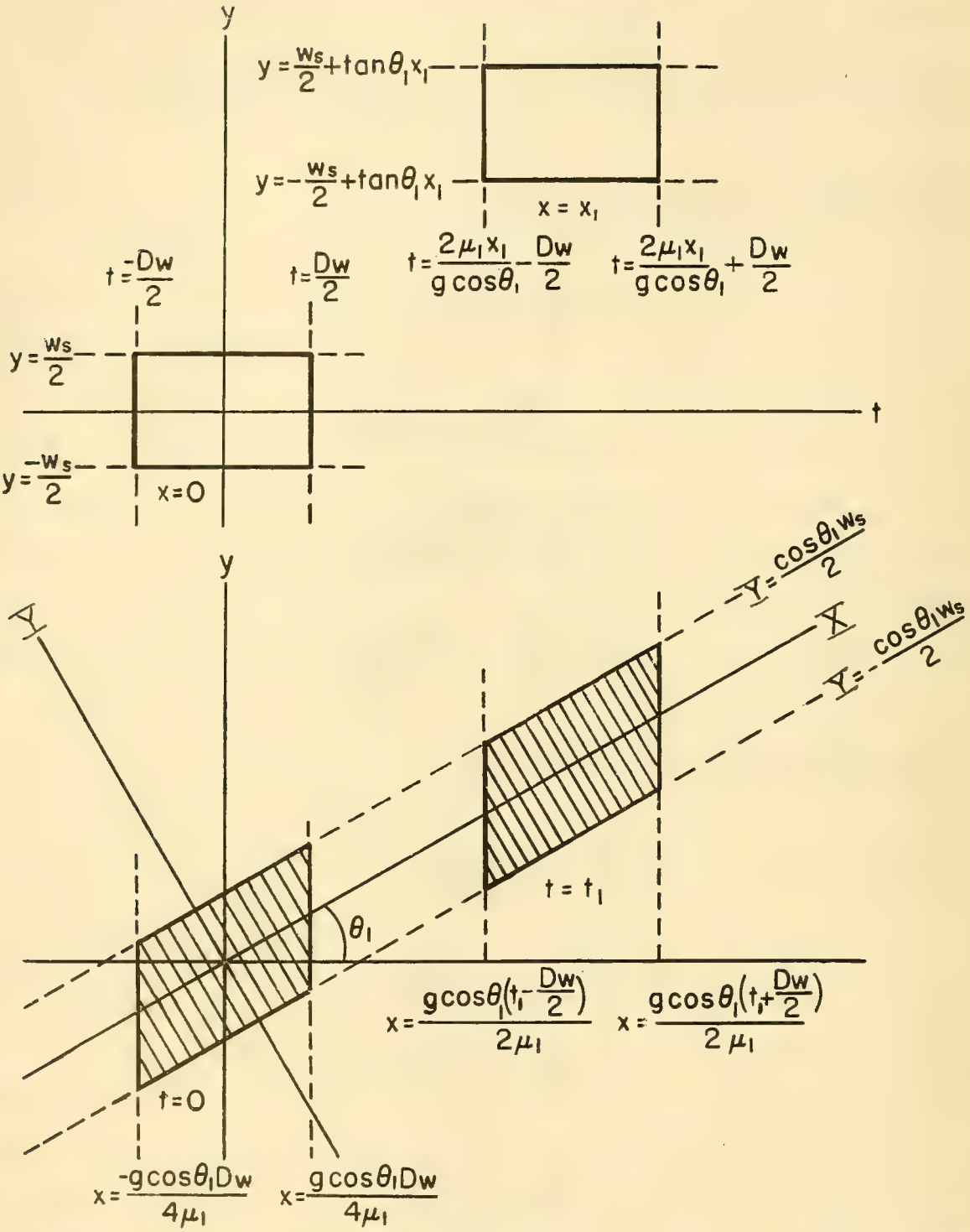

Fig 18. The Quarter Power Boundaries of the Envelope of the Solution. The heavy lines are the boundaries. The dashed lines are portions of the equations of the boundaries. The wave crests are shown in the xy plane.

When x is not zero, as a function of y, the profile of FF(x,y,t) where it exists looks at an edge like the dashed curve in figure 9. Similarly when x is not zero, as a function of t the same profile would be found. The product of the two profiles is rather complex at the corners of the rectangle.

As x approaches zero in equation (8.62) the radicals in the integrand become infinite. The quarter power lines move to the position indicated at the origin of the y,t plane in figure 20. This shows that the solution reduces to the initial values given in the formulation of the problem despite the approximations employed in evaluating the integral.

N ow the function will be studied for fixed values of t as a function of x and y. A second set of coordinate axes defined by $\bar{X}$ and $\bar{Y}$ as given in equations (8.52) and (8.53) are also useful. The bottom graph in figure 18 shows the two coordinate systems. The quarter power points in the $\bar{Y}$ direction are given simply by equations (8.67) and (8.68). In the x direction, they are given by equations (8.69) and (8.70). The area in the x,y plane occupied by the waves is consequently a parallelogram with sides parallel to the $\bar{Y}$ axis and the x axis. The individual wave crest segments are parallel to the $\bar{Y}$ axis and travel in the positive $\bar{X}$ direction. On the $\bar{X}$ axis, the value of $\bar{X}$ for the forward edge of the disturbance is given by $\bar{X} = x/\cos\theta_1 = g(t + D_w/2)/2\mu_1$ which shows that the forward edge of the disturbance travels in the positive $\bar{X}$ direction with the group velocity of waves with a period μ_1.

The accuracy of the approximations employed

Two approximations were employed in the derivation of the solution. The first approximation was in the formulation of the integral representation given by equation (8.37). This integral representation permits some of the spectral components to have a component of travel in the negative x direction. By the arguments given in Chapter 5 for the simpler case, this approximation is probably not too bad. The effect of the other approximation, namely that given in equation (8.49), is probably more important. The approximation is more accurate for small values of θ_1. With θ_1 greater than $\pi/4$ or less than $-\pi/4$, the approximation becomes poorer. A more accurate evaluation of the integral might show that the parallelogram form in the x,y plane shown in figure 18 would tend to lose the sharper corner and assume the shape of a rectangle with sides parallel to the $\bar{X}$ and $\bar{Y}$ axes as it travels along. The approximation is adequate in the sense that it locates the disturbance fairly precisely and shows where it is not located to a great degree of accuracy.

Additional comments

It would be possible to take the two initial value problems given in this chapter and manufacture some model wave systems from storms at sea which have properties which would be analogous to those models studied in Chapter 6. Models with discrete spectral components which would travel in all directions within a 180° sector could be manufactured. They could be made to be infinite in duration and width, infinite in duration and finite in width, finite in duration and infinite in width, and finite

in duration and width. The elemental unit of construction would be a finite wave group which would last for only a few minutes and be only a few kilometers wide as it passed the line $x = 0$ near a point $y = y_o$.

The most realistic model possible by these methods would be a model something like the last model described briefly in Chapter 6. The analysis of the properties of the model would turn out to be very complex, and the results would be indecisive because of the difficulties involved in evaluating the potential energy.

None of the above possible models would be Gaussian in character, and since there is evidence that a wave record is very nearly Gaussian in character as shown in Chapter 7, they would all be unrealistic. For this reason, none of these models will be treated.

Instead, in Chapter 9, the Gaussian case for a short crested sea surface will be treated, and $FF(x,y,t)$ as derived in this chapter will be applied as a filter to the Gaussian case in order to forecast the spectrum of the waves in the area of decay.

Chapter 9. THE MATHEMATICAL REPRESENTATION OF A SHORT CRESTED SEA SURFACE BY A LEBESGUE STIELTJES POWER INTEGRAL AND THE PROBLEM OF FORECASTS FOR A STORM OF FINITE WIDTH AND FINITE DURATION OVER A FETCH OF LENGTH, F.

Introduction

Now that wave systems have been represented for the short crested case by Fourier Integral Theory, the next step in generality is to represent an area of a short-crested sea surface by a Lebesgue-Stieltjes Power Integral. It will then be possible by extending the methods of Chapter 7 to devise a forecasting procedure for an actual short crested irregular sea surface in a storm at sea of finite duration and finite width.

The Lebesgue Stieltjes Power Integral for short crested wave systems

The logical extension of equation (7.1) to a short crested sea surface is given by equation (9.1). The integral could also be considered as if x were zero and the term x cos θ were absent. It would then follow from the properties of gravity waves in deep water that the term x cos θ could be added immediately under the assumption that the disturbance occupies all of the x,y,t space. Note that the integral is not completely general in that it does not represent waves traveling in all possible directions. All component waves have a component of motion in the positive x direction. A more general representation would later on necessitate evaluation of derivatives of the sea surface. For most systems, equation (9.1) is general enough.

The Lebesgue Stieltjes Power Integral for Short Crested Wave Systems

$$\eta(x,y,t)=\int_0^{\infty}\int_{-\frac{\pi}{2}}^{\frac{\pi}{2}}\cos\left(\frac{\mu^2}{g}(x\cos\theta+y\sin\theta)-\mu t+\psi(\mu,\theta)\right)\sqrt{d^2E_2(\mu,\theta)} \quad (9.1)$$

$E_2(o,\theta)=0$ (9.2) $E_2(\mu,\frac{-\pi}{2})=0$ (9.3) $0\leq E_2(\mu,\theta)<M$ for all μ and θ (9.4)

if $\mu_K<\mu_{K+1}$ (9.5) and $\theta_J<\theta_{J+1}$ (9.6) and if $E_2(\mu_K,\theta_J)\leq E_2(\mu_{K+1},\theta_J)$ (9.7)

$E_2(\mu_K,\theta_{J+1})\leq E_2(\mu_{K+1},\theta_{J+1})$ (9.8) $E_2(\mu_K,\theta_J)\leq E_2(\mu_K,\theta_{J+1})$ (9.9)

$E_2(\mu_{K+1},\theta_J)\leq E_2(\mu_{K+1},\theta_{J+1})$ (9.10) and finally if

$E_2(\mu_{K+1},\theta_{J+1})-E_2(\mu_{K+1},\theta_J)\geq E_2(\mu_{K+1},\theta_J)-E_2(\mu_K,\theta_J)$ (9.11) one finds that

$E_2(\mu_{K+1},\theta_{J+1})-E_2(\mu_{K+1},\theta_J)\geq E_2(\mu_K,\theta_{J+1})-E_2(\mu_K,\theta_J)$ (9.12) and also

$E_2(\mu_{K+1},\theta_{J+1})-E_2(\mu_{K+1},\theta_J)-E_2(\mu_K,\theta_{J+1})+E_2(\mu_K,\theta_J)\geq 0$ (9.13)

let $0<\mu_1<\mu_2<\mu_3<\mu_4<\mu_5<\ldots\ldots<\mu_K<\mu_{K+1}\mu_{K+2}\ldots<\mu_{2R}<\infty$ (9.14)

where $\mu_{K+1}-\mu_K\leq\Delta_1\mu$ (9.15) $\mu_{L+1}-\mu_L\leq\Delta_2\mu$ (9.16) and where $\Delta_2\mu\leq\mu_{K+1}-\mu_K\leq\Delta_1\mu$ (9.17)

and let $-\frac{\pi}{2}\leq\theta_0<\theta_1<\theta_2<\theta_3<\ldots\ldots\ \theta_J<\theta_{J+1}<\ldots\ldots<\theta_{2S}\leq\frac{\pi}{2}$ (9.18)

where $\theta_{J+1}-\theta_J=\Delta_1\theta$ (9.19) $\theta_{I+1}-\theta_I\leq\Delta_2\theta$ (9.20) and where $\Delta_2\theta\leq\theta_{J+1}-\theta_J\leq\Delta_1\theta$ (9.21)

Then $\eta(x,y,t)=\lim_{\substack{\mu_{2S}\to\infty\\ \frac{\pi}{2}-\theta_{2R}\to 0\\ \Delta_1\mu\to 0\\ \Delta_1\theta\to 0}}\sum_{N=0,1,2}^{S-1}\cdot\sum_{P=0,1,2}^{R-1}\cdot\cos\left(\frac{(\mu_{2N+1})^2}{g}(x\cos\theta_{2P+1}+y\sin\theta_{2P+1})-\mu_{2N+1}t+\psi(\mu_{2N+1},\theta_{2P+1})\right)$

$$\cdot\sqrt{E_2(\mu_{2N+2},\theta_{2P+2})-E_2(\mu_{2N},\theta_{2P+2})-E_2(\mu_{2N+2},\theta_{2P})+E_2(\mu_{2N},\theta_{2P})} \quad (9.22)$$

Plate XXXVI

$E_2(\mu,\theta)$ is the cumulative power distribution in the μ ,θ plane. It represents the amount of power present in the system below the wave frequency μ and between the directions $-\pi/2$ and θ. $E_2(\mu,\theta)$ is defined for values of θ between $-\pi/2$ and $\pi/2$ and for all positive values of μ . As required by equations (9.2), (9.3), and (9.4), $E_2(\mu,\theta)$ is zero at the origin, zero along the line $\theta = -\pi/2$, and bounded from above for all μ and θ.

Equations (9.5) through (9.10) require that $E_2(\mu,\theta)$ be monotonically non-decreasing in both μ and θ.

Some properties of $E_2(\mu,\theta)$ at a set of four points at the corners of an elemental area element are also needed. The required property is stated in equation (9.11). Equation (9.11) yields equation (9.12) and equation (9.13) through the usual operations with inequalities. Equation (9.13) is very important. This particular combination of the values of $E_2(\mu,\theta)$ at the four corners of the area element must always be greater than or equal to zero, if equations (9.5) through (9.11) hold.

In order to define the integral given by equation (9.1), it is first necessary to define a net over the μ ,θ plane described above. The μ axis is first broken up into a finite number of intervals as given in equation (9.14). Equations (9.15), (9.16), and (9.17) state that the smallest interval is $\Delta_2\mu$ and that the largest interval is $\Delta_1\mu$. Next, the angular coordinate, θ, is broken up into 2S angular segments in the interval between $-\pi/2$ and $\pi/2$. Equations (9.19), (9.20) and (9.21) state that the smallest angular segment is $\Delta_2\theta$ and that the largest is $\Delta_1\theta$.

Equation (9.1) is then the limit of the partial sum given by

equation (9.22) as μ_{2S} approaches infinity, θ_{2R} approaches $\pi/2$ from values less than $\pi/2$, and the mesh of the net approaches zero. The rule for picking $\psi(\mu,\theta)$ must also be given before the partial sum is formed. For some forms of the integral $\psi(\mu,\theta)$ can be a continuous function; for other forms of the integral, it must be defined in very special ways. The value under the square root sign is always positive by virtue of equation (9.13).

An imporant property of the Lebesgue Stieltjes Power Integral for a short crested sea surface

From the properties of $E_2(\mu,\theta)$, it follows that $E_2(\mu,\theta)$ has a definite limiting value when $\theta = \pi/2$ as μ approaches infinity. This limiting value will be called E_{2max}, and it should be noted that the free surface considered as a function of time (when squared and averaged over time) for some fixed x and y may or may not be related to the E_{max} of Chapter 7. For this reason the difference between E_{2max} and E_{max} must be kept in mind until their relationship is studied in Chapter 10.

When the free surface defined by equation (9.1) is squared and averaged over the y,t plane, it can be proved that equation (9.24) is the result. The potential energy averaged over the y,t plane is then given by equation (9.25).

Equation (9.24) can be proved by the procedures given in equation (9.26) and the steps which follow it. In equation (9.26) the definition of the integral given by equation (9.24) has been substituted for $\eta(x,y,t)$. By a correct application of the various limiting procedures, the result can be proved. In equation

Since $0 \leqslant E(\mu,\theta) < M$ for all μ and θ it follows that $\lim_{\mu\to\infty} E(\mu,\frac{\pi}{2}) = E_{2max} \leqslant M$ (9.23)
and from equations (9.2) through (9.10).

$$\lim_{\substack{\bar{T}\to\infty \\ L\to\infty}} \frac{1}{\bar{T}L}\int_{y^*}^{y^*+L}\int_{t^*}^{y^*+\bar{T}} (\eta(x,y,t))^2\,dt\,dy = \frac{E_{2max}}{2} \qquad \text{for any } x. \tag{9.24}$$

$$\overline{PE}^{yt} = \lim_{\substack{\bar{T}\to\infty \\ L\to\infty}} \frac{\rho g}{2\bar{T}L}\int_{y^*}^{y^*+L}\int_{t^*}^{t^*+\bar{T}} (\eta(x,y,t))^2\,dt\,dy = \frac{\rho g}{4} E_{2max} \qquad \text{for any } x. \tag{9.25}$$

$$\frac{E_{2max}}{2} = \lim_{\substack{\bar{T}\to\infty \\ L\to\infty}} \frac{1}{\bar{T}L}\int_{y^*}^{y^*+L}\int_{t^*}^{t^*+\bar{T}} \left[\lim_{\substack{\mu_{2S}\to\infty \\ \frac{\pi}{2}-\theta_{2R}\to 0 \\ \Delta_1\mu\to 0 \\ \Delta_1\theta\to 0}} \sum_{n=0}^{S-1}\sum_{p=0}^{R-1} \cdot \cos\left(\frac{(\mu_{2n+1})^2}{g}(x\cos\theta_{2P+1} + y\sin\theta_{2P+1}) - \mu_{2\mu+1}t + \psi(\mu_{2\mu+1},\theta_{2P+1})\right)\cdot \right.$$
$$\left. \cdot\sqrt{E_2(\mu_{2n+2}\theta_{2p+2}) - E_2(\mu_{2n}\theta_{2p+2}) - E_2(\mu_{2n+2}\theta_{2p}) + E_2(\mu_{2n}\theta_{2p})}\right]^2 dt\,dy \tag{9.26}$$

$$\frac{E_{2max}}{2} = \lim \frac{1}{\bar{T}L}\int_{y^*}^{y^*+L}\int_{t^*}^{t^*+\bar{T}} \left[\sum_{n=0}^{S-1} \cos\left(\frac{(\mu_{2n+1})^2}{g}(x\cos\theta_1 + y\sin\theta_1) - \mu_{2n+1}t + \psi(\mu_{2m-1}\theta)\right)\cdot \right.$$
$$\cdot\sqrt{E_2(\mu_{2n+2}\theta_2) - E_2(\mu_{2n+2}\theta_0) - E_2(\mu_{2n}\theta_2) + E_2(\mu_{2n}\theta_0)}$$
$$+\cos\left(\frac{(\mu_{2n+1})^2}{g}(x\cos\theta_3 + y\sin\theta_3) - \mu_{2n+1}t + \psi(\mu_{2n+1}\theta_1)\sqrt{E_2(\mu_{2n+2}\theta_4) - E_2(\mu_{2n+2}\theta_2) - E_2(\mu_{2n}\theta_4) + E_2(\mu_{2n}\theta_2)}\right.$$
$$+ + \ldots.$$
$$+ \ldots.$$
$$\left.+\cos\left(\frac{(\mu_{2n+1})^2}{g}(x\cos\theta_{2R-1} + y\sin\theta_{2R-1}) - \mu_{2n+1}t + \psi(\mu_{2n+1}\theta_{2R-1})\sqrt{E_2(\mu_{2n+2}\theta_{2R}) - E_2(\mu_{2n+2}\theta_{2R-2}) - E_2(\mu_{2n}\theta_{2R}) + E_2(\mu_{2n}\theta_{2R-2})}\right]^2 dt\,dy \tag{9.27}$$

(9.27) all of the limiting processes have been designated by the simple notation, lim, and the summation over n has been written out in full. In equation (9.28), the summation over p has also been written out in full, and the trigonometric terms have been designated by a shorter notation.

The next expression in equation (9.28) indicates the process of squaring the entire large bracket. Each term in the sum will occur as a square, and there will also be a large number of cross product terms. Each squared term will be of the form of the square of one of the indicated square roots times the square of a cosine term, and since, for example, $(\cos \alpha)^2 = (1 + \cos 2\alpha)/2$, a term equal to one half of the sums of the squares of all of the indicated square roots will occur. There will also be a great many terms which are periodic in either y or t or both. Some of the terms which are periodic in either y or t or both occur first as the product of two trigonometric terms. In every case, however, either the values of μ in the two terms or the values of θ in the two terms will be different, and the product can therefore be written as the sum of two trigonometric terms which involve the sum and difference of the arguments.

The sum of all of the values of $E_2(\mu,\theta)$ at the points of the net telescopes into the value of $E_2(\mu_{2S},\theta_{2R})$ by virtue of the properties of the net and the properties of $E_2(\mu,\theta)$. For example, the first row of terms in equation (9.28) becomes simply $E_2(\mu_{2S},\theta_2)$. All terms occur once positively in the sum and once negatively except $E_2(0,0)$, $E(0_2,\theta_2)$, $E_2(\mu_{2S},0)$ and $E_2(\mu_{2S},\theta_2)$. All but $E_2(\mu_{2S},\theta_2)$ are zero by definition. The second row of terms, of which only the first is shown, becomes $E(\mu_{2S},\theta_4)$ -

An Important Property of the Lebesgue Stieltjes Power Integral for a Short Crested Sea Surface.

$$\frac{E_{2\max}}{2} = \lim \frac{1}{TL}\int_{y^*}^{y^*+L}\int_{t^*}^{t^*+\bar{T}}\Big[\cos(\mu_1,\theta_1,\psi_{11})\sqrt{E_2(\mu_2\theta_2)-E_2(\mu_2\theta_0)-E_2(\mu_0\theta_2)+E_2(\mu_0\theta_0)} +$$

$$+\cos(\mu_3\theta_1\psi_{31})\sqrt{E_2(\mu_4\theta_2)-E_2(\mu_4\theta_0)-E_2(\mu_2\theta_2)+E_2(\mu_2\theta_0)}+\ldots+\cos(\mu_{2S-1}\theta_1\psi_{2S-1,1})\sqrt{E_2(\mu_{2S}\theta_2)-E_2(\mu_{2S}\theta_0)-E_2(\mu_{2S-2}\theta_2)+E_2(\mu_{2S-2}\theta_0)}+$$

$$+\cos(\mu_1\theta_3\psi_{13})\sqrt{E_2(\mu_2\theta_4)-E_2(\mu_2\theta_2)-E_2(\mu_0\theta_4)+E_2(\mu_0\theta_2)}+\ldots+\cos(\mu_1\theta_{2R-1}\psi_{1,2R-1})\sqrt{E_2(\mu_2\theta_{2R})-E_2(\mu_2\theta_{2R-2})-E_2(\mu_0\theta_{2R})+E_2(\mu_0\theta_{2R-2})}+\ldots$$

$$+\ldots.\quad+\cos(\mu_{2S-1}\theta_{2R-1}\psi_{2S-1,2R-1})\sqrt{E_2(\mu_{2S}\theta_{2R})-E_2(\mu_{2S-2}\theta_{2R})-E_2(\mu_{2S}\theta_{2R-2})+E_2(\mu_{2S}\theta_{2R-2})}\Big]^2\,dt\,dy =$$

$$=\lim \frac{1}{TL}\int_{y^*}^{y^*+L}\int_{t^*}^{t^*+\bar{T}}\Big[\Sigma \text{ squares} + \text{cross product terms}\Big]\,dt\,dy$$

$$=\lim \frac{1}{TL}\int_{y^*}^{y^*+L}\int_{t^*}^{t^*+\bar{T}}\frac{1}{2}\Big[E_2(\mu_2\theta_2)-E_2(\mu_2\theta_0)-E_2(\mu_0\theta_2)+E_2(\mu_0\theta_0)+E_2(\mu_4\theta_2)-E_2(\mu_4\theta_0)-E_2(\mu_2\theta_2)+E_2(\mu_2\theta_0)+E_2(\mu_6\theta_2)-E_2(\mu_6\theta_0)-$$

$$-E_2(\mu_4\theta_2)+E_2(\mu_4\theta_0)+\ldots+E_2(\mu_{2S}\theta_2)-E_2(\mu_{2S}\theta_0)-E_2(\mu_{2S-2}\theta_2)+E_2(\mu_{2S-2}\theta_0)$$

$$+E_2(\mu_2\theta_4)-E_2(\mu_2\theta_2)-E_2(\mu_0\theta_4)+E_2(\mu_0\theta_2)+\ldots.$$

$$+E_2(\mu_2\theta_{2R})-E_2(\mu_2\theta_{2R-2})-E_2(\mu_0\theta_{2R})+E_2(\mu_2\theta_{2R-2})+\ldots.+\ldots.+E_2(\mu_{2S}\theta_{2R})-E_2(\mu_{2S-2}\theta_{2R})-E_2(\mu_{2S}\theta_{2R-2})+E_2(\mu_{2S-2}\theta_{2R-2})\Big]+$$

$$+\Big[\text{terms periodic in either y or t or both}\Big]\,dt\,dy$$

$$=\lim_{\substack{\mu_{2S}\to\infty\\ \frac{\pi}{2}-\theta_{2R}\to 0\\ \Delta_1\mu\to 0\\ \Delta_1\theta\to 0}}\frac{1}{2}E_2(\mu_{2S}\theta_{2R})=\lim_{\substack{\mu_{2S}\to\infty\\ \Delta_1\mu\to 0\\ \Delta_1\theta\to 0}}\frac{1}{2}E_2(\mu_{2S}\tfrac{\pi}{2})=\lim_{\substack{\Delta_1\mu\to 0\\ \Delta_1\theta\to 0}}\frac{1}{2}E_{2\max}=\frac{1}{2}E_{2\max} \qquad (9.28)$$

PLATE XXXVIII

$E_2(\mu_{2S},\theta_2)$, and the sum of the first and second row then becomes $E_2(\mu_{2S},\theta_4)$. Finally, the complete sum is simply $E_2(\mu_{2S},\theta_{2R})$.

Figure 19 illustrates this property of the net. The net as shown is not a very close one, but it is seen that if the indicated signs are assigned to each corner of the elemental areas of the grid system, and if the sum of all the terms is then taken, every value of $E_2(\mu,\theta)$ which occurs will be cancelled out by a term of opposite sign except the ones for $E_2(0,0)$, $E_2(0,\theta_{12})$, $E_2(\mu_8,0)$ and $E_2(\mu_8,\theta_{12})$. The only one not zero of those that are not cancelled out is $E_2(\mu_8,\theta_{12})$.

The next step is to integrate over y and t and pass to the limit as L and $\bar{T}$ approach infinity. The only term remaining is $\frac{1}{2}E_2(\mu_{2S},\theta_{2R})$. (See for example equation (6.64).) Then as θ_{2R} approaches $\pi/2$, the next expression is obtained. And as μ_{2S} approaches infinity, $E_{2max}/2$ is obtained. Finally, the same results hold as $\Delta_1\mu$ and $\Delta_1\theta$ approach zero. Therefore equation (9.24) is proved.

The results hold for any value of x. Consequently, they hold for an average over x also. In other words, equation (9.24) and (9.25) could be modified by another integration from x* to x* + L* and a division by L*. Then the limits as $\bar{T}$, L, and L* approach infinite would be the same as the limits as they are given.

Some examples

Various examples of the integration of equation (9.1) will now be described. These examples will all be examples of the non-Gaussian case. They are of interest because they show that all of the systems which were infinite in duration and width in the

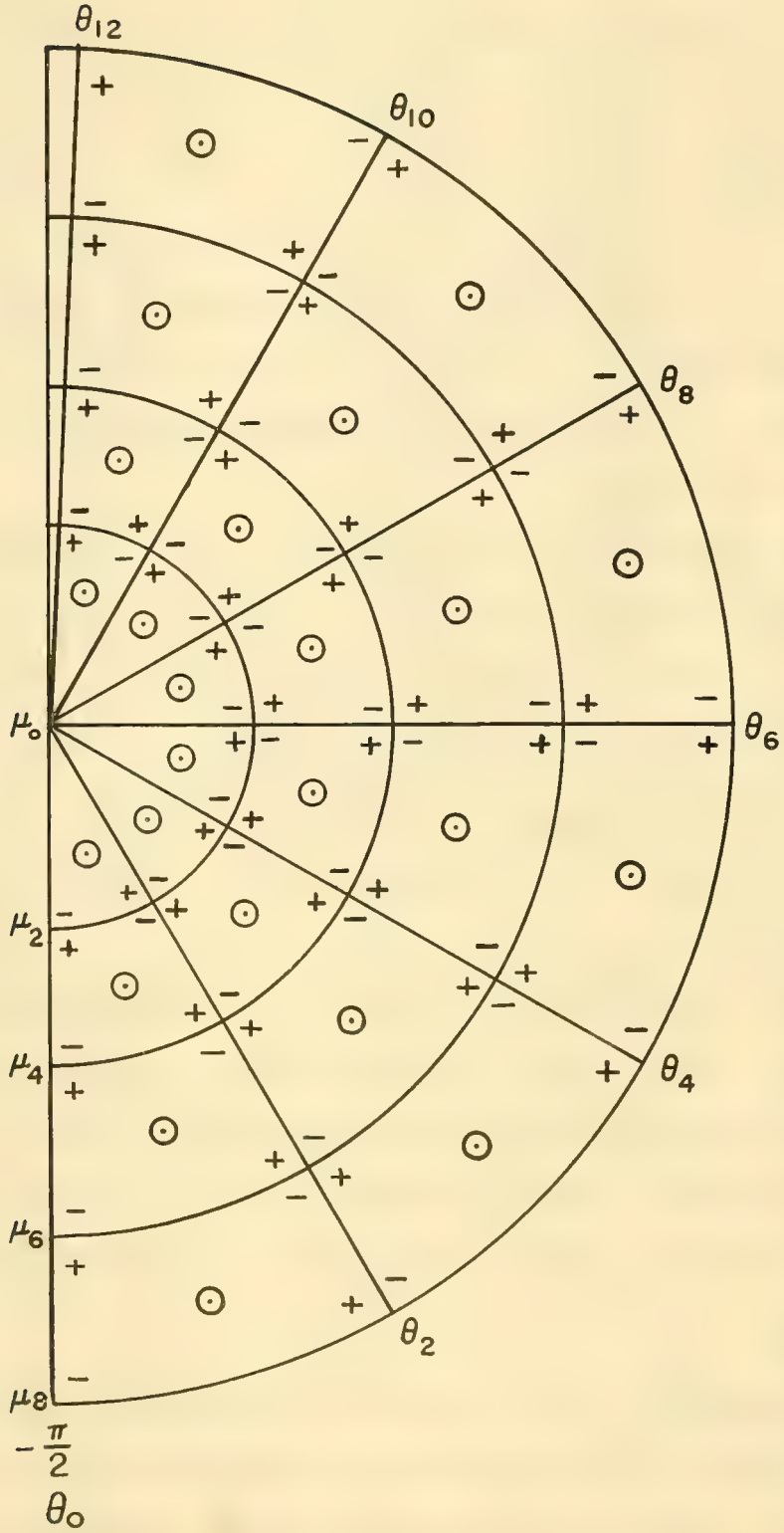

Fig 19 The Properties of the Net in the (μ,θ) Polar Coördinate System.

past chapters come under the properties of this particular integral.

The form of $E_2(\mu,\theta)$, for example one is given by equation (9.29). $\psi(\mu,\theta)$ is zero. $E_2(\mu,\theta)$ is indicated schematically by the little polar coordinate sketch on the left. Graphed as a surface in the three dimensional $\mu,\theta,E_2(\mu,\theta)$ space, $E_2(\mu,\theta)$ would look like a vertical cliff along the curve $\mu = \mu_I$, between $\theta = 0$ and $\theta = \pi/2$, and the curve $\theta = 0$, between $\mu = \mu_I$ and $\mu = \infty$. There will be a sharp corner at the point $(\mu_I,0)$. A plateau of height A^2 would exist to the upper right behind these two curves, and $E_2(\mu,\theta)$ would be zero everywhere else.

Now consider a partial sum such as equation (9.22). For any net, a portion of the net will look like the magnified part shown in the plate. There will always be an area element in the μ,θ plane which encloses the point $(\mu_I,0)$. For this particular net, the appropriate corner points are given by (μ_{2i},θ_{2m}), (μ_{2i+2},θ_{2m}), $(\mu_{2i+2},\theta_{2m+2})$ and (μ_{2i},θ_{2m+2}) in a counterclockwise order. The square root of the appropriate term in the partial sum then has the value, A, for this set of four points as shown by equation (9.31). All other elements in the net contribute nothing to the partial sum. For example, the contribution of the element to the right of the one just considered, yields a value of zero as shown by equation (9.32). Consequently, for this particular partial sum, the value of the partial sum is given by equation (9.33). There is always some set of four net points such that equations (9.34) and (9.35) hold, and as $\Delta_1\mu$ and $\Delta_1\theta$ go to zero, the final result is equation (9.36). Consequently, example one is simply a single sinusoidal wave traveling in the positive x direction of

Some Examples

Example I

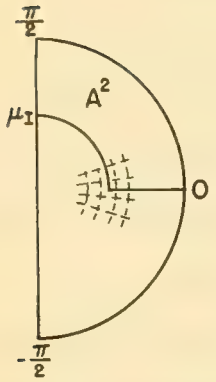

$$E_2(\mu,\theta)\begin{cases} 0\,;\ \theta<0 \\ 0\,;\ \mu<\mu_I \\ A\,;\ \text{otherwise} \end{cases} \qquad (9.29)$$

$$\psi(\mu,\theta)=0 \qquad (9.30)$$

magnified part of net

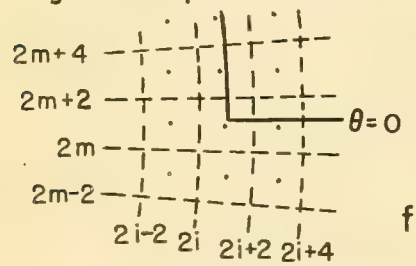

for a partial sum

$$\sqrt{E_2(\mu_{2i+2},\theta_{2N+2})-E_2(\mu_{2i},\theta_{2N+2})-E_2(\mu_{2i+2}\theta_{2M})+E_2(\mu_{2i},\theta_{2M})}=\sqrt{A^2-0-0+0}=A \qquad (9.31)$$

$$\sqrt{E_2(\mu_{2i+4},\theta_{2M+2})-E_2(\mu_{2i+2},\theta_{2M+2})-E_2(\mu_{2i+4},\theta_{2M})+E_2(\mu_{2i+2},\theta_{2M})}=\sqrt{A^2-A^2-0-0}=0 \qquad (9.32)$$

all other elements of the net, but the first one give a contribution of zero

therefore $\eta(x,y,t)=A\cos\left(\frac{(\mu_{2i+1})^2}{g}(x\cos\theta_{2M+1}+y\sin\theta_{2M+1})-\mu_{2i+1}t\right)$ (9.33)

since there is always some set of four net points such that $\mu_{2i+2}>\mu_I>\mu_{2i}$

and $\theta_{2M+2}>0>\theta_{2M}$ (9.34) in the limit $\eta(x,y,t)=A\cos\left(\frac{(\mu_I)^2}{g}x-\mu_I t\right)$ (9.35)

Plate XXXIX

constant period and amplitude in deep water.

The form of $E_2(\mu,\theta)$ for example two is given by equation (9.36a) and the appearance of the function is given on the little figure to the left. $\psi(\mu,\theta)$ is defined in small strips which cover the jumps in $E_2(\mu,\theta)$, and it can be anything otherwise as shown by equation (9.37a). A partial sum, if the net points are close together, for the element which encloses the point $(\mu_{II},0)$, then yields for the square root term the value

$$((A_1^2 + A_2^2) - A_1^2 - 0 + 0)^{1/2} = A_2.$$

The final result, in the limit is given by equation (9.38a). From the above two examples, it is evident that all of the examples given in Chapter 7 are special cases of the integral given by equation (9.1) in which the sea surface does not vary in the y direction.

In example three, $E_2(\mu,\theta)$ is given by equation (9.36b), and $\psi(\mu,\theta)$ is zero. For the area element which encloses the point $(\mu_I,\pi/6)$, the radical in the partial sum for that term is given by $(2A^2 - 0 - A^2 + 0)^{1/2} = A$. The integral is consequently given by equation (9.38b). Equation (9.38b) is just a specific example of equation (8.4) as far as the direction of the two waves is concerned.

In example four, the form of $E_2(\mu,\theta)$ is given by equation (9.39), and $\psi(\mu,\theta)$ equals $3\pi/2$. The integral is then a special case of equation (8.5). In fact, the integral is equal to the equation given in figure ~~19~~ 17 when t is zero. $E_2(\mu,\theta)$ is an interesting function in this particular case, and a three dimensional sketch of the surface involved is given in figure 20. Note the

Some Examples

Example II

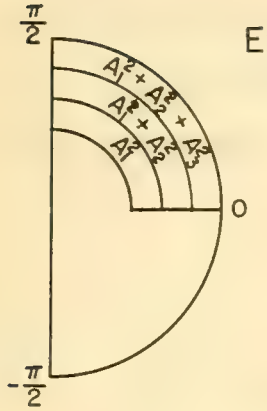

$$E_2(\mu,\theta) = \begin{cases} 0;\ \theta<0 & \\ 0;\ \mu<\mu_I & \\ A_1^2;\ \mu_I\leq\mu<\mu_{II} & 0\leq\theta<\frac{\pi}{2} \\ A_1^2+A_2^2;\ \mu_{II}\leq\mu<\mu_{III} & 0\leq\theta<\frac{\pi}{2} \\ A_1^2+A_2^2+A_3^2;\ \mu_3\leq\mu<\infty & 0\leq\theta<\frac{\pi}{2} \end{cases} \quad (9.36\,a)$$

$$\psi(\mu,\theta) = \begin{cases} 0;\ |\mu-\mu_I|<\epsilon \\ \frac{3\pi}{2};\ |\mu-\mu_{II}|<\epsilon \\ \pi;\ |\mu-\mu_{III}|<\epsilon \\ \text{anything otherwise} \end{cases} \quad (9.37\,a)$$

Then $\eta(x,y,t) = A_1\cos(\frac{\mu_I^2}{g}x-\mu_I t) + A_2\sin(\frac{\mu_{II}^2}{g}x-\mu_{II}t) - A_3\cos(\frac{\mu_{III}^2}{g}x-\mu_{III}t)$ (9.38 a)

Example III

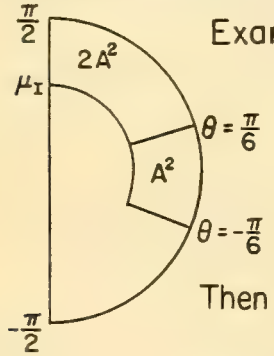

$$E_2(\mu,\theta) = \begin{cases} 0;\ \theta<-\frac{\pi}{6} & \\ 0;\ \mu<\mu_I & \\ A^2;\ \mu_I\leq\mu<\infty & -\frac{\pi}{6}<\theta<\frac{\pi}{6} \\ 2A^2;\ \mu_I\leq\mu<\infty & \frac{\pi}{6}\leq\theta<\frac{\pi}{2} \end{cases} \quad (9.36\,b)$$

$$\psi(\mu,\theta) = 0 \quad (9.37\,b)$$

Then $\eta(x,y,t) = A\cos(\frac{\mu_I^2}{g}(x\cos\frac{\pi}{6}-y\sin\frac{\pi}{6})-\mu_I t) +$
$+A\cos(\frac{\mu_I^2}{g}(x\cos\frac{\pi}{6}+y\sin\frac{\pi}{6})-\mu_I t)$ (9.38 b)

Example IV

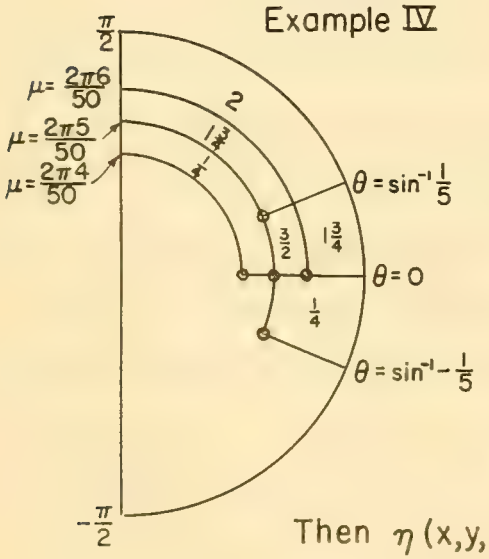

$$E_2(\mu,\theta) = \begin{cases} 0;\ \theta\ \sin^{-1}(-\frac{1}{5}) & \\ 0;\ \sin^{-1}(-\frac{1}{5})<\theta<0 & \text{and } \mu<\frac{2\pi5}{10} \\ 0;\ \mu<\frac{2\pi4}{50} & \\ \frac{1}{4};\ \frac{2\pi5}{50}\leq\mu<\infty & \sin^{-1}(-\frac{1}{5})<\theta<0 \\ \frac{1}{4};\ 0<\theta<\frac{\pi}{2} & \frac{2\pi4}{50}\leq\mu<\frac{2\pi5}{50} \\ \frac{3}{2};\ 0<\theta<\sin^{-1}(\frac{1}{5}) & \frac{2\pi4}{50}\leq\mu<\frac{2\pi5}{50} \\ 1\frac{3}{4};\ \sin^{-1}(\frac{1}{5})<\theta<\frac{\pi}{2} & \frac{2\pi5}{50}\leq\mu<\frac{2\pi6}{50} \\ 1\frac{3}{4};\ 0<\theta<\sin^{-1}(\frac{1}{5}) & \frac{2\pi6}{50}\leq\mu<\infty \\ 2;\ \sin^{-1}(\frac{1}{5})<\theta<\frac{\pi}{2} & \frac{2\pi6}{50}\leq\mu<\infty \end{cases} \quad (9.39)$$

$$\psi(\mu,\theta) = \frac{3\pi}{2} \quad (9.40)$$

Then $\eta(x,y,0)$ = Equation given on Figure ~~19~~ 17

Plate XI

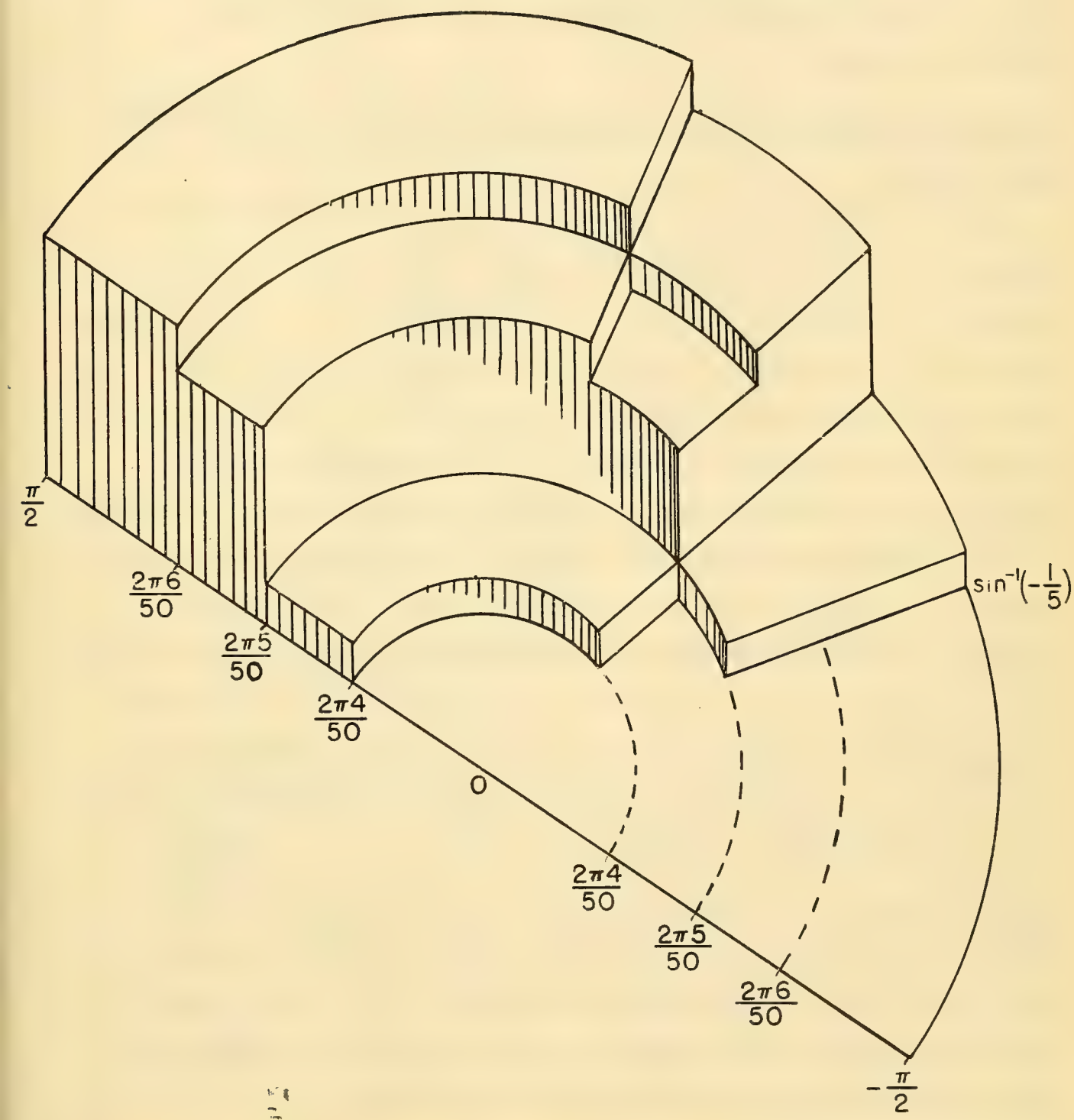

Figure 20 The Form of $E_2(\mu,\theta)$ for equation (9.39)

point at $(2\pi\ 6/50, \sin^{-1} 1/5)$. An area element from the net which covers this point gives no contribution since $(2 - 7/4 - 7/4 + 3/2) = 0$. Also note that $\eta(x,y,0)$ for a fixed y is an almost periodic function in x since $(24/25)^{1/2}$ is an irrational number.

The Gaussian case of the Lebesgue Power Integral for short crested wave systems

By the techniques employed above, many strange and wonderful sea surfaces can be created. It appears that none of them would be quite as strange and wonderful and realistic as the one which will now be described. The short crested wave system given by the Gaussian case of the Lebesgue Stieltjes Power Integral appears to describe the actual surface of the sea in the best possible way within the limits of the linearization assumptions of Chapter 2.

The Gaussian case can be obtained in the following way. Equations (9.2) through (9.13) are still imposed. In addition, if a small circle of radius δ is placed around any point, say, (μ_k, θ_j), then it is required that the absolute value of the difference between $E_2(\mu,\theta)$ at the point and at any other point in the circle be smaller than an epsilon (which may depend on delta). Stated another way, $E_2(\mu,\theta)$ is a continuous function in both variables, and it is monotonic non-decreasing in both variables (see Courant, Vol. I). Equations (9.41) and (9.42) are another way to impose these conditions. Finally, $\Psi(\mu,\theta)$ must have a value between zero and 2π, and its value is picked by the probability law given in equations (9.44) and (9.45).

If equations (9.2) through (9.13) hold, and if the conditions

The Gaussian Case of the Lebesgue Power Integral for Short Crested Wave Systems.

Equations (9.2) through (9.13) hold in addition

$$\text{if } (\mu_{K+1}-\mu_K)^2+(\theta_{j+1}-\theta_j)^2<\delta^2 \tag{9.41}$$

$$\text{then } E_2(\mu_{K+1},\theta_{j+1})-E_2(\mu_K,\theta_j)<\epsilon(\delta) \tag{9.42}$$

and

$$0<\psi(\mu,\theta)<2\pi \tag{9.43}$$

$$p(0<\psi(\mu_{2n+1},\theta_{2p+1})<\alpha\,2\pi)=\alpha \tag{9.44}$$

where

$$0\le\alpha\le 1 \tag{9.45}$$

then equations (9.22) and (9.24) still hold.
also if $E_2(\mu,\theta)$ has continuous first derivatives

$$d^2E_2(\mu,\theta)=\frac{\partial^2E_2(\mu,\theta)}{\partial\mu\,\partial\theta}d\mu d\theta$$

$$=[A_2(\mu,\theta)]^2 d\mu\,d\theta \tag{9.46}$$

alternate formulation of integral

$$\eta(x,y,t)=\int_0^{\infty}\int_{-\frac{\pi}{2}}^{\frac{\pi}{2}}\cos\left[\frac{\mu^2}{g}(x\cos\theta+y\sin\theta)-\mu t+\psi(\mu,\theta)\right]\sqrt{[A_2(\mu,\theta)]^2 d\mu\,d\theta} \tag{9.47}$$

$$\eta(x,y,t)=\lim_{\substack{\mu_{2S}\to\infty\\ \frac{\pi}{2}-\theta_{2R}\to 0^+\\ \Delta_1\mu\to 0\\ \Delta_1\theta\to 0}}\sum_{n=0}^{S-1}\sum_{p=0}^{R-1}\cdot\cos\left(\frac{(\mu_{2n+1})^2}{g}(x\cos\theta_{2p+1}+y\sin\theta_{2p+1})-\mu_{2n+1}t+\psi(\mu_{2n+1},\theta_{2p+1})\right)\cdot\sqrt{(A_2(\mu_{2n+1},\theta_{2p+1}))^2(\mu_{2n+2}-\mu_{2n})(\theta_{2p+2}-\theta_{2p})}$$

$$=\lim_{\substack{\mu_{2S}\to\infty\\ \frac{\pi}{2}-\theta_{2R}\to 0\\ \Delta_1\mu\to 0\\ \Delta_1\theta\to 0}}\operatorname{Re}\sum^{S-1}\cdot\sum^{R-1}e^{i\left(\frac{(\mu_{2n+1})^2}{g}(x\cos\theta_{2p+1}+y\sin\theta_{2p+1})-\mu_{2n+1}t+\psi(\mu_{2n+1},\theta_{2p+1})\right)}\cdot\sqrt{(A_2(\mu_{2n+1},\theta_{2p+1}))^2(\mu_{2n+2}-\mu_{2n})(\theta_{2p+2}-\theta_{2p})} \tag{9.48}$$

Plate XLI

given by equations (9.41) through (9.45) are added, then the limit of the partial sum defined by equation (9.22) still exists, and the integral given by equation (9.1) still has the property given by equation (9.24).

If $E_2(\mu,\theta)$ has a continuous second mixed partial derivative, it must be everywhere greater than or equal to zero. Consequently, it can always be written as the square of some function $A_2(\mu,\theta)$, and under some conditions equation (9.46) is another way to write $d^2E_2(\mu,\theta)$. Substitution of equation (9.46) in equation (9.1) yields equation (9.47) which has a meaning only in the Gaussian case. The expressions for the partial sums can then be written in the forms given in equation (9.48). In the last expression in equation (9.48), the partial sum has again been expressed as a vector in the complex plane. It will be shown in Chapter 10 that for a fixed x and y as t varies, the short crested sea surface as observed at a point has all the properties studied in Chapter 7 for $\eta(t)$. The exact relations between $E_2(\mu,\theta)$, $E(\mu)$, $(A_2(\mu,\theta))^2$ and $[A(\mu)]^2$ will also be discussed at that time.

Some examples of cumulative power density functions and their power spectra

Values of $[A_2(\mu,\theta)]^2$ have never been obtained for an actual sea surface because the observations needed on which the computation of the function depend have never been obtained. Some examples of what the function might look like can be given, and then the consequences of the form of $[A_2(\mu,\theta)]^2$ in the results of a hypothetical forecast can be described. It will be seen that the nature of the forecasted values depends critically on the

Some Examples of Cumulative Power Density Functions and Their Power Spectra.

Example I

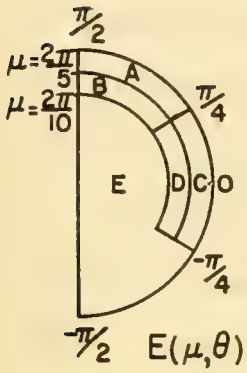

$$A;\ E_2(\mu,\theta) = \left(\frac{2\pi}{5} - \frac{2\pi}{20}\right)\frac{\pi}{2}K^*$$

$$B;\ E_2(\mu,\theta) = \left(\frac{2\pi}{5} - \frac{2\pi}{20}\right)\left(\theta + \frac{\pi}{4}\right)K^*$$

$$C;\ E_2(\mu,\theta) = \left(\mu - \frac{2\pi}{20}\right)\frac{\pi}{2}K^*$$

$$D;\ E_2(\mu,\theta) = \left(\mu - \frac{2\pi}{20}\right)\left(\theta + \frac{\pi}{4}\right)K^*$$

$$E;\ E_2(\mu,\theta) = 0 \qquad (9.49)$$

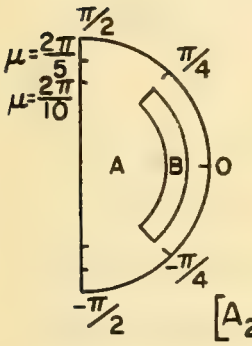

$$A;\ [A_2(\mu,\theta)]^2 = 0$$

$$B;\ [A_2(\mu,\theta)]^2 = K^* \qquad (9.50)$$

Example II

$$E_2(\mu,\theta) = 0 \qquad \text{if } -\pi/2 < \theta < -3\pi/8$$

$$E_2(\mu,\theta) = \int_{-3\pi/8}^{\theta}\int_{0}^{\mu} K\mu^* e^{-\mu^* T_1/2\pi}\left(1+\cos\frac{8}{3}\theta^*\right)d\mu^* d\theta^*$$

$$= \frac{K(2\pi)^2}{T_1^2}\left(1 - e^{-\mu T_1/2\pi} - \frac{\mu T_1}{2\pi}e^{-\mu T_1/2\pi}\right)\left(\frac{3\pi}{8}+\theta+\frac{3}{8}\sin\frac{8\theta}{3}\right)$$

$$\text{if } -\frac{3\pi}{8} < \theta < \frac{3\pi}{8}$$

$$E_2(\mu,\theta) = \int_0^{\mu}\frac{3\pi}{4}K\mu^* e^{-\mu^* T_1/2\pi}du^* = \frac{K(2\pi)^2}{T_1^2}\frac{3\pi}{4}\left(1 - e^{-\mu T_1/2\pi} - \frac{\mu T_1}{2\pi}e^{-\mu T_1/2\pi}\right)$$

$$\text{if } \frac{3\pi}{8} < \theta < \frac{\pi}{2} \qquad (9.51)$$

$$[A_2(\mu,\theta)]^2 = K\mu e^{-\mu T_1/2\pi}\left(1+\cos\frac{8\theta}{3}\right) \qquad \text{if } -\frac{3\pi}{8} < \theta < \frac{3\pi}{8}$$

$$[A_2(\mu,\theta)]^2 = 0 \quad \text{otherwise} \qquad (9.52)$$

nature of the sea surface in the storm.

Example one is a possible form for $E_2(\mu,\theta)$. The μ ,θ polar coordinate system is broken up into five areas as shown in the little sketch on the side of the plate. In area A, the value of $E_2(\mu,\theta)$ is constant and equal to the values given in equation (9.49). The figure is cut off at finite values of μ , but the same value holds for θ between $\pi/4$ and $\pi/2$ and μ greater than $2\pi/5$. In the other areas, the values of $E_2(\mu,\theta)$ are given by the appropriate functions in equation (9.49). Note that $E_2(\mu,\theta)$ is continuous.

Area D is the only area in which $E_2(\mu,\theta)$ is a function of both θ and μ . The second mixed partial derivative is different from zero only in this area. $[A_2(\mu,\theta)]^2$ is equal to K* in this area, and it is zero everywhere else. For any partial sum, with a small enough net, there would be no component wave crests traveling in directions between $-\pi/2$ and $-\pi/4$, and in directions between $\pi/4$ and $\pi/2$, and there would be no component wave crests with periods greater than 10 seconds or less than 5 seconds. In the limit, if the phases were random, the wave system would still be Gaussian.

In equations (9.49) and (9.50), if K* equals $1.69\ 10^5$ cm^2 sec, then E_{2max} equals $2.5\ 10^5$ cm^2. The potential energy in the system averaged over y and t is then equal to $6.25\ 10^7$ $ergs/cm^2$ (if the product ρg equals 10^3 gm/cm^2sec^2).

Example one is physically not a very realistic example. It would not be expected that a turbulent process such as the one which produces waves in a storm at sea could produce such a sharp

cornered power spectrum. Example one is given so that it can be compared with the next example in order to show how remarkably different the forecast results can be.

Example two is somewhat more realistic, although it must be emphasized again that very little is known about the actual values of $E_2(\mu,\theta)$ in nature. In example two, $E_2(\mu,\theta)$ is zero for θ between $-\pi/2$ and $-3\pi/8$. It is given by equation (9.51) between $-3\pi/8$ and $3\pi/8$. For θ between $3\pi/8$ and $\pi/2$, it is a function of μ alone.

The second mixed partial derivative is different from zero only for θ between $-3\pi/8$ and $3\pi/8$. $[A_2(\mu,\theta)]^2$ is then given by equation (9.52).

$E_2(\mu,\theta)$ and $[A_2(\mu,\theta)]^2$ are shown in figures 21 and 22, respectively. The isopleths of constant $E_2(\mu,\theta)$ for θ greater than $3\pi/8$ follow the circles of the coordinate system since there is no variation in θ. The power spectrum has a peak at $\theta = 0$ and $\mu = 2\pi/T_1$. The values of the parameters in the equations for the evaluation are given by

$$K = 2.68\ 10^5\ cm^2sec^2,$$

and $T_1 = 10$ seconds. E_{2max} is then given by $2.5\ 10^5\ cm^2$. The average potential energy in the system is then equal to $6.25\ 10^7$ erg/cm^2 (if the product ρg equals 10^3 g,/cm^{2}sec^2). This is the same amount of potential energy averaged over y and t which would be found in a simple sinusoidal wave with an amplitude (crest to mean water level) of five meters. The same amount of energy as in the power spectrum given in example one has been used for purposes of comparison later.

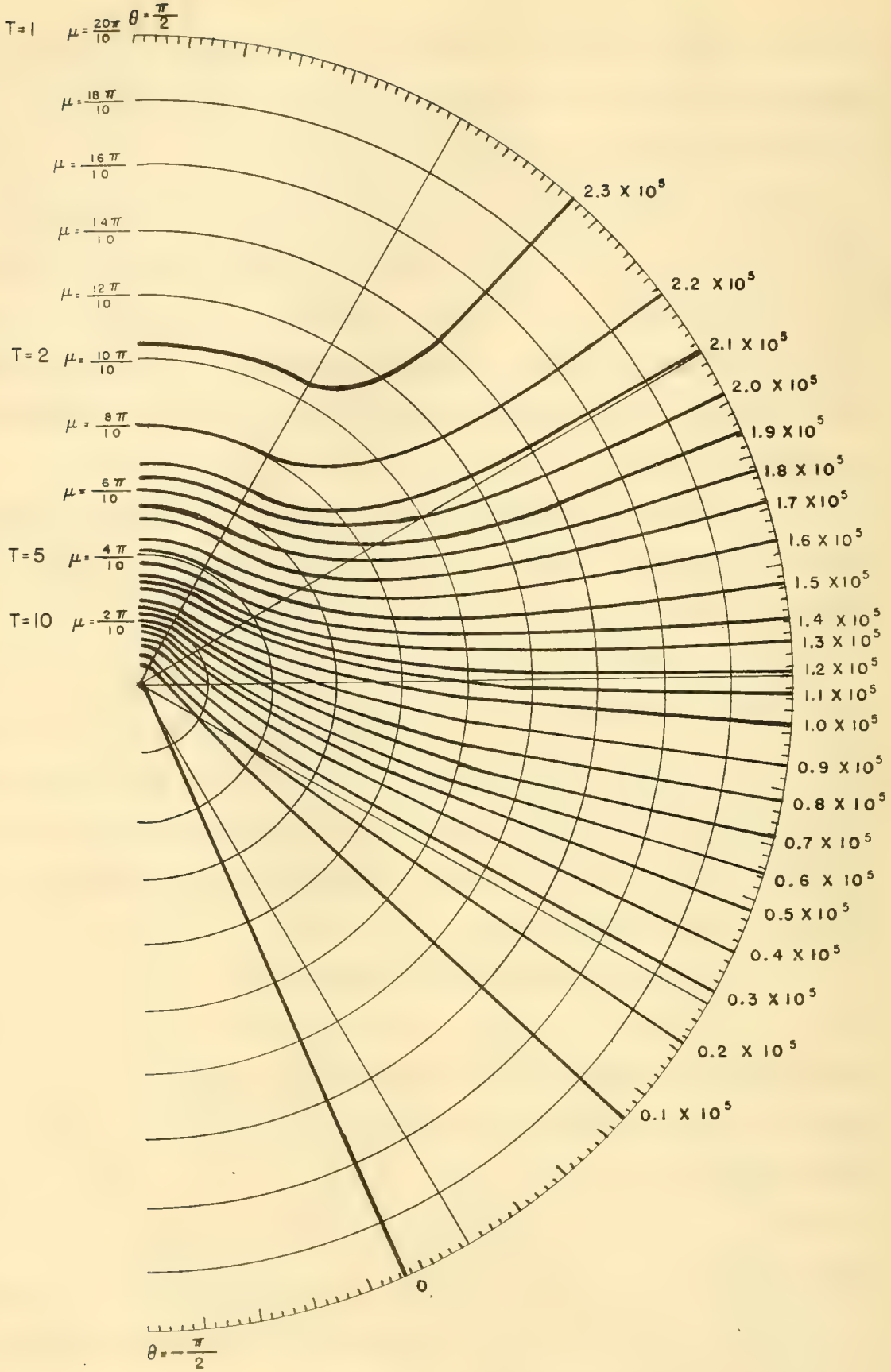

FIG. 21 THE FORM OF $E_2(\mu,\theta)$ FOR EQUATION (9.51).

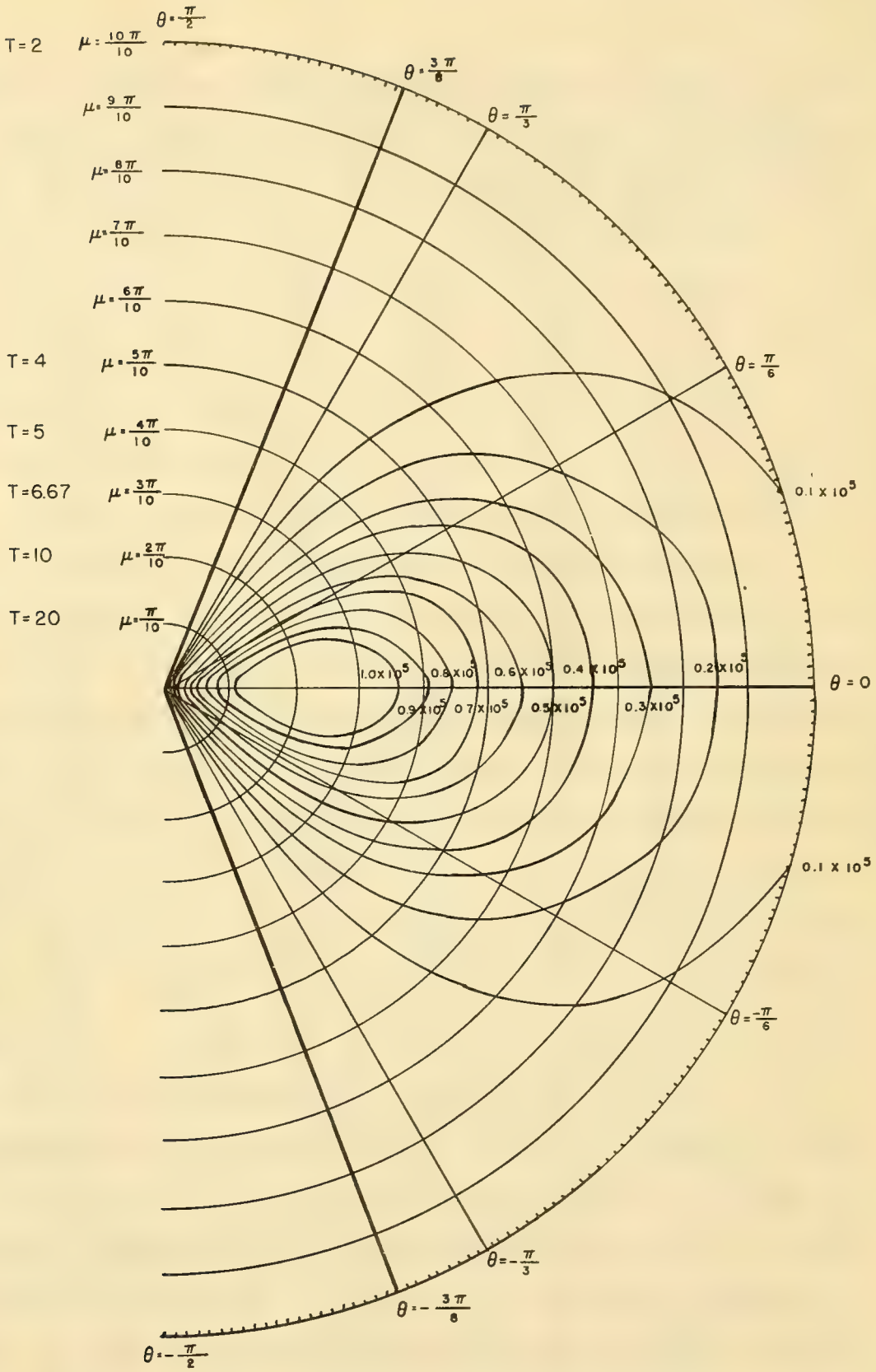

FIG. 22 THE FORM OF $\left[A_2(\mu,\theta)\right]^2$ FOR EQUATION (9.52).

The forecasting problem for a sea level surface represented by short crested waves, a Gaussian Lebesgue Power Integral, and waves that last D_w seconds at the edge of a storm of width W_s.

Equation (9.1) has the same nature as equation (7.1) in that the disturbance exists everywhere and has the same character everywhere, once $E_2(\mu,\theta)$ is fixed. If the disturbance were observed as a function of y and t at x = 0, it would be represented by equation (9.53). The limit of the partial sum given in equation (9.54) is again a representation for equation (9.53).

In order to produce a localized storm, instead of a disturbance everywhere, the representation given by equation (9.54) can be multiplied by a slowly varying function of y and t as given by $\tilde{F}(y,t)$. For a particular example, $\tilde{F}(y,t)$ can be represented by equation (9.55). Other functional forms for $\tilde{F}(y,t)$ with smoother sides might be employed for somewhat more realistic results, but the form given in equation (9.55) at least has the property that the area covered by the waves has a finite width and that the waves are of finite duration at the source. Waves produced by storms in nature are not so sharply defined as this model.

The argument now follows the same line as the one which was used in equation (7.39). If $\tilde{F}(y,t)$ as given in equation (9.55) is applied to $\eta(0,y,t)$ as given in equation (9.54), the disturbance which results is observed at the source only over a distance of length W_s and only for a time D_w. If the disturbance is observed within the time interval indicated, it will be indistinguishable from a similar short observation at any time and place in

The Forecasting Problem for a Sea Surface Represented by Short Crested Waves, a Gaussian Lebesgue Power Integral, and Waves that last D_w Seconds at the Edge of a Storm of Width W_s.

$$\eta(o,y,t) = \int_0^{\infty} \int_{-\frac{\pi}{2}}^{\frac{\pi}{2}} \cos\left(\frac{\mu^2}{g} y\sin\theta - \mu t + \psi(\mu,\theta)\right) \sqrt{d^2E_2(\mu,\theta)} \tag{9.53}$$

$$\eta(o,y,t) = \lim_{\substack{\mu_{2S}\to\infty \\ \frac{\pi}{2}-\theta_{2R}\to 0 \\ \Delta_1\mu\to 0 \\ \Delta_1\theta\to 0}} \sum_{n=0}^{S-1}\cdot\sum_{p=0}^{R-1} \cdot \cos\left[\frac{(\mu_{2n+1})^2}{g} y\sin\theta_{2p+1} - \mu_{2n+1}t + \psi(\mu_{2n+1},\theta_{2p+1})\right] \sqrt{\left[A_2(\mu_{2n+1},\theta_{2p+1})\right]^2 (\mu_{2n+2}-\mu_{2n})(\theta_{2p+2}-\theta_{2p})} \tag{9.54}$$

$$F(y,t) = \begin{cases} 1 \ ; \ 0<t<D_w; \ -\frac{W_s}{2}<y<\frac{W_s}{2} \\ 0 \ ; \ \text{otherwise} \end{cases} \tag{9.55}$$

$$FF(x,y,t,\mu,\theta) = \frac{1}{4}\left[\left(\int_{\sqrt{\frac{2\mu\cos\theta}{2\pi x g}}\left(\frac{Y}{\cos\theta}-\frac{W_s}{2}\right)}^{\sqrt{\frac{2\mu\cos\theta}{2\pi x g}}\left(\frac{Y}{\cos\theta}+\frac{W_s}{2}\right)} \cos\frac{\pi}{2}\delta^2 d\delta\right)^2 + \left(\int_{\sqrt{\frac{2\mu\cos\theta}{2\pi x g}}\left(\frac{Y}{\cos\theta}-\frac{W_s}{2}\right)}^{\sqrt{\frac{2\mu\cos\theta}{2\pi x g}}\left(\frac{Y}{\cos\theta}+\frac{W_s}{2}\right)} \sin\frac{\pi}{2}\delta^2 d\delta\right)^2\right] \cdot \left[\left(\int_{\sqrt{\frac{2x\cos\theta}{3\pi g}}\left(\frac{\mu}{\cos\theta}-\frac{g(t_{ob}-D_w)}{2x}\right)}^{\sqrt{\frac{2x\cos\theta}{3\pi g}}\left(\frac{\mu}{\cos\theta}-\frac{gt_{ob}}{2x}\right)} \cos\frac{\pi}{2}\delta^2 d\delta\right)^2 + \left(\int_{\sqrt{\frac{2x\cos\theta}{3\pi g}}\left(\frac{\mu}{\cos\theta}-\frac{g(t_{ob}-D_w)}{2x}\right)}^{\sqrt{\frac{2x\cos\theta}{3\pi g}}\left(\frac{\mu}{\cos\theta}-\frac{gt_{ob}}{2x}\right)} \sin\frac{\pi}{2}\delta^2 d\delta\right)^2\right] \tag{9.56}$$

$$Y_u = -\sin\theta_u x + \cos\theta_u y = -\frac{W_s}{2}\cos\theta_u \tag{9.57}$$

$$\tan\theta_u = \frac{y+\frac{W_s}{2}}{x} \tag{9.58}$$

$$Y_L = -\sin\theta_L x + \cos\theta_L y = \frac{W_s}{2}\cos\theta_L \tag{9.59}$$

$$\tan\theta_L = \frac{y-\frac{W_s}{2}}{x} \tag{9.60}$$

$$\tan\theta_D = \frac{y}{x} \tag{9.61}$$

$$S.F.G.W. = \begin{cases} 1 \ ; \ \text{if } \tan^{-1}\frac{y-\frac{W_s}{2}}{x} \le \theta \le \tan^{-1}\frac{y+\frac{W_s}{2}}{x} \ ; \ \text{and if } \frac{g(t_{ob}-D_w)}{2x} \le \frac{\mu}{\cos\theta} \le \frac{gt_{ob}}{2x} \\ 0 \ ; \ \text{otherwise} \end{cases} \tag{9.62}$$

$$S.F.G.W. = \begin{cases} 1 \ ; \ \text{if } \tan^{-1}\frac{y-\frac{W_s}{2}}{x} \le \theta \le \tan^{-1}\frac{y+\frac{W_s}{2}}{x} \ ; \ \text{and if } \frac{g(t_{ob}-D_w)}{2R} \le \mu \le \frac{gt_{ob}}{2R} \\ 0 \ ; \ \text{otherwise} \end{cases} \tag{9.63}$$

PLATE XLIII

the disturbance covering the whole y,t plane. $\tilde{F}(y,t)$ can be applied to each term in any finite partial sum. As the indicated limit is approached, the result of the operation by $\tilde{F}(y,t)$ can be treated as a filter operation on $[A_2(\mu,\theta)]^2$ in order to find the power spectrum at other times and places as the concentrated disturbance at the source disperses and spreads over the x,y plane.

The problem of the result of the application of $\tilde{F}(y,t)$ to a particular term in the partial sum was solved in Chapter 8, apart from minor modifications necessitated by the arbitrary phase, $\psi(\mu_{2m+1},\theta_{2p+1})$. These modifications only serve to complicate the algebra in the analysis and the same filter function is obtained. The end result is FF(x,y,t) as given in equation (8.62). This filter function is repeated with modifications in equation (9.56). The time variable has been referred to t_{ob} by a change of variables, and the filter is also given as a function of μ and θ. If x, y, t_{ob}, D_w and W_s are fixed, $FF(x,y,t,\mu,\theta)$ can be varied as a function of μ and θ, and the filter properties can then be determined.

The θ-band cutoff points

The Fresnel filter, $FF(x,y,t,\mu,\theta)$, has the disadvantages of the corresponding filter given in equation (7.50) in that it oscillates rapidly near the quarter power points as a function of μ and θ. It can be approximated as before by the square cutoff filter. In the first term given by equation (9.56) the quarter power points occur where equations (8.67) and (8.68) are satisfied. With the use of equations (8.53), (8.51) and (8.31), equation (8.68) can be

put in the form of equation (9.57). The points x and y are treated as constants. θ is treated as a variable, and when θ equals θ_u, as θ is increased, the term in the filter passes through the value one half. For θ greater than θ_u the term rapidly becomes zero. The result is that tan θ_u is given by $[y + W_s/2)]/x$. Similarly equation (8.67) yields equation (9.59). For θ less than θ_L, the term in the filter is nearly zero, when θ equals θ_L it is one half, and for θ greater than θ_L but less than θ_u, the term is essentially two.

The properties of the filter which cause it to cut off all but a certain angular band width of the power spectrum at the source can be explained by reference to figure 18 and to figure 23. Figure 18 shows that for a fixed value of θ, the disturbance in the x,y plane remains between the two lines, $\bar{Y}_L = \cos \theta_L W_s/2$ and $\bar{Y}_L = - \cos \theta_L W_s/2$. Consider then in the x,y plane, the area which can be occupied by a disturbance which travels along the line $\bar{Y}_u = 0$, for a fixed point $x = x_1$ and $y = y_1$. The lowermost part of that disturbance as shown by the dashed line $\bar{Y}_u = - \cos \theta_u W_s/2$ will just miss the point $x_1 y_1$, and any disturbance which leaves the source at directions greater than θ_u will never be observed at the point $x_1 y_1$. Similarly the disturbance which travels along the line $\bar{Y}_L = 0$, will pass just below the point x_1, y_1, as shown by the dashed line, $\bar{Y}_1 = \cos \theta_L W_s/2$. Any disturbance which leaves the source with a direction less than θ_L will never be observed at the point x_1, y_1. Equations (9.58) and (9.60) have a simple interpretation in terms of these considerations when interpreted with the

aid of the upper part of figure 23. Another important direction namely the direction to the point x_1, y_1, is given by equation (9.61).

The μ -band cutoff points

The second term in equation (9.56) can be studied as a function of μ and θ for a fixed value of x and t_{ob}. The upper and lower ranges of integration when set equal to zero, yield the information that when $\mu/\cos\theta$ is less than $g(t_{ob} - D_w)/2x$, the disturbing element in the partial sum will already have passed, and that when $\mu/\cos\theta$ is greater than $gt_{ob}/2x$ the disturbance will not yet have arrived. When the θ band width is small, the variation of $\cos\theta$ is small and the range of the values determines the range of μ essentially.

The square filter for the Gaussian case of a short crested sea surface in a disturbance which lasts D_w seconds at the edge of a storm of width, W_s

Under the assumption that the Fresnel fringes will cancel out because of the finite time of observation, the square cutoff filter for this model wave system can be given by equation (9.62). Since $\theta_L < \theta_D < \theta_u$, and if $\theta_u - \theta_L$ is small, the value of $\mu/\cos\theta$ can be approximated by $\mu/\cos\theta_D$. θ_D is the angular direction of the point x_1, y_1, from the point x = 0, y = 0. The second inequality in equation (9.62) can then be multiplied through by $\cos\theta_D$, and the result is a factor of the form $(\cos\theta_D)/x$. The factor, $(\cos\theta_D)/x$ is simply equal to the reciprocal of the distance a given elemental disturbance must travel to reach the point (x_1, y_1), and consequently it is equal to 1/R. The value of R is measured from the center of the forward edge of the storm to the point of forecast. With this

slight approximation the square cutoff filter is given by equation (9.63). The result is then an equation analogous to equation (7.45), in which R has been substituted for x. Equations similar to equations (7.46), (7.47) and (7.48) would also result and remarks similar to those in Chapter 7 could be made about them.

The θ-band width

From equation (9.58) and (9.60), it is possible to form the difference given by $\theta_u - \theta_L$ and determine the θ-band width. The result is equation (9.64) where $\Delta\theta$ is the angular width of the square cutoff filter.

The θ-band width is not of equal width above and below the value θ_D. This is shown in equations (9.65) and (9.66) which show that $\Delta\theta_u$, the variation in radians from θ_D to θ_u (the upper cutoff angle), is smaller than $\Delta\theta_L$, the variation in radians from the lower cutoff angle to θ_D.

The square filter for the Gaussian case of a short crested sea surface generated by a storm of finite duration D_s, finite width, W_s, over a fetch of length, F.

With the realization that the wave systems under study are only a first approximation to actual wave systems from a storm at sea (mainly because of the nature of the functional form of $\tilde{F}$ which has been assumed; and not because of the inadequacy of the Gaussian Lebesgue Power Integral), it is possible to account for the effect of a fetch of finite length. If a wave record is observed at a point x = 0, y = 0, (or any value between $\pm W_s/2$), there is of course an ambiguity as to where the waves come from

The Θ Band Width and the Forecasting Problem for a Sea Surface Represented by Short Crested Waves, a Gaussian Lebesgue Power Integral for a Storm of Width, W_s, of Duration, D_s, over a Fetch of Length, F.

$$\Delta\theta = \theta_u - \theta_L = \tan^{-1}\left(\frac{y+\frac{W_s}{2}}{x}\right) - \tan^{-1}\left(\frac{y-\frac{W_s}{2}}{x}\right) = \tan^{-1}\left(\tan\left(\tan^{-1}\left(\frac{y+\frac{W_s}{2}}{x}\right) - \tan^{-1}\left(\frac{y-\frac{W_s}{2}}{x}\right)\right)\right) = \tan^{-1}\frac{W_s}{x}\left[\frac{x^2}{x^2+\left(y^2-\frac{W_s^2}{4}\right)}\right] \tag{9.64}$$

$$\Delta\theta_u = \theta_u - \theta_D = \tan^{-1}\left[\frac{W_s}{2x}\left[\frac{x^2}{x^2+\left(y+\frac{W_s}{2}\right)y}\right]\right] \cong \tan^{-1}\left[\frac{W_s}{2x}\left[1-\frac{y^2}{x^2}-\frac{W_s y}{2x^2}\right]\right] \tag{9.65}$$

$$\Delta\theta_L = \theta_D - \theta_L = \tan^{-1}\left[\frac{W_s}{2x}\left[\frac{x^2}{x^2+\left(y-\frac{W_s}{2}\right)y}\right]\right] \cong \tan^{-1}\left[\frac{W_s}{2x}\left[1-\frac{y^2}{x^2}+\frac{W_s y}{2x^2}\right]\right] \tag{9.66}$$

$$F_F(y,t,\mu) = \begin{cases} 1 & \text{if } 0 < t < D_s + \frac{2\mu F}{g}; \text{ and if } -\frac{W_s}{2} < y < \frac{W_s}{2} \\ 0 & \text{otherwise} \end{cases} \tag{9.67}$$

$$\text{S.F.G.W.F} = \begin{cases} 1 & \text{if } g\frac{(t_{ob}-D_s)}{2(R+F)} \le \mu \le \frac{g t_{ob}}{2R} \text{ and if } \tan^{-1}\left(\frac{y-\frac{W_s}{2}}{x}\right) \le \theta \le \tan^{-1}\left(\frac{y+\frac{W_s}{2}}{x}\right) \\ 0 & \text{otherwise} \end{cases} \tag{9.68}$$

where $$\Delta\mu = \frac{gD_s}{2R} + \frac{gF(t_{ob}-D_s)}{2R(R+F)} \tag{9.69}$$

$$\Delta\theta = \tan^{-1}\left[\frac{W_s x}{R^2-\left(\frac{W_s^2}{4}\right)}\right] \tag{9.70}$$

Final Forecast Formula for Deep Water

$$\eta(x,y,t) = \int_0^{\infty}\int_{-\frac{\pi}{2}}^{\frac{\pi}{2}} \cos\left[\frac{\mu^2}{g}(x\cos\theta + y\sin\theta) - \mu t + \psi(\mu,\theta)\right]\sqrt{[\text{S.F.G.W.F}]\,[A_2(\mu,\theta)]^2}\,d\mu\,d\theta \tag{9.71}$$

Plate XLIV

behind the y axis. The lower part of figure 23 illustrates two possibilities which could occur. Suppose that an area of relatively strong winds covers the region between $x = 0$ and $x = -F$, and $y = W_s/2$ and $y = -W_s/2$. Also suppose that the winds last D_s units of time. Then at the time $t = D_s$ an elemental wave which has left the storm area would occupy the area ahead of the y axis which is bounded by the solid lines. When the winds stop at $t = D_s$, the area behind the y axis bounded by the solid lines might be occupied by an elemental wave component which could travel off in the θ_1 direction after $t = D_s$. This would imply a rather peculiar behavior of the wave component, and the two obliquely oriented areas would sweep out a rather peculiar area as they travel along.

In an actual storm the area covered by the winds merges gradually into the area of relative calm. In addition the wind direction varies turbulently over the storm area. It would therefore be equally consistent to assume that the area occupied by the wave element traveling in the θ_1 direction could be given by the dashed area at the time, $t_{ob} = D_w$. At any time after $t_{ob} = 0$, one observation, sufficiently detailed to determine $E_2(\mu, \theta)$ at $x = 0$, $y = 0$, would yield only enough information to show that either of the two assumed areas could be used. A system of weather maps which could yield such a pattern and which could occur in an actual meteorological situation, will be described in a later chapter. The filter under discussion will be derived under the assumption that the elemental wave system occupies the area bounded by the dashed lines.

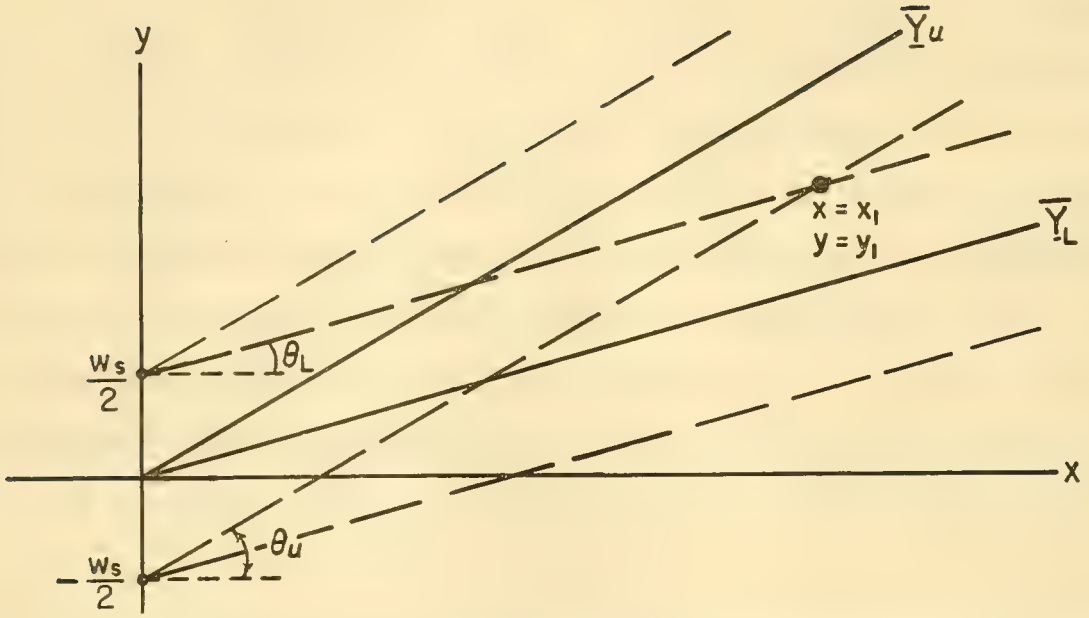

The determination of the angular bond width of the filter for a storm of finite width.

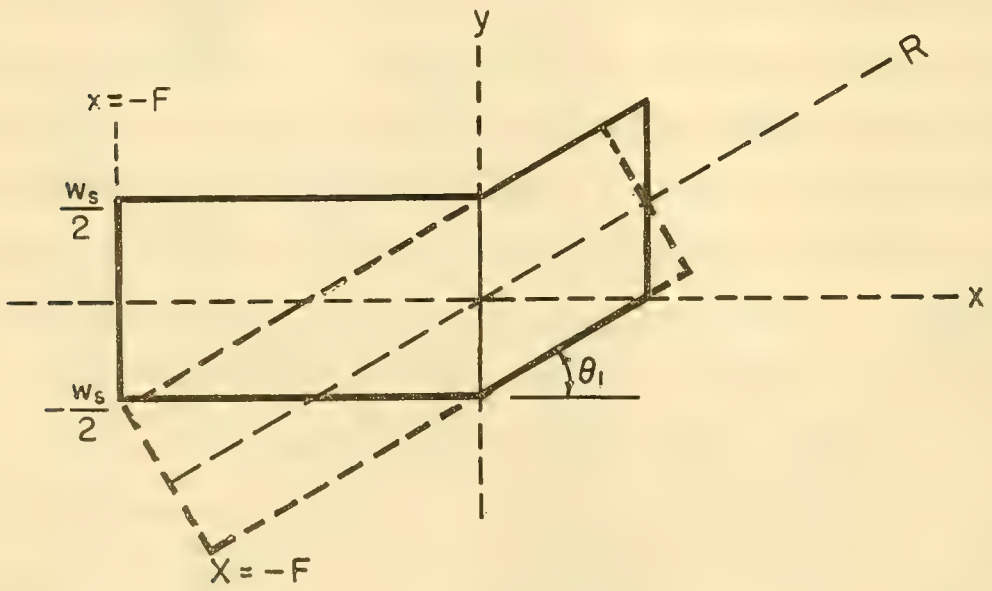

——— Possible area covered by waves at $t = D_s$ for storm of finite width.

– – – – Assumed area for the computations of the square cut-off filter for the storm of finite width.

Fig. 23 Filter Considerations for a Storm of Finite Width.

Under the above assumptions, the modulating function $\tilde{F}_F(y,t,\mu)$ is given by equation (9.67). Equation (7.51) of Chapter 7 modified by the requirement that the storm be of finite width has been employed, and the argument that shorter period waves require a longer time to travel from the rear edge of the fetch to the point, x = 0, y = 0, is employed.

The square cutoff filter for the Gaussian case of a storm of finite width and duration over a fetch of finite length under the above assumptions, is then given by equation (9.68). The μ cutoff values are given by an equation similar to equation (7.57) except that they are determined by the distance R and not by x. The θ cutoff values are given by equation (9.64). The μ band width is given by equation (9.69), and the θ band width is given by equation (9.70) in which R^2 equals $x^2 + y^2$. It should be noted that equations (9.64) and (9.70) hold only if $R^2 > W_s^2/4$, that is, outside of a semi-circle with a center at x = 0, y = 0, of radius $W_s/2$. If the point of observation is inside of this circle, the expressions for $\Delta\theta_u$ and $\Delta\theta_L$ given by equations (9.65) and (9.66) can be employed. The filter might be smoothed by arguments similar to those employed in deriving equation (7.61).

The final forecast formulas for waves in deep water

If the entire forecast is to be carried out in deep water, the final forecast formula is then given by equation (9.71). If the short crested disturbance at the source is given by equation (9.47), and if the disturbance is produced by a storm of finite width and finite duration over a fetch of length, F, then the forecast formula states that the short crested disturbance in

the vicinity of the point x_1, y_1, t_{ob} is given approximately by multiplying $[A_2(\mu, \theta)]^2$ by the cutoff filter given by equation (9.68) and integrating the resulting Lebesgue Power Integral for the Gaussian case.

More precisely, the wave system at the source is one system from a whole statistical class of systems given by all the possible forms the free surface can assume upon forming all of the possible limiting partial sums which can be obtained from equation (9.48) with all possible combinations of the random phases. Thus the disturbance at the source is one of an infinite number of possible disturbances for a fixed functional form for $[A_2(\mu, \theta)]^2$, and the disturbance in the area of decay is one of an infinite number of possible disturbances for a fixed functional form of S.F.G.W.F. times $[A_2(\mu, \theta)]^2$. Also more precisely, when, as in the last paragraph, integration of equation (9.71) is referred to so glibly, one should think only of some finite partial sum evaluated with a sufficiently small net to yield a result adequate for the problem under study. In addition, the indicated forecasted sea surface should be considered to be valid only for a relatively short time, and only over a relatively small area of the sea surface.

Practical evaluation of the filters

Three sharp cutoff filters have been described above in equations (9.62), (9.63) and (9.68). For a fixed value of x, y, and t_{ob}, they determine an area in the μ, θ plane. Inside of this area in the μ, θ plane the power spectrum is the same

as at the source, and outside of this area the spectrum is zero. In all three filters, the θ cutoff values are given by the same expression. In each of the three filters the μ cutoff values are slightly different. The determination of the θ cutoff values and the θ-band width will be described first; then the various μ-band width determinations will be described; and finally some sample filters will be graphed.

Determination of the θ-band width and the θ cutoff points

The angles θ_D, $\Delta\theta_u$, and $\Delta\theta_L$ are functions of x, y, and W_s. For a storm of given width, the values of x and y then determine these angles. If the width of the storm is doubled, and if the values of x and y are doubled, the same values for the angles result. Consequently, if x and y are measured in units of W_s, the angular cutoff values are in a sense independent of the actual width of the storm. In figure 24, lines of constant θ_D, $\Delta\theta_u$, and $\Delta\theta_L$ are shown on an x,y coordinate system with units marked off in terms of the width of the storm. Note that $\Delta\theta_L$ is slightly greater at each point than $\Delta\theta_u$. Given $[A_2(\mu,\theta)]^2$ and the point in the x,y plane at which the forecast is to be made, measure x and y in terms of W_s and enter the point on figure 24 to read off θ_D, $\Delta\theta_u$, and $\Delta\theta_L$. Then in the μ,θ polar coordinate plane draw a line through μ equals zero along a radius at the value θ_D. Mark off an angular increment in the positive θ direction equal to $\Delta\theta_u$ units from the values θ_D, and a decrement in the negative θ direction equal to $\Delta\theta_L$. Draw the two radii obtained. The two outside lines then cut off a sector of

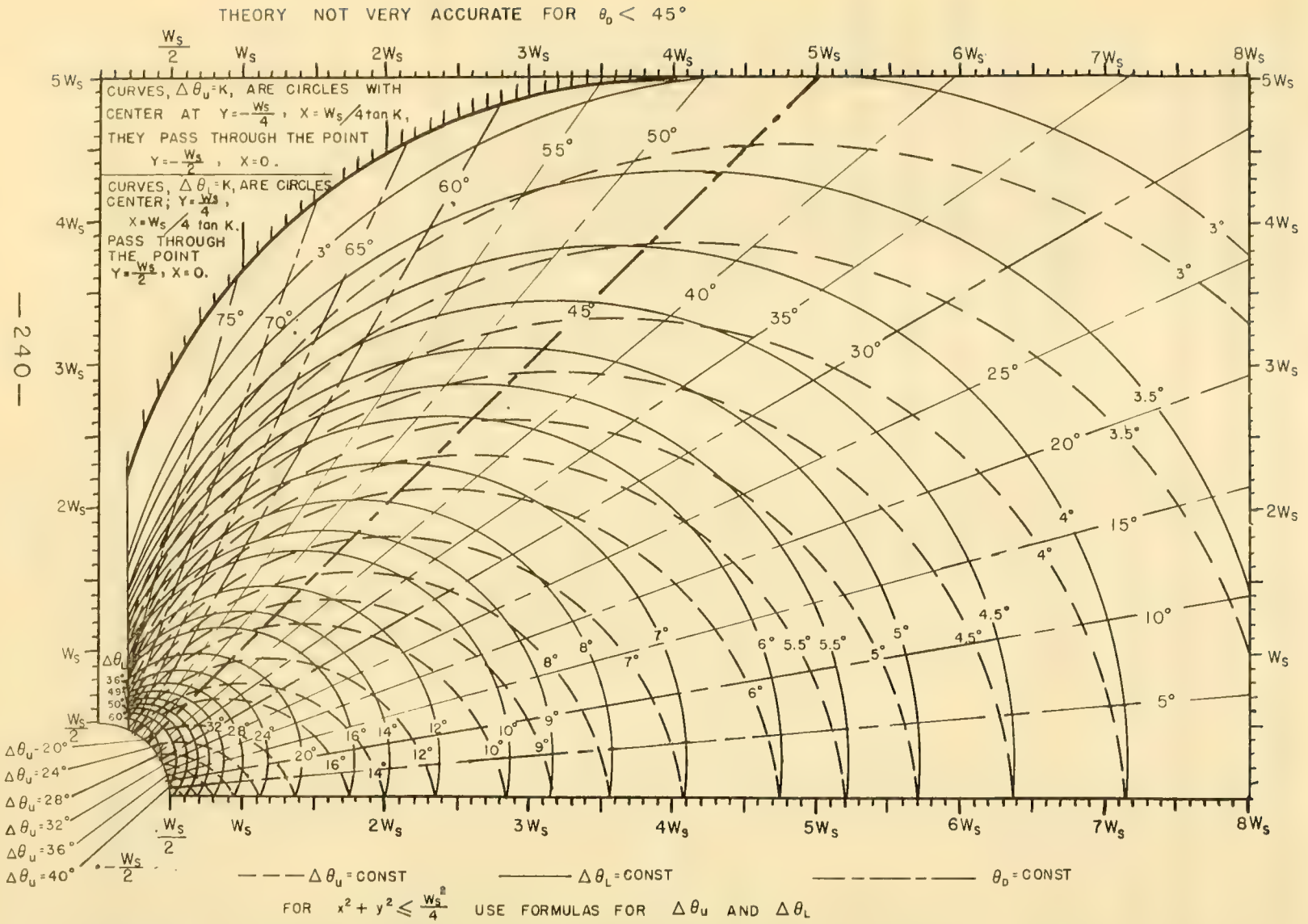

FIG. 24 ISOPLETHS OF θ_D, $\Delta\theta_u$, AND $\Delta\theta_L$ FOR THE X,Y PLANE IN UNITS OF STORM WIDTH, W_s.

the μ,θ plane which determines the θ cutoff values. Note that the θ cutoff values do not depend upon time, and that for a given storm and a given point of forecast, they are fixed once and for all for all forecasts. Note the complete symmetry upon reflection in the θ equals zero axis of the coordinate system as given by the equation. Only the first quadrant is shown in figure 24 for this reason.

Determination of the μ cutoff values

In equation (9.62), the ratio, $\mu/\cos\theta$, must lie between two fixed numbers, once t_{ob}, D_w and x are fixed. An equation of the form, $\mu/\cos\theta$ = const, is an equation of a circle in the μ,θ polar coordinate system which passes through the two points ($\mu = 0, \theta = \pi/2$, and $\mu = \text{const}/\cos\theta_D, \theta = \theta_D$). The circle has a center on the line $\theta = 0$. The intersection of the two curves $\mu/\cos\theta = \text{const}_u$ and $\mu/\cos\theta = \text{const}_L$ and the two lines, $\theta = \theta_D + \Delta\theta_u$ and $\theta = \theta_D - \Delta\theta_L$, then determines an area in the μ,θ plane bounded by segments of two straight lines and two circles.

In equation (9.63) in which $\cos\theta_D$ has replaced $\cos\theta$, μ_u is given by $t_{ob}/2R$ and μ_L by $g(t_{ob} - D_w)/2R$. Figure 15 can then be employed, upon reading R for x, to find the band width and the upper and lower cutoff values for the point and the time of the forecast. In the μ,θ plane the area bounded by $\mu = \mu_u$, $\mu = \mu_L$, $\theta = \theta_D + \Delta\theta_u$ and $\theta = \theta_D - \Delta\theta_L$ then determines the edges of the filter given by equation (9.63) once x, y, W_s, t_{ob}, and D_w are given. (D_w is ten hours for figure 15, but the extension to any value of D_w is simple.)

In equation (9.68), figure 16 can be employed to find the μ band width and the μ cutoff values for a storm with a duration of ten hours and with any length fetch. The μ band width depends upon D_s, R, F, and t_{ob}.

Final forecast diagrams

Figure 24 and figure 25 are all the equipment needed to determine the filter characteristics for the filter given by equation (9.68). Figure 25 is simply a graph of the straight lines given by $t_{ob} = 2\mu_u R/g$ (see Chapter 7, page 162) on a t_{ob}, μ coordinate system for various values of the parameter, R. Given D_s, F, t_{ob}, and R, the appropriate graph of the straight line $t_{ob} - D_s = 2\mu_L(R + F)/g$ can also be found, and the intersection of various lines on the diagram then determines μ_u and μ_L for the filter.

The entire procedure for the evaluation of equation (9.68) for a fixed set of parameters with the use of figures 24 and 25 will now be described. The given parameters, which could theoretically be evaluated from weather maps are: storm width, 200 km (W_s); fetch, 200 km (F); duration of storm, 15 hours (D_s); x, 600 km; y, 600 km; and time of observation, 40 hours (t_{ob}).

The evaluation of the θ-band width proceeds as follows. Tan $\theta_D = y/x = 1$, and $\theta_D = 45°$. $x = y = 3W_s$, and from figure 24, $\Delta\theta_u = 4.4°$ and $\Delta\theta_L = 5.2°$. The θ-band width is therefore 9.6° and the θ cutoff points are at 49.4° and 39.8°. (From equations (9.65) and (9.66), $\Delta\theta_u = \tan^{-1}(1/13)$ and $\Delta\theta_L = \tan^{-1}(1/11)$.

The evaluation of the μ band width proceeds as follows. R equals $\sqrt{2}$ 600 which equals 848 km. In figure 25, locate the line t_{ob} = 40 hours, and the line labeled 848($\tilde{=}$ 850) km. The

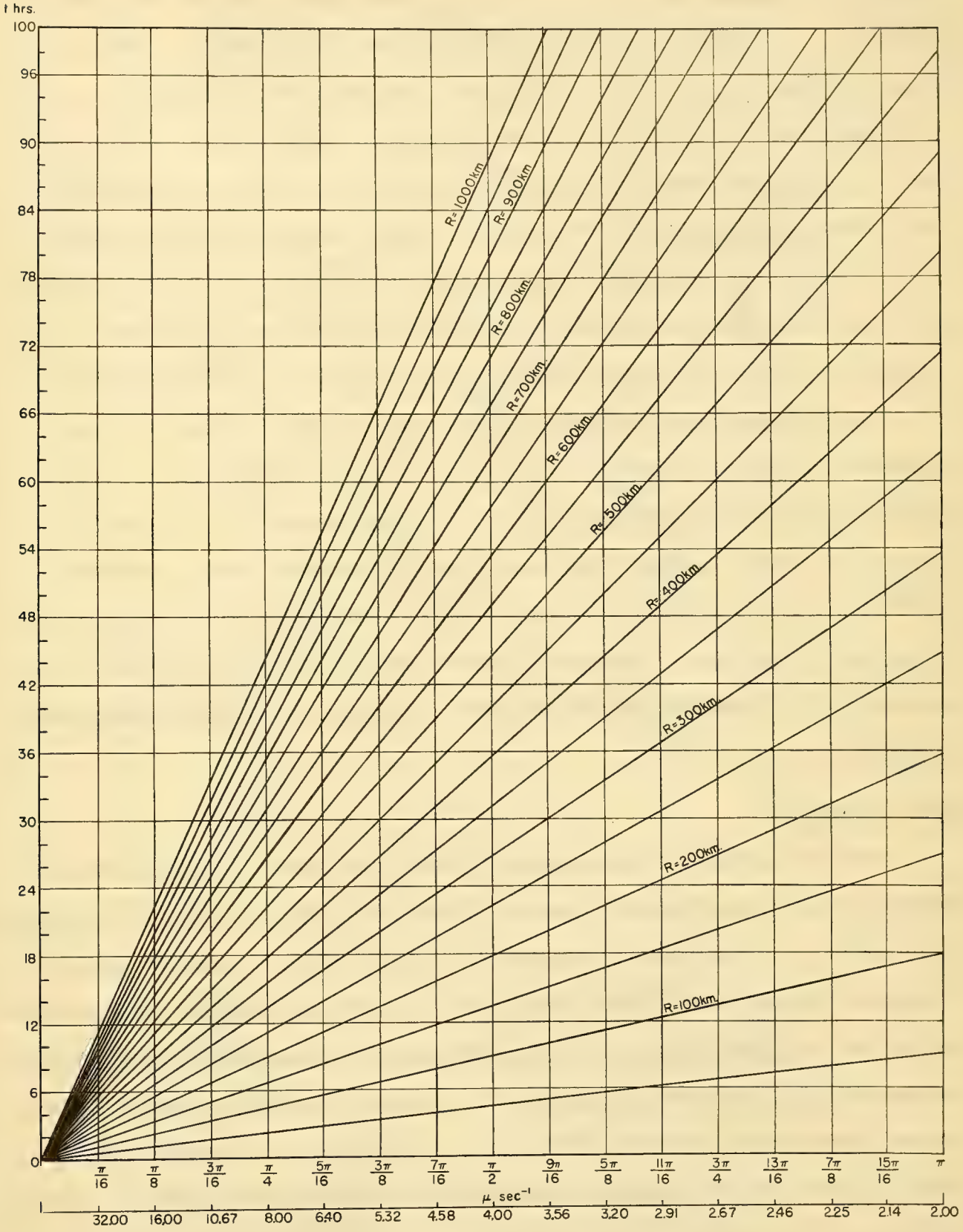

Fig.25. Forecast Diagram For The Determination Of The Band Width.

point of intersection in the μ ,t_{ob} plane then determines the value of μ_u which is equal to .81 radians per second. Next locate the line t_{ob} - 15 hrs = 25 hrs, and the line labeled 1050 km($\cong$ 848 + 200). The intersection of these two lines in the μ ,t_{ob} plane then determines the value of μ_L which equals .402 radians per second. The value, .402, corresponds to a period of 15.63 sec, and .81 corresponds to a period of 7.75 seconds. All spectral periods greater than 15.63 seconds or less than 7.75 seconds will not be present at the point and time of observation.

The filter for the given set of parameters then equals one inside of an area element in the μ ,θ plane bounded by θ_u = 49.4 degrees, θ_L = 39.8 degrees, μ_u = .81, (a segment of a circle), and μ_L = .402. Inside this area the forecasted power spectrum equals the power spectrum at the source, and outside of this area, it is equal to zero. The wave system at the point and time of observation is then the Lebesgue Power Integral over this forecasted power spectrum.

Some examples

The filter given by equation (9.62) can best be evaluated by brute force. The filter given by equation (9.63) is simply a special case of the filter given by equation (9.68) when F equals zero. Figure 26 shows the cutoff boundaries of the three filters described above for various values of the parameters. The values appropriate to equation (9.62) are shown by the dotted lines when needed. The values appropriate to equation (9.63) are shown by dashed lines when needed and the values appropriate to equation (9.68) are given by the solid lines. The θ band width is the same for all three

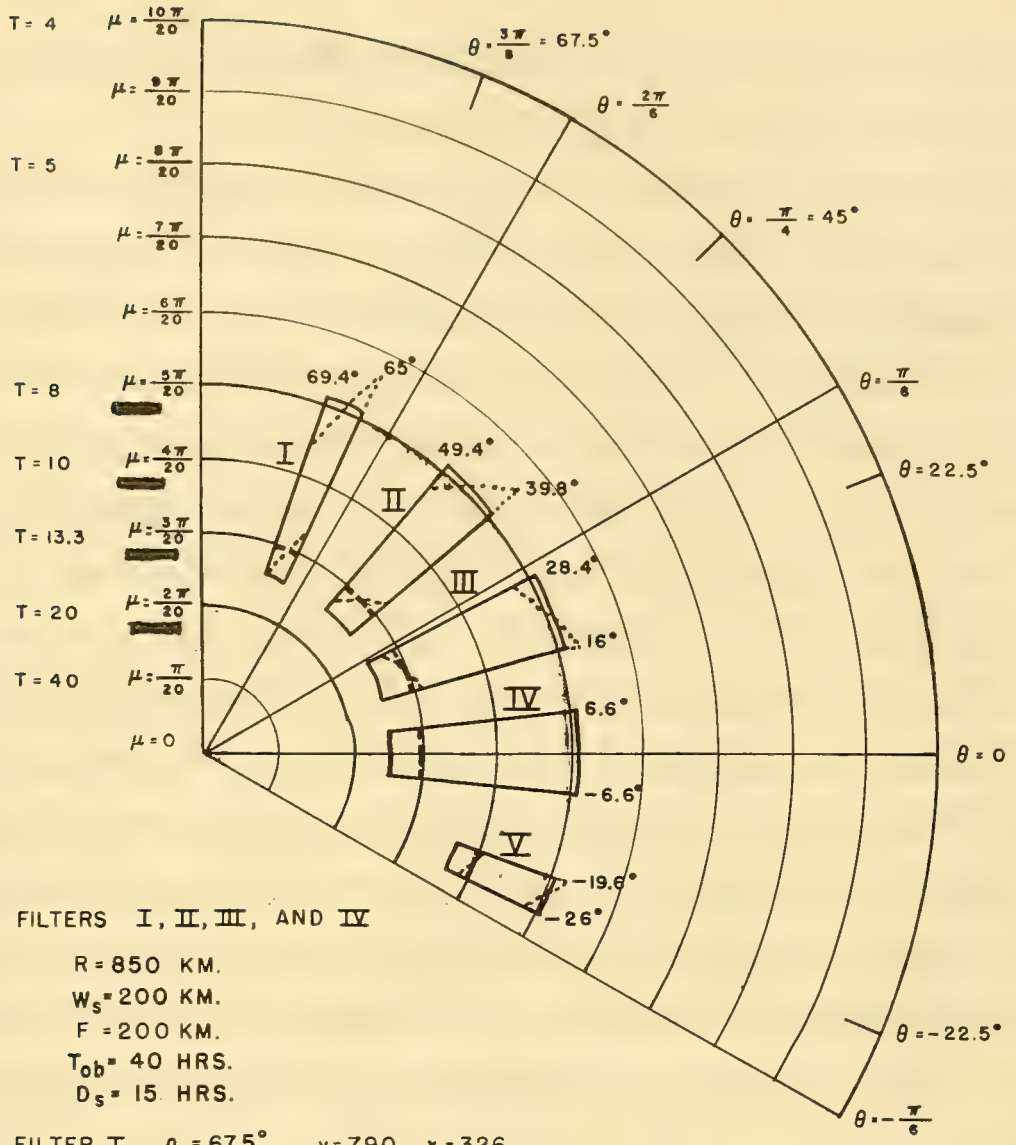

FILTERS I, II, III, AND IV

R = 850 KM.
W_S = 200 KM.
F = 200 KM.
T_{ob} = 40 HRS.
D_S = 15 HRS.

FILTER I $\theta_D = 67.5°$, y = 790, x = 326
FILTER II $\theta_D = 45°$, y = 600, x = 600
FILTER III $\theta_D = 22.5°$, y = 326, x = 790
FILTER IV $\theta_D = 0$, y = 0, x = 850

FILTER V

R = 1700 KM.
W_S = 200 KM.
F = 200 KM.
T_{ob} = 80 HRS.
D_S = 15 HRS.
$\theta_D = -22.5°$
x = 1580
y = −652

FIG. 26 SOME EXAMPLES OF THE SHARP CUT—OFF FILTERS FOR EQUATIONS (9.62), (9.63) AND (9.68).
(NOTE THE SMALL EFFECT OF THE 200 KM. FETCH EVEN FOR SUCH A SHORT DURATION STORM).

—— SOLID LINE FILTER FOR SFGWF (9.68)

– – – DASHED LINE FILTER FOR SFGW (9.63) (NO FETCH, $\theta \cong \theta_D$)

-----DOTTED LINE FILTER FOR SFGW (9.62) (NO FETCH)

filters and the lines are given by solid lines for all three filters. See the legend at the bottom of the figure.

The greater the departure of θ_D from zero the more the filter for equation (9.62) departs from the other filters. The approximations employed in obtaining the other filters is therefore most accurate for small θ_D. In addition the original Fresnel filter was more accurate for small values of θ_D. Consequently, these results should not be applied too strictly at large angles.

If the power spectrum given in figure 22 for equation (9.52) were to represent the disturbance at the source, then the application of the filters given in figure 26 would result in various quite different sea surfaces at the various points and times of forecast. There would be a very small disturbance at the point and time used to determine the particular filter labeled number I, because the power spectrum is identically zero for θ greater than 67.5° and very low for θ near 67.5°. In contrast for the power spectrum given by equation (9.50), the disturbance would be identically zero.

For filter number III, the power spectrum given in figure 22 would result in considerably higher waves at the point R = 850, and θ_D = 22.5° (corresponding to y = 326, x = 790 km) than at the point determined by filter number I. For equation (9.50) and the value of K given for equation (9.50) the waves determined by the filter at the above point would be considerably lower compared to those determined by figure 22 because only the components from 10 seconds to 7.75 seconds would be present (due to the original nature of the power spectrum).

A study of the effects of given filters upon the two power spectra under consideration thus shows that the forecasted values would be completely different in many cases for the same storm parameters and the same point and time of observation. For many forecasts based upon equation (9.50) there would simply be no waves present, whereas for the same forecasts based upon figure 22 (equation 9.52) an appreciable disturbance would be present. These two examples therefore make it evident that there is no hope for consistently accurate wave forecasts until $E_2(\mu,\theta)$ has been measured for wave systems at the edge of an actual storm at sea. Dealing with the significant waves at the edge of the storm without regard to the underlying power spectrum can never yield consistent results. At this time, the hope that $E_2(\mu,\theta)$ will in some way be a function which depends consistently upon the wind velocity, and the air mass in which the winds are blowing so that it can be predicted is expressed. Methods for measuring $E_2(\mu,\theta)$ will be given in the next chapter.

Decrease in wave height with travel

For the same power spectrum at the source (say figure 22), the effect of doubling R and t_{ob} is interesting to study. Filter V for $\theta_D = -22.5°$ for example could be reflected in the $\theta = 0$ axis. Then it would correspond to the filter for the same parameters given on the figure except θ_D would then equal + 22.5°. Thus doubling R (or x and y) and t_{ob}, results in a power spectrum at the new point of observation with the same value of μ_u, but $\Delta\mu$ and $\Delta\theta$ are approximately halved. Consequently the potential

energy averaged over y and t are the new point of observation is only one fourth of what it was at the closer point. The wave height which is (crudely) proportional to the square root of the average potential energy therefore decreases like 1/R.

In particular, for waves observed on the x axis, at large values of x, $\Delta\mu \cong gD_s/2x$ and $\Delta\theta \cong W_s/x$. The effect of the short crestedness of the sea surface at the source is then of the same order of magnitude as the effect of dispersion, and the average potential energy decreases like $1/x^2$. Consequently, the actual short crestedness of waves from a storm at sea cannot be neglected in an adequate wave forecasting theory.

At this point, reference is made to H.O. Publication No. 604, Techniques for Forecasting Wind Waves and Swell. This book contains the lates theory for forecasting significant waves as developed by Sverdrup and Munk. Consider, in particular, Plate VI of the above publication. It can also be found as figure 3 in Forecasting Ocean Waves by Munk and Arthur [1951]. It gives values of H_D/H_F as functions of T_F. For T_F in the plate, equal to 10 seconds, H_D/H_F is 0.8 at 200 nautical miles, 0.63 at 400 nautical miles, 0.43 at 800 nautical miles, and 0.26 at 1600 nautical miles. The numbers squared are given by 0.64 at 200 nautical miles, 0.40 at 400 nautical miles, 0.17 at 800 nautical miles and 0.07 at 1600 nautical miles. Roughly these values decrease by a little more than one half as the decay distance is doubled.

The theory discussed above in this paper says that at great distances the values should decrease by one fourth as the decay distance is doubled. The methods employed in the derivation of the theory on which the figure in H.O. Pub. No. 604 is based,

depend upon, among other things, the assumption that the decrease in wave height is caused by friction against the air. The width and the duration of the storm are not considered. Groen and Dorrestein [1950] attribute the decay of waves to eddy viscosity in the water, but again their theory does not account for wave dispersion and lateral spreading. The theory discussed in this paper predicts greater decreases in wave height simply due to dispersion and angular spreading from a storm of finite width and duration than are predicted by the Sverdrup-Munk theory without these considerations.

Storms <u>are</u> of finite width and duration. A storm which is wide compared to the decay distance but which lasts a relatively short time would cause waves at distant points which decrease in height like $1/\sqrt{R}$ simply due to dispersion. A storm which is narrow compared to the decay distance but which lasts a long time would cause waves which decrease in height like $1/\sqrt{R}$ simply due to angular spreading. Other small, short duration storms would behave differently. Storms which cover a large area and which last a long time would behave still differently. The curves in H.O. Pub. No. 604 are based on wave observations from many storms of many different widths, durations, and fetch lengths. Consequently, the curves average in many errors even if there is some slight loss due to friction.

From these considerations, and since the significant height and period have been shown to be inadequate in many other respects, it must be concluded that the decrease of wave height with distance traveled can best be explained by the methods derived herein and

that friction effects are negligible, or of second order in importance, in the problem of wave forecasting.

Transformation of sea into swell

The results of Chapter 8 and of this chapter also explain all of the known effects which accompany the transformation of sea into swell. Short crested waves are simply sums of waves with infinitely long crests such as equation (8.5). A short crested Gaussian sea surface is given by an integral of the form of equation (9.47). The greater the variation of $[A_2(\mu,\theta)]^2$ over μ and θ the more irregular, choppy, and short crested the sea surface will be at the source. The apparent crests will actually vary in direction depending upon what particular terms happen by chance to reinforce at a particular time and place. For example, if $[A_2(\mu,\theta)]^2$ were given by, say, figure 22, and if a partial sum such as equation (9.48) were formed over a net containing about fifty elemental net areas, the resulting equation for $\eta(x,y,t)$ would represent a very complex irregular short crested sea surface which would approximate (even for such a coarse net) many of the features of waves at the edge of a storm at sea.

Now consider the power spectrum given by applying filter V to figure 22. For any partial sum, all the elemental waves would be traveling in directions only a few degrees from -22.5° and all the elemental waves would have nearly the same spectral periods. The sea surface would therefore have to consist of large areas of waves of nearly uniform height with quite long crests all traveling in the same apparent direction. Arguments similar to

those in Chapter 7 show that a wave group would have to last a considerable length of time before the elemental vectors in the partial sum become sufficiently out of phase to cancel out the wave amplitude. Note the change in the direction of the apparent crests. The crests appear to be coming from a point source at these distances.

Period increase of swell

If figure 22 were actually to approximate the power spectrum at the source, the period increase of ocean swell can also be explained by this model. The "significant" period for the highest waves passing a point of observation would increase from a value of approximately seven seconds in the storm to a value of ten seconds at distant points of observation, but it would not increase indefinitely.

Complete reality of the final model

The decrease in wave height with travel, the transformation from an irregular choppy short crested "sea" to a regular "long crested" smooth "swell," the arrival of waves at points at an angle to the main direction of the winds in the storm, the period increase of the swell and the so-called forerunners of swell are all explained by this model. Note that the "swell" is still Gaussian. The author has yet to see a natural wave record even approximately equal to A sin $2\pi t/T$ over a time interval of 20 minutes.

Additional comments on the final forecast formula

The final forecast formula, given by equation (9.71) and the auxiliary formulas given by equations (9.24), (9.25), (9.46),

(9.47), (9.48), (9.65) through (9.70), and equations (7.55) and (7.56) (with R replacing x), is the most realistic forecast formula of all those that have been presented. The above formulas are the only ones out of over three hundred in this paper (so far) which are needed to carry out a wave forecast. Actually only two diagrams given by figures 24 and 25 are needed along with the concept of the Gaussian case of the Lebesgue Power Integral for short crested sea surface. All of the other attempts to represent the sea surface and to forecast ocean waves serve only to illustrate forcefully the inadequacy of the models employed. A system which depends on the gross characteristics of a storm at sea, namely its duration, width, and fetch, and on the properties of a very special integral has yielded results which explain all known properties of waves from a storm at sea by the use of the classical concepts of gravity wave theory.

In actual practice, the square cutoff filter will be only a first approximation to the actual wave systems because the winds which produce the waves require time to build up to full amplitude and die down from full amplitude, and because of smoothing effects due to the finite time required for observation and the finite area which must be observed. The waves build up with the wind, and they have different characteristics at the edges of the storm and at the rear of the storm than they do at the center of the forward edge. The actual filters will then be smoothed in some way with respect to the theoretical filters. Their actual nature awaits detailed analysis and study of the sea surface.

Moving storms and hurricanes

Storms with rapidly moving edges (from which the waves leave the storm) and hurricanes produce wave systems which are not covered by the above theoretical considerations. The theory can probably be applied to slowly moving storms without too great an error. Also various successive temporarily stationary positions of a moving storm might yield fairly good results upon application of the theory. Hurricanes just do not come under the scope of the theory for reasons mentioned in Chapter 2. The Gaussian Lebesgue Power Integral has a different form and a hurricane has no width because it is circular. Possibly in another paper and at another time, the problem will be treated for moving storms and for hurricanes. The above forecast model ought to work for a large number of practical cases.

Something left out

There is still a joker in the deck. The functional forms of $E_2(\mu,\theta)$ for storm waves at sea are still unknown. From the results of Deacon [1949], Donn [1949], Arthur [1949], and Barber and Ursell [1948], a particular $E_2(\mu,\theta)$ must vary considerably over a range of μ corresponding to a period range exceeding values of from below five seconds to above twenty seconds and over a range of θ from forth-five to sixty degrees above and below the dominant direction of the winds in the storm. In the next chapter, adequate methods for the analysis of ocean wave records, and adequate procedures for the determination of $E_2(\mu,\theta)$ will be given. Then

after a sufficient amount of correctly obtained data has been assembled and analyzed, and after the variations of $E_2(\mu, \theta)$ as a function of the properties of the storm have been obtained, it will then be possible to prepare correct wave forecasts.

Chapter 10. METHODS FOR THE DETERMINATION OF POWER SPECTRA

Introduction

In Chapter 7, the sea surface as a function of time alone, at a fixed point was first studied. In Chapter 9, some properties of a short crested sea surface were derived. It is still necessary to show that a short crested sea surface observed at a fixed point is a Gaussian case of the Lebesgue Power Integral as a function of time. When this is accomplished it will also be possible to show that the functions, $E(\mu)$, $E_2(\mu,\theta)$, $[A(\mu)]^2$ and $[A_2(\mu,\theta)]^2$ are interrelated.

The techniques of Tukey [1949] and Tukey and Hamming [1949] will then be applied in order to obtain the relationships between the non-normalized auto-correlation function and the power spectrum, and procedures for the estimation of the various power spectra will then be described.

Other properties of a short crested sea surface will then be obtained. Finally methods for computing $[A_2(\mu,\theta)]^2$ will be presented.

Where and when the methods apply

The methods to be presented in this chapter strictly speaking apply only when the sea surface is in a steady state. That is $[A(\mu)]^2$ or $[A_2(\mu,\theta)]^2$ when determined by these methods should have the same value about any point of the sea surface at any time. It has already been pointed out that under these conditions wave forecasts and methods of wave analysis would not be needed because the

waves everywhere would be the same. Waves at the forward edge of a storm can be thought of as being in a steady state along that forward edge if $[A_2(\mu,\theta)]^2$ and $[A(\mu)]^2$ do not change with time during the duration of the storm. Since the methods of analysis to be presented can be applied to time intervals which are short compared to the duration of the storm and to areas which are small compared to the dimensions of the storm, the methods are valid in the analysis of actual wave records at the edge of a storm or over a wave generation area.

The methods of analysis which will be presented are also valid in the area of wave decay. The filters described in Chapters 7 and 9 are slowly varying functions of time. If $[A(\mu)]^2$ is analyzed from a wave record thirty or forty minutes long, the wave system will be so slowly varying that the methods will be valid. If $[A_2(\mu,\theta)]^2$ is determined over an area of the sea surface thirty or forty miles on a side, and for thirty or forty minutes, the wave system will be so slowly varying that the methods will be valid.

An analogy to electronic practices might clarify the situation. An engineer designs a radio to operate on 60 cycle AC current. The design of the power supply is based mainly on the formula $E = E \sin 2\pi t/T$. For nearly all practical purposes, the fact that the radio is turned on or off can be ignored, and the fact that the voltage is actually given by an equation like equation (5.1) is not important.

Similarly, the amplification sections of a radio are treated as if they were amplifying constant musical notes. A small enough

section of speech, although in reality the frequencies are slowly varying (compared to the duration of one cycle), can be treated this way without any serious consequences.

Consequently, the results of this chapter will apply to almost any wave situation. If there is reason to believe that the waves are changing very, very rapidly, the results of the analysis should be questioned, but for slowly varying situations the results can be interpreted in the light of the theoretical considerations given in the previous chapters.

For these reasons, $[A(\mu)]^2$ and $[A_2(\mu,\theta)]^2$ will represent power spectra for any sea surface either at the edge of a storm or in the area of decay. No special notation will be used to designate special conditions.

Non-Gaussian short crested sea surfaces

Consider, for example, the short crested sea surface given by equation (8.1). For this representation of the sea surface, it is possible to pick some fixed point on the sea surface, say x_1 and y_1, and observe the wave system at that point as a function of time. Evidently, there will be places at which very small (or zero) amplitudes will be observed, and at other places the amplitudes will be quite large.

In equation (10.1), the potential energy averaged over time at the point (x_1,y_1) is computed. The result shows that the value obtained is still a function of y_1. At some points, $\overline{\text{P.E.}}^t$ is $\rho g A^2/4$; at others, $\overline{\text{P.E.}}^t$ is zero. The potential energy averaged over y and t is $\rho g A^2/8$. (See also equation (8.5).)

At first, the point just made above does not appear to be

The Properties of a Short Crested Sea Surface as Observed as a Function of Time at a Fixed Point in Space.

$$\overline{P.E.}^{t} = \lim_{\bar{T}\to\infty} \frac{\rho g}{2\bar{T}} \int_{t^*}^{t^*+\bar{T}} \left[A\cos\frac{4\pi^2}{gT^2}\alpha y_1 \cdot \cos\left(\frac{4\pi^2}{gT^2}\sqrt{1-\alpha^2}\, x_1 - \frac{2\pi t}{T}\right)\right]^2 dt = \frac{\rho g}{4} A^2 \left[\cos\frac{4\pi^2}{gT^2}\alpha y_1\right]^2 \tag{10.1}$$

In general for the non-Gaussian case $\overline{P.E.}$ is a function of point of observation (10.2)

For the Gaussian case $P.E. = \frac{\rho g}{4} E_{2\,max}$ at all points. (10.3)

$$\text{Proof } \eta(x_1,y_1,t) = \int_0^{\infty}\int_{-\pi/2}^{\pi/2} \cos\left(\frac{\mu^2}{g}(x_1\cos\theta + y_1\sin\theta) - \mu t + \psi(\mu,\theta)\right)\sqrt{d^2E_2(\mu,\theta)} \tag{10.4}$$

consider a smaller subdivision of some $\Delta\mu$ in equation (7.14) such that

$$0 < \mu_K = \mu_{2k} < \mu_{2k+1} < \mu_{2k+2} < \cdots < \mu_{2k+2j} < \mu_{2k+2j+1} < \cdots < \mu_{2k+2N} = \mu_{K+2} < \infty \tag{10.5}$$

where $\mu_{2k+2N} - \mu_{2k} = \Delta\mu_{K+2} - \mu_K$ (10.6)

and consider a full net over θ_{oj} for each value of $\mu_{2K+2j+2}$

$$-\frac{\pi}{2} = \theta_{oj} < \theta_{1j} < \theta_{2j} \cdots < \theta_{2p+1,j} < \cdots < \theta_{2R,j} = \frac{\pi}{2} \tag{10.7}$$

where θ is the first value of θ for the net subdivions between $\mu_{2k+2j+2}$ and μ_{2k+2j} (10.8)

$$\eta_{\Delta\mu}(x_1,y_1,t) = \lim_{\substack{N\to\infty \\ R\to\infty}} \sum_{j=0}^{N}\sum_{p=0}^{R-1} \cos\left[\frac{(\mu_{2k+2j+1})^2}{g}(x_1\cos\theta_{2p+1,j} + y_1\sin\theta_{2p+1,j}) - \mu_{2k+2j+1}t + \psi(\mu_{2k+2j+1},\theta_{2p+1,j})\right]$$

$$\cdot\sqrt{E_2(\mu_{2k+2j+2},\theta_{2p+2,j}) - E_2(\mu_{2k+2j+2},\theta_{2p,j}) - E_2(\mu_{2k+2j},\theta_{2p+2,j}) + E_2(\mu_{2k+2j},\theta_{2p,j})} \tag{10.9}$$

very important. But wave records at present are observed at a fixed point as a function of time. If this very simple example of a short crested sea surface yields such widely varying records and such widely varying values of the average potential energy, what assurance is there that actual wave records as a function of time represent the sea surface in the neighborhood of the point of observation, and that the average of the squared wave record is actually related to the potential energy of the sea surface?

For the non-Gaussian case, that is for sea surfaces of the form of equation (8.5), the potential energy averaged over time varies from place to place. Stated another way, it is a function of the point of observation as shown by equation (10.2).

Gaussian short crested sea surfaces

For the Gaussian case of a short crested sea surface, it can be proved that the potential energy averaged over time at any point on the sea surface is given by equation (10.3). This property of the Gaussian case is very important because it shows that the current wave records as obtained as a function of time do contain important information worthy of more detailed and refined methods of analysis.

The proof of the statement made by equation (10.3) is somewhat lengthy, and some other important results are also obtained. Consider first the integral definition of the short crested sea surface as given by equation (10.4) in which x_1 and y_1 are given subscripts to point out that the sea surface is being observed as a function of time at a fixed point. In Chapter 9, the inte-

gral was defined by a net over the μ ,θ plane as the mesh of the net was shrunk to zero. Consider the two values of μ given by μ_K and μ_{K+2} in the net defined by equation (9.14), and break up this small increment, $\Delta\mu$, into N much smaller increments as shown by equation (10.5). The relations between the various μ 's involved are given by equation (10.6). Also consider a full net over θ from $-\pi/2$ to $\pi/2$, for each of the smaller nets given in equation (10.5). The values of θ at the net points will also need to depend on the particular net interval, μ_{2k+2j} to $\mu_{2k+2j+2}$, and they are therefore designated by subscripts like θ_{1j} as shown by equation (10.8).

One property that these Lebesgue Power Integrals have (and which has not been proved in this paper) is that they are the same as the ordinary Riemann integral in that it is possible to break up the area of integration into small touching but non-overlapping pieces and the total integral is the sum of the integrals over the smaller pieces. Consequently, the contribution to the total disturbance created by the power in the semicircular strip from μ_K to μ_{K+2} and from $-\pi/2$ to $\pi/2$ is given by the limit of the partial sum given by equation (10.9).* $\eta\Delta\mu(x_1,y_1,t)$ is thus the contribution of this strip to the total integral as observed at the fixed point x_1,y_1. The proof of equation (10.3) consists essentially of picking an appropriate sub-net in this semicurcular strip to obtain the desired properties.

In equation (10.10), it is pointed out that for any

---

*Note that the R here has nothing to do with the R of Chapter 9. It is just an integer.

$\mu_{2k+2j+1}$ and $\theta_{2p+1,j}$ with x_1 and y_1 fixed it is always possible to subtract and integral number of 2π's from the sum in order to find a new $\psi'(j,p_j)$, (short notation for $\psi'(\mu_{2k+2j+1},\theta_{2p+1,j})$) such that $\psi'(j,p_j)$ has the same probability distribution as the original ψ .

In equation (10.11), for a fixed j, the net over θ for this small subdivision of the original strip has been picked so that each of the terms under the square root sign in the evaluation of the integral has the same numerical value, given by the increment in $E(\mu,\pi/2)$ from μ_{2k+2j} to $\mu_{2k+2j+2}$ divided by R, the total number of elemental areas in the small strip. This can obviously always be done. Each term in the sum over p is thus given by $\Delta E_j/R$.

Equations (10.10) and (10.11) are next substituted into equation (10.9) in order to obtain the first expression in equation (10.12). The cosine term is then expanded by trigonometric identity in the second expression, and the summation over p is moved inside. An expression of the form $A\cos\theta + B\sin\theta$ can be written in the form $[A^2 + B^2]^{1/2}\cos(\theta - \psi)$ and this has been done in the last expression in equation (10.12). The complete expression for $\psi'(j)$ is given by equation (10.13).

The next step is to simplify the coefficient of the cosine term in equation (10.13). In equation (10.14) this is done by writing the cosine and sine in complex notation. When the first expression on the right in equation (10.14) is expanded, only the cross product terms remain and the second expression results. The sum from p equals zero to R - 1 of $\exp(i\,\psi'(j,p_j))$ is a sum

The Properties of a Short Crested Sea Surface as Observed as a Function of Time at a Fixed Point in Space

$$0 < \frac{(\mu_{2K+2j+1})^2}{g}\left(x_1\cos\theta_{2p+1,j}+y_1\sin\theta_{2p+1,j}\right)+\psi(\mu_{2K+2j+1},\theta_{2p+1,j})-2\pi M=\psi'(j,p_j)\leq 2\pi \tag{10.10}$$

let $E_2(\mu_{2K+2j+2},\theta_{2,j})-E_2(\mu_{2K+2j+2},\theta_{0,j})-E_2(\mu_{2K+2j},\theta_{2,j})+E_2(\mu_{2K+2j},\theta_{0,j})$

$= E_2(\mu_{2K+2j+2},\theta_{4,j})-E_2(\mu_{2K+2j+2},\theta_{2,j})-E_2(\mu_{2K+2j},\theta_{4,j})+E_2(\mu_{2K+2j},\theta_{2,j})$

$$=\cdots=\frac{E_2(\mu_{2K+2j+2},\frac{\pi}{2})-E_2(\mu_{2K+2j},\frac{\pi}{2})}{R}=\frac{\Delta E_j}{R} \tag{10.11}$$

$$\eta_{\Delta\mu}(x_1,y_1,t)=\lim_{\substack{N\to\infty\\R\to\infty}}\sum_{j=0}^{N}\sum_{p=0}^{K-1}\cos(-\mu_{2K+2j+1}t+\psi'(j,p_j)\sqrt{\frac{\Delta E_j}{R}}$$

$$=\lim_{\substack{N\to\infty\\R\to\infty}}\sum_{j=0}^{N}\left[\sum_{P=0}^{R-1}\cos\psi'(j,p_j)\sqrt{\frac{\Delta E_j}{R}}\cos(\mu_{2K+2j+1}t)+\sum_{P=0}^{R-1}\sin\psi'(j,p_j)\sqrt{\frac{\Delta E_j}{R}}\sin(\mu_{2K+2j+1}t)\right]$$

$$=\lim_{\substack{N\to\infty\\R\to\infty}}\sum_{j=0}^{N}\left[\left(\sum_{P=0}^{R-1}\sqrt{\frac{\Delta E_j}{R}}\cos\psi'(j,p_j)\right)^2+\left(\sum_{P=0}^{R-1}\sqrt{\frac{\Delta E_j}{R}}\sin\psi(j,p_j)\right)^2\right]^{1/2}\cdot\cos\left[\mu_{2K+2j+1}t-\psi'(j)\right] \tag{10.12}$$

$$\psi'(j)=\sin^{-1}\frac{\sum_{p=0}^{R-1}\sqrt{\frac{\Delta E_j}{R}}\sin\psi'(j,p_j)}{\left[\left(\sum_{p=0}^{R-1}\sqrt{\frac{\Delta E_j}{R}}\cos\psi'(j,p_j)\right)^2+\left(\sum_{p=0}^{R-1}\sqrt{\frac{\Delta E_j}{R}}\sin\psi'(j,p_j)\right)^2\right]^{1/2}} \tag{10.13}$$

Plate XLVI

of R vectors of unit length all pointing in randomly picked directions. Let the sum be the complex vector given by $B_{jR}\exp(i\theta_j)$. The other sum is a sum of R vectors and every vector in this sum points in exactly the opposite direction to the corresponding term in the first sum. The sum is therefore of the form $B_{jR}\exp(-i\theta_j)$ and it points in exactly the opposite direction. The complex product is therefore always a real positive number $(B_{jR})^2$, as given by the last expression in equation (10.14).

From equation (10.13), the sine of $\psi(j)$ can be written in the various forms given in equation (10.15). The results of equation (10.14) permit the use of terms like $B_{jR}\exp(i\theta_{jR})$, and in this case the B_{jR} cancel out. The sum therefore represents the sine of some angle, θ_{jR}. But from the nature of the sums discussed in the paragraph above, the value of θ_{jR} for a large value of R is equally probably any value from zero to 2π. Equation (10.16) is therefore the result, and the probability distribution of $\psi'(j)$ is the same as that required originally in equation (7.28).

These results are next substituted into equation (10.17). Since the values of the B_{jR} are not one, one begins to suspect that things are getting complicated. Also the results are beginning to look something like the results which were obtained in Chapter 7.

So far in the proof only one small strip between μ_{2k+2j} and $\mu_{2k+2j+2}$ has been treated. There are N of these strips between μ_K and μ_{K+2}. The values of ΔE_j can, by picking the points μ_{2k+2j}, all be made equal to $[E_2(\mu_{K+2},\pi/2) - E_2(\mu_K,\pi/2)]/N$ as shown in equation (10.18).

$$\lim_{R\to\infty}\left[\left(\sum_{p=0}^{R-1}\sqrt{\frac{\Delta Ej}{R}}\cos\psi'(j,p_j)\right)^2+\left(\sum_{p=0}^{R-1}\sqrt{\frac{\Delta Ej}{R}}\sin\psi'(j,p_j)\right)^2\right]=\lim_{R\to\infty}\frac{\Delta Ej}{R}\left(\left(\sum_{p=0}^{R-1}\frac{e^{i\psi'(j,p_j)}}{2}+\sum_{p=0}^{R-1}\frac{e^{-i\psi'(j,p_j)}}{2}\right)^2+\left(\sum_{p=0}^{R-1}\frac{e^{i\psi'(j,p_j)}}{2i}-\sum_{p=0}^{R-1}\frac{e^{-i\psi'(j,p_j)}}{2i}\right)^2\right)$$

$$=\lim_{R\to\infty}\frac{\Delta Ej}{R}\sum_{p=0}^{R-1}e^{i\psi'(j,p_j)}\sum_{p=0}^{R-1}e^{-i\psi'(j,p_j)}$$

$$=\lim_{R\to\infty}\frac{\Delta Ej}{R}B_{jR}e^{i\theta_{jR}}\;B_{jR}e^{-i\theta_{jR}}=\lim_{R\to\infty}\frac{\Delta Ej}{R}B_{jR}^2 \qquad (10.14)$$

$$\sin\psi'(j)=\frac{e^{i\psi'(j)}}{2i}-\frac{e^{-i\psi'(j)}}{2i}$$

$$=\lim_{R\to\infty}\frac{\sum_{p=0}^{R-1}\sin\psi'(j,Pj)}{\left[\sum_{p=0}^{R-1}e^{i\psi'(j,p_j)}\sum_{p=0}^{R-1}e^{-i\psi'(j,p_j)}\right]^{\frac{1}{2}}}=\lim_{R\to\infty}\frac{1}{2i}\left(\frac{\sum_{p=0}^{R-1}e^{i\psi'(j,p_j)}}{\sum_{p=0}^{R-1}e^{-i\psi'(j,p_j)}}\right)^{\frac{1}{2}}-\frac{1}{2i}\left(\frac{\sum_{p=0}^{R-1}e^{-i\psi(j,p_j)}}{\sum_{p=0}^{R-1}e^{i\psi(j,p_j)}}\right)^{\frac{1}{2}}$$

$$=\lim_{R\to\infty}\frac{1}{2i}\left(\frac{B_{jR}e^{i\theta_{jR}}}{B_{jR}e^{-i\theta_{jR}}}\right)^{\frac{1}{2}}-\frac{1}{2i}\left(\frac{B_{jR}e^{-i\theta_{jR}}}{B_{jR}e^{i\theta_{jR}}}\right)^{\frac{1}{2}}=\lim_{R\to\infty}\frac{1}{2i}e^{i\theta_{jR}}-\frac{1}{2i}e^{-i\theta_{jR}}=\lim_{R\to\infty}\sin\theta_{jR} \qquad (10.15)$$

but for R large all directions are equally probable and therefore

$$p(0<\psi'(j)<\alpha 2\pi)=\alpha \qquad (10.16)$$

where $0<\alpha<1$

This increment in power is designated by $\Delta E(K+2,K)/N$.

The next step is to compute the power contributed by $\eta_{\Delta\mu}(x_1,y_1,t)$ with the use of equation (10.17). The phases drop out and since the μ's are different, by the arguments given in other parts of this paper, the first two expressions on the bottom line of equation (10.19) can be obtained.

It is now necessary to investigate the limiting process more carefully. N and R must both approach infinity together. That is, each term in approaching the limit is found by picking fixed N and R and forming the net which has the property that each elemental area in the net contributes the same power (namely $\Delta E(K+2,K)/NR$). For the next N and R picked larger to approach the limit a completely different net will have to be found.

Now as N and R become large, B_{jR} becomes larger and larger but if it is divided by $\sqrt{R}$, the number $B_{jR}/\sqrt{R}$ has a probability distribution given by considering it to be a sample from a normal (Gaussian) population with a zero mean and a unit standard deviation. This is stated by equation (10.20). Proof can be found in the statistical references cited elsewhere. Thus the sum over N of the $(B_{jR})^2/NR$ becomes more and more like the sum of N terms each of which is the square of a number taken from a normal population with zero mean and unit standard deviation. This sum of N terms is precisely the second moment of a sample of N values from the population, and by Tchebycheff's theorem and the law of large numbers, this sample second moment can be made to differ from one by as little as desired by picking N large enough. Therefore the limit as N and R approach infinity

$$\eta_{\Delta\mu}(x,y,t) = \lim_{\substack{N\to\infty \\ R\to\infty}} \sum_{j=0}^{N} \left[\frac{\Delta E_j}{R} B_{jR}^2\right]^{\frac{1}{2}} \cdot \cos(\mu_{2k+2j+1} t - \psi'(j)) \tag{10.17}$$

can also pick $\Delta E_1 = \Delta E_2 = \Delta E_3 = \cdots = \dfrac{E_2(\mu_{K+2}, \pi/2) - E_2(\mu_K, \pi/2)}{N} = \dfrac{\Delta E(K+2,K)}{N}$ (10.18)

$$\lim_{\bar{T}\to\infty} \int_{t^*}^{t^*+\bar{T}} (\eta_{\Delta\mu}(x,y,t))^2 dt = \lim_{\bar{T}\to\infty} \int_{t^*}^{t^*+\bar{T}} \lim_{\substack{N\to\infty \\ R\to\infty}} \left[\sum_{j=0}^{N} \left(\frac{\Delta E(K+2,K)}{NR} (B_{jR})^2\right)^{\frac{1}{2}} \cdot \cos(\mu_{2k+2j+1} t - \psi'(j))\right]^2 dt$$

$$= \lim_{\substack{N\to\infty \\ R\to\infty}} \sum_{j=0}^{N} \frac{\Delta E(K+2,K)}{2NR} (B_{jR})^2 = \frac{\Delta E(K+2,K)}{2} \lim_{\substack{N\to\infty \\ R\to\infty}} \sum_{j=0}^{N} \frac{(B_{jR})^2}{NR} = \frac{\Delta E(K+2,K)}{2} \tag{10.19}$$

since $P(-\infty < B_{jR}/\sqrt{R} < D) = \dfrac{1}{\sqrt{\pi}} \int_{-\infty}^{D} e^{-\xi^2/2} d\xi$ for large R (10.20)

which implies that $\lim \sum_{j=0}^{N} \dfrac{(B_{jR})^2}{NR} = 1$ (The $B_{jR}/\sqrt{R}$ are samples from a normal population with a zero mean and a unit standard deviation) (The average of the sum of squares of a random sample from a normal population with a zero mean and unit standard deviation is one as the size of the sample tends toward infinity.)

Therefore if $\eta(x_i,y_i,t)$ is evaluated by any finite net, the same results are obtained as in the evaluation

$$\eta(0,0,t) = \int_0^{\infty} \cos(\mu t + \psi(\mu)) \sqrt{dE_2(\mu, \pi/2)} \tag{10.22}$$

Also for all finite nets (consequently for all practical purposes), $E_2(\mu,\theta)$ and $E(\mu)$ can be thought of as simple continuous functions, with piecewise continuous derivatives, and

$$E_2(\mu, \tfrac{\pi}{2}) = E(\mu) \tag{10.23}$$

$$\frac{\partial E(\mu)}{\partial \mu} = [A(\mu)]^2 = \int_{-\frac{\pi}{2}}^{\frac{\pi}{2}} \frac{\partial^2 E_2(\mu,\theta)}{\partial\mu\partial\theta} d\theta = \int_{-\frac{\pi}{2}}^{\frac{\pi}{2}} [A_2(\mu,\theta)]^2 d\theta = \frac{\partial E_2(\mu, \pi/2)}{\partial \mu} \tag{10.24}$$

of the expression given in equation (10.21) is one, and it is possible to write $\Delta E(K + 2,K)/2$ as the last expression in equation (10.19).

The power in $\eta_{\Delta\mu}(x_1,y_1,t)$ over the strip bounded by μ_K, μ_{K+2}, $-\pi/2$, and $\pi/2$ is therefore given by

$$[E_2(\mu_{K+2},\pi/2) - E_2(\mu_K,\pi/2)]/2$$

at the point x_1,y_1 when the sea surface is observed as a function of time at that point. (Note $E_2(\mu_{K+2},-\pi/2)$ and $E_2(\mu_K,-\pi/2)$ are zero by definition.)

For θ fixed at $\pi/2$, $E_2(\mu,\pi/2)$ is consequently connected with $E(\mu)$ as defined in Chapter 7. The Lebesgue Power Integral given by equation (10.22), evaluated as a function of time by any finite net (no matter how small), is by virtue of equation (10.19) indistinguishable from the result of evaluating the Lebesgue Power Integral given by equation (9.1) at a fixed point as a function of time.

In addition, for all practical purposes, equation (10.23) and equation (10.24) determine the relationships between $E_2(\mu,\theta)$, $E(\mu)$, $[A(\mu)]^2$, and $[A_2(\mu,\theta)]^2$.

Equations (10.23) and (10.24) are not strictly true. The functional relationships given do not hold <u>exactly</u> point for point. The relationships are true, however, in the sense that given that $E_2(\mu,\theta)$ is a continuous function with piecewise continuous first partial derivatives, then $E(\mu)$, and $[A(\mu)]^2$ are point set functions with definite properties in a probability sense.

To show this, consider the function $E(\mu)$,* as yet not defined, and the function $E(\mu)$ defined by (10.23). Also consider the

function $[A(\mu)]^2*$, as yet not defined, and the function $[A(\mu)]^2$ defined by equation (10.24). $E(\mu)$ is assumed to have a piecewise continuous partial derivative with respect to μ. Form a net over the μ axis. Also find $[A(\mu)]^2$. For each net interval, μ_{2n+2} to μ_{2n}, take the value of $[A(\mu_{2n+1})]^2$. Pick a number from a Gaussian distribution with a zero mean and unit standard deviation and multiply $[A(\mu_{2n+1})]^2$ by its square. Assign the result to the entire net interval, μ_{2n+2}, μ_{2n}. The resulting new function is piecewise continuous, and as, say, a function of $\mu*$ it can be integrated from 0 to μ to find a new cumulative power distribution. The new cumulative power distribution will be continuous, since the integral of a piecewise continuous function is continuous.

Now consider the class of all possible functions which would result from this operation as the mesh of the net approaches zero. There are an infinite number. Define the function, $[A(\mu)]^2*$, mentioned above, to be one of the functions; and define the function $E(\mu)*$ to be the integral of $[A(\mu)]^2*$.

How does $[A(\mu)]^2*$ differ from $[A(\mu)]^2$? First of all it is continuous no where. Each point value of $[A(\mu)]^2*$ can differ from the value at any nearby point by any amount. The function, $[A(\mu)]^2*$, cannot be graphed, but it can be visualized as a cloud of points scattered above, below, and on the graph of $[A(\mu)]^2$ such that no point is above any other point and there is a point for every point of $[A(\mu)]^2$. In addition, if a new net is taken over $[A(\mu)]^2*$, the Lebesgue integral from μ_{2n} to μ_{2n+2} of this function has the same value as the integral from μ_{2n} to μ_{2n+2} of $[A(\mu)]^2$. This statement can be proved by methods similar to

those used in equations (10.1) to (10.22).

How does $E(\mu)^*$ differ from $E(\mu)$? $E(\mu)^*$ is continuous, and it has the same value as $E(\mu)$ at each point. But it has a derivative at no point, because the slopes at two neighboring points can be completely different.

The above considerations are admittedly very crude explanations of what are, in reality, very complex properties of some of the more abstract functions treated in the theory of functions of a real variable. A study of the derivation given above from equations (10.1) to (10.22) shows that actually functions like $E(\mu)^*$ and $[A(\mu)]^{2*}$ are approached instead of functions like $E(\mu)$ and $[A(\mu)]^2$.

However, and this is the important point, it is impossible to tell the difference between the starred and unstarred functions by any numerical or physical (electronic and/or mechanical) method of analysis of the original wave record. In any numerical method, a finite net must be taken, and the abstract differences between the functions cannot be detected. In an electronic or mechanical method of analysis, at some time in the analysis the record is sent through a tuned circuit of finite band width and again the abstract differences between the functions cannot be detected. For a further consideration along these lines, the papers of Tukey [1949] and Tukey and Hamming [1949] can be consulted.

In conclusion, then, it is possible to think of the power spectrum and the cumulative power distribution as nice, smooth, elementary functions, to work with them as such, and differentiate, integrate, and transform them as such. With these considerations in mind, equations (10.22), (10.23) and (10.24) can be used with

complete freedom in subsequent theoretical and practical work.

Numerical methods for the determination of $[A(\mu)]^2$ from a sample from a stationary time series

Ocean wave records are obtained on both coasts of the United States and in England. A few are or have been analyzed by Deacon [1949], Barber and Ursell [1948], and Klebba [1946,1949] with the aid of mechanical-electrical wave analyzers. Others are being or have been analyzed by Seiwell [1949, 1950, 1950] and Seiwell and Wadsworth [1949] and Rudnick [1949] by autocorrelation methods. Two have been analyzed by Tukey and Hamming [1949].* All the rest of the wave records have suffered the inglorious fate of being analyzed for "significant" height and period. Given the "significant" height and period, it is usually impossible even to estimate the average potential energy (in part, because the records are pressure records). In fact, from the two numbers which result, it is impossible to tell if the waves are all from one source, and in general it is frequently difficult to tell whether the record was of a "sea" or of a "swell."

The numerical methods of analysis of stationary time series or "temporarily homogeneous" time series (Tukey) as derived and presented by Tukey [1949] and Tukey and Hamming [1949] are the basis for a correct analysis of wave records because they are the only methods in which the errors of the analysis can be precisely defined by statistical methods. Any analysis of a short section of

*These results will be discussed in greater detail in a later chapter. It suffices to say now that the error in Seiwell's interpretation was that he failed to consider the whole autocorrelation function of the records he studied. They actually die down to zero if carried out far enough with a long enough record. The wave analyzer records of the records he studied are more realistic than his interpretation.

a stationary time series always introduces errors of a statistical nature. The techniques given by Tukey [1949] tell us how big the error is and how to make it smaller if desired.

In addition, Tukey and Hamming [1949] discuss design criteria of physical wave analyzers. The numerical methods can be used to calibrate the wave analyzers, to tell how much in error the physical analysis is, and to determine possible improvements in the design of the instruments. More will be discussed on these points later.

Statement of problem

A wave record is a short section of a very nearly temporarily homogeneous longer record. It can to a first approximation be treated as a stationary process. Such a wave record could be, say, seven minutes long (the usual Beach Erosion Board practice), twenty minutes long (Barber and Ursell [1948]) or an hour long. Consider such a record. Read off the values of the record at, say, one second intervals of the record and tabulate the values in terms of their departure from the mean of the record at the time of observation. The result is a sample from a stationary time series, and there are N points representing N values as given in equation (10.25). The problem of numerical wave record analysis is to find an estimate of the function $[A(\mu)]^2$ from these N numbers, and to tell how reliable this estimate is.

Preliminary investigation: the non-normalized autocorrelation function

The problem is to find $[A(\mu)]^2$. It will be found first by abstract methods, and then by practical numerical methods. The

procedure is to find first the non-normalized autocorrelation function and then to determine $[A(\mu)]^2$ from it.

The non-normalized autocorrelation function is given by Q(p), where p is a continuous variable, in equation (10.26). In the first expression on the right in the top line of equation (10.26) Q(p) is defined in terms of $\eta(t)$, the free surface as a function of time, as observed at a fixed point. The variable, p, has the dimensions of time, and $\eta(t + p)$ is simply the value of η which is found p seconds after the time, t. In the second expression, the Lebesgue Stieltjes representation for $\eta(t)$ is substituted for $\eta(t)$. On the next line, the integral is represented by the limit of a partial sum. The results are equally valid for the non-Gaussian cases discussed in Chapter 7.

For q not equal to n, the product term which results can be written as the sum of two trigonometric terms which when averaged over time average to zero, and consequently the expression simplifies to the third expression. Upon rearrangement, the fourth expression is obtained in which the square of the cosine term has a net positive mean, and the cosine sine term averages to zero. The fifth expression extracts the constant part of the cosine squared term; all other terms are sines and cosines, and in the limit, average to zero. Integration over time yields the bottom expression on the left, and, in the limit, the last two integral forms are the result. These integrals are ordinary Stieltjes integrals without the square root sign as in the power integrals. If $[A(\mu)]^2$ is a piecewise continuous function, the last integral is an ordinary Riemann integral (i.e. the kind one can often look up in tables of integrals to evaluate).

Numerical Methods for the Determination of $[A(\mu)]^2$ from a Sample of a Stationary Time Series

Given; $\eta(t)$ at $\eta(t_1), \eta(t_2), \eta(t_3), \eta(t_4) \cdots\cdots \eta(t_n)$ (10.25)

Problem; Find an estimate of $[A(\mu)]^2$ from above data, and find how reliable this estimate is

Preliminary Investigation; The Non-normalized Auto-correlation Function

$$Q(P) = \lim_{\bar{T}\to\infty} \frac{2}{\bar{T}} \int_{t^*}^{t^*+\bar{T}} \eta(t)\eta(t+p)\,dt = \lim_{\bar{T}\to\infty} \frac{2}{\bar{T}} \int_{t^*}^{t^*+\bar{T}} \left[\int_0^\infty \cos(\mu t+\psi(\mu))\sqrt{dE(\mu)}\right]\left[\int_0^\infty \cos(\mu(t+p)+\psi(\mu))\sqrt{dE(\mu)}\right] dt$$

$$= \lim_{\bar{T}\to\infty} \frac{2}{\bar{T}} \int_{t^*}^{t^*+\bar{T}} \left(\lim_{\substack{\Delta_2\mu\to 0 \\ \mu_{2R}\to\infty}} \sum_{N=0}^{R} \cos(\mu_{2n+1}t+\psi(\mu_{2n+1}))\sqrt{E(\mu_{2n+2})-E(\mu_{2n})}\right)\left(\lim_{\substack{\Delta_{2\mu}\to 0 \\ \mu_{2R}\to\infty}} \sum_{q=0}^{R} \cos(\mu_{2q+1}(t+p)+\psi(\mu_{2q+1}))\sqrt{E(\mu_{2q+2})-E(\mu_{2q})}\right) dt$$

$$= \lim_{\bar{T}\to\infty} \frac{2}{\bar{T}} \int_{t^*}^{t^*+\bar{T}} \lim_{\substack{\Delta_2\mu\to 0 \\ \mu_{2R}\to\infty}} \sum_{n=0}^{R} \cos(\mu_{2n+1}t+\psi(\mu_{2n+1}))\cdot\cos(\mu_{2n+1}(t+P)+\psi(\mu_{2n+1}))(E(\mu_{2n+1})-E(\mu_{2n}))\,dt$$

$$= \lim_{\bar{T}\to\infty} \frac{2}{\bar{T}} \int_{t^*}^{t^*+\bar{T}} \lim_{\substack{\Delta_2\mu\to 0 \\ \mu_{2R}\to\infty}} \sum_{n=0}^{R} \left[\cos^2(\mu_{2n+1}t+\psi(\mu_{2n+1}))\cos\mu_{2n+1}P - (\cos(\mu_{2n+1}t+\psi(\mu_{2n+1}))\sin(\mu_{2n+1}t+\psi(\mu_{2n+1}))\sin\mu_{2n+1}P\right]$$
$$\cdot(E(\mu_{2n+2})-E(\mu_{2n}))\,dt$$

$$= \lim_{\bar{T}\to\infty} \frac{2}{\bar{T}} \int_{t^*}^{t^*+\bar{T}} \lim_{\substack{\Delta_2\mu\to 0 \\ \mu_{2R}\to\infty}} \sum_{n=0}^{R} \cos\mu_{2n+1}P\,\frac{1}{2}(E(\mu_{2n+2})-E(\mu_{2n}))\,dt + \text{periodic terms which average to zero.}$$

$$= \lim_{\substack{\Delta_2\mu\to 0 \\ \mu_{2R}\to\infty}} \sum_{n=0}^{R} \left[E(\mu_{2n+2})-E(\mu_{2n})\right]\cos(\mu_{2n+1}P) = \int_0^\infty \cos\mu p\,dE(\mu) = \int_0^\infty \cos\mu p\left[A(\mu)\right]^2 d\mu \qquad (10.26)$$

At this point a very important theorem due to Wiener [1930] is used. The theorem states that the power spectrum of the stationary process is given by the Fourier cosine transformation of the autocorrelation function. The theorem is much more general than needed here, and its proof will be given here only for the specific cases under study.

The proof of equation (10.27) follows in equation (10.28). The infinite integral is replaced by the limit as M approaches infinity of the integral from 0 to M in the first expression on the right. The integral form for Q(p) given in equation (10.26) is also substituted for Q(p). The steps thereafter are straightforward, and upon the application of the lemma given in Chapter 8, the result is obtained immediately. The second term in the next to the last expression is zero because the range of integration does not cover α equal to zero.

Tukey's formulas

The problem of numerical analysis was stated in equation (10.25), but then it was necessary to carry out some preliminary theoretical derivations before continuation of the description of the numerical methods. Equation (10.29) states that it is more convenient to take the points of the record at equally spaced intervals of time, designated by Δt. The three basic formulas for the numerical estimation of the power spectrum as presented by Tukey [1949] and Tukey and Hamming [1949] are given by equations (10.30), (10.31) and (10.32).

Equation (10.30) is the finite difference analogue of equation (10.26). It describes a procedure for finding an estimate of the

Numerical Methods for the Determination of $[A(\mu)]^2$ from a Sample of a Stationary Time Series

To prove $[A(\mu^*)]^2 = \frac{2}{\pi}\int_0^\infty Q(p)\cos\mu^* p \; dp$ (10.27)

$$[A(\mu^*)]^2 = \lim_{M\to\infty}\frac{2}{\pi}\int_0^M\int_0^\infty \cos\mu p\,[A(\mu)]^2 d\mu\,\cos\mu^* p\,dp = \lim_{M\to\infty}\frac{2}{\pi}\int_0^\infty [A(\mu)]^2\int_0^M \cos\mu p\,\cos\mu^* p\,dp\,d\mu$$

$$= \lim_{M\to\infty}\frac{2}{\pi}\int_0^\infty [A(\mu)]^2\int_0^M \left[\tfrac{1}{2}\cos(\mu-\mu^*)p + \tfrac{1}{2}(\mu+\mu^*)p\right]dp\,d\mu = \lim_{M\to\infty}\frac{2}{\pi}\int_0^\infty [A(\mu)]^2\left[\frac{\frac{1}{2}\sin(\mu-\mu^*)p}{(\mu-\mu^*)} + \frac{\frac{1}{2}\sin(\mu+\mu^*)p}{(\mu+\mu^*)}\right]_0^M d\mu$$

$$= \lim_{M\to\infty}\frac{1}{\pi}\int_0^\infty [A(\mu)]^2\left[\frac{\sin(\mu-\mu^*)M}{(\mu-\mu^*)} + \frac{\sin(\mu+\mu^*)M}{(\mu+\mu^*)}\right]d\mu = \lim_{M\to\infty}\frac{1}{\pi}\int_{-\mu^*}^\infty [A(\alpha+\mu^*)]^2\frac{\sin\alpha M}{\alpha}d\alpha + \lim_{M\to\infty}\frac{1}{\pi}\int_{\mu^*}^\infty [A(\alpha-\mu^*)]^2\frac{\sin\alpha M}{\alpha}d\alpha = [A(\mu^*)]^2 \quad (10.28)$$

Tukey's Formulas for Numerical Estimation: Let $t_2-t_1 = t_3-t_2 = \ldots\ldots t_{N+1}-t_N = \Delta t$ (10.29)

$Q_p = \frac{2}{N-p}\sum_{n=1}^{N-p}\eta(t_n)\eta(t_{n-p})$ $(p=0,1,\ldots\ldots m)$ (10.30) $L_h = \frac{1}{m}\left(Q_0 + 2\sum_{p=1}^{m-1} Q_p\cos\frac{\pi p h}{m} + Q_m\cos\pi h\right)$ $(h=0,1,\ldots\ldots m)$ (10.31)

$E(\mu_{h+\frac{1}{2}}) - E(\mu_{h-\frac{1}{2}}) = U_h = .23L_{h-1} + .54L_h + .23L_{h+1}$ $(h=0,1,\ldots\ldots m)$ (10.32)

$\mu_h = \frac{\pi h}{\Delta t m}$ (10.33) μ band from $\frac{\pi(h-\frac{1}{2})}{\Delta t m}$ to $\frac{\pi(h+\frac{1}{2})}{\Delta t m}$ (10.34)

$[A(\mu_h)]^2 = \frac{1}{\pi}[E(\mu_{h+\frac{1}{2}}) - E(\mu_{h-\frac{1}{2}})]\Delta t m = \frac{U_h \Delta t m}{\pi}$ (10.35) $T_h = \frac{2\Delta t m}{h}$ (10.36) $L_{-1} = L_1$ and $L_{m+1} = L_{m-1}$ (10.37)

Plate L

non-normalized autocorrelation function. There are a total of m lags shown, and m numbers are the result, as designated by Q_o, Q_1, $Q_2 \cdots\cdots Q_{m-1}$, and Q_m.

Equation (10.31) is the finite difference analogue of equation (10.27) except that it yields increments in $E(\mu)$ instead of $[A(\mu)]^2$. It yields the "raw" or uncorrected values of quantities related to $[A(\mu)]^2$, (Tukey [1949]).

Equation (10.32) finally yields the difference values between $E(\mu_{h+1/2})$ and $E(\mu_{h-1/2})$. It is a correction of the "raw" data which is necessitated by the inherent inaccuracies introduced in the procedure by taking only N points and by the finite difference procedures. It essentially smooths the values of L_h by giving the correct factors which determine the interrelation between adjacent values.

After the various multiplications and summations indicated by equations (10.30) through (10.32) have been carried out the result is m numbers which represent the increments in $E(\mu)$ from μ equal to $\pi(h - 1/2)/\Delta tm$ to μ equal to $\pi(h + 1/2)/\Delta tm$ as given by equation (10.34). The center of each band is at μ_h equal to $\pi h/\Delta tm$ as given by equation (10.33). Note that the dimensions of the various quantities are correct. The most representative value of $[A(\mu)]^2$ for the point, μ_h, is then given by equation (10.35). The period, T_h, which corresponds to the spectral frequency μ_h is given by equation (10.36).

For μ equal to zero and μ equal to $\pi/\Delta t$, the statements given above must be modified because of the edge effect. For h equal to zero in equation (10.32), μ_h should be given by $E(\mu_{1/2}) - E(0)$ and the band is only one half of those in the

center. Similarly for h equal to m, μ_h should be given by $E(\mu_h) - E(\mu_{h-1/2})$. In addition the formulas given in equation (10.37), must be employed in equation (10.32) in order to determine the appropriate values for h equal to zero or m. The formulas follow from more detailed considerations based upon the fact that Q(p) is an even function; i.e., in equation (10.29) summation over p equals zero, minus one, etc., to minus m, will result in the same numerical values for Q(-p) as for Q(p).

Planning the analysis and the work involved

The point is rapidly being approached where it will be necessary to use a computing machine, an I.B.M. machine, or an autocorrelator such as the one at Woods Hole in order to carry out the numerical work indicated in equations (10.29), (10.30), and (10.31). The word "work" is chosen advisedly because it will be work to do a sufficient number of wave records in order to calibrate the various mechanical electrical wave analyzers now in use.

This work can be planned. It is possible to decide beforehand how reliable the values need to be and how to get these values as economically as possible. An example will be given later which will show how easily much effort can be wasted.

The choice of Δt and the determination of the amount of aliasing

From equations (10.25) and (10.29), the data to be analyzed are presented as point values of the original time series at equal time intervals. The problem of the choice of Δt is very important. If Δt is picked too small, too many computations have to be made, and the final results often lead to the result that the power spectrum is negligible above a certain value of μ. If Δt is

picked too large, the power per division on the μ axis as shown in equation (10.34) can have other values of power from other parts of the μ axis aliased into (or added into) the true values for the particular band desired.

Consider the sketch at the top of Plate LI. If only the four values labeled 1, 2, 3, and 4 are given, it is not possible to tell the difference between the dashed sine curve and the solid sine curve. In fact, since the numerical method of analysis assigns all of the power present to spectral values between zero and $2\pi/2\,\Delta t$, if the solid curve represents a spectral value greater than $2\pi/2\,\Delta t$, it will be aliased by the method of analysis into a spectral value associated with the dashed curve on the plate. These features are explained in greater detail by the values shown in (10.38). The spectral frequency given by $2\pi h/2\,\Delta tm$ for h equal to zero, one, two....through m has aliases given by $(2\pi/2\,\Delta t) + (2\pi h/2\,\Delta tm)$, $(4\pi/2\,\Delta t) \pm (2\pi h/2\,\Delta tm)$, $(6\pi/2\,\Delta t) \pm (2\pi h/2\,\Delta tm)$ and so forth. From the little table it is seen that the value of the aliased cosine terms is the same at the points $t = 0$, Δt, $2\,\Delta t$.....as the value of the true component at these points. The sketch below shows this effect in another way. The power associated with the first little black strip shows up in that range of the spectrum upon analysis, but if there is any power associated with the other little black strips, it will show up in the range where the true values occur.

The important point is to pick Δt small enough so that there is no appreciable power in the power spectrum for spectral frequencies above $2\pi/2\,\Delta t$. Stated another way, components with

Aliasing

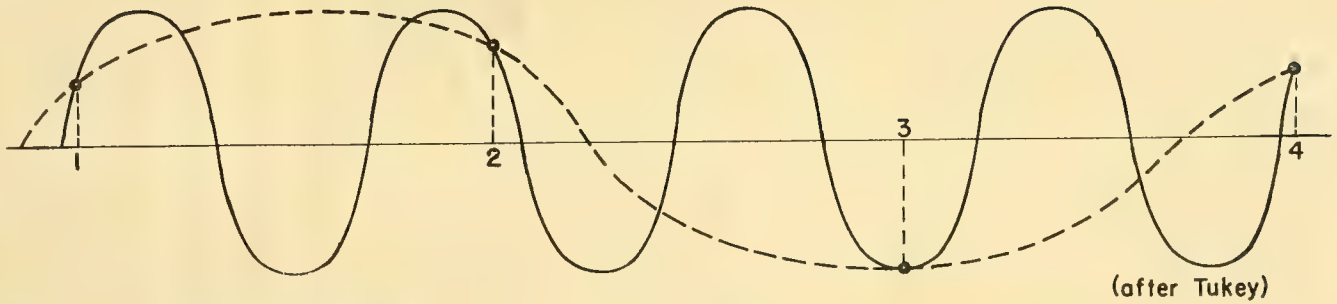

Point	True Component	Aliased Components
	$\cos\frac{2\pi h}{2\Delta t m}t$	$\cos(\frac{2\pi}{2\Delta t}+\frac{2\pi h}{2\Delta t m})$, $\cos(\frac{4\pi}{2\Delta t}\pm\frac{2\pi h}{2\Delta t m})t$, $\cos(\frac{6\pi}{2\Delta t}\pm\frac{2\pi h}{2\Delta t m})t$
$t=0$	$\cos 0 = 1$	$\cos 0 = 1$, $\cos 0 = 1$, $\cos 0 = 1$
$t=\Delta t$	$\cos\frac{\pi h}{m}$	$\cos(\pi+\frac{\pi h}{m})=-\cos\frac{\pi h}{m}$, $\cos(2\pi\pm\frac{\pi h}{m})=\cos\frac{\pi h}{m}$, $\cos(3\pi\pm\frac{\pi h}{m})=\cos-\frac{\pi h}{m}$
$t=2\Delta t$	$\cos\frac{2\pi h}{m}$	$\cos(\pi+\frac{2\pi h}{m})=-\cos\frac{2\pi h}{m}$, $\cos(4\pi\pm\frac{2\pi h}{m})=\cos\frac{2\pi h}{m}$, $\cos(3\pi\pm\frac{2\pi h}{m})=-\cos\frac{2\pi h}{m}$
(etc)		(10.38)

Degrees of freedom per elemental Band of Derived Power Spectrum if Spectrum is very slowly varying

$$f = \frac{N - \frac{m}{4}}{\frac{m}{2}} \qquad (10.39)$$

Plate L1

periods shorter than $2\Delta t$ should be negligible in the record. Wave records obtained by pressure recorders are an excellent illustration of this point. If, for example, the depth of the water is 22.5 feet, then waves with wave lengths less than 45 feet have very little effect upon the pressure at the bottom. Consequently components with periods less than three seconds will have very little effect on the pressure at the bottom and will not show up in either the record or the power spectrum. In this example, then, a Δt of 1.5 seconds would be sufficiently small to be sure that there was no aliasing in the analysis of the pressure record. This point will be discussed in greater detail later.

Resolution and the choice of m

For a fixed value of Δt, the larger the value of m, the more points are determined for the power spectrum, and the greater the ability of the analysis to determine the finer details of the power spectrum. For example, if it was suspected that a wave record contained a sharp peak near a certain frequency, say $2\pi/5$, then the sharp peak could be determined more accurately by taking a larger value of m. For Δt equal to 1 and for m equal to 10, then frequencies from $2\pi 3/20$ to $2\pi 5/20$ are present in the band containing $2\pi/5$. For Δt equal to 1, and for m equal to 50, then frequencies from $2\pi 19/100$ to $2\pi 21/100$ would be present in the band containing $2\pi/5$.* If the power were actually concentrated

*Periods from 6.67 to 4 seconds in the first case, and periods from 5.26 to 4.76 seconds in the second case.

near $2\pi/5$, the second value of m would show this more clearly.

Accuracy of the final values obtained

The power integrals under study in this paper are extremely complicated functions. Their analysis is consequently also extremely complicated. The numerical methods presented by Tukey [1949] and Tukey and Hamming [1949] are the only methods of analysis which permit as a final result a correct estimate of how accurate the calculated power spectrum is.*

Associated with the final m numbers obtained in the analysis is a value, f, which is called the number of degrees of freedom of the value of U_h. The value of f can be computed from equation (10.39). The larger the value of f, the more reliable the power estimates of the spectrum. Equation (10.39) shows that the larger the value of N the larger the value of f and that the larger the value of m, the smaller the value of f. Thus greater resolution, which requires a large m, sacrifices accuracy of analysis unless a very large N is chosen.

The number of degrees of freedom of the sample, f, can be used to determine the reliability of the power spectrum estimates. Tukey and Hamming [1949] have shown that the values of U_h given by equation (10.32) are distributed according to a χ^2 distribution with f degrees of freedom. Table 16 gives the important numbers connected with this distribution. The first values are expressed in decibels for the convenience of electronic engineers

*This statement is made with the knowledge that many incorrect and inadequate methods for determining hidden periodicities and their significance are to be found in current geophysical studies. A prime example of how to do things wrong is found in the current claims of Langmuir [1950].

Table 16. Reliability of power spectrum estimates

f	Points of χ^2/f in db					Departure from true value					Possible error in observed value				
	$2\frac{1}{2}\%$	5%	50%	95%	$97\frac{1}{2}\%$	$2\frac{1}{2}\%$	5%	50%	95%	$97\frac{1}{2}\%$	$2\frac{1}{2}\%$	5%	50%	95%	$97\frac{1}{2}\%$
1	-30	-24	-3.4	5.8	7.0	.001	.004	.46	3.8	5	1000	250	3.1	.26	.2
2	-16	-13	-1.6	4.8	6.7	.025	.05	.69	3.0	4.7	40	20	1.5	.33	.21
3	-11.5	-9.3	-1.1	4.2	5.0	.971	.12	.78	2.7	3.2	14	8.5	1.3	.36	.32
4	-9.2	-7.5	-0.8	3.8	4.4	.12	.18	.83	2.4	2.8	8.3	5.63	1.2	.42	.36
5	-7.8	-6.4	-0.6	3.4	4.1	.17	.23	.87	2.2	2.6	6.0	4.37	1.15	.46	.39
6	-6.8	-5.6	-0.5	3.2	3.8	.21	.27	.89	2.1	2.4	4.8	3.6	1.12	.48	.42
8	-5.8	-4.6	-0.4	2.9	3.4	.26	.35	.91	2.0	2.2	3.8	2.8	1.10	.51	.46
10	-4.9	-4.1	-0.3	2.6	3.1	.32	.39	.93	1.8	2.0	3.1	2.6	1.07	.55	.49
15	-3.8	-3.2	-0.2	2.2	2.6	.42	.48	.95	1.66	1.82	2.4	2.1	1.05	.60	.55
20	-3.2	-2.6	-0.1	2.0	2.3	.48	.55	.98	1.60	1.70	2.1	1.8	1.02	.63	.59
50	-1.9	-1.6	-0.1	1.3	1.6	.65	.69	.98	1.35	1.45	1.55	1.45	1.02	.74	.69
100	-1.3	-1.1	-0.0	1.0	1.1	.74	.78	1.00	1.25	1.29	1.35	1.29	1.00	.79	.78
Large	$\frac{-12}{\sqrt{f}}$	$\frac{-10}{\sqrt{f}}$	~0	$\frac{+10}{\sqrt{f}}$	$\frac{+12}{\sqrt{f}}$		$10^{-1/\sqrt{f}}$	1	$10^{1/\sqrt{f}}$			$10^{1/\sqrt{f}}$	1	$10^{-1/\sqrt{f}}$	

After Tukey

who think in such terms. The second set of values entitled "Departure from True Values" is simply ten to the power one tenth of the numbers in the first set of tables. The third set of values is the reciprocal of the second set of values.

Estimate of sampling error

Suppose that some fixed power spectrum is chosen. From the power spectrum suppose that a section of the function, $\eta(t)$, is constructed. And then suppose that a U_h from (10.32) is found as an estimate of the power in some band by the use of equations (10.29), (10.30), (10.31) and (10.32). The true value is known from the chosen form of the fixed power spectrum, and the estimate is known by the procedures given by Tukey and Hamming [1949]. How far off can the estimate be? The answer to the question can be given in a probability sense. The estimate is a sample from a population of possible samples. That is, many different samples could have been taken from many different $\eta(t)$ constructed from the same fixed power spectrum.

For a particular example, suppose that there are ten degrees of freedom (i.e. f = 10). Then there is one chance in forty that the estimate will be less than 32% of the true value. There is one chance in twenty that the estimate will be less than 39% of the true value. There are nine chances in ten that the estimate will lie between 39% and 180% of the true value. There is one chance in twenty that the estimate will exceed the true value by 180%. Finally there is one chance in forty that the estimate will exceed 200% of the true value. The estimate (from the center column) will be too low more often than it is too high. There

is one chance in two that the estimate will be lower than 93% of the true value.

The same example can be expressed in another way. Suppose that from the same fixed power spectrum a large number of different sections of η (t) are given, and suppose that the power in a given band is estimated for each of these sections. Then from this large number of estimates, the ratio of the number less than 32% of the true value to the total number will approach the fraction 1/40 as the total number of estimates is increased. Similar statements for each of the other values can be made.

Thus for ten degrees of freedom, it is not possible to be very sure of the accuracy of one single estimate of the power in a given band. The value will be wrong by more than a factor of two one time out of ten.

The error of a particular estimate

Usually the true value of the power in the band under analysis is not known, and usually only one sample of η(t) is available. Thus only one estimate of the power in the band is available and no additional analysis of the data can be carried out. The last table permits an interpretation of the accuracy of this one number. Thus, if U_h from equation (10.32) is, say, ten thousand cm^2, then the true value of the power in the band will lie between twenty-six thousand cm^2 and five thousand five hundred cm^2 nine times out of ten for ten degrees of freedom.

As the number of degrees of freedom is increased the range of values such that the true value will be included 90% of the time becomes smaller. For one hundred degrees of freedom, and

for U_h equal to ten thousand cm^2, the true value will lie between thirteen thousand cm^2 and eight thousand cm^2 ninety percent of the time.

The reliability of a seven minute wave record

Seven minute long samples of a function related to $\eta(t)$, namely P(t), are taken every four hours at Long Branch, New Jersey by a pressure recorder in approximately thirty feet of water.* Spectral components with periods less than 3.5 seconds will not show up in the records. A Δt of 1.7 seconds is therefore the value which will exclude aliases and eliminate dangers from that feature of the analysis. There are 420 seconds in a seven minute wave record and therefore N is 246. If m is chosen to be twenty, then one band would cover periods from 7.14 to 4.56 seconds. The value of f would be 24, and approximately 90% of the time the true value of the power in the band would lie between 1.8 times and .63 times the estimated value. The same possible error could occur for the estimate of each of the bands, and the total power in the record can also be incorrect.

These results are not too surprising. Consider again the records shown in figure 12. The records are over one hour long. One tenth of the record is about seven minutes long. It is evident from the records that strips seven minutes long can be found which would yield much smaller values for the simple estimate of the number, E_{max}, than would be obtained from the estimate over the entire record. Similarly, much higher values could also be found. It is therefore necessary to conclude that the data which can be

---

* See the next two chapters.

obtained from a seven minute record are not very reliable.

Wave analysis

The wave analyzer constructed by Klebba [1946, 1949] and the one used by Deacon [1949] find some function related to $[A(\mu)]^2$, possibly its square root. Tukey and Hamming [1949] give some design criteria for such devices. One extremely important point is that they can be just as much in error as the numerical method estimates for low values of f, and if the tuned circuit in the device is too sharply peaked they can be even more in error. The modifications which could improve the design of Klebba's instrument will be described in a later chapter. They are not too difficult to make. Even as it is now constructed it is a very valuable instrument, and it can be made even more valuable by these modifications.

Very slowly varying

Equation (10.39) gives the number of degrees of freedom per elemental band of the derived power spectrum if the spectrum is very slowly varying over that band. If the spectrum varies rapidly, then the true number of degrees of freedom is less. For additional details see Tukey and Hamming [1949]. The considerations given above serve as design criteria and the real errors may be somewhat worse than are indicated by the table.

The work involved

Tukey and Hamming [1949] have estimated that $(m + 1)(N + \frac{m}{2} + 2)$ additions, $(m + 1)(N + \frac{m}{2} + 4) + 2$ multiplications, and $m + 3$ divisions have to be made to carry out one numerical analysis without checks for accuracy. Simplifications of procedure are given in the above reference. With a desk calculator, and with N equal

to 600 and m equal to 60 (assuming all the necessary trigonometric terms are available in a matrix), it should take about one eight hour day with a skilled operator. For punch cards on an IBM machine, about four hours are needed. High speed calculators require two and a half minutes, plus the time required to code the machine. It might be well worth while to set up a high speed calculator for the permanent part of the process and process a great many observations in one single day.

The determination of $[A_2(\mu,\theta)]^2$

The function, $[A_2(\mu,\theta)]^2$, is very difficult to evaluate. It is a function of two variables, and, over a complex sea surface, especially at the edge of a storm, the short crested waves imply a wide variation of the function. The needed measurements can be made and it is theoretically possible to determine the structure of the function.

There are two instruments discussed in the literature which, along with an ordinary pressure (or spar) type wave recorder, make it possible to measure the appropriate functions. One instrument is the airborne wave recorder described by Deacon, Darbyshire, and Smith [1949]. It measures elevation of the sea surface along some chosen line over the sea surface at practically an instant of time. It will be assumed in this derivation that the speed of the aircraft is so great compared to the variation with time of the sea surface that the values obtained are essentially instantaneous. Minor (in principle) modifications of the procedures which will follow could eliminate this assumption. The second instrument would have to be an extension of the stereoptican methods to high

to high altitude, wide base line, aerial photographs. The sea surface as a function of x and y at an instant of time would then be the observed quantity.

The functions which are observed by these instruments will be described in the course of the development of the method for the determination of $[A_2(\mu,\theta)]^2$. Of course, $[A_2(\mu,\theta)]^2$ can only be estimated for some finite net in the same way that $[A(\mu)]^2$ was determined by the methods given by Tukey.

Preliminary investigation

Consider the airborne altimeter. It yields a graph of the height of the sea surface along the path taken by the aircraft. Suppose that the aircraft were flying at a speed of 200 mph in a dense fog over a perfectly sinusoidal wave system (which does not exist in nature). What would the record look like? The disturbance is given by equation (10.40) where θ_1 and μ_1 are fixed. Of course the pilot does not know the orientation of the x axis, and he does not know the direction of orientation of the wave crests. Rotate the coordinate system with respect to the sea surface so that x' is the direction along which the aircraft is flying on a straight course. The equations for the rotation are given by equations (10.41) and (10.42). The sea surface in the new coordinate system is given by equation (10.43). Since the aircraft is flying so fast, as a first approximation consider t to be fixed at an instant of time and since the aircraft is flying in the x' direction, y' is fixed. The recorder, if calibrated in distance traveled by the aircraft, will then record an observed wavelength, L_o, given in equation (10.44) and (10.45). If the aircraft is

The Determination of $\left[A_2(\mu,\theta)\right]^2$

Preliminary Investigation

$$\eta(t) = A\cos\left(\frac{\mu_1^2}{g}(x\cos\theta_1 + y\sin\theta_1) - \mu_1 t\right) \tag{10.40}$$

Let $x = x'\cos\theta^* - y'\sin\theta^*$ (10.41)

$y = x'\sin\theta^* + y'\cos\theta^*$ (10.42)

$$\eta(t) = A\cos\left[\frac{\mu_1^2}{g}\left(x'\cos(\theta_1-\theta^*) + y'\sin(\theta_1-\theta^*)\right) - \mu_1 t\right] \tag{10.43}$$

fix y' and t, and let $\mu = \frac{2\pi}{T_1}$

$$\frac{2\pi x'}{L_o} = \frac{4\pi^2}{g T_1^2}\cos(\theta_1-\theta^*)\,x' \tag{10.44}$$

$$L_o = \frac{g T_1^2}{2\pi(\cos(\theta_1-\theta^*))} \tag{10.45}$$

$$\frac{g T_1^2}{2\pi} \leq L_o \leq \infty \tag{10.46}$$

The Gaussian Case

$$\eta(x,y,t) = \int_0^{\infty}\int_{-\frac{\pi}{2}}^{\frac{\pi}{2}} \cos\left[\frac{\mu^2}{g}(x\cos\theta + y\sin\theta) - \mu t + \psi(\mu,\theta)\right]\sqrt{\left[A_2(\mu,\theta)\right]^2}\,d\mu\,d\theta$$

$$= \int_0^{\infty}\int_{-\frac{\pi}{2}}^{\frac{\pi}{2}} \cos\left[\frac{\mu^2}{g}\left[x'\cos(\theta-\theta^*) + y'\sin(\theta-\theta^*)\right] - \mu t + \psi(\mu,\theta)\right]\sqrt{\left[A_2(\mu,\theta)\right]^2}\,d\mu\,d\theta \tag{10.47}$$

Let $\nu_o = \frac{\mu^2}{g}\cos(\theta-\theta^*)$ (10.48) and $\theta_o = \theta - \theta^*$ (10.49)

then $\mu^2 = \frac{g\nu_o}{\cos\theta_o}$ (10.50) and $\theta = \theta_o + \theta^*$ (10.51)

$$\frac{\delta(\mu,\theta)}{\delta\nu_o\,\delta\theta_o} = \begin{vmatrix} \frac{\delta\mu}{\delta\nu_o} & \frac{\delta\mu_o}{\delta\theta_o} \\ \frac{\delta\theta}{\delta\nu_o} & \frac{\delta\theta}{\delta\theta_o} \end{vmatrix} = \begin{vmatrix} \frac{1}{2}\left(\frac{g}{\cos\theta_o\nu_o}\right)^{\frac{1}{2}} & \frac{1}{2}\left(\frac{g\nu_o}{\cos\theta_o}\right)^{\frac{1}{2}}\tan\theta_o \\ 0 & 1 \end{vmatrix} = \frac{1}{2}\left(\frac{g}{\cos\theta_o\nu_o}\right)^{\frac{1}{2}} \tag{10.52}$$

$$\eta(x',y',t) = \int_0^{\infty}\int_{-\frac{\pi}{2}-\theta^*}^{\frac{\pi}{2}-\theta^*} \cos\left(\nu_o x' + \nu_o\tan\theta_o\,y' - \left(\frac{g\nu_o}{\cos\theta_o}\right)^{\frac{1}{2}}t + \psi(\nu_o\theta_o)\right)\sqrt{\left[A_2\left(\left(\frac{g\nu_o}{\cos\theta_o}\right)^{\frac{1}{2}},\ \theta_o+\theta^*\right)\right]\cdot\frac{1}{2}\left(\frac{g}{\cos\theta_o\nu_o}\right)^{\frac{1}{2}}}\,d\nu_o\,d\theta_o \tag{10.53}$$

flying in the true direction of travel of the crests (i.e. $\theta_1 = \theta^*$), the true wave length of the waves will be observed. If not, some wave length greater than the true value will be observed as shown by equation (10.46). It is not possible to record a wave length shorter than the true value. Conversely, the wave number given by $\nu_o = 2\pi/L_o$ will vary between zero and its true value, and it will not be greater than its true value.

The problem is quite simple in this case if the pilot wishes to discover the true wave length of the waves below the aircraft in the fog. Many passes are made over the sea surface at various headings until a heading is found such that the length of the recorded waves increases when either the aircraft is turned to the right or left. This minimum length is then the true wave length. By then flying very very slowly, or sending out a helicopter, the direction of wave travel could be determined by the Doppler effect.

For the other simple cases discussed previously, similar techniques could be used and the resolution of five or six sinusoidal waves of different periods and directions would not be too difficult a feat by ordinary techniques. However, the true sea surface is best represented by a Lebesgue-Stieltjes power integral over $[A_2(\mu,\theta)]^2$, and, as such, it is composed of an infinite number of infinitesimal sine waves traveling in all directions from (it is hoped) $-\pi/2$ to $\pi/2$ with respect to the dominant direction of the crests and with all possible spectral frequencies over a considerable range of the μ axis. For these reasons, the determination of $[A_2(\mu,\theta)]^2$ is a complicated problem.

The determination of $[A_2(\mu,\theta)]^2$, observed quantities

Consider the short crested Gaussian sea surface given by equation (9.47) and apply equations (10.41) and (10.42) so that the sea surface can be studied as a function of x'. The result is equation (10.47). For convenience θ equals zero should be picked to be the dominant direction of travel of the apparent crests, and the direction θ equals zero is therefore along the x axis. The angle, θ^*, then measures the angle between the x axis and the line of flight. The observed spectral wave number, ν_o, then depends upon the spectral frequency and the cosine of the difference between θ and θ^*. Angular directions above and below θ^* are determined by an angle, θ_o.

The procedure is now to transform the μ ,θ polar coordinate system and the integration over $[A_2(\mu,\theta)]^2$ to a ν_o,θ_o polar coordinate system and an integration over a new function $[A_2(\nu_o,\theta_o,\theta^*)]^2$. The variables, ν_o and θ_o, are defined in terms of μ and θ by equations (10.48) and (10.49). The inverse transformation which defines μ and θ in terms of ν_o and θ_o is given by equations (10.50) and (10.51). The Jacobian of the transformation is given by equation (10.52). Substitution of $(g\,\nu_o/\cos\theta_o)^{1/2}$ for μ and $\theta_o + \theta^*$ for θ in equation (10.47), and the use of the Jacobian to preserve the mapping then yields equation (10.53). The Jacobian is needed because the function $[A_2(\mu,\theta)]^2$ has been distorted by the mapping, and in order to preserve the total power in the wave system it must be amplified for low values of ν_o and $\cos\theta_o$ and decreased for high values of ν_o. Stated another way, an increment, $\Delta\mu$, maps into a much smaller $\Delta\nu_o$ if it is at the

low end of the μ scale than it does at the high end of the μ scale. From the properties of the Jacobian, it then follows that equation (10.54) holds and E_{max} is given by both an integration over the μ ,θ plane and the ν_o,θ_o plane (see Courant [1937]). The integration over the θ_o coordinate then can be defined to yield the function $[A(\nu_o,\theta_o*)]^2$ as given by equation (10.55). The angle, $\theta*$, is, of course, fixed for each single flight.

It is now possible to describe the functions which can be recorded by current instrumental techniques. First, the free surface as a function of time at a fixed point in space can be recorded. The function which results is a Gaussian Lebesgue Power integral of the form of equation (10.56) (or (7.1)) as has been proved at the start of this chapter for the case of a short crested sea surface. Secondly, for a fixed $\theta*$ the sea surface as a function of x' can be recorded. In equation (10.53), if y' and t' are fixed, then by exactly the same techniques that were employed to study the short crested sea surface as a function of time it is possible to prove that the free surface as a function of x' for a fixed y' and t is given by equation (10.57).

Both functions are samples of stationary series and both can be analyzed by the methods presented above in order to determine $[A(\mu)]^2$ and $[A(\nu_o,\theta*)]^2$ for a finite net. In addition many different values of $\theta*$ can be chosen and a whole set of functions of the form of $[A(\nu_o,\theta*)]^2$ for different $\theta*$ can be found. Thus the observed power spectra are given by equation (10.58). From these data, the problem is to find an estimate of $[A_2(\mu,\theta)]^2$.

THE DETERMINATION OF $\left[A_2(\mu,\theta)\right]^2$

$$E_{max} = \int_0^\infty \int_{-\frac{\pi}{2}}^{\frac{\pi}{2}} \left[A_2(\mu,\theta)\right]^2 d\theta\, d\mu = \int_0^\infty \int_{-\frac{\pi}{2}-\theta^*}^{\frac{\pi}{2}-\theta^*} \left[A_2\left(\left(\frac{g\,\nu_o}{\cos\theta_o}\right)^{\frac{1}{2}}, (\theta_o+\theta^*)\right)\right]^2 \frac{1}{2}\left(\frac{g}{\cos\theta_o \nu_o}\right)^{\frac{1}{2}} d\theta_o\, d\nu_o \tag{10.54}$$

$$\int_{-\frac{\pi}{2}-\theta^*}^{\frac{\pi}{2}-\theta^*} \left[A_2\left(\left(\frac{g\,\nu_o}{\cos\theta_o}\right)^{\frac{1}{2}}, \theta_o+\theta^*\right)\right]^2 \frac{1}{2}\left[\frac{g}{\cos\theta_o \nu_o}\right]^{\frac{1}{2}} d\theta_o = \int_{-\frac{\pi}{2}}^{\frac{\pi}{2}} \left[A_2\left(\frac{g\,\nu_o}{\cos(\theta_o-\theta^*)}\right)^{\frac{1}{2}} \theta\right)\right] \frac{1}{2}\left(\frac{g}{\cos(\theta-\theta^*)\nu_o}\right)^{\frac{1}{2}} d\theta = \left[A(\nu_o,\theta^*)\right]^2 \tag{10.55}$$

Statement of Problem.

The observed functions are

$$\eta(x_1,y_1,t) = \int_o^\infty \cos\left[\mu t + \psi(\mu)\right] \sqrt{\left[A(\mu)\right]^2 d\mu} \tag{10.56}$$

$$\eta(x',y',t_1) = \int_o^\infty \cos\left[\nu_o x' + \psi(\nu_o)\right] \sqrt{\left[A(\nu_o,\theta^*)\right]^2 d\nu_o} \tag{10.57}$$

The observed power spectra are

$$\left[A(\mu)\right]^2 \quad \text{and} \quad \left[A(\nu_o,\theta^*)\right]^2 \tag{10.58}$$

Problem; Find $\left[A(\mu,\theta)\right]^2$ (10.59)

Solution; Let $\mu_c = \frac{2\pi}{2\Delta t}$ (10.60) and $\nu_c = \frac{4\pi^2}{(2\Delta t)^2 g}$ (10.61)

can find $\left[A(0)\right]^2, \left[A\left(\frac{\mu_c}{m}\right)\right]^2, \left[A\left(\frac{\mu_c 2}{m}\right)\right]^2, \ldots\ldots\ldots, \left[A(\mu_c)\right]^2$ (10.62)

which will be designated by $A(h)$; $h = 0, 1 \ldots\ldots m$ (10.63)

can observe for $\theta^* = -\frac{\pi}{2}, \frac{\pi}{2}\left(\frac{-q+1}{q}\right), \ldots\ldots -\frac{\pi}{2q}, 0, \frac{\pi}{2q}, \ldots\ldots\ldots, \frac{\pi}{2}$ (10.64)

which will be designated by $\theta^* = \frac{\pi}{2}\frac{j^*}{q}$; $j^* = -q \ldots\ldots\ldots +q$ (10.65)

and for a fixed θ^* can find

$$\left[A\left(0, \frac{\pi}{2}\frac{j^*}{q}\right)\right]^2, \left[A\left(\frac{\nu_c}{m}, \frac{\pi}{2}\frac{j^*}{q}\right)\right]^2, \left[A\left(\frac{\nu_c 2}{m}, \frac{\pi}{2}\frac{j^*}{q}\right)\right]^2, \ldots\ldots\ldots \left[A\left(\nu_c, \frac{\pi}{2}\frac{j^*}{q}\right)\right]^2 \tag{10.66}$$

which will be designated by $A(h', j^*)$; $h' = 0, 1, \ldots\ldots\ldots m$ (10.67)

This yields $m+1$ numbers from (10.63) and $2q(m+1)$ values from (10.67) or a (10.68)

total of $(2q+1)(m+1)$ numbers. (10.69)

since $A(h', -q) = A(h', q)$

PLATE LIII

The determination of $[A_2(\mu,\theta)]^2$; solution

For convenience in notation let μ_c be defined by equation (10.60) and ν_c by equation (10.61). These are the cutoff values of the spectral wave frequencies and the spectral wave number. If there is no aliasing for μ greater than μ_c, then the largest spectral wave number which can be observed is ν_c.

Then for m lags of $\eta(t)$, m + 1 values of $[A(\mu)]^2$ can be found as given by equation (10.62). These values will be designated by A(h) as h runs from 0 to m for simplicity of notation as given by equation (10.63). $[A(\mu_c \frac{h}{m})]^2$ is given by equation (10.35) after the use of equations (10.30), (10.31), and (10.32).

It is possible to pick 2q + 1 directions for θ^* as given by equation (10.64), and θ^* can be designated by $\pi j^*/2q$ as j^* is summed from minus q to plus q as shown by equation (10.65). The θ^* are equally spaced angular values above and below θ equal to zero.

For each value of θ^*, the stationary series which is observed can be analyzed by numerical methods exactly like equations (10.30), (10.31), and (10.32). The space separation of points in the series is given by Δx_1 equals $(2\Delta t)^2 g/2\pi$. For each value of θ^*, that is for j^* fixed, the power in m + 1 bands of the ν_o axis can be estimated. Values of the form $[A(\nu_c \frac{h}{m}, \pi j^*/2q)]^2$, can be obtained. These values will be designated by A(h',j*) as h' runs from zero to m for simplicity as given by equation (10.67).

From equation (10.63), m + 1 numbers are the result. From equation (10.67),(2q + 1)(m + 1) numbers are the result since j^* ranges from minus q to plus q, but for j^* equal to plus and minus

q the results are the same because the same track is retraced in the opposite direction. Equation (10.69) states formally that $A(h',-q)$ equals $A(h',q)$. Thus m + 1 numbers are duplicates and can be discarded. Finally $(2q+1)(m+1)$ numbers result from the application of the procedures given by Tukey and Hamming [1949] to the recorded data. This is stated in (10.68). As a check, the total area under A(h) in cm^2 should equal the total area under $A(h',j^*)$ for each j^* to a high degree of accuracy. If not, the value of N is too small and the value of m is too large for reliable results.

It is now necessary to study how the μ,θ plane maps into the ν_o,θ_o plane and how area net elements in the first plane map into area net elements in the second plane. For this purpose, pick the values given by equation (10.70) for the μ axis and the values given by equation (10.71) for the θ axis. The curves defined by the double lines are boundary curves of area elements. The unknown number, $A_2(h,j)$, will designate the value of

$$[A_2(\frac{\mu_c h}{m}\ ,\ \frac{\pi}{2}\ \frac{j}{q})]^2$$

over the net area element defined by equations (10.73) and (10.74). It will be assumed that $A_2(h,j)$ is constant over the area element.

Figure 27 is an example of such a net of the μ,θ plane for the special case of m equal to 10 and q equal to 3. The values of $A_2(h,j)$ are shown in each of the area elements. The $A_2(h,j)$ are the unknowns which must be found to determine an approximation of $[A_2(\mu,\theta)]^2$. Near the origin of the coordinate system some of the values of $A_2(h,j)$ are not shown because the figure would be too crowded. There are $(m+1)(2q+1)$ unknown values of $A_2(h,j)$.

The Determination of $[A_2(\mu,\theta)]^2$

In the μ,θ, pick the following net $\mu = 0, \frac{\mu_c}{2m}, \frac{\mu_c}{m}, \frac{3\mu_c}{2m}, \frac{2\mu_c}{m}, \frac{5\mu_c}{2m} \ldots\ldots \frac{2m-1}{2m}\mu_c, \mu_c$ (10.70)

$\theta = -\frac{\pi}{2}, (\frac{-2q+1}{2q})\frac{\pi}{2}, \ldots\ldots \frac{\pi}{2}(\frac{-1}{2q}), 0, \frac{\pi}{2}(\frac{1}{2q}), \ldots\ldots \frac{\pi}{2}$ (10.71)

The curves defined by the double = are boundary curves. The curves defined by the single — define center points. Let $[A_2(\frac{\mu_c h}{m}, \frac{\pi}{2}\frac{j}{q})]^2 = A_2(h,j)$ (10.72) where (10.72) is assumed constant over the area defined by $\mu_c(\frac{2h-1}{2m}) < \mu < \mu_c(\frac{2h+1}{2m})$ (10.73) $\frac{\pi}{2}(\frac{2j-1}{2q}) < \theta < \frac{\pi}{2}(\frac{2j+1}{2q})$ (10.74)

In the ν_0,θ_0 plane for a fixed θ^*, pick the following net $\nu = 0, \frac{\nu_c}{2m}, \frac{\nu_c}{m}, \frac{3\nu_c}{2m} \ldots\ldots \nu_c$ (10.75)

$\theta_0 = -\frac{\pi}{2}, \ldots\ldots -\frac{\pi}{2}(\frac{1}{2q}), 0, \frac{\pi}{2}(\frac{1}{2q}), \ldots\ldots \frac{\pi}{2}$ (10.76) Let $[A_2(\frac{\nu_c h'}{m}, \frac{\pi}{2}\frac{j'}{q}, \frac{\pi}{2}\frac{j^*}{q})]^2 = A_2(h',j',j^*)$ (10.77)

Where (10.77) is assumed constant over the area defined by $\nu_c(\frac{2h'-1}{2m}) < \nu_c < \nu_c(\frac{2h'+1}{2m})$ (10.78)

$\frac{\pi}{2}(\frac{2j'-1}{2q}) < \theta < \frac{\pi}{2}(\frac{2j'+1}{2q})$ (10.79)

Plate LIV

In the ν_o,θ_o plane for a fixed θ^*, pick the net defined by equation (10.75) for ν_o and (10.76) for θ_o. Over the area element defined by equation (10.78) and (10.79), the value of $[A_2(\nu_o,\theta,\theta^*)]^2$ can be designated by $A_2(h',j',j^*)$ in equation (10.77).

The net for the ν_o,θ_o plane for θ^* equal to $\pi/6$ and for m equal to 10 and q equal to 3 is shown in figure 28 by the dashed lines. The circles shown by the solid lines show what happens to the lines μ equal to a constant in the μ,θ plane as they are mapped into the ν_o,θ_o plane. (See equations (10.48) and (10.49).)

Consider what happens to the boundary curves which define the area covered by $A_2(h,j)$. The curve μ equal to $\mu_c(2h + 1)/2m$ maps into ν_o equal to $\nu_c \cos\theta(2h + 1)^2/(2m)^2$ as stated by equation (10.80). Similarly equation (10.81) is the mapping of μ equal to $\mu_c(2h - 1)/2m$. The straight line θ equal to $\pi(2j - 1)/4q$ maps into θ_o equal to $\pi(2(j - j^*) - 1)/4q$ as stated by equation (10.82). Similarly, equation (10.83) shows the mapping of θ equal to $\pi(2j + 1)/4q$. Equations (10.80)and (10.81) are equations of circles which pass through the point ν_o equal to zero and θ_o equal to plus or minus $\pi/2$. They are shown, for example, in figure 28. From these considerations, the area element $A_2(8,1)$ maps into the shaded area shown in figure 28. It therefore covers part of $A_2(6',0',1^*)$ and $A_2(7',0',1^*)$.

Power is conserved by the mapping. Since $A_2(h,j)$ is the constant value for the power spectrum over an individual area element, the integral over the area element in the μ,θ plane is given by equation (10.84). After the mapping the integral over the area defined by equations (10.80), (10.81), (10.82), and (10.83) becomes an

The Determination of $[A_2(\mu,\theta)]^2$

The boundaries of $A_2(h,j)$ map into the following curves in the ν_0,θ_0 plane for a fixed $\theta^*=\frac{\pi}{2}\frac{j^*}{q}$

Lower Boundary, $\nu_0=\nu_c\left(\frac{2h-1}{2m}\right)^2\cos\theta_0$ (10.80) Upper Boundary, $\nu_0=\nu_c\left(\frac{2h+1}{2m}\right)^2\cos\theta_0$ (10.81)

Lower θ_0, $\theta_0=\frac{\pi}{2}\left(\frac{2(j-j^*)-1}{2q}\right)$ (10.82) Upper $\theta_0=\frac{\pi}{2}\left(\frac{2(j-j^*)+1}{2q}\right)$ (10.83)

$$\int_{\frac{\pi}{2}\left(\frac{2j-1}{2q}\right)}^{\frac{\pi}{2}\left(\frac{2j+1}{2q}\right)}\int_{\mu_c\left(\frac{2h-1}{2m}\right)}^{\mu_c\left(\frac{2h+1}{2m}\right)} A_2(h,j)\,d\mu\,d\theta=\frac{\pi}{2q}\frac{\mu_c}{m}A_2(h,j) \quad (10.84)$$

$$\int_{\frac{\pi}{2}\left(\frac{2(j-j^*)-1}{2q}\right)}^{\frac{\pi}{2}\left(\frac{2(j-j^*)+1}{2q}\right)}\int_{\nu_c\left(\frac{2h-1}{2m}\right)^2\cos\theta_0}^{\nu_c\left(\frac{2h+1}{2m}\right)^2\cos\theta_0} A_2(h,j)\frac{1}{2}\left(\frac{g}{\cos\theta_0\,\nu_0}\right)^{1/2}d\nu_0\,d\theta_0=A_2(h,j)\frac{\pi\mu_c}{2qm} \quad (10.85\,a)$$

$$\int_{\frac{\pi}{2}\left(\frac{2(j-j^*)-1}{2q}\right)}^{\frac{\pi}{2}\left(\frac{2(j-j^*)+1}{2q}\right)} A_2(h,j)\left(\frac{g}{\cos\theta_0}\right)^{1/2}\left[\sqrt{\nu_0}\right]_{\nu_c\left(\frac{2h-1}{2m}\right)^2\cos\theta_0}^{\nu_c\left(\frac{2h+1}{2m}\right)^2\cos\theta_0}d\theta_0=\int_{\frac{\pi}{2}\left(\frac{2(j-j^*)-1}{2q}\right)}^{\frac{\pi}{2}\left(\frac{2(j-j^*)+1}{2q}\right)} A_2(h,j)(g)^{\frac{1}{2}}\frac{\sqrt{\nu_c}}{m}d\theta_0=A_2(h,j)\frac{\pi}{2q}\frac{\mu_c}{m} \quad (10.85\,b)$$

Assume $j^*=0$, $j^*=0$ (10.86) with respect to $A_2(h,j)$ $\nu_{0\,MAX}=\nu_c\left(\frac{2h+1}{2m}\right)^2\cos\left(\frac{\pi}{2}\frac{2j-1}{2q}\right)$ (10.87)

$\nu_{0\,MIN}=\nu_c\left(\frac{2h-1}{2m}\right)^2\cos\left(\frac{\pi}{2}\frac{2j+1}{2q}\right)$ (10.88)

Plate LV

integral over a portion of the ν_o,θ_o plane. The integral is evaluated in equation (10.85) which proves that power is conserved.

Consider figure 29. The dashed lines bound the area elements of $A_2(h',j',j^*)$ and they form a net over $[A_2(\nu_o,\theta_o,\theta^*)]^2$. For this particular case θ^* equals zero. The shaded area shows the area mapped into by $A_2(8,1)$. For this case, j is greater than zero and j^* is zero, as assumed for a special consideration in equation (10.86). Then after $A_2(h,j)$ has been mapped into $[A_2(\nu_o,\theta_o,\theta^*)]^2$, the greatest value of ν_o, $\nu_{o_{max}}$, is then found by substituting the smallest value θ_o can have, namely equation (10.82), into the upper boundary curve, namely equation (10.81), and the result is equation (10.87). Similarly equation (10.88) gives the minimum value of ν_o.

For the net in the ν_o,θ_o plane, $A_2(h,j)$ therefore occupies part of several area elements given by $A_2(h',j',0^*)$. In fact, there exists some value of h', say K, such that $\nu_{o_{min}}$ and $\nu_{o_{max}}$ are sandwiched between $\nu_o(2K - 1)/2m$ and $\nu_o(2K + P)/2m$ as stated by equation (10.89). Finally on mapping $A_2(h,j)$ into $A_2(h',j',0^*)$, $A_2(h,j)$ contributes part of its power to the $A_2(h',j',0^*)$ for h' ranging from K to $[K + (p - 1)/2]$ and for j' equal to j as stated by equation (10.90).

Consider equation (10.91). The right hand side of the equation gives the power in the area element, $A_2(h,j)$ in the μ,θ plane. $A_2(h,j)$ has the dimensions of cm^2sec/radian, and the whole term has the dimensions of cm^2. The number $B(h,j,h',j',j^*)$ is a number which partitions the right hand side into contributions to the various elements $A_2(h',j',j^*)$ in the ν_o,θ_o plane. Equation (10.92)

The Determination of $A_2[(\mu,\theta)]^2$

There exists some value of h', say K, such that $\nu_c\frac{2K-1}{2m} \leq \nu_{o\,MIN} < \nu_c\frac{2K+1}{2m} < \nu_c\frac{2K+3}{2m} \ldots\ldots \leq \nu_{o\,MAX} \leq \nu_c\frac{2K+P}{2m}$ (10.89)

Therefore $A_2(h,j)$ contributes to $A_2(h',j',\theta^*)$ for $h'=k,k+1,\ldots\ldots,k+(\frac{P-1}{2})$ and $j'=j$ (10.90)

Define $\sum_{h'} B(h,j,h',j',j^*)A_2(h,j)=\frac{\mu_c\pi}{2qm}A(h,j)$ (10.91) $\frac{2qm}{\mu_c\pi}\sum_{h'} B(h,j,h',j',j^*)=1$ (10.92)

where $\frac{2qm}{\mu_c\pi}B(h,j,h',j',j^*)$ determines the fractional part of $A_2(h,j)$ in the net element $A(h',j',j^*)$

For this example, $B(h,j,h',j',o)=0$ if $h'<K$ and if $h'>K+\frac{P-1}{2}$ (10.93)

$$\int_{\frac{\pi}{2}(\frac{2j'-1}{2q})}^{\frac{\pi}{2}(\frac{2j'+1}{2q})}\int_{\nu_c(\frac{2h'-1}{2m})}^{\nu_c(\frac{2h'+1}{2m})} A(h',j',j^*)\,d\nu_o\,d\theta_o=\frac{\pi}{2q}\frac{\nu_c}{m}A(h',j',j^*) \quad (10.94) \quad \sum_{j'} A(h',j',j^*)\frac{\pi}{2q}\frac{\nu_c}{m}=\frac{\nu_c}{m}A(h',j^*) \quad (10.95)$$

$\sum_{j',h,j} B(h,j,h',j',j^*)A(h,j)=\frac{\nu_c}{m}A(h',j^*)$ (10.96) for $j^*=-q+1$ to q and $h'=0,1,\ldots\ldots m$ (10.97)

$\sum_{j}\frac{\pi}{2q}\frac{\mu_c}{m}A(h,j)=\frac{\mu_c}{m}(A(h))$ (10.98) for $h=0,1,2,\ldots\ldots m$ (10.99)

Plate LVI

follows from equation (10.91). The dimensionless number, $2\pi qm\ B(h,j,h',j',j^*)/\mu_c\pi$, determines that fractional part of $A_2(h,j)$ which is contributed to the value of $A_2(h',j',j^*)$. For the examples in the plates, $B(h,j,h',j',j^*)$ is zero if $h' < K$ and if $h' > (2K + P - 1)/2$ as stated by equation (10.93). It is also zero if $j^* \neq j'$.

The power in an area element in the ν_o,θ_o plane is given by equation (10.94). $A_2(h',j',j^*)$ has the dimensions of cm^3/radian, and the right hand side of (10.94) has the dimensions of cm^2. The integral over θ_o (see equation (10.55)) then becomes the sum given by equation (10.95). $A(h',j^*)$ has the dimensions of cm^3 and the right hand side has the dimensions of cm^2.

All of the terms of the form of $B(h,j,j',j',\ j^*)\ A_2(h,j)$, which have the dimensions cm^2, can be treated for a fixed h' and j*. Summed over all possible j', h, and j, they will be all contributions to the net elements in the ν_o,θ_o plane for a fixed h'. In fact, they must again equal the right hand side of equation (10.95) as is stated by equation (10.96).

Equation (10.96) thus involves known values of $B(h,j,j',j',j^*)$ and a known value for the right hand side given by the values found in equation (10.67). The unknowns are given by the $A_2(h,j)$. Separate equations for each value of h' and j* result as shown by equation (10.97), and equation (10.96) with equation (10.97) therefore stands for a system of $2q(m + 1)$ linear equations.

Also equation (10.98) follows from equation (10.24). The right hand side is known from equation (10.63). There are $m + 1$ equations of the form of equation (10.98) as stated by the condition (10.99). The unknowns are $A_2(h,j)$.

Equations (10.96), (10.97), (10.98) and (10.99) therefore define a system of $(2q + 1)(m + 1)$ inhomogeneous simultaneous linear equations and there are $(2q + 1)(m + 1)$ unknown values of $A_2(h,j)$. Such a system has a solution if the determinant of the equations is not zero. It has not been proved that this is the case, but further investigation has shown that sub sets of the equation starting with h and h' equal to m can be solved. It appears that a process similar in the abstract to the concrete process of peeling the outside rings off one half of a slice of a Bermuda onion one by one will yield the values of $A_2(h,j)$.

Corrections to the equations

Some of the area elements in the μ ,θ plane and in the ν_o,θ_o plane contribute only half of the power to the total power that is contributed by area elements in the center of the system. Others at the corners of the system contribute only a quarter of the amount of those at the center. Equation (10.94), for example, must be modified if h' equals m. Also the terms in (10.95) for j' equal to -q and q have a factor of one half in them. At various places in these equations, then, factors of one half and one fourth must be inserted. These factors have been omitted in order to simplify the notation since it is not intended actually to solve such a system. (For one reason, the needed data are not available.)

Further explanations

Figures 27, 28, 29 and 30 can be studied together in order to understand better the procedures described above. In these figures $A_2(8,1)$ in the μ ,θ plane is traced as it is mapped into

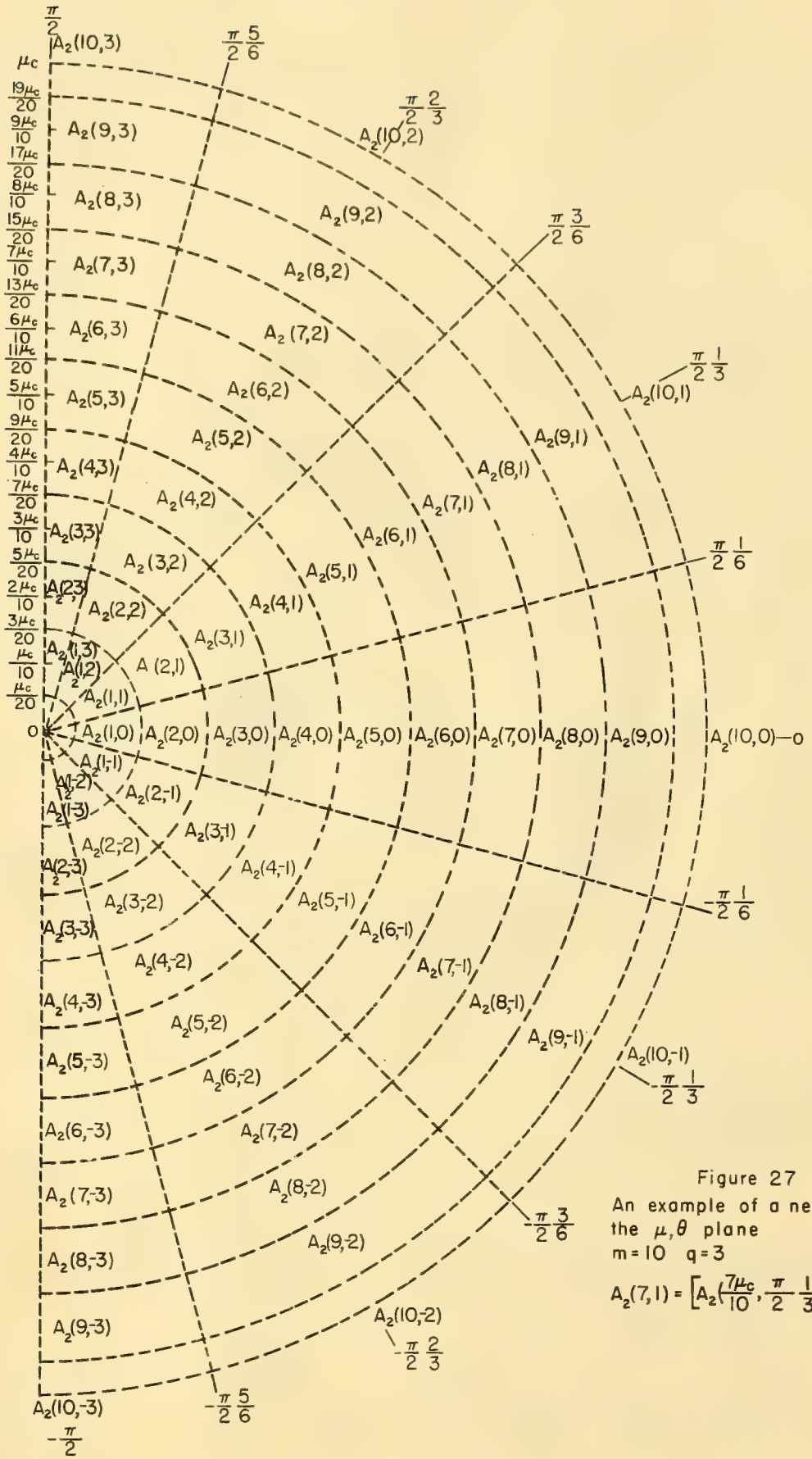

Figure 27

An example of a net over the μ, θ plane

$m = 10 \quad q = 3$

$$A_2(7,1) = \left[A_2\left(\frac{7\mu_c}{10}, \frac{\pi}{2}\frac{1}{3}\right)\right]^2$$

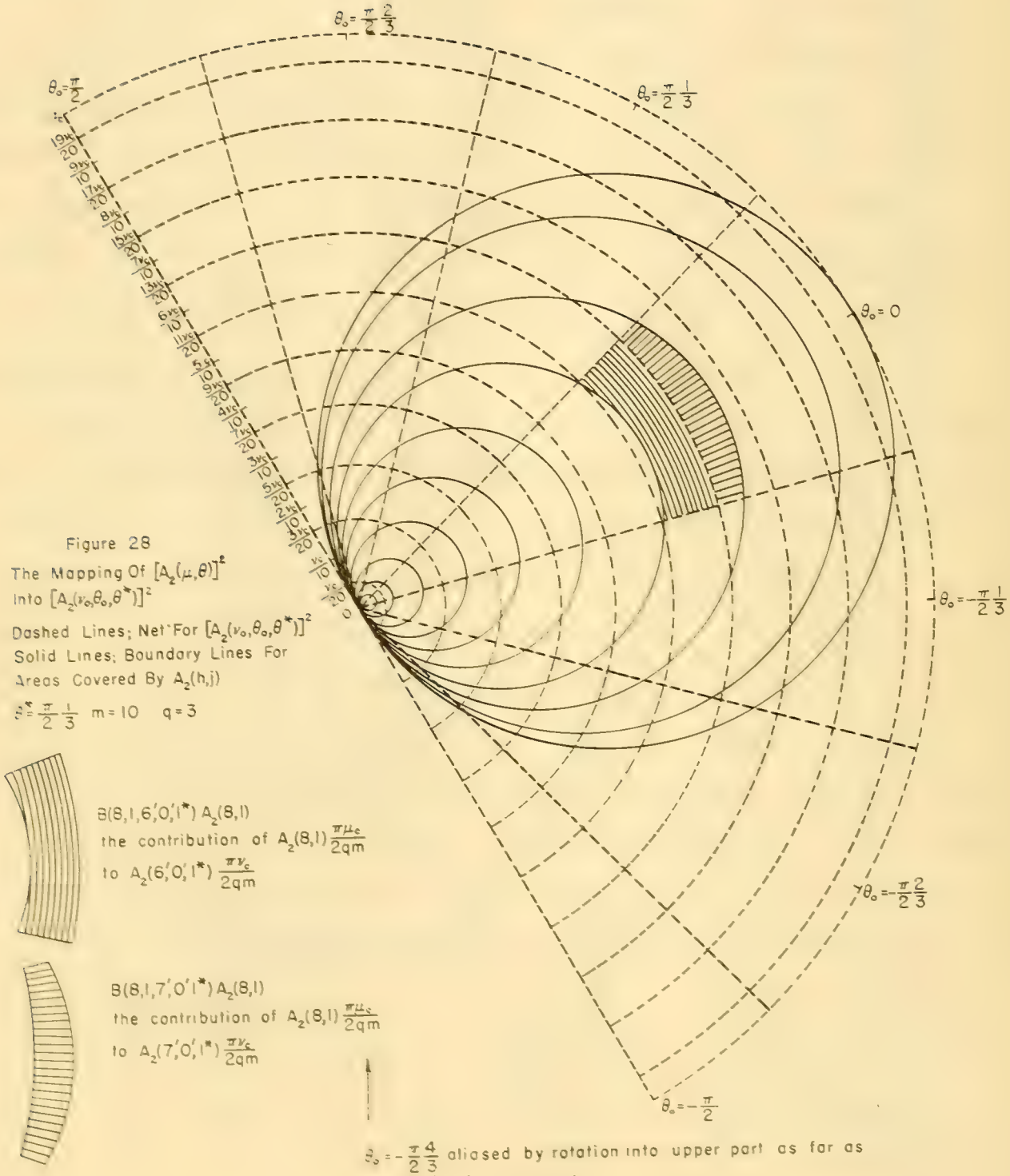

Figure 28

The Mapping Of $[A_2(\mu,\theta)]^2$ Into $[A_2(\nu_o,\theta_o,\theta^*)]^2$

Dashed Lines; Net For $[A_2(\nu_o,\theta_o,\theta^*)]^2$

Solid Lines; Boundary Lines For Areas Covered By $A_2(h,j)$

$\theta^* = \frac{\pi}{2}\frac{1}{3}$ $m=10$ $q=3$

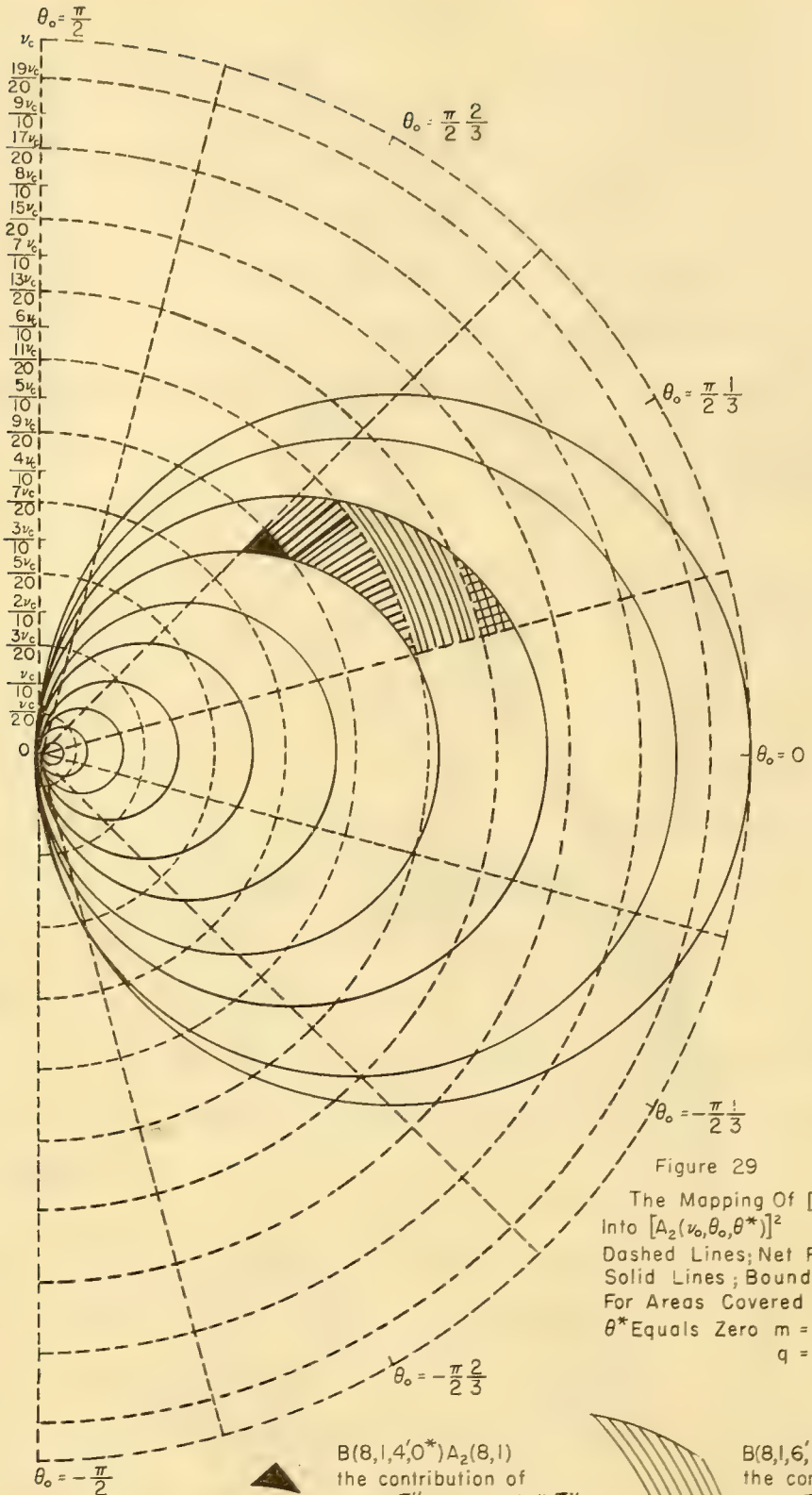

Figure 29

The Mapping Of $[A_2(\mu,\theta)]^2$
Into $[A_2(\nu_o,\theta_o,\theta^*)]^2$
Dashed Lines; Net For $[A_2(\nu_o,\theta_o,\theta^*)]^2$
Solid Lines; Boundary Lines
For Areas Covered By $A_2(h,j)$
θ^* Equals Zero $m = 10$
$q = 3$

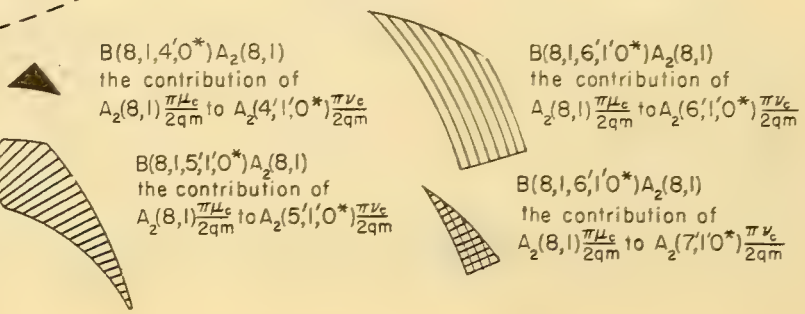

Figure 30

The Mapping Of $[A_2(\mu,\theta)]^2$ Into $[A_2(\nu_o,\theta_o\theta^*)]^2$

Dashed Lines; Net For $[A_2(\nu_o,\theta_o,\theta^*)]^2$

Solid Lines; Boundary Lines For Areas Covered by $A_2(h,j)$

$\theta^* = -\frac{\pi}{2}\frac{1}{3}$ $m = 10$ $q = 3$

$B(8,1,2',2',-1)A_2(8,1)$; the contribution of $A_2(8,1)\frac{\pi\mu_c}{2qm}$ to $A_2(2',2',-1^*)\frac{\pi\nu_c}{2qm}$

$B(8,1,3',2',-1^*)A_2(8,1)$; the contribution of $A_2(8,1)\frac{\pi\mu_c}{2qm}$ to $A_2(3',2',-1^*)\frac{\pi\nu_c}{2qm}$

$B(8,1,4',2',-1^*)A_2(8,1)$; the contribution of $A_2(8,1)\frac{\pi\mu_c}{2qm}$ to $A_2(4',2',-1^*)\frac{\pi\nu_c}{2qm}$

$B(8,1,5',2',-1^*)A_2(8,1)$; the contribution of $A_2(8,1)\frac{\pi\mu_c}{2qm}$ to $A_2(5',2',-1^*)\frac{\pi\nu_c}{2qm}$

$\theta_o = \frac{\pi}{2}\frac{4}{3}$ aliased by the rotation into lower part as far as integration is concerned

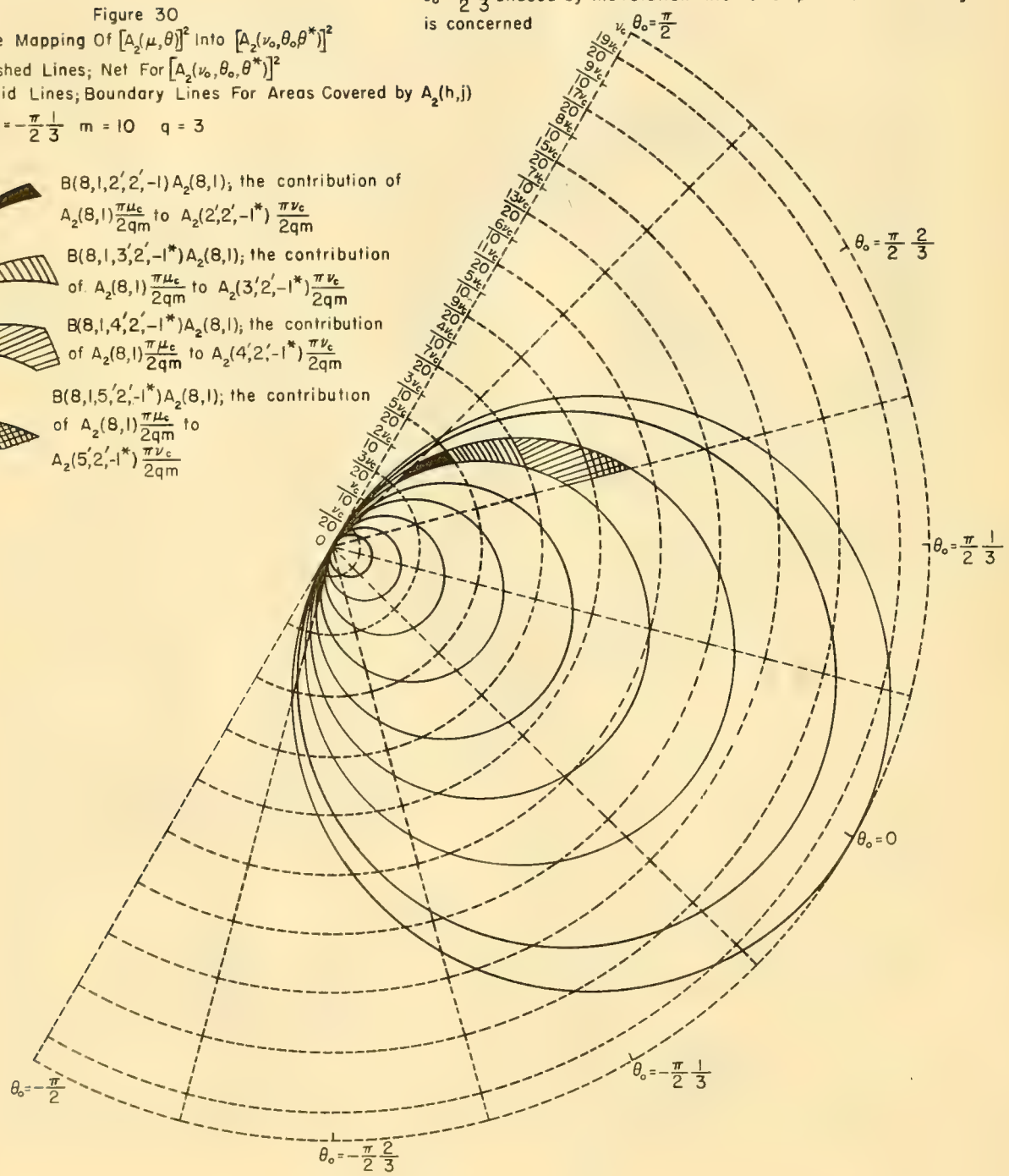

the functions $[A_2(\nu_o,\theta_o,\pi/6^*)]^2$, $[A_2(\nu_o,\theta_o,0^*)]^2$ and $[A_2(\nu_o,\theta_o,-\pi/6^*)]^2$.* In figure 28, the elemental waves in $A_2(8,1)$ are traveling very nearly in the direction $\theta^* = \pi/6$. $A_2(8,1)$ then goes into a symmetric figure which contributes part of its power to $A_2(6',0',1^*)$ and the other part to $A_2(7',0',1^*)$. Note also that the range of integration in equation (10.53) is from $-\pi/2 - \theta^*$ to $\pi/2 - \theta^*$ and that the figure shows $A(\nu_o,\theta_o,\pi/6^*)$ as if it varies from $-\pi/2$ to $\pi/2$. The true figure can be obtained by slicing figure 28 along the line $\theta_o = 2\pi/6$ and rotating the pie-shaped sector obtained counterclockwise until $\theta_o = \pi/2$ touches $\theta_o = -\pi/2$. Then θ_o varies from $-4\pi/6$ to $2\pi/6$.

For θ^* equals zero, the mapping is given by figure 29. The shaded areas again show what happens to $A_2(8,1)$. The power in $A_2(8,1)$ is distributed over $A_2(4',1',0^*)$, $A_2(5',1',\theta^*)$, $A_2(6',1',0^*)$ and $A_2(7',1',0^*)$. The wave elements in the elemental area, $A_2(8,1)$, are now at an angle to the direction of observation. For θ^* equals $-\pi/6$ the power in $A_2(8,1)$ is contributed to $A_2(2',2',-1^*)$, $A_2(3',2',-1^*)$, $A_2(4',2',-1^*)$ and $A_2(5',2',-1^*)$ as shown by figure 30. The angle between the wave direction and the direction of x' is now greater.

The computation of $B(h,j,h',j',j^*)$

The value of $B(h,j,j',j',j^*)$ depends only on the properties of the net and not on any unknown quantities. There are $(m+1)^2 \cdot (2q+1)^3$ possible values but most of them are zero and many of them are numerically the same. There are a possible 77 values for $B(8,1,h',j',0^*)$ if m is 10 and q is 3, but for j' not

*Note how the circles shown by the solid lines squeeze down to the origin. One of them is so small, in fact, that it is not shown.

equal to 1 they are zero, and for h' less than 4 or greater than 7 they are zero. Therefore only four values have to be found out of the 77. From figures 29 and 30, B(8,1,7',1',0*) and B(8,0,7',1,-1*) have the same numerical value. Thus only a few of the values actually have to be determined.

The evaluation of B(8,1,5',1',0*) will be discussed as a particular example. It is the number which results from the double integration of $(1/2)(g/\cos\theta_o \nu_o)^{1/2}\, d\nu_o d\theta_o$ over the shaded area indicated in figure 29. Three sections of the boundary curves are given by constant values of ν_o and θ_o. Two of the boundary curves are functions of ν_o and θ_o. By breaking up the area shown into three sub-areas shown by the heavy lines, and then, by integration over ν_o first, the center area works out immediately with respect to the next integration over θ_o. The other two areas become elliptic integrals over θ_o which can be evaluated from tables such as those in Janke-Emde [1945].

Estimate of the work involved

For a complicated function, $[A_2(\nu,\theta)]^2$, and for m equal to 10 and q equal to 3 as in the figures, seven analyses of the form described by Tukey and Hamming [1949] would have to be carried out. Each might require four or five hours on a computing machine. The evaluation of the B(h,j,j',j',j*) might require several days. The result would be 77 linear inhomogeneous simultaneous equations with 77 unknowns. The matrix of the equations has certain symmetry properties and if its inverse could be found easily, then the numerical work would involve another day of work. With time for checks of the computation, it would take about ten days to determine the

function. For larger values of m and j, the time required increases very rapidly, and the use of electronic computers might be advisable.

The reliability of the results

If $[A_2(\mu,\theta)]^2$ were determined by the procedures described above, there would be some doubt as to the reliability of the results, especially for small values of m and q. They would at least give an indication of the values of the function but the degree of confidence in the final numerical results in terms of the number of degrees of freedom cannot be given at this time.

The airborne altimeter might introduce additional error by reflecting in part the effect of atmospheric turbulence as suggested by Tukey in a recent conference. A stereoptican measurement of $\eta(x')$ for different θ^* from a photograph would eliminate errors due to the effect of turbulence.

If $[A_2(\mu,\theta)]^2$ is a function which has been filtered by the travel of the disturbance from the source so that it is confined to a small area of the μ,θ plane, just a few directions of θ^* would yield, along with the observation of $\eta(t)$, a great deal of information about $[A_2(\mu,\theta)]^2$.

Other methods for the determination of $[A_2(\mu,\theta)]^2$

In a recent conference, Tukey suggested another method for the determination of $[A_2(\mu,\theta)]^2$ by the use of the stereoptican measurements. The method depends on many parallel measurements for different y' in the x' direction. Waves not traveling in the x' direction can be partly filtered out by the addition of values on a line y' equals constant. The details of the procedure

have not been investigated by the author, and possibly they can be worked out in some future paper. The method has definite advantages over the method described above according to Tukey.

A final method for the determination of $[A_2(\mu,\theta)]^2$ depends upon the acceptance of the results of Chapter 9. The oceans act as a filter on the waves which propagate from the edges of the storms over them. Swell simultaneously recorded on a line of pressure wave recorders (on the California coast, for example) spaced several hundred miles apart can be analyzed by the equations given in this section. The θ band width and filter characteristics could be determined from the dimensions of the storm, and the power spectrum at the edge of the storm could be computed from the observed power spectra after the propagation of the waves over a long distance of decay. $[A_2(\mu,\theta)]^2$ at the edge of many storms must also be determined by the methods described in previous paragraphs in order to verify the statement made in this paper that friction effects are negligible. If this statement is verified, and many arguments have been given which make it appear to be true, the method described in this paragraph will then be a very important way to study the variation of $[A_2(\mu,\theta)]^2$ with wind velocity and air mass properties.

APPENDIX

The foregoing chapters are all of the material available in finished form for publication at the present time. Some detailed wave analyses will be carried out in a later chapter. This appendix has been added in order to show six very interesting figures which illustrate the great range of possible wave records and the interpretation which can be put upon them in the light of the foregoing chapters.

Figures A-1, A-2, A-3, A-4, A-5 and A-6 are from the original paper by Klebba (1946). They have been furnished through the cooperation of Admiral E. H. Smith of Woods Hole Oceanographic Institution. The figures which show wave records are numbered on the right and the corresponding wave record analyses on figures A-3 and A-6 have been numbered to correspond to the wave records for comparison purposes.

The sharp jagged tops of the spectra shown (which are not necessarily power spectra) are probably due to design faults of the instrument and to sampling error. The band width of the tuned circuit of the instrument is probably so narrow that the instrument responds very erratically to portions of the record near certain critical frequencies. For example in figure A-3, the sharp jagged tops in the spectra numbered 13 and 14 could be drastically smoothed in order to obtain a spectrum more like the one numbered 15.

These data are not quantitative in any way because the instrument has a gain control and the gain of the electronic circuits was readjusted for the various analyses. (See for example records

17, 18, and 19 and spectra 17, 18, and 19.)

Finally note that the spectra yield very little information for periods less than 6 seconds. The depth of location of the pressure recorder was 78 feet in one case (B Station) and 103 feet for the other case (A Station). Periods less than 5.6 seconds and 6.5 seconds are hardly detected by the pressure recording instrument.

With these qualifications in mind, the records can first be studied qualitatively and then compared qualitatively with the spectra. Note record 22, for example, in figure A-4. By scanning the record, it is seen that the departure from the mean value is most of the time much less than the peak values of the record. It is not too difficult to accept the hypothesis that enough points taken at random would have a Gaussian distribution. Now note the tremendous variability of the record as a function of time. The time intervals between successive apparent crests vary over a wide range. An autocorrelation of the record with itself would rather rapidly die down to zero which would mean that what happens, say, one minute in the future has very little to do with the behavior of the record at the time of observation.

Now note record number 6. It is much lower in amplitude, but again the departure from the mean of the record is much less most of the time than the departure when the few peak values occur. Again, it is not too difficult to accept the hypothesis that the distribution is Gaussian. The variability of this record is much less than that of the former record in that the time interval between successive crests is much less variable. An autocorrelation

of the record with itself would die down to zero much less rapidly than in the former case (if both were normalized to one at the start). In fact, it is even possible to imagine that one could say something about the behavior of the record one minute into the future given that, say, one of the "groups" was just starting up.

Now compare the spectrum for record 22 with the wave record. The spectrum has amplitudes of importance in the entire band from six seconds to twelve seconds. The wave record is just about what one might expect from such a power spectrum.

Finally compare the spectrum for record 6 with the wave record. The spectrum covers a much narrower band from eight to eleven seconds. (It even looks as if it could have been obtained by the forecast procedures.) The character of the record fits the nature of the spectrum qualitatively.

Trouble occurs though in trying to apply too precise a reasoning to the records and the corresponding spectra. Record number 5, for example, differs only a little (to the eye) from record number 6 and yet the two spectra are very different. It is believed that the differences are due to instability of the instrument and not to a marked change in the sea surface during the three hour interval from record 5 to 6. More precise analysis along the lines described herein would eliminate this trouble.

In conclusion, for part one, quantitative methods of wave analysis have been described herein. They appear to be able to make it possible to put wave analysis and wave forecasting on a

much firmer theoretical and practical basis. It should eventually be possible to analyze records such as those just given accurately, quickly, and quantitatively, by both numerical and physical methods and to relate the power spectra to the storms which produced the waves.

WAVE RECORDS TAKEN AT "A" STATION

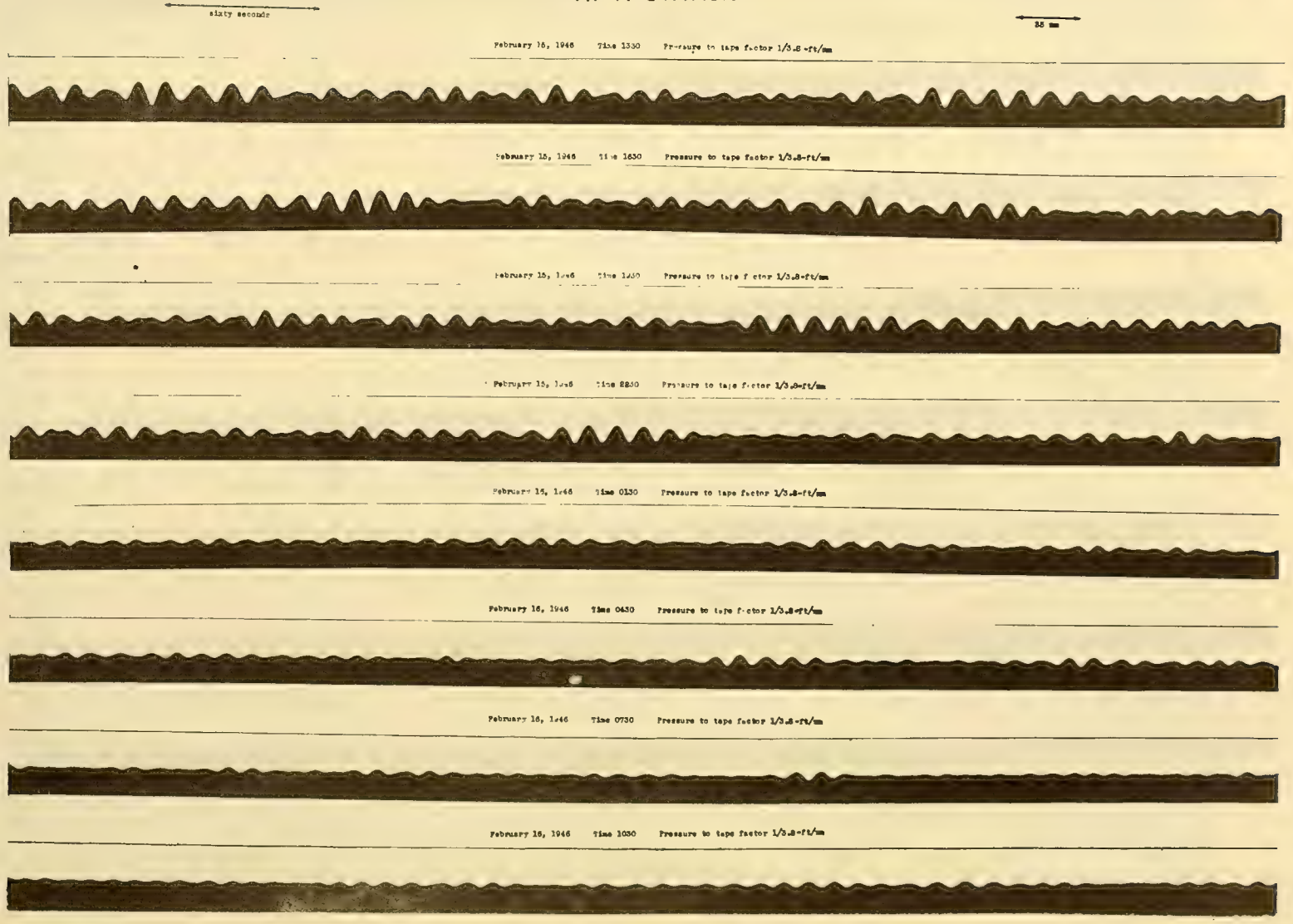

Fig. A1

WAVE RECORDS TAKEN AT "A" STATION

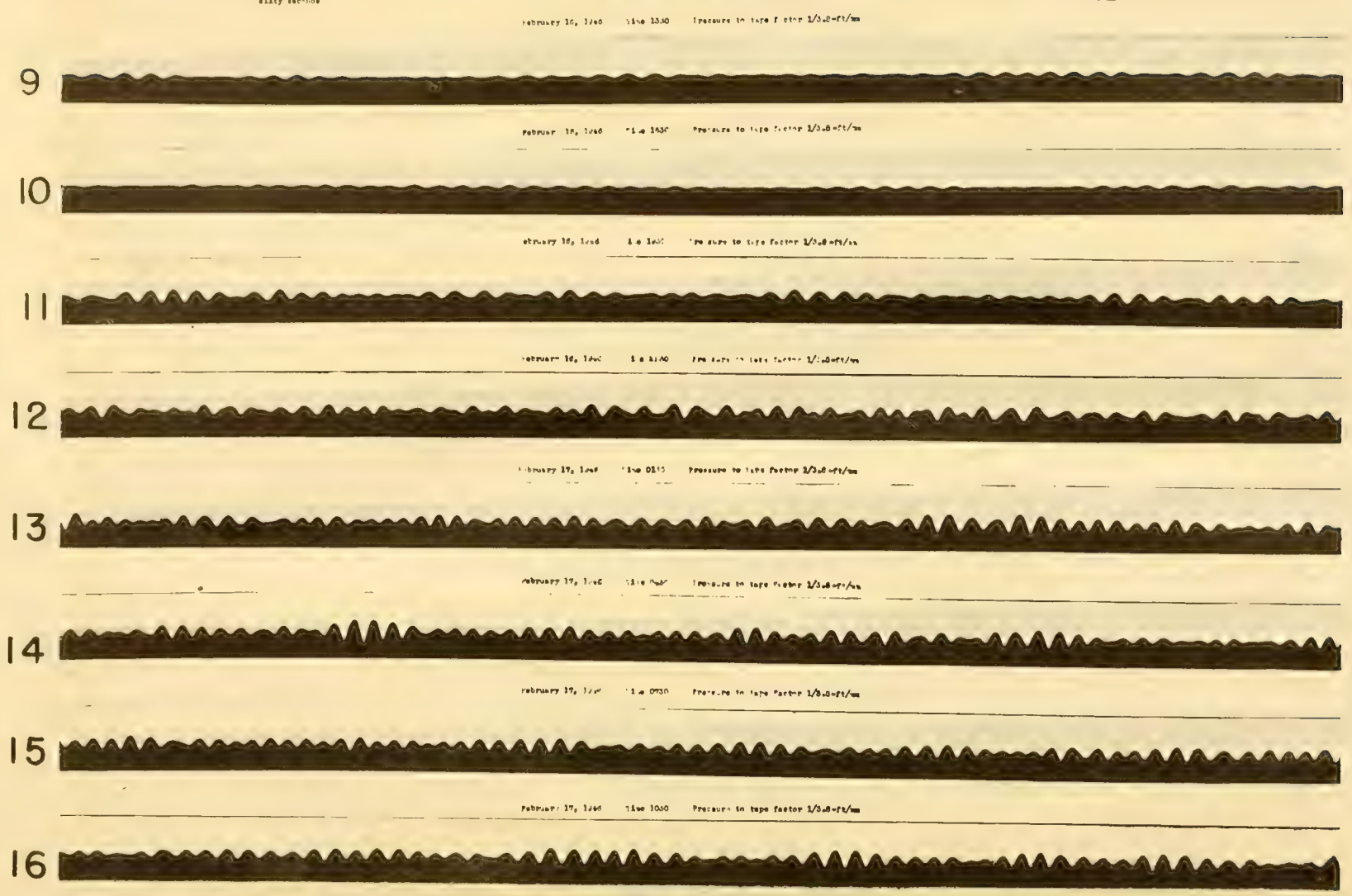

Fig. A2

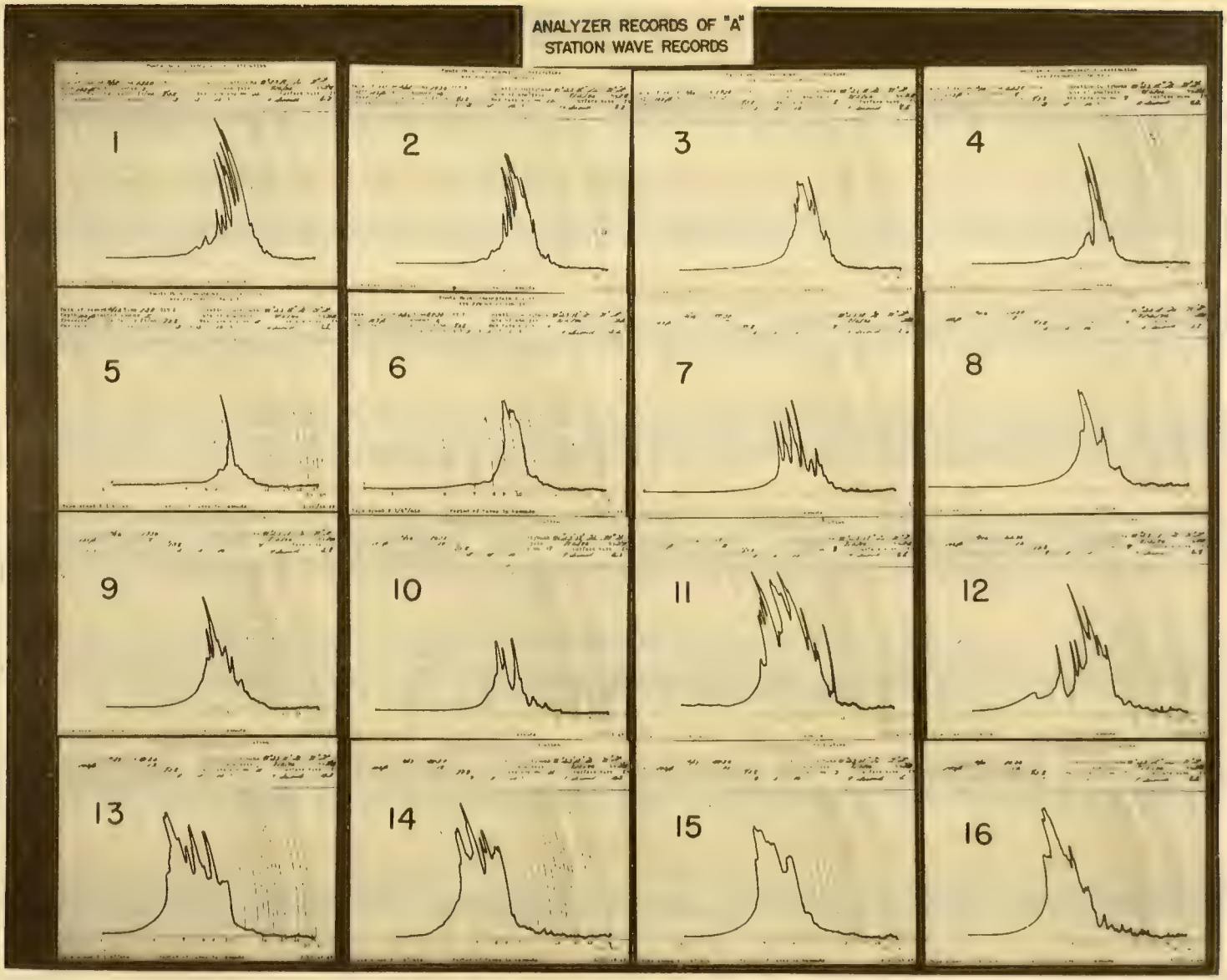
ANALYZER RECORDS OF "A"
STATION WAVE RECORDS
1
2
3
4
5
6
7
8
9
10
11
12
13
14
15
16

Fig. A 3

WAVE RECORDS TAKEN
AT "B" STATION

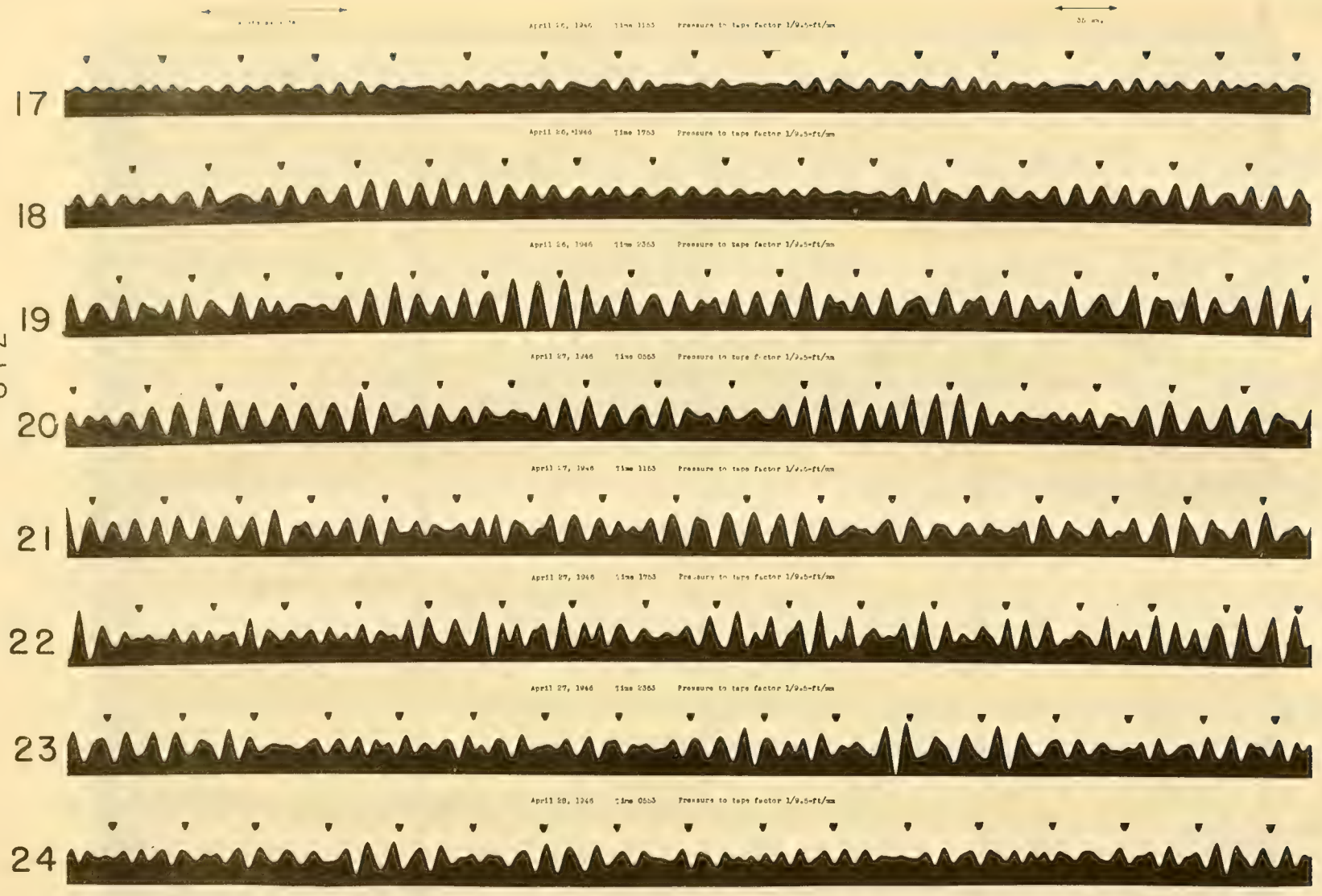

Fig A 4

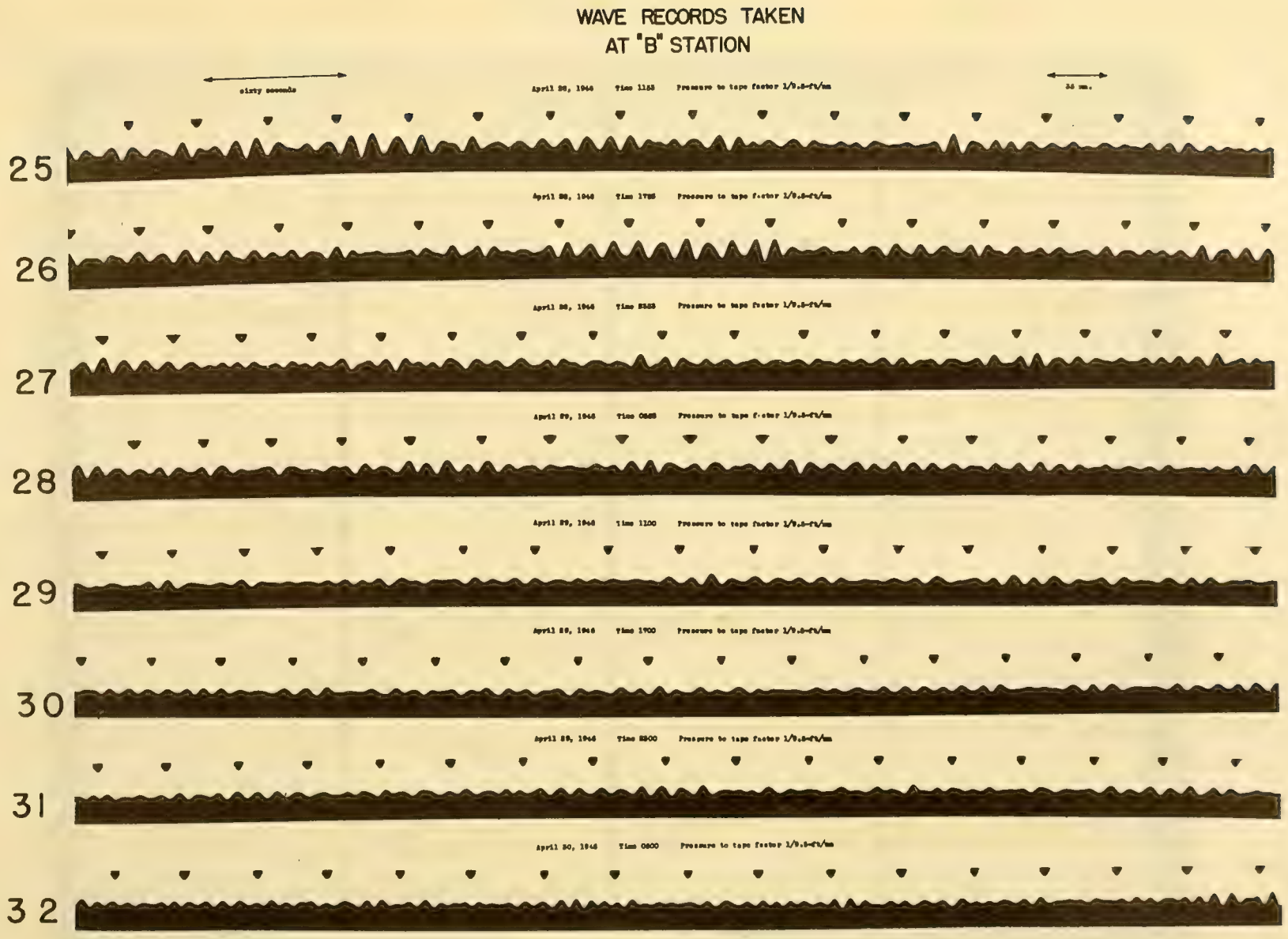
WAVE RECORDS TAKEN
AT "B" STATION
sixty seconds
30 sec.
25
26
27
28
29
30
31
32

Fig. A 5

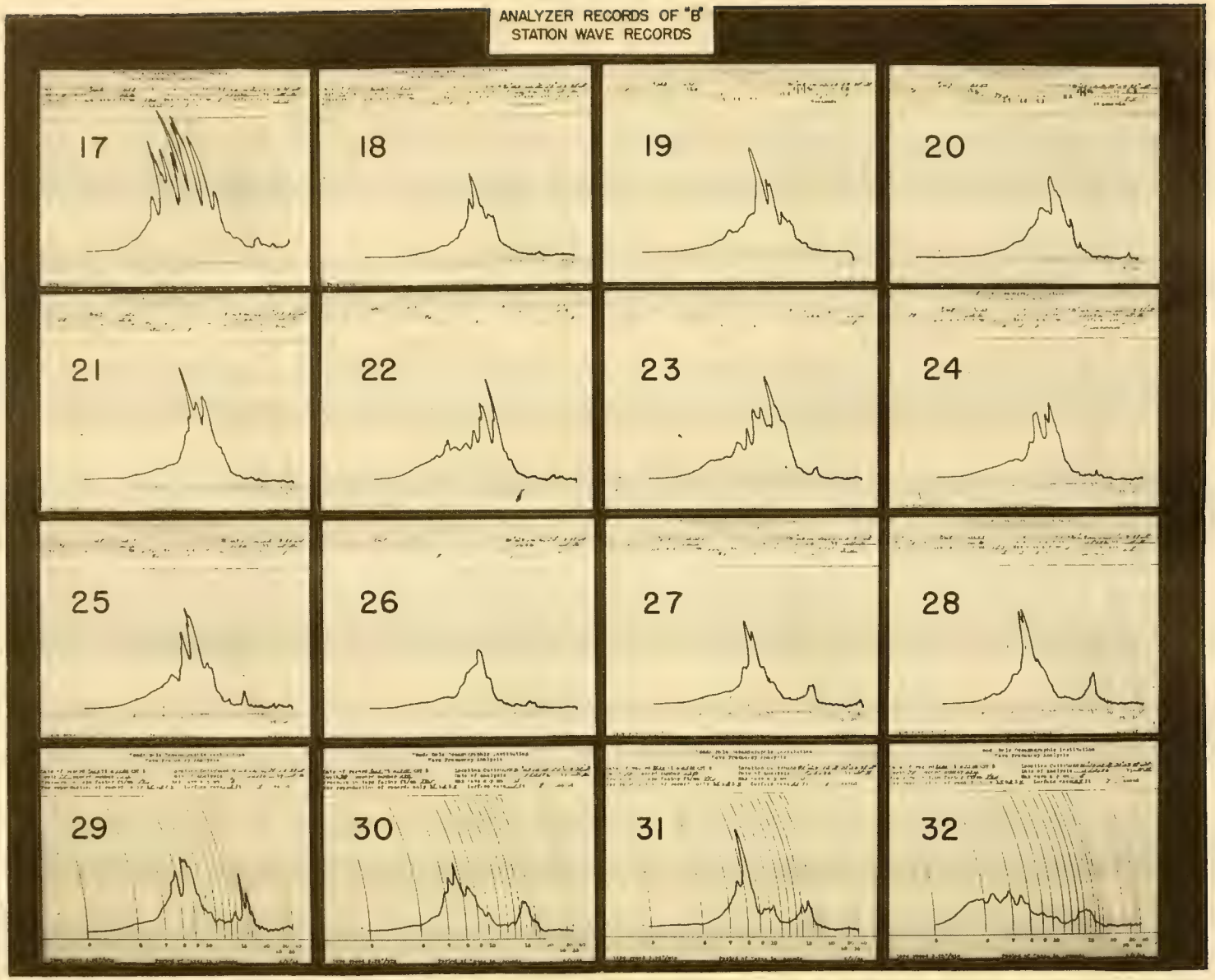
ANALYZER RECORDS OF "B"
STATION WAVE RECORDS
17
18
19
20
21
22
23
24
25
26
27
28
29
30
31
32

Fig. A 6

Acknowledgements

The author wishes to express his sincere thanks to the many people who have helped in the preparation of this work. The list is long, and it consists of many persons from many organizations from all over the United States.

At New York University, there are those who were and are on the immediate staff of the project. Mr. D. P. Martineau, now of Woods Hole and Mr. Richard James, now of A. H. Glenn and Associates, helped in the early part of this work. Mr. Wilbur Marks, Mr. Tony Isnardi, and Mr. John Woolley helped to prepare this book. Professor Bernhard Haurwitz, director of the Beach Erosion Board project, helped by critical discussion and by suggested improvements of the final draft. Professor Hans A. Panofsky, now of Pennsylvania State College, helped in many early stimulating discussions of power spectra.

At the Institute for Mathematics and Mechanics of New York University, Professor Joseph B. Keller and Professor Eugene Isaacson helped me in discussions of some of the mathematical details involved.

In addition at New York University, there are those on the regular University staff who helped in the preparation of this work. My thanks are due to Mrs. Sadelle Wladaver who typed the text and Mr. Gerhard Reinert and Mr. Arthur Klein who drafted the many plates and figures.

At the Office of Naval Research, I wish to express my

appreciation for the cooperation and help provided by Mr. Knauss, Mr. Gordon Lil, and Mr. Rowe.

At the Beach Erosion Board, the entire organization has followed the progress of this paper with great interest. The help and cooperation of Colonel Gessler, Dr. Martin A. Mason, Mr. R. O. Eaton, Mr. Joseph Caldwell, Mr. Jay V. Hall, and Mr. Thorndyke Saville, Jr. are deeply appreciated.

At Woods Hole Oceanographic Institution, Admiral E. H. Smith has helped by providing the staff for the auto-correlation analysis of a wave record. Mrs. Mary Hunt directed the work involved. Theoretical discussions with Columbus Iselin have suggested many future refinements.

At Scripps Institution of Oceanography, I wish to thank Professor R. S. Arthur and Professor W. H. Munk for the many stimulating conferences on wave forecasting we have had and for their continued correspondence on various points of wave theory. The set of lecture notes prepared at Scripps is an excellent supplemented source on wave theory.

Professor John W. Tukey of Princeton University is one person to whom very special thanks are due. Without his help, suggestions, and previous works, this book could never have been written. The author was bogged down at the end of Chapter 6 when Professor Tukey suggested the mechanism of the filters employed in Chapter 7 for the more realistic wave systems studied in that chapter. The tremendous importance of the methods which he has developed

is just now being realized in many geophysical applications, and it is hoped that this book will show how to use these methods in the study and analysis of ocean waves as they really are.

March 1, 1952

Willard J. Pierson, Jr.
Department of Meteorology
New York University

INDEX TO THE FIGURES

Page

Frontispiece. A Photograph of a Short Crested Sea Surface. Photograph through the courtesy of Prof. Robert S. Arthur. Scripps Institution of Oceanography.

Figure 1. Graphs of the Continuous Spectra of Finite Wave Groups for Various Values of σ and T 43

Figure 2. Form of the Graph of the Argument of $S(\eta)$ 54

Figure 3. Form of the Finite Wave Group as a Function of Time When it Passes Various Points. $\sigma = 1/20$ T = 10 68

Figure 4. Form of the Finite Wave Group as a Function of Time When it Passes Various Points. $\sigma = 1/20$ T = 20

Figure 5. Envelope of the Finite Wave Group as a Function of x for Fixed Times. $\sigma = 1/100$ sec^{-1} T = 10 sec . . 70

Figure 6. Graphs of $b(\mu)$ for Various Values of n. Coordinate Scales Differ for Different n for bottom graph as shown 88

Figure 7. G^* and H^* Graphed as a Function of $(g/4\pi x_1)^{1/2}t'$ 93

Figure 8. Graphs of the Finite Wave Train as a Function of t' for Various Values of x_1. T = 10 sec n = 1800 . 95

Figure 9. Variation of the Envelope, the Average Potential Energy, and the Phase of the Crests for Relatively Large Values of x_1 as a Function of t' 97

Figure 10. Graphs of Segments of Equations (6.4) (6.5) and (6.6b) 104

Figure 11. Dispersion Curve for Model Wave System 113

Figure 12. Some Very Condensed Sample Wave Records 124

Figure 13. Graphs of the Functions Involved in the Various Examples of the Lebesgue Stieltjes Power Integral . . . 133

Figure 14. Histograms of Wave Height and Pressure Amplitude Distributions from Sample Wave Records 141

Page

Figure 15. Forecasting Diagram for the Square Cornered Filter and the Fresnel Filter for the Case of a Very Short Fetch 153

Figure 16. Forecasting Diagram for the Square Cornered Filter for the Case of a Fetch of Length, F 163

Figure 17. A Portion of a Short Crested Sea Surface 177

Figure 18. The Quarter Power Boundaries of the Envelope of the Solution 202

Figure 19. The Properties of the Net in the μ ,θ Polar Co-ordinate System 214

Figure 20. The Form of $E_2(\mu,\theta)$ for Equation (9.39) 219

Figure 21. The Form of $E_2(\mu,\theta)$ for Equation (9.51) 226

Figure 22. The Form of $[A_2(\mu,\theta)]^2$ for Equation (9.52) . . . 227

Figure 23. Filter Considerations for a Storm of Finite Width 236

Figure 24. Isopleths of $\theta_p, \Delta\theta_u$, and $\Delta\theta_L$ for the x,y plane in units of Storm Width, W_s 240

Figure 25. Forecast Diagram for the Determination of the Band Width 243

Figure 26. Some Examples of the Sharp Cut-off Filters for Equations (9.62), (9.63) and (9.68) 245

Figure 27. An Example of a Net over the μ ,θ Plane. m = 10, q = 3 303

Figure 28. The Mapping of $[A_2(\mu,\theta)]^2$ into $[A_2(\mu_o,\theta_o,\theta^*)]^2$. $\theta^* = \pi/6$ 304

Figure 29. The Mapping of $[A_2(\mu,\theta)]^2$ into $[A_2(\mu_o,\theta_o,\theta^*)]^2$. $\theta^* = 0$ 305

Figure 30. The Mapping of $[A_2(\mu,\theta)]^2$ into $[A_2(\mu_o,\theta_o,\theta^*)]^2$. $\theta^* = -\pi/6$ 306

INDEX TO THE PLATES

Page

Plate I. Irrotational Non-Linear and Irrotational Linear Equations for Motion Bounded by a Free Surface and a Bottom of Variable Depth
Equations (2.1) through (2.10) 5

Plate II. Form of the Irrotational Linear Equations When the Requirement that the Solution be Periodic in Time is Imposed
Equations (2.11) through (2.23) 12

Plate III. Periodic Wave Solutions for Infinitely Deep Water Expressed in Terms of Angular Wave Frequencies
Equations (2.24) through (2.29) 18

Plate IV. Types of Periodic Functions and Non-periodic Functions and Their Representation by Discrete and Continuous Spectra
Equations (3.1) through (3.9) 27

Plate V. The Propagation of a Finite Wave Group in Infinitely Deep Water
Equations (4.1) through (4.7) 36

Plate VI. Finite Wave Group (Solution)
Equations (4.8) through (4.10) 41

Plate VII. Properties of the Solution
Equations (4.11) through (4.23) 45

Plate VIII. Properties of the Solution (Continued)
Equations (4.24) through (4.35) 72

Plate IX. The Propagation of a Finite Wave Train in Infinitely Deep Water
Equations (5.1) through (5.5) 79

Plate X. The Propagation of a Finite Wave Train in Infinitely Deep Water (Continued)
Equations (5.6) through (5.11) 81

Plate XI. The Propagation of a Finite Wave Train in Infinitely Deep Water (Continued)
Equations (5.12) through (5.14) 83

Plate XII. Finite Wave Train (Solution)
Equations (5.15) through (5.22) 85

Page

Plate XIII. Finite Wave Train (Properties of the Solution)
Equations (5.23) through (5.30) 92

Plate XIV. Model Wave Systems with Infinitely Long Crests
Equations (6.1) through (6.6b) 103

Plate XV. An Infinite Periodic Train of Wave Groups . . .
Equations (6.7) through (6.13) 107

Plate XVI. A Finite Train of Regular Wave Groups
Equations (6.14) through (6.17) 110

Plate XVII. Energy Considerations
Equations (6.18) through (6.25) 117

Plate XVIII. The Lebesgue Stieltjes Power Integral
Equations (7.1) through (7.10) 126

Plate XIX. Some Examples
Equations (7.11) through (7.26) 131

Plate XX. The Gaussian Case
Equations (7.27) through (7.34) 135

Plate XXI. The Forecasting Problem for a Sea Surface Represented by the Gaussian Case of the Lebesgue Power Integral with Infinitely Long Crests in the y Direction
Equations (7.35) through (7.50) 149

Plate XXII. The Forecasting Problem for a Sea Surface Represented by Infinitely Long Crests, a Gaussian Wave Record, and Winds that Lasts D_s Seconds Over a Fetch of Length, F.
Equations (7.51) through (7.61) 159

Plate XXIII. Short Crested Waves
Equations (8.1) through (8.5) 175

Plate XXIV. A Useful Lemma
Equations (8.6) through (8.13) 179

Plate XXV. The Initial Value Problem in the y,t Plane for a Disturbance of Finite Duration and Width
Equations (8.14) through (8.17) 181

Plate XXVI. The Initial Value Problem in the y,t Plane for a Disturbance of Finite Duration and Width
Equations (8.18) through (8.20) 184

Page

Plate XXVII. The Initial Value Problem in the y,t Plane for a Disturbance of Finite Duration and Width
Equations (8.21) through (8.24) 186

Plate XXVIII. The Initial Value Problem in the y,t Plane for a Disturbance of Finite Duration and Width
Equations (8.25) through (8.28) 188

Plate XXIX. The Initial Value Problem in the x,y Plane for a Disturbance over a Finite Area
Equations (8.29) through (8.33) 189

Plate XXX. The Initial Value Problem in the y,t Plane for a Wave Train of Finite Width and Finite Duration
Equations (8.34) through (8.36) 191

Plate XXXI. The Initial Value Problem in the y,t Plane for a Wave Train of Finite Width and Finite Duration
Equations (8.37) through (8.48) 193

Plate XXXII. The Initial Value Problem in the y,t Plane for a Wave Train of Finite Width and Finite Duration
Equations (8.49) through (8.53) 195

Plate XXXIII. The Initial Value Problem in the y,t Plane for a Wave Train of Finite Width and Finite Duration
Equations (8.54) through (8.60) 197

Plate XXXIV. The Initial Value Problem in the y,t Plane for a Wave Train of Finite Width and Finite Duration
Equations (8.61) through (8.62) 199

Plate XXXV. Interpretation of Results
Equations (8.63) through (8.70) 201

Plate XXXVI. The Lebesgue Stieltjes Power Integral for Short Crested Wave Systems
Equations (9.1) through (9.22) 207

Plate XXXVII. An Important Property of the Lebesgue Stieltjes Power Integral for a Short Crested Sea Surface
Equations (9.23) through (9.27) 210

Plate XXXVIII. An Important Property of the Lebesgue Stieltjes Power Integral for a Short Crested Sea Surface
Equation (9.28) 212

Plate XXXIX. Some Examples
Equations (9.29) through (9.35) 216

Page

Plate XL. Some Examples
Equations (9.36a) through (9.40). 218

Plate XLI. The Gaussian Case of the Lebesgue Power Integral for Short Crested Wave Systems
Equations (9.41) through (9.48) 221

Plate XLII. Some Examples of Cumulative Power Density Functions and Their Power Spectra
Equations (9.49) through (9.52) 223

Plate XLIII. The Forecasting Problem for a Sea Surface Represented by Short Crested Waves, a Gaussian Lebesgue Power Integral, and Waves that Last D_W Seconds at the Edge of a Storm of Width, W_s
Equations (9.53) through (9.63) 229

Plate XLIV. The θ-Band Width and the Forecasting Problem for a Sea Surface Represented by Short Crested Waves, a Gaussian Lebesgue Power Integral for a Storm of Width, W_s, of Duration, D_s, over a Fetch of Length, F
Equations (9.64) through (9.71) 234

Plate XLV. The Properties of a Short Crested Sea Surface as Observed as a Function of Time at a Fixed Point in Space
Equations (10.1) through (10.9) 258

Plate XLVI. The Properties of a Short Crested Sea Surface as Observed as a Function of Time at a Fixed Point in Space
Equations (10.10) through (10.13) 262

Plate XLVII. The Properties of a Short Crested Sea Surface as Observed as a Function of Time at a Fixed Point in Space
Equations (10.14) through (10.16) 264

Plate XLVIII. The Properties of a Short Crested Sea Surface as Observed as a Function of Time at a Fixed Point in Space
Equations (10.17) through (10.24) 266

Plate XLIX. Numerical Methods for the Determination of $[A(\mu)]^2$ from a Sample of a Stationary Time Series
Equations (10.25) through (10.26) 273

Page

Plate L. Numerical Methods for the Determination of $[A(\mu)]^2$ from a Sample from a Stationary Time Series
Equations (10.27) through (10.37) 275

Plate LI. Planning the Analysis and the Work Involved
Equations (10.38) through (10.39) 279

Plate LII. The Determination of $[A_2(\mu,\theta)]^2$
Equations (10.40) through (10.53) 289

Plate LIII. The Determination of $[A_2(\mu,\theta)]^2$
Equations (10.54) through (10.69) 293

Plate LIV. The Determination of $[A_2(\mu,\theta)]^2$
Equations (10.70) through (10.79) 296

Plate LV. The Determination of $[A_2(\mu,\theta)]^2$
Equations (10.80) through (10.88) 298

Plate LVI. The Determination of $[A_2(\mu,\theta)]^2$
Equations (10.89) through (10.99) 300

INDEX TO THE TABLES

Page

Tables 1 to 4:

Values of the Envelope of the Free Surface at Fixed Points as a Function of Time.

Table 1. $\sigma = 1/100$ sec^{-1} T = 5 T = 10 48

Table 2. $\sigma = 1/50$ sec^{-1} T = 5 T = 10 49

Table 3. $\sigma = 1/30$ sec^{-1} T = 5 T = 10 50

Table 4. $\sigma = 1/20$ sec^{-1} T = 5 T = 10 T = 20 . . . 51

Tables 5 to 13:

Apparent Local Period of the Free Surface at Fixed Points.

Table 5. $\sigma = 1/100$ T = 5 (Table 1) 58

Table 6. $\sigma = 1/50$ T = 5 (Table 2) 59

Table 7. $\sigma = 1/30$ T = 5 (Table 3) 60

Table 8. $\sigma = 1/20$ T = 5 (Table 4) 61

Table 9. $\sigma = 1/100$ T = 10 (Table 1) 62

Table 10. $\sigma = 1/50$ T = 10 (Table 2) 63

Table 11. $\sigma = 1/30$ T = 10 (Table 3) 64

Table 12. $\sigma = 1/20$ T = 10 (Table 4) 65

Table 13. $\sigma = 1/20$ T = 20 (Table 4) 66

Table 14. Component periods, amplitudes, and 1000 KM travel times for the important wave trains in equation (6.4) . 112

Table 15. Chi Square Test of the Upper Histogram in Figure 14 142

Table 16. Reliability of Power Spectrum Estimates 282

Arthur, R. S., [1948]: Revised wave forecasting graphs and procedure. Scripps Institution of Oceanography, Wave report no. 73, 14 pp. + 10 pl.

_____, [1949]: Variability in direction of wave travel. Ocean Surface Waves. Annals of the New York Academy of Sciences, v. 51, pp. 511-522.

Barber, N. F. and F. Ursell, [1948]: The generation and propagation of ocean waves and swell. I Wave Periods and Velocities. Phil. Trans. Royal Soc. of London, No. 824, v. 240, pp. 527-560.

Bierens de Haan, D., [1867]: Nouvelles tables d'integrales defines, (ed. of 1867). Reprint Stechert, New York, 1939.

Biesel, F., [1951]: Effect of gradually varying depth on wave propagation. Symposium on Gravity Waves, National Bureau of Standards.

Birkhoff, G., and J. Koteg, [1951]: Fourier analysis of one-dimensional gravity wave trains. Symposium on Gravity Waves, National Bureau of Standards.

Bohr, H., [1947]: Almost Periodic Functions. Chelsea Publishing Company, New York, New York

Caldwell, J., [1948]: An ocean wave measuring instrument. Beach Erosion Board Technical Memorandum No. 6.

Conrad, V., [1946]: Methods in Climatology. Harvard University Press.

Coulson, C. A., [1943]: Waves. Interscience Publishers, Inc., New York, New York.

Courant, R., [1937]: Differential and Integral Calculus. Vol. I and Vol II. Interscience Publishers, Inc., New York.

Cramer, H., [1946]: Mathematical Methods of Statistics. Princeton University Press.

Davies, T. V., [1951]: Finite amplitude gravity waves. Symposium on Gravity Waves, National Bureau of Standards.

Deacon, G. E. R., [1949]: Recent studies of waves and swell. Ocean Surface Waves. Annals of the New York Academy of Sciences, v. 51, pp. 475-482.

Deacon, G. E. R, J. Darbyshire, and N. D. Smith [1949]: Use of the airborne sea and swell records to measure changes in the wave spectrum from west to east across the Irish Sea. Admiralty Research Laboratory, Teddington, Middlesex. A.R.L./R1/103-18/W.

Donn, W. L., [1949]: Studies of waves and swell in the Western North Atlantic Ocean. Trans. American Geophysical Union, v. 30, no. 4.

Eckart, C., [1951]: The propagation of gravity waves from deep to shallow water. Symposium on Gravity Waves, National Bureau of Standards.

Ewing, M., and F. Press, [1949]: Notes on surface waves. Ocean Surface Waves. Annals of the New York Academy of Sciences, v. 51, pp. 453-462.

Glenn, A. H., [1950]: Wave, tide, current, and hurricane problems in coastal operations. The Oil and Gas Journal, June 22, 1950.

Groen, P., and R. Dorrestein, [1950]: Ocean swell, its decay and period increase. Nature 165, pp. 445-447.

Hoel, P. G., [1947]: Introduction to Mathematical Statistics. Wiley and Sons, New York.

Hydrographic Publication No. 604, [1951]. Techniques for forecasting wind waves and swell. U. S. Navy Hydrographic Office, Washington, D. C.

Isaacs, J. V., and T. Saville, Jr., [1949]: A comparison between recorded and forecast waves on the Pacific coast. Ocean surface waves. Annals of the New York Academy of Sciences, v. 51, art. 3, pp. 502-510.

James, G., and R. C. James, [1949]: Mathematical Dictionary. D. Van Nostrand Company, Inc., New York.

Jahnke, E., and F. Emde, [1945]: Functionentafeln mit Formeln und Kurven. Fourth revised edition, Dover Publications.

Johnson, J. W., [1949]: Scale effects in hydraulic models involving wave motion. Trans. American Geophysical Union, v. 30, no. 4.

Johnson, J. W., M. P. O'Brien, and J. D. Isaacs [1948]: Graphical construction of wave refraction diagrams. H. O. Publ. no. 605.

Keller, J., [1949]: The solitary wave and periodic waves in shallow water. Ocean Surface Waves. Annals of the New York Academy of Sciences, v. 51, pp. 345-350.

Kennard, E. H., [1938]: Kinetic Theory of Gases. McGraw Hill Book Company, New York.

Klebba, A. A., [1946]: Progress report on shore wave recorder and ocean wave analyzer. Memorandum for File. Woods Hole Oceanographic Institution.

_____, [1949]: Details of shore based wave recorder and ocean wave analyzer. Ocean Surface Waves. Annals of the New York Academy of Sciences, v. 51, pp. 533-544.

Lamb, H., [1932]: Hydrodynamics. 6th ed., Dover Publications.

Langmuir, I., [1950]: A seven day periodicity in weather in United States during April 1950. Bull. Amer. Meteor. Soc., v. 31, no. 10.

Levy, Paul, [1948]: Processes Stochastiques et Mouvement Brownien. Paris, Gauthier-Villars, Imprimeur - Editeur (Suivi d'une Note de M. Loeve). (See Chapter 4.)

Lowell, S. C., [1949]: The propagation of waves in shallow water. Communications on Pure and Applied Mathematics, v. 2, no. 2/3

_____, [1950]: Gravity waves of finite amplitude. Office of Naval Research London Technical Report, ONRL-111-50.

Margenau, H., and G. M. Murphy, [1947]: The Mathematics of Physics and Chemistry. D. Van Nostrand Company, New York.

Munk, W. H., [1947]: Increase in the period of waves traveling over large distances: with applications to tsunamis, swell and seismic surface waves. Trans. American Geophysical Union, v. 28, pp. 198-217.

_____, [1949]: The solitary wave theory and its application to surf problems. Ocean Surface Waves. Annals of the New York Academy of Sciences, v. 51, art. 3, pp. 376-401.

Munk, W. H., and R. S. Arthur, [1951]: Forecasting ocean waves. Compendium of Meteorology, American Meteorological Society, Boston, Mass.

Peters, A. S., [unpublished]: Water waves on sloping beaches and the solution of a mixed boundary value problem for $\nabla^2\varphi - k^2\varphi = 0$ in a sector. (To be published in Communications on Pure and applied Mathematics,- possibly v. 5, no. 1.)

Pierce, B. O., [1929]: A Short Table of Integrals. Ginn and Company, New York.

Pierson, W. J., Jr., [1951a]: The interpretation of crossed orthogonals in wave refraction phenomena. Beach Erosion Board Technical Memorandum, no. 21.

_____, [1951b]: The accuracy of present wave forecasting methods with reference to problems in beach erosion on the New Jersey and Long Island coasts. Beach Erosion Board Technical Memorandum, no. 24.

_____, [1951c]: On the propagation of waves from a model fetch at sea. Symposium on Gravity Waves, National Bureau of Standards.

Putz, R. R., [1950a]: Idealized reconstructions of ocean surface waves as inferred from measurements on twenty five subsurface pressure records. Technical Report 116-317, University of California, Institute of Engineering Research.

_____, [1950b]: Wave height variability; prediction of distribution function. Technical Report HE 116-318, University of California, Institute of Engineering Research.

_____, [1951]: Wave period variability; prediction of distribution function. Technical Report HE 116-325, University of California, Institute of Engineering Research.

Rudnick, P., [1949]: A system for recording and analyzing random processes. Symposium on Applications of Autocorrelation Analyses to Physical Problems. Woods Hole, Mass. 13-14, ONR, Department of the Navy, Washington, D. C.

Seiwell, H. R., [1949a]: The principles of time series analysis applied to ocean wave data. Proc. Nat. Acad. of Sciences, v. 35, no. 9, pp. 518-528.

_____, [1949b]: Ocean wave analyses. Symposium on Applications of Autocorrelation Analysis to Physical Problems. Woods Hole, Mass. 13-14 June, 1949, ONR Dept. of Navy, Washington, D. C.

_____, [1950a]: A new mechanical autocorrelator. The Review of Scientific Instruments, v. 21, no. 5, pp. 481-484.

_____, [1950b]: Problems in the statistical analyses of geophysical time series. Science, v. 112, no. 2905, pp. 243-246.

Seiwell, H. R., and C. P. Wadsworth, [1949]: A new development in ocean wave research. Science, v. 109, no. 2829, pp. 271-274.

Sommerfeld, A., [1949]: Partial Differential Equations in Physics. Academic Press, Inc., New York.

Stoker, J. J., [1947]: Surface waves in water of variable depth. Quart. Applied Mathematics, v. 5, no. 1.

_____,[1948]: Formation of breakers and bores. Communications on Applied Mathematics, I(1) 1-87.

_____, [1949]: The breaking of waves in shallow water. Ocean Surface Waves. Annals of the New York Academy of Sciences, v. 51, art. 3, pp. 360-375.

Stokes, G. G., [1847]: On the theory of oscillatory waves. Cambridge Transactions viii (papers i 177).

Sverdrup, H. U., [1947]: Period increase of ocean swell. Trans. American Geophysical Union, v. 28, no. 3.

Sverdrup, H. U., and W. H. Munk, [1944a]: Wind, waves and swell: Principles in Forecasting. HO Misc. 11275.

_____, [1944b]: Breakers and surf. U. S. Hydrographic Office Publ. No. 234.

_____, [1947]: Wind, sea and swell; theory of relations for forecasting. U. S. Navy Hydrographic Office. HO P_{ub}. No. 601.

Tukey, J. W., [1949]: The sampling theory of power spectrum estimates. Symposium on Applications of Autocorrelation Analysis to Physical Problems. Woods Hole, Mass. 13-14 June 1949. ONR Dept. of the Navy, Washington, D. C.

Tukey, J. W., and R. W. Hamming, [1949]: Measuring Noise Color 1.

Wiener, N., [1930]: Generalized Harmonic Analysis. Acta Math 55.

_____, [1949]: Extrapolation Interpolation and Smoothing of Stationary Time Series. John Wiley and Sons, Inc., New York.